EVOLUTION OF ANIMAL MICROBIAL COMMUNITIES IN RESPONSE TO ENVIRONMENTAL STRESS

EDITED BY: Teresa Nogueira, Ana Pombo Botelho, Lucas David Bowler and Joao Inacio

PUBLISHED IN: Frontiers in Microbiology

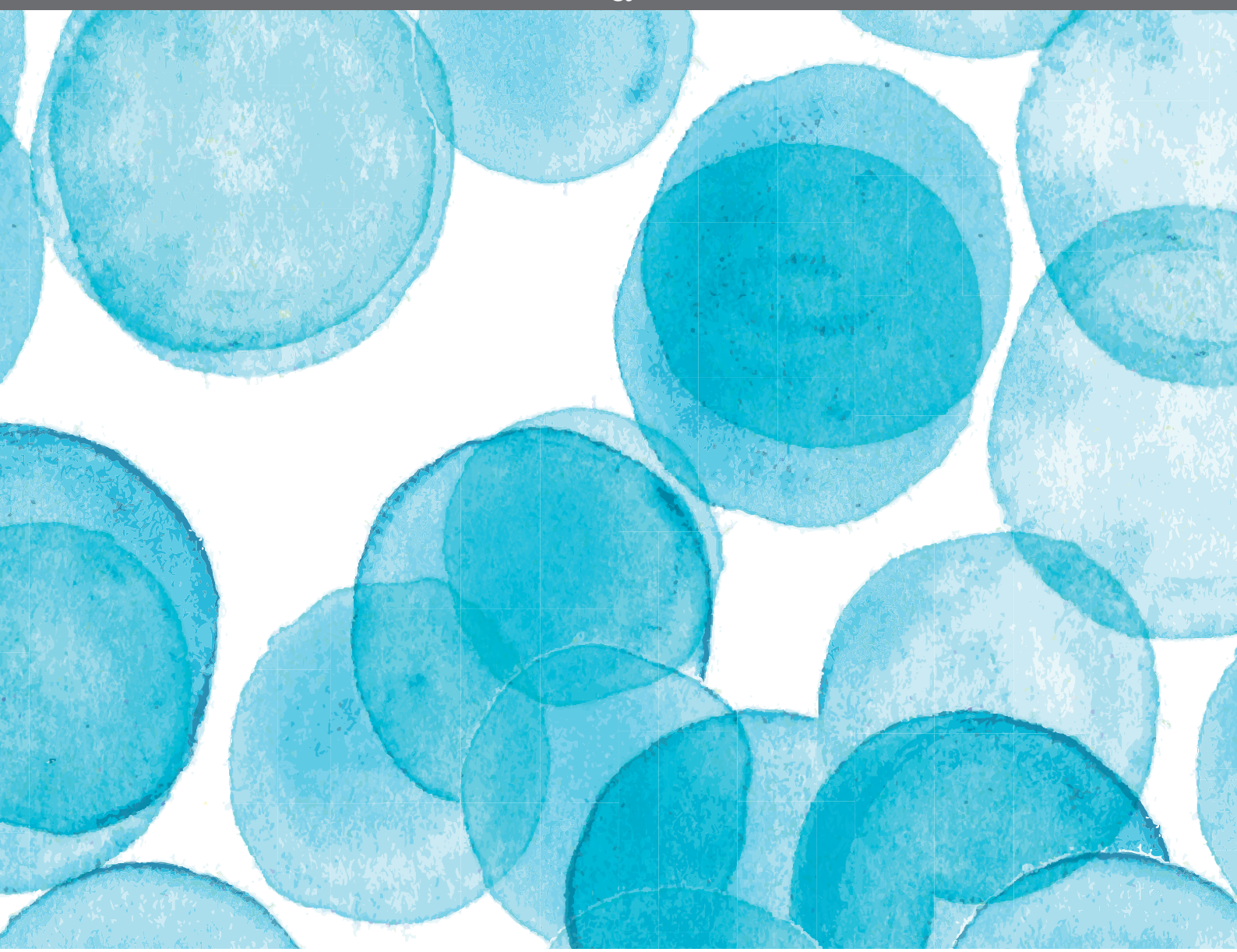

frontiers Research Topics

ISSN 1664-8714
ISBN 978-2-88974-972-0
DOI 10.3389/978-2-88974-972-0

About Frontiers

Frontiers is more than just an open-access publisher of scholarly articles: it is a pioneering approach to the world of academia, radically improving the way scholarly research is managed. The grand vision of Frontiers is a world where all people have an equal opportunity to seek, share and generate knowledge. Frontiers provides immediate and permanent online open access to all its publications, but this alone is not enough to realize our grand goals.

Frontiers Journal Series

The Frontiers Journal Series is a multi-tier and interdisciplinary set of open-access, online journals, promising a paradigm shift from the current review, selection and dissemination processes in academic publishing. All Frontiers journals are driven by researchers for researchers; therefore, they constitute a service to the scholarly community. At the same time, the Frontiers Journal Series operates on a revolutionary invention, the tiered publishing system, initially addressing specific communities of scholars, and gradually climbing up to broader public understanding, thus serving the interests of the lay society, too.

Dedication to Quality

Each Frontiers article is a landmark of the highest quality, thanks to genuinely collaborative interactions between authors and review editors, who include some of the world's best academicians. Research must be certified by peers before entering a stream of knowledge that may eventually reach the public - and shape society; therefore, Frontiers only applies the most rigorous and unbiased reviews.
Frontiers revolutionizes research publishing by freely delivering the most outstanding research, evaluated with no bias from both the academic and social point of view. By applying the most advanced information technologies, Frontiers is catapulting scholarly publishing into a new generation.

What are Frontiers Research Topics?

Frontiers Research Topics are very popular trademarks of the Frontiers Journals Series: they are collections of at least ten articles, all centered on a particular subject. With their unique mix of varied contributions from Original Research to Review Articles, Frontiers Research Topics unify the most influential researchers, the latest key findings and historical advances in a hot research area! Find out more on how to host your own Frontiers Research Topic or contribute to one as an author by contacting the Frontiers Editorial Office: frontiersin.org/about/contact

EVOLUTION OF ANIMAL MICROBIAL COMMUNITIES IN RESPONSE TO ENVIRONMENTAL STRESS

Topic Editors:
Teresa Nogueira, Instituto Nacional Investigaciao Agraria e Veterinaria (INIAV), Portugal
Ana Pombo Botelho, Instituto Nacional Investigaciao Agraria e Veterinaria (INIAV), Portugal
Lucas David Bowler, University of Brighton, United Kingdom
Joao Inacio, University of Brighton, United Kingdom

Citation: Nogueira, T., Botelho, A. P., Bowler, L. D., Inacio, J., eds. (2022). Evolution of Animal Microbial Communities in Response to Environmental Stress. Lausanne: Frontiers Media SA. doi: 10.3389/978-2-88974-972-0

Table of Contents

frontiers in Microbiology

EDITORIAL
published: 30 March 2022
doi: 10.3389/fmicb.2022.860609

Editorial: Evolution of Animal Microbial Communities in Response to Environmental Stress

Teresa Nogueira[1,2]*, *Ana Botelho*[1], *Lucas Bowler*[3] and *João Inácio*[3]

[1] Bacteriology and Mycology Laboratory, Instituto Nacional Investigação Agrária e Veterinária (INIAV), Oeiras, Portugal, [2] Centro de Ecologia, Evolução e Alterações Ambientais (cE3c), Universidade de Lisboa, Lisbon, Portugal, [3] School of Applied Sciences, University of Brighton, Brighton, United Kingdom

Keywords: microbiomes, adaptation, ecology and population biology, environment, stress response, microbial evolution, microbiome and dysbiosis, microbiome in health and disease

Editorial on the Research Topic

Evolution of Animal Microbial Communities in Response to Environmental Stress

We live in a microbial world in which bacteria, viruses, fungi, and other microscopic organisms such as parasites live together in microbial communities, where they establish ecological interactions, cooperative and competitive behaviors, driving to environmental adaptation and genome evolution.

A microbiome represents the collection of the microorganisms that inhabit a specific environment along with their genomic content. They are present everywhere and in many niches of the human body. Metagenomics brings together microbiology, genetics, genomics, and bioinformatics, enabling an integrated approach to the understanding of the natural microbial communities to capture the ecology, evolution, and dynamics of these microbial communities.

In a changing environment, microorganisms evolve and adapt, and the balance between species and strains within the community can also be disrupted or shifted to another level of steady-state. Human and other animal microbiomes can be under diverse sources of disturbance: physiological changes due to diet or health/illness, exposure to medications, or even environmental changes, among others. To understand and study the effect of these changes on animal microbial communities' dynamics, the most appropriate sampling design tools must be applied, and mathematical and computational methods must also be developed to deal with this challenging subject. This Research Topic "*Evolution of Animal Microbial Communities in Response to Environmental Stress*" addresses the dynamics of microbial (symbiotic) communities under environmental changes.

The microbiome of individuals who share the same household or social contacts is more likely to share similar microbes (Brito et al., 2019). Thus, cohabitation has been reported to be a driver of the transfer and sharing of the oral, gut, and nasopharyngeal microbiomes from person to person in a physical social network, as well as, for example, a major factor facilitating the typical asymptomatic transmission of SARS-CoV-2 (Hu et al., 2020). Chen Y. et al. conducted a confined experiment in which healthy individuals were enclosed together in a space capsule on the ground for 180 days, which revealed that both the structure and diversity of the nasal and oropharyngeal microbiota changed over time and were shared between the participants, during the study. A work by Fu et al. shows that domestication is also a modulator of gut microbiome diversity in yak which paves the way for the development of new commercial strains in livestock based on the biotechnology of gut microbiota.

OPEN ACCESS

Edited and reviewed by:
M. Pilar Francino, Fundación para el Fomento de la Investigación Sanitaria y Biomédica de la Comunitat Valenciana (FISABIO), Spain

***Correspondence:**
Teresa Nogueira
teresainogueira@gmail.com

Specialty section:
This article was submitted to Microbial Symbioses, a section of the journal Frontiers in Microbiology

Received: *23 January 2022*
Accepted: *10 February 2022*
Published: *30 March 2022*

Citation:
Nogueira T, Botelho A, Bowler L and Inácio J (2022) Editorial: Evolution of Animal Microbial Communities in Response to Environmental Stress. Front. Microbiol. 13:860609. doi: 10.3389/fmicb.2022.860609

The microbial community of the Qinghai-Tibet Plateau (QTP) includes parasites of mammalian hosts, such as some rodent species. Wu et al. have demonstrated that the altitude of the Qinghai-Tibet Plateau is a driver of diversity, not only of plants and animals but also of microorganisms such as parasites and their microscopic larvae of Taeniidae species.

A classic example of the adaptive response of populations and communities is exposure to antibiotics. The study by Chen C.-M. et al. demonstrates that changes in the gut microbiota following maternal exposure to antibiotics during pregnancy can be transmitted to offspring, also leading to a disruption in gut development in neonatal mice.

Dietary modification can also have an effect as a modulator of the gut microbiota, inducing the appearance of new genomic variants in the gut microbiome. For example, one study shows that changing the diet to one rich in fiber, in children with Prader-Willi syndrome and obese children, led not only to changes in microbial diversity but also to the evolution of the microbial genome with the appearance of variants corresponding to SNPs related to traits of adaptation to the use of nutrients from the diet, thus opening the prospect of investigating new therapeutic pathways (Li et al.). Diet is also involved in modeling gut microbiota and the immune stimulation of sows, which may reduce the diarrhea rate of their offspring (Zhang et al.).

The human gut is an ecosystem comprising trillions of microbes that reacts to diet and interacts with the host influencing its health. Close relationships between dietary modifications, microbiota composition and health status have been established (Enam and Mansell, 2019). Furthermore, gut microbes develop catabolic activity to circumvent the antimicrobial activity of certain food additives such as vanillin. Gene clusters specific for the vanillin metabolism and intermediary metabolic pathways have been identified by metagenomic analysis in several gut microbial populations (Yadav et al.). The metabolomic analysis brings forth the functionality of the vanillin catabolic pathway. These results highlight the human gut microbial features and metabolic bioprocess involved in vanillin catabolism to overcome its antimicrobial activity.

Another example of the relationship between the diversity of the gut microbiome and health is presented by Ma et al. that have demonstrated that there is a correlation between native Tibetans and Han immigrants' gut microbiome and their hematological profile, which may also relate to the Tibetans' adaptation to high altitudes.

The determination of the vaginal microbiome in women undergoing different types of treatments and the correlation with clinical outcomes have been the object of several studies (Hyman et al., 2012). The changes in the composition of the vaginal microbiome under the effect of menopausal hormonal therapies consist in a decrease in microbial diversity and a preponderance of *Lactobacillus* (Geng et al.). In contrast, the non-treated vaginal microbiome is enriched with anaerobic and facultative anaerobic bacteria, namely, *Gardnerella, Prevotella, Escherichia, Shigella, Streptococcus, Atopobium, Aerococcus, Anaerotruncus, and Anaerococcus*, apart from *Chlamydia* and *Streptococcus*. These changes have consequences in the symptoms of the genitourinary syndrome in menopause that are more severe without the effect of hormonal therapies.

It is known that the natural respiratory tract microbiome plays an important role in controlling nosocomial infections. However physiological conditions and interventions of critical respiratory tract patients, such as mechanical ventilation and antibiotics administration, dramatically alter the respiratory tract microbiome, leading to dysbiosis and favoring the colonization by opportunistic and resistant pathogens (Pérez-Cobas et al.). Therefore, this microbial imbalance is linked with various diseases and significantly reduces the quality of one's life. Varying inflammatory profiles are associated with specific microbial compositions, while the same is true for many disease conditions and environmental exposures. A shift in the microbial composition is also detected upon the administration of numerous therapeutics, highlighting other beneficial and adverse side effects (Elgamal et al., 2021).

The commensal bacteria that show the potential to inhibit pathobionts and modulate host immunity should be further studied for their potential to stimulate a resilient microbiota that is resistant to infection. The development of *in vivo* and *in vitro* models that assess microbial competition and interactions within the microbiota will further the understanding of the complex relationships that exist and will help develop probiotic solutions for respiratory tract infections.

AUTHOR CONTRIBUTIONS

TN, AB, LB, and JI contributed to conception of the aim of the Research Topic. TN and AB wrote the manuscript. All authors contributed to manuscript revision, read, and approved the submitted version.

FUNDING

Fundação para a Ciência e a Tecnologia (FCT), I.P., supports TN by contract ALG-01-0145-FEDER-028824 and PTDC/BIA-MIC/28824/2017 and cE3c-FCUL through contract UIDP/00329/2020.

ACKNOWLEDGMENTS

We would like to thank Todd Treangen and Sara Vieira-Silva for the fruitful discussions and suggestions during the preparation of the Research Topic.

REFERENCES

Brito, I. L., Gurry, T., Zhao, S., Huang, K., Young, S. K., Shea, T. P., et al. (2019). Transmission of human-associated microbiota along family and social networks. *Nat. Microbiol.* 4, 964–971. doi: 10.1038/s41564-019-0409-6

Elgamal, Z., Singh, P., and Geraghty, P. (2021). The upper airway microbiota, environmental exposures, inflammation, and disease. *Medicina* 57, 823. doi: 10.3390/medicina57080823

Enam, F., and Mansell, T. J. (2019). Prebiotics: tools to manipulate the gut microbiome and metabolome. *J. Ind. Microbiol. Biotechnol.* 46, 1445–1459. doi: 10.1007/s10295-019-02203-4

Hu, Z., Song, C., Xu, C., Jin, G., Chen, Y., Xu, X., et al. (2020). Clinical characteristics of 24 asymptomatic infections with COVID-19 screened among close contacts in Nanjing, China. *Sci. China Life Sci.* 63, 706–711. doi: 10.1007/s11427-020-1661-4

Hyman, R. W., Herndon, C. N., Jiang, H., Palm, C., Fukushima, M., Bernstein, D., et al. (2012). The dynamics of the vaginal microbiome during infertility therapy with in vitro fertilization-embryo transfer. *J. Assist. Reprod. Genet.* 29, 105–115. doi: 10.1007/s10815-011-9694-6

Conflict of Interest: The authors declare that the research was conducted in the absence of any commercial or financial relationships that could be construed as a potential conflict of interest.

frontiers in Microbiology

ORIGINAL RESEARCH
published: 16 October 2020
doi: 10.3389/fmicb.2020.588545

Catabolic Machinery of the Human Gut Microbes Bestow Resilience Against Vanillin Antimicrobial Nature

Monika Yadav[1], *Rajesh Pandey*[2]* *and Nar Singh Chauhan*[1]*

[1] Department of Biochemistry, Maharshi Dayanand University, Rohtak, India, [2] Genomics and Molecular Medicine, CSIR-Institute of Genomics and Integrative Biology (CSIR-IGIB), New Delhi, India

Vanillin is a phenolic food additive commonly used for flavor, antimicrobial, and antioxidant properties. Though it is one of the widely used food additives, strategies of the human gut microbes to evade its antimicrobial activity await extensive elucidation. The current study explores the human gut microbiome with a multi-omics approach to elucidate its composition and metabolic machinery to counter vanillin bioactivity. A combination of SSU rRNA gene diversity, metagenomic RNA features diversity, phylogenetic affiliation of metagenome encoded proteins, uniformly (R = 0.99) indicates the abundance of Bacteroidetes followed by Firmicutes and Proteobacteria. Manual curation of metagenomic dataset identified gene clusters specific for the vanillin metabolism (*ligV, ligK*, and *vanK*) and intermediary metabolic pathways (*pca* and *cat* operon). Metagenomic dataset comparison identified the omnipresence of vanillin catabolic features across diverse populations. The metabolomic analysis brings forth the functionality of the vanillin catabolic pathway through the Protocatechuate branch of the beta-ketoadipate pathway. These results highlight the human gut microbial features and metabolic bioprocess involved in vanillin catabolism to overcome its antimicrobial activity. The current study advances our understanding of the human gut microbiome adaption toward changing dietary habits.

Keywords: human gut microbes, food metabolism, vanillin catabolism, food additives, metabolomics, metagenomics, antimicrobial resistance

OPEN ACCESS

Edited by:
Ana Rosa Botelho, Instituto Nacional Investigaciao Agraria e Veterinaria (INIAV), Portugal

Reviewed by:
Monica Rosenblueth, National Autonomous University of Mexico, Mexico
Debarati Paul, Amity University, India

***Correspondence:**
Rajesh Pandey
rajeshp@igib.res.in
Nar Singh Chauhan
nschauhan@mdurohtak.ac.in; nschauhanmdu@gmail.com

Specialty section:
This article was submitted to Microbial Symbioses, a section of the journal Frontiers in Microbiology

Received: *29 July 2020*
Accepted: *17 September 2020*
Published: *16 October 2020*

Citation:
Yadav M, Pandey R and Chauhan NS (2020) Catabolic Machinery of the Human Gut Microbes Bestow Resilience Against Vanillin Antimicrobial Nature. Front. Microbiol. 11:588545. doi: 10.3389/fmicb.2020.588545

INTRODUCTION

The human gut microbiome is a stratified, metabolically active, and resilient biotic component of the human body (Yadav et al., 2018). Its progressive establishment starts with human birth and matures by the adulthood of the host (Vemuri et al., 2018). The gut microbes continuously interact, mostly as commensals with the host for their survival (Parker et al., 2018) and maintenance of the healthy host physiology (Yadav et al., 2018). An adult gut microbiome is primarily enriched with Firmicutes and Bacteroidetes (Chauhan et al., 2018). The human gut microbiome enriches the host gene pool with additional 300,000 + genetic features to enrich the metabolic potential of the host (Qin et al., 2010; Oliphant and Allen-Vercoe, 2019). Role of the gut microbes in food digestion is being elucidated for decades, however, their role in xenobiotic/drug metabolism has only been recently discovered (Clarke et al., 2019). Human gut microbes are equipped with efficient metabolic machinery to metabolize polyphenols (Theophylline and Caffeine) (Yu et al., 2009) as well as pharmaceutical drugs (Zimmermann et al., 2019). Despite these discoveries, research toward

unveiling the role of human gut microbes in the metabolism of food additives needs further attention.

Vanillin is the principal flavor and aroma component of the vanilla beans (Ramachandra Rao and Ravishankar, 2000). In addition to the flavoring properties, is also characterized by antimicrobial, antifungal, antioxidant, anticlastogenic, and antitumor properties (Durant and Karran, 2003; Shyamala et al., 2007; Sinha et al., 2008; Guo et al., 2018). Due to its flavoring and medicinal properties, it was used in Indian food preparations for many centuries (Menon and Nayeem, 2013). The natural preservative and flavoring properties of vanillin make it a commonly used food additive (Fitzgerald et al., 2004). Additionally, the degradation of lignin compounds also contributes (Furuya et al., 2015; Chen et al., 2016) to the availability of vanillin (10 mg/kg of the body weight in the human body) (Furuya et al., 2015; Chen et al., 2016). Continuous exposure of the vanillin exposes human gut microbes toward its antimicrobial property (Fitzgerald et al., 2004; Endo et al., 2009). It possibly challenges human gut microbes to either develop efficient metabolic machinery to respond to antimicrobial behavior of vanillin or a compromised survival trajectory. If microbes were unable to efficiently metabolize vanillin, it could lead to microbial dysbiosis, followed by the onset of microbial dysbiosis associated human disorders. On the contrary, vanillin is known to improve the gut microbiome composition (Guo et al., 2018), as well as protect the host from the onset of various human disorders (Yan et al., 2017). Thus, it indicates the possible presence of efficient vanillin catabolic machinery among the human gut microbes; however, an effort to explore these metabolic pathways is warranted. In the current study, we have explored the human gut microbiome composition, its genetic content, and metabolic efficiency to catabolize vanillin using a culture-independent multi-omics approach. This is a pioneer study to rationalize the role of human gut microbes in vanillin catabolism. The findings of this study hold potential to enrich our understanding of the gut microbial functionaries in the xenobiotic metabolism and evolution of the human gut microbiome with dietary habits.

MATERIALS AND METHODS

Ethics Statement

The study was conducted after receiving ethical clearance from the Human Ethical Committee at M. D. University, Rohtak, Haryana, India. Strict human ethical guidelines were followed and written consent was sought from each enrolled individual in this study.

Metagenomic DNA Isolation

The fecal samples were collected from healthy individuals ($n = 8$, Age 29–36 years, Male). Alkali-lysis method was adopted to isolate high molecular weight metagenomic DNA (Kumar et al., 2016). Qualitative and quantitative analysis of Metagenomic DNA was performed with agarose-gel electrophoresis and Qubit dsDNA HS Assay Kit (Invitrogen, United States) respectively.

Small Subunit rRNA Gene Analysis

The V1 to V4 region of the SSU rRNA gene was amplified from the metagenomic DNA using region-specific primers (Morowitz et al., 2011). The amplified product was sequenced with Roche 454 GS FLX + using GS FLX Titanium XL$^+$ Sequencing Kit (Gupta et al., 2017). Quantitative Insights into Microbial Ecology (QIIME) 1.9.1 pipeline was implemented for quality filtering, OTU picking, taxonomic assignment, alpha and beta diversity analysis (Kapono et al., 2018).

Metagenome Sequencing and Sequence Analysis

The metagenomic DNA was sequenced with MiSeq Next-Generation Sequencing (NGS) platform with paired-end sequencing chemistry using MiSeq Reagent Kit v3 (600-cycle) (Illumina, United States). The reads were preprocessed and uploaded into the Metagenome Rapid Annotation using Subsystem Technology (MG-RAST) server 4.0.3 (Meyer et al., 2008). The metagenome sequence dataset was quality filtered (Denoising and normalization with DynamicTrim, removal of host DNA sequences with Bowtie2) and processed for the identification of rRNA gene features (by rRNA genecalling) and protein features (with genecalling using cutoff similarity% > 70%). Potential ribosomal RNA genes were clustered with CD-HIT and checked for their homologs in the Greengene database (e-value $<10^{-5}$, sequence similarity < 60% and word size > 15 bp). FragGeneScan 1.3.1 was employed for the identification of all putative protein-coding features (Rho et al., 2010). Predicted protein features were clustered (90% identity) and processed for similarity search using BLAT (BLAST-Like Alignment Tool) algorithm (Kent, 2002) against the M5NR protein database, RefSeq database (O'Leary et al., 2016), COG database (Database of Clusters of Orthologous Groups of proteins) (Tatusov, 2000) with stringent search parameters (e-value $<10^{-5}$, minimum identity < 60%). Protein feature abundance, Lowest Common Ancestor (LCA) abundance profile, and Data source abundance profile were used to predict taxonomic and functional affiliation of the predicated protein features (Milanese et al., 2019).

Identification and Mapping of Features Associated With Vanillin Catabolism

Functional annotation of predicted protein features was performed by searching homologs in the Subsystems database (Overbeek, 2005) using stringent search parameters (e-value < 10^{-5}, minimum identity < 60%, word size > 15). Vanillin catabolic features were manually curated from the annotated protein features and mapped on to the metabolic pathway. Sequence (both gene and protein) of the potential vanillin catabolic features were extracted from the metagenomic dataset and used for phylogenetic characterization using KAIJU webserver 1.7.3 (Menzel et al., 2016).

Comparative Metagenome Analysis

To explore the omnipresence of the vanillin catabolic features across gender, age, geographical location, the human gut

metagenomic datasets of the United States, Sweden, Venezuela, Japan, and Malaysia were used for comparative analysis (**Supplementary Table S1**). All these metagenomic datasets were processed with the MG-RAST server. Predicted RNA features were clustered and checked for their homologs in the Greengene database (*e*-value $<10^{-5}$, sequence similarity < 60% and word size > 15 bp). Predicted protein features were clustered and searched for their homologs in the RefSeq database (O'Leary et al., 2016), COG database (Database of Clusters of Orthologous Groups of proteins) (Tatusov, 2000) (*e*-value $<10^{-5}$, minimum identity < 60%). Functional annotation of the predicated protein features was performed after searching homologs (*e*-value $< 10^{-5}$, minimum identity < 60%, word size > 15) in the Subsystems database. Vanillin catabolic features were manually curated from each dataset. Each search output was normalized before the Pearson correlation analysis, Principle Component Analysis (PCA), and heatmap generation (Koch et al., 2018).

Functional Assessment of Vanillin Catabolism

Human fecal suspensions (n = 8) (500 mg/ml in phosphate buffer saline pH 7.4) were used for the purification of the microbial pellet (Kumar et al., 2016). The microbial pellet was incubated in vanillin solution (5 mM) at 37°C. A control sample without the vanillin solution was also incubated at 37°C simultaneously. The samples were withdrawn in small fractions at various intervals of time (0, 0.5, 2, 4, 6, 12, and 24 h). Samples were centrifuged at 13,000 rev min^{-1} for 2 min. Samples were quenched and processed for extraction of metabolites (**Supplementary Method SM1**). A 400 μl of acetonitrile was added to the metabolite fraction and centrifuged at 5,000 rev min^{-1} for 10 min. The supernatant was collected and loaded in autosampler for injection in LC-MS analysis. High-performance liquid chromatography coupled to quadrupole-time of flight mass spectrometry (HPLC/Q-TOF MS), possessing an Exion LC system integrated with X-500 QTOF (SCIEX Technology, United States) was used to obtain the metabolic profiles in the filtered supernatant (**Supplementary Method SM2**). Both negative and positive modes of electrospray ionization were used to capture the metabolic profile. LC-MS spectra were analyzed with SCIEX OS software 1.4 using ALL in One HR-MS/MS spectral library (SCIEX, United States) using an untargeted metabolic mapping workflow using default parameters.

RESULTS

SSU rRNA Gene Amplicons Based Human Gut Microbiome Composition

A total of 208,726 sequence reads were obtained after sequencing the SSU rRNA amplicons (V1–V4 region) from human stool metagenomic DNA. The removal of ambiguous sequences, quality (>Q30), and chimeric sequences, resulted in a total of 149,342 high quality reads for downstream analysis. *De novo* clustering of all sequences with QIIME 1.9.1 resulted in a total of 1,453 OTUs. Microbial diversity analysis of SSU rRNA sequences identified sequences corresponding to a total of 11 microbial phyla. Among all, the majority of sequences were of Bacteroidetes (80.18 ± 11.6%), Firmicutes (17.8 ± 11.67%), and Proteobacteria (1.85 ± 1.6%) lineages (**Figures 1A,B**). Additionally, representation of Actinobacteria, Acidobacteria, Chloroflexi, Fusobacteria, Lentisphaerae, Tenericutes, and Verrucomicrobia was also observed at lower proportions (**Figures 1A,B**). Within Bacteroidetes, majority of SSU rRNA sequences (90.16 ± 8.26%) were found affiliated to *Prevotella* sp., while *Ruminococcaceae* (40.82 ± 23.1%) and *Lachnospiraceae* (31.05 ± 17.85%) were found to be predominant among Firmicutes (**Supplementary Figure S1**).

Taxonomic Characterization of the Human Gut Metagenomic Dataset

A total of 20,136,917 sequences were generated after shotgun sequencing of the human gut metagenomic DNA with the MiSeq paired-end sequencing chemistry (Illumina, United States) (**Supplementary Table S2**). The151554 sequences were identified to possess ribosomal RNA features. The majority of these ribosomal features were phylogenetically affiliated with the bacterial clade (99.98 ± 0.01%), whereas 0.01 ± 0.008% remained unclassified. Amidst bacterial clade, rRNA features shared homology with rRNA gene sequences of Bacteroidetes, Firmicutes, Proteobacteria, Actinobacteria, Verrucomicrobia, Cyanobacteria, Tenericutes, Chlorobi, Synergistetes, Planctomycetes, and Spirochetes (**Figure 1C**). Among these groups, Bacteroidetes were predominant (66.11 ± 24.67%) followed by Firmicutes (17.47 ± 16.95%), and Proteobacteria (2.86 ± 2.47%). The ribosomal features based gut microbiome analysis shared a good correlation (R = 0.9916) with the outcome of the SSU rRNA gene-based microbial diversity analysis. This highlights the significant concordance among the microbial diversity observed after whole metagenome sequencing and targeted V1–V4 region of 16S rRNA gene sequencing.

RefSeq database search analyses indicated taxonomic affiliation within bacteria (99.62 ± 0.1%), archaea (0.21 ± 0.06%), eukaryota (0.14 ± 0.03%), and viruses (0.035 ± 0.01%). These protein features showed similar phylogenetic distribution as observed after analysis of SSU rRNA genes and rRNA features (**Figure 1D** and **Supplementary Table S3**). Despite of a slightly higher diversity of the encoded protein features, a good correlation was observed among phylogenetic affiliation of encoded protein features and SSU rRNA gene-based diversity analysis (R = 0.975).

Functional Characterization of the Human Gut Metagenomic Dataset

A total of 2,581 clusters of orthologous groups (COGs) have been observed with a role in various cellular physiological processes. Of this, 48.93 ± 2.30% of orthologous features were found associated with cellular metabolism, while 20.10 ± 0.17% were involved in cellular processes and signaling. A slightly lower proportion (19.01 ± 2.07%) was found associated with information storage and processing, while remaining

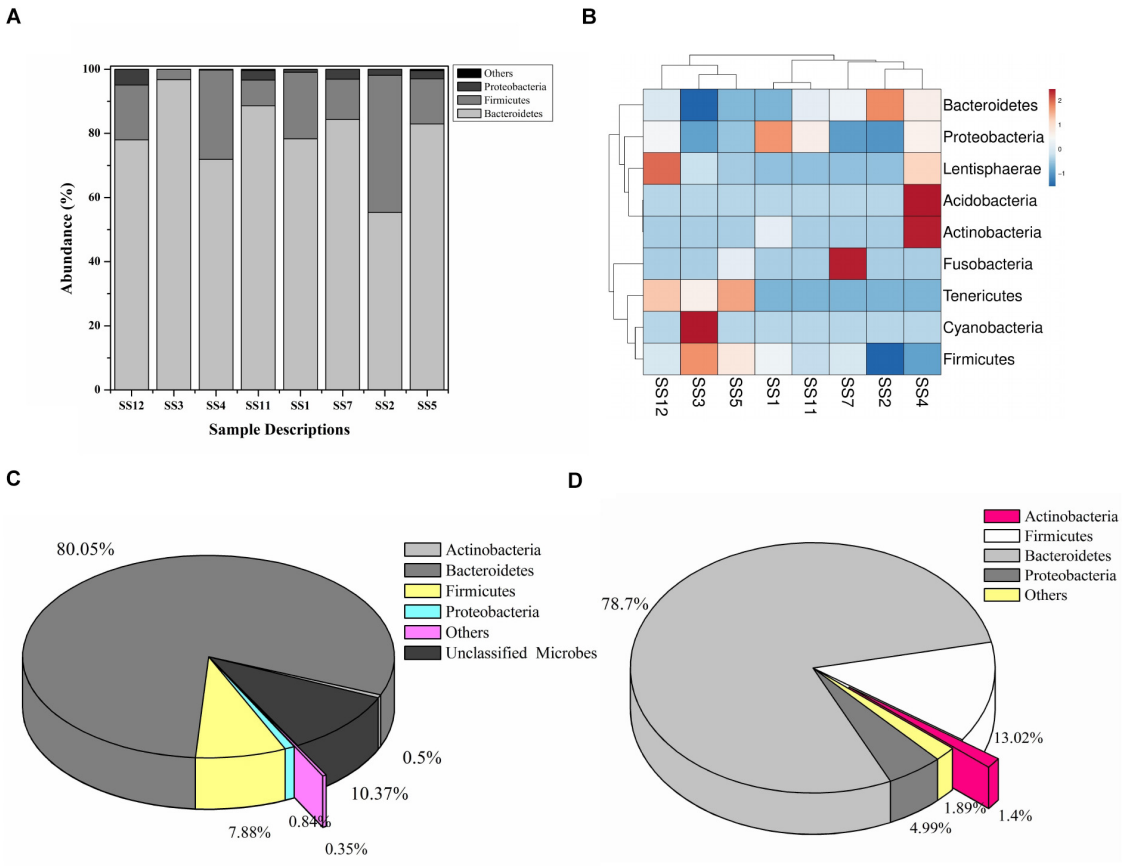

FIGURE 1 | Microbiome composition based on SSU rRNA gene analysis, rRNA features, and protein features. Phylogenetic distribution of SSU rRNA genes **(A)** and their interrelationship among samples **(B)**. Phylogenetic distribution of human gut metagenomic rRNA features **(C)** and protein features **(D)**.

(11.94 ± 0.16%) were poorly characterized proteins. Among cellular metabolism-associated COGs, the majority of proteins were associated with carbohydrate transport and metabolism (30.18 ± 0.69%) and amino acid transport and metabolism (23.53 ± 0.17%). We observed a very low percentage of COGs (3.11 ± 0.11% and 0.57 ± 0.03%) associated with defense and secondary metabolism (**Supplementary Table S4**). The human gut is considered a more stable ecosystem than its environmental counterparts (soil, water, etc.). Hence human gut microbes were not subjected to challenging environmental conditions (variations in temperature, pH, water contents, scarcity of nutrients, etc.) (Tian et al., 2017). Human gut microbiome evolution might have allowed human gut microbes to perform genetic restructuring toward gut conditions for better harvesting of energy and nutrients for their growth and proliferation (Hooper, 2001).

Vanillin Catabolism Genetic Machinery of the Human Gut Microbiome

To date there is no scientific evidence of vanillin catabolism among human gut microbes; however, its catabolism has been studied in various free-living microbes like *Rhodococcus jostii* RHA1 (Chen et al., 2012), *Pseudomonas putida* (Plaggenborg et al., 2003), *Sphingomona spaucimobilis* SYK-6 (Masai et al., 2007), and *Streptomyces* sp. NL15-2K (Nishimura et al., 2018). Vanillin is generally metabolized in two phases; vanillin is catabolized into protocatechuate by two-step process catalyzed by vanillin dehydrogenase (LigV) and vanillate O-demethylase (LigM) in the first phase (Kamimura et al., 2017). Phase II includes bioconversion of protocatechuate through a central aromatic intermediate metabolic pathway into TCA cycle intermediates (Grant and Patel, 1969; Romero-Steiner et al., 1994; Parke, 1995).

Manual curation of the human gut metagenome dataset identifies protein features and their respective genes potentially associated with vanillin metabolism (**Table 1**). Homologs of the decoded genes are part of *lig*, *pca*, and *cat* operons. Encoded products of vanillin membrane transporter gene (*vanK*), *lig* genes (*ligV* and *ligM*) could perform cellular transport and catabolism of vanillin into protocatechuate, respectively (**Figure 2**). Identified vanillin membrane transporter (VanK) was found to be a member of the aromatic acid/H + symport family MFS transporter involved in the transport of aromatic compounds across cytoplasmic membranes (Chaudhry et al., 2007). The *lig* operon genes *ligV*, and *ligM* encode putative vanillin

TABLE 1 | Human gut microbiome protein features mapped for vanillin catabolism.

Vanillin metabolism	Protein features	Representative features
Phase I	Vanillin dehydrogenase, LigV (EC 1.2.1.65)	4
(Vanillin biotransformation)	Vannilate transporter, VanK	5
	Vanillate O-demethylase, LigM (EC 1.14.13.82)	21
Phase II	Protocatechuate 3,4-dioxygenase alpha chain, PcaG (EC 1.13.11.3)	4
(Ring fission)	Protocatechuate 3,4-dioxygenase beta chain, PcaH (EC 1.13.11.3)	12
	3-carboxy-cis,cis-muconate cycloisomerase, PcaB (EC 5.5.1.2)	11
	4-carboxymuconolactone decarboxylase, PcaC (EC 4.1.1.44)	553
	Beta-ketoadipate enol-lactone hydrolase, PcaD (EC 3.1.1.24) or 3-oxoadipate enol-lactonase, PcaD (EC 3.1.1.24)	2
	3-oxoadipate CoA-transferase subunit A, Pcal (EC 2.8.3.6)	7
	3-oxoadipate CoA-transferase subunit B, PcaJ (EC 2.8.3.6)	1
	Beta-ketoadipyl CoA thiolase, PcaF (EC 2.3.1.16)	5
	Pca operon regulatory protein, PcaR	19
	Succinyl-CoA:3-ketoacid-coenzyme A transferase subunit A, ScoA (EC 2.8.3.5)	2
	4-hydroxybenzoate transporter, PcaK	15
	Catechol 1,2-dioxygenase, CatA (EC 1.13.11.1)	7
	Muconate cycloisomerase, CatB (EC 5.5.1.1)	13
	Muconolactone isomerase, CatC (EC 5.3.3.4)	1

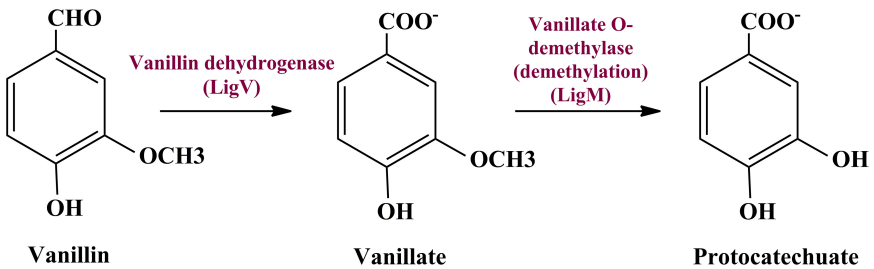

FIGURE 2 | The delineated phase I of the vanillin catabolic pathway. Vanillin dehydrogenase (VanD) and vanillate O-demethylase (VanM) metabolize vanillin into protocatechuate.

dehydrogenase (LigV) and putative vanillin-O-demethylase (LigM). Homologs of these proteins catalyze the conservation of vanillin to vanillic acid and vanillic acid to protocatechuate (Chen et al., 2012). Putative vanillin dehydrogenase (LigV) sequence was found to harbor a ALDH_VaniDH_like (*Pseudomonas putida* vanillin dehydrogenase-like) conserved domain (cd07150) characterized for $NAD(P)^+$-dependent dehydrogenase activity against vanillin. Additionally, putative LigV features shared a good homology of (65–90%) with their characterized homolog of *Pseudomonas putida* KT2440 indicating its activity as a vanillin dehydrogenase. The sequences of putative LigM were found to possess START/RHO_alpha_C/PITP/Bet_v1/CoxG/CalC (SRPBCC) ligand-binding domain. The SRPBCC domain was characterized by Rieske-type non-heme iron aromatic ring-hydroxylating oxygenases. Additionally, putative LigM shared a very good homology of 98 and 96% with vanillin-O-demethylase of *Enterobacter hormaechei* and *Klebsiella pneumonia* respectively. Presence of a domain for Rieske-type non-heme iron aromatic ring-hydroxylating oxygenases, and high identity with vanillin-O-demethylase indicates its potential activity as vanillin-O-demethylase to convert vanillic acid into protocatechuate. Phylogenetic characterization indicates that the VanK, LigV, and LigM shared homology with the proteins belonging to the *Azotobacter vinelandii*, *Azoarcus* sp., *Enterobacter hormaechei, Klebsiella pneumonia, Pseudomonas putida*, *Rhodopseudomonas palustris*, and *Serratia proteamaculans* indicating their origin from the proteobacterial clade.

Metagenomic exploration identifies genes associated with the catechol branch of the beta-ketoadipate pathway and the protocatechuate branch of the beta-ketoadipate pathway (**Table 1**). The *pcaIJFBDKCHG* operon is well-established as genetic machinery to catabolize protocatechuate to TCA cycle intermediates through the beta-ketoadipate pathway (Gerischer et al., 1998). Manual curation of the current metagenomics dataset indicates several genes sharing homology with *pcaB*, *pcaC*, *pcaD*, *pcaG/H, pcaI, pcaJ, pcaK, pcaF*, and *pcaR* (**Table 1**). Encoded proteins of these genes systematically catabolize protocatechuate into succinate and acetyl CoA (**Figure 3**). These putative proteins share homology with the proteins associated with Proteobacteria, Firmicutes, and FCB group microbes (*Acidovorax* sp., *Bacteroides*

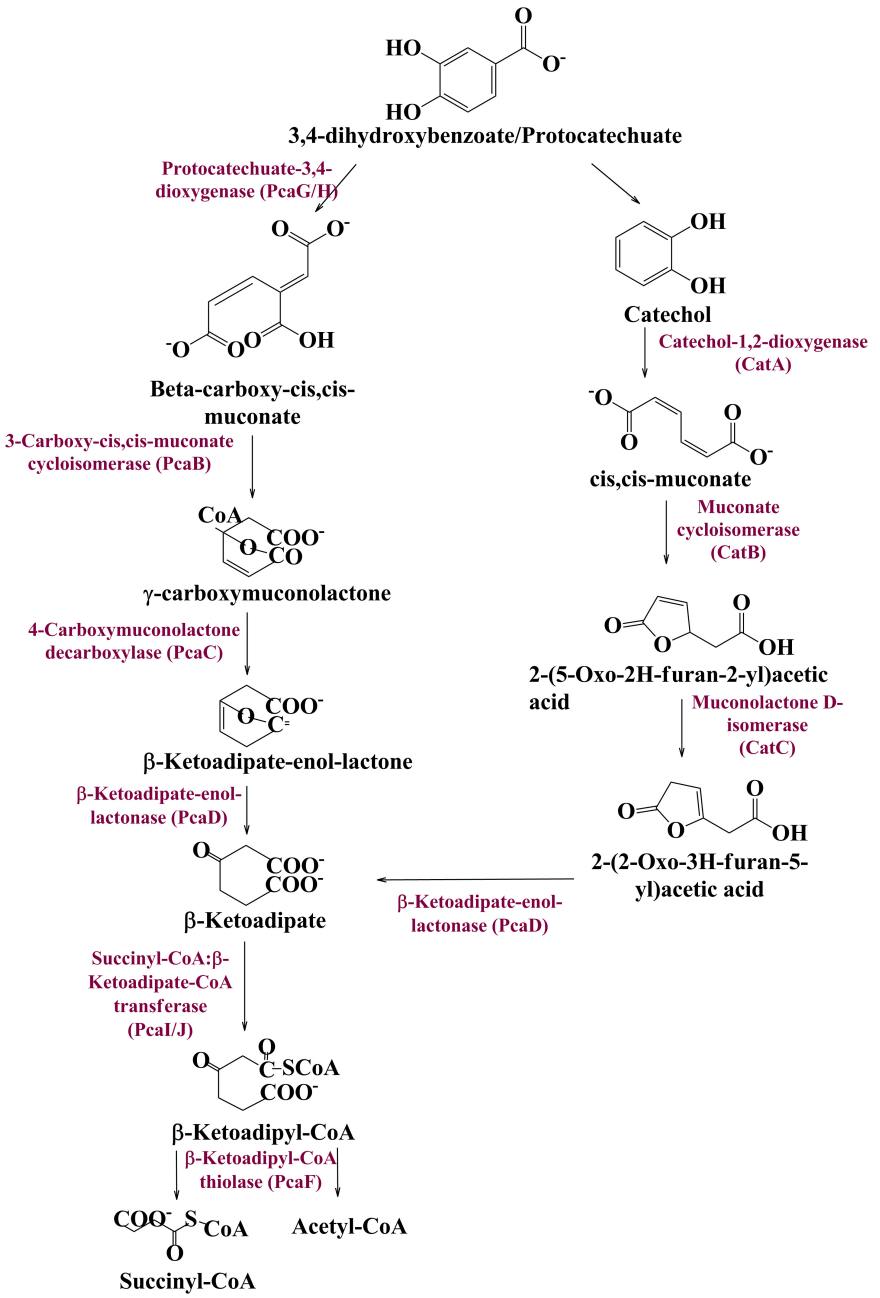

FIGURE 3 | The delineated phase II of the vanillin catabolic pathway. Protocatechuate could be metabolized either directly into TCA cycle intermediates or through catechol mediated ortho ring cleavage.

fragilis, *Dethiosulfovibrio peptidovorans*, *Eggerthella lenta*, *Escherichia coli, Eubacterium rectale*, *Klebsiella pneumoniae, Lactobacillus acidophilus*, *Lactobacillus brevis*, *Lactobacillus gasseri*, *Lactobacillus reuteri*, *Leuconostoc mesenteroides*, *Methanosarcina barkeri*, *Marinomonas*, *Pediococcus pentosaceus*, *Pseudomonas syringae*, *Rhodospirillum centenum*, *Ruegeria pomeroyi*, and *Streptococcus mutans*).

Catechol mediated protocatechuate metabolism is an alternative catabolic pathway (Grant and Patel, 1969), catabolized by Catechol-1,2-dioxygenase, Muconate cycloisomerase, and Muconolactone D-Isomerase (**Figure 3**) encoded by *catA*, *catB*, and *catC* genes of cat operon, respectively. In-depth human gut metagenome analysis showed several protein features homologous to the CatA, CatB, and CatC proteins (**Table 1**). Human gut metagenomic putative Catechol 1,2-dioxygenase (*catA*) were found phylogenetically affiliated with proteins of the *Klebsiella pneumoniae*, while the putative Muconate cycloisomerase (*catB*) shared homology with the

proteins of *Bacteroides vulgatus, Dokdonia donghaensis*, and *Clostridium difficile* origin. Muconolactone isomerase (*catC*) shared homology with Crenarchaeota (*Sulfolobus tokodaii*) originated proteins.

Contrary to the vanillin catabolic gene clusters, *pca*, and *cat* operon encoded proteins shared homology with diversified microbial groups (**Figure 4**). These observations indicate that vanillin metabolism might be either carried out in a synergistic way or there is a division of labor where only one microbial group is assigned to do this job.

Comparative Metagenomic Analysis

Current human gut metagenomic datasets were compared with other gut metagenome datasets (**Supplementary Table S1**) to assess its similarity and uniqueness. Selected gut metagenomic datasets represented the individual of diverse geographical locations (United States, Sweden, Venezuela, Japan, and Malaysia), varied age group (infants, children, teenagers, and adults) (Yatsunenko et al., 2012), gender (male and female). Presence of vanillin catabolic features among this varied representation would confirm their omnipresence.

Ribosomal features of the current metagenomic dataset showed a good correlation with ribosomal features identified in other metagenomic datasets at the domain level ($R > 0.99$), however, it is drastically reduced at lower taxonomic levels (**Supplementary Table S5**). Principal component analysis (PCA) indicates a clustering of the current metagenomic dataset with the metagenomic dataset of Japan and Venezuela at the domain level (**Supplementary Figure S2A**); however, no clustering was observed at other taxonomic analysis (**Supplementary Figures S2B,C**). Heatmap indicates variable clustering of the current metagenomic dataset with a metagenomic dataset at different taxonomic levels (**Supplementary Figure S3**). These results cumulatively indicate that the gut metagenomic datasets are comparatively similar at a higher taxonomic level; however, phylogenetic variability enhances at lower taxonomic levels.

COGs analysis of the metabolic features showed a very good correlation at level 1 ($R > 0.99$) and level 2 ($R > 0.96$, $R > 0.98$, $R > 0.95$, $R > 0.9606$, $R > 0.98$, and $R > 0.95$) of COG classification with the features identified in various metagenomic datasets (Malawi, Japan, Europe, United States, and Venezuela, respectively). However, a lower correlation ($R = 0.45$) was observed with Malaysian population gut metagenomic dataset at level 2 of COG classification. Principal component analysis (PCA) also makes a similar observation (**Figure 5A**). Heatmap of the subsystem database identified protein features showed clustering of the current metagenomic datasets with Malawi, Japan, Europe, United States, Venezuela in a group, while Malaysian metagenome was in the distant group (**Figure 5B**). Comparative functional profiling of metagenomic datasets indicates that despite taxonomic diversity, all the metagenomic dataset harbors similar functional profile.

Explorations of the metagenomic datasets for vanillin catabolic features indicate their omnipresence with differential abundance profile (**Supplementary Table S6**). Principal component analysis (PCA) and heatmap indicated clustering of Japan (MGP4778) and United States metagenomes with the current dataset (**Figure 6**). The omnipresence of vanillin catabolic features indicates the metabolic potential of the gut microbiome. However, their functioning needs to be assessed through functional assays.

Validation of Vanillin Catabolism

Metabolomics profiling identified several metabolites associated with vanillin metabolism (**Table 2**). Significantly enriched metabolites were mapped to the proposed metabolic pathway confirming the functionality of the proposed vanillin metabolic pathway. LC-MS spectra analysis indicates that the vanillin was completely metabolized by human gut microbes within 24 h of incubation (**Supplementary Figure S4**). The disappearance of vanillin was negatively correlated with the appearance of the Protocatechuate ($r = -0.987$), Catechol ($r = -0.978$). These results established the protocatechuate and catechol-mediated vanillin catabolism among human gut microbes.

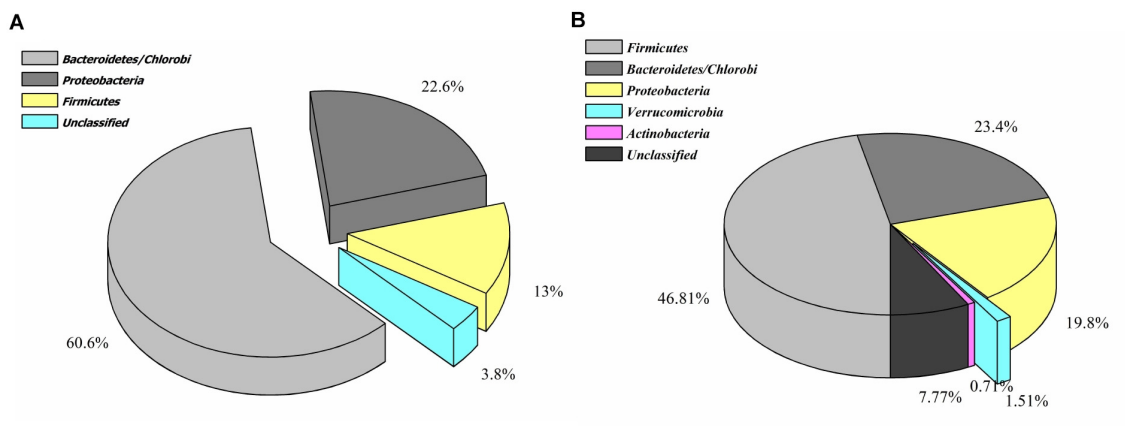

FIGURE 4 | Phylogenetic affiliation of the features associated with catechol **(A)** and protocatechuate **(B)** catabolism.

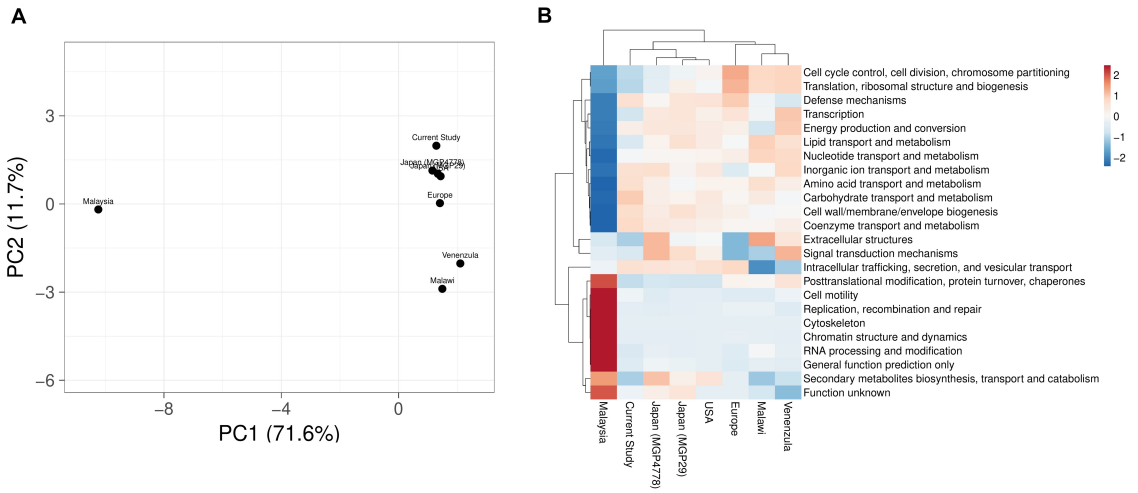

FIGURE 5 | A comparison of the metabolic potential of the gut metagenomes across diversified populations. Principle component analysis **(A)** and heatmap **(B)** showing the relationship among various gut metagenomes.

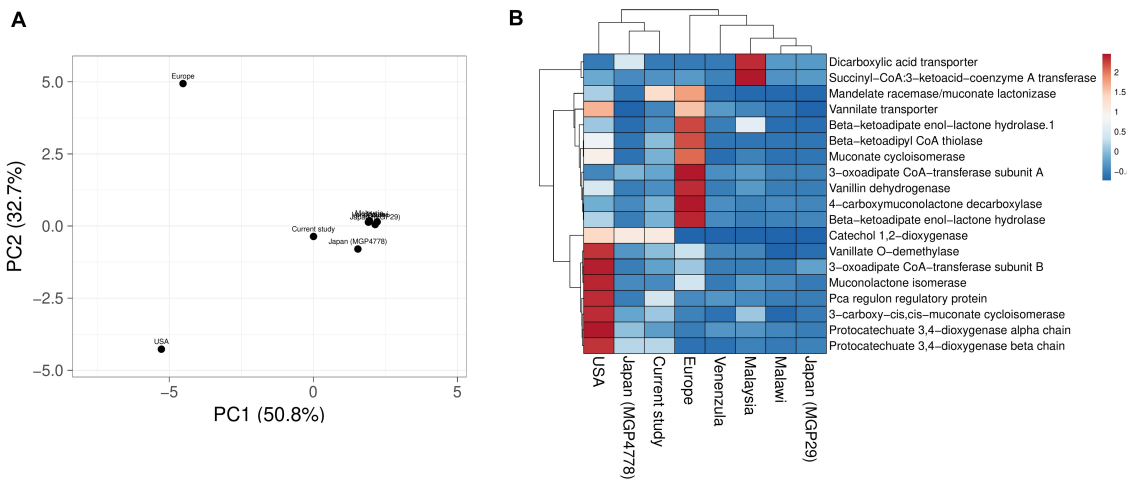

FIGURE 6 | Vanillin catabolic features across various gut metagenomes. Principal component analysis **(A)** and heatmap **(B)** showing the relationship among various gut metagenomes.

DISCUSSION

The human microbiome is a specialized dynamic organ that plays a vital role in the maintenance of host physiology. The human gut microbiome complements with host machinery to metabolize a wide range of ingested foods (Yadav et al., 2018). Along with improving the metabolic capacity of the host, the gut microbes play a significant role in drug detoxification (Jourova et al., 2016) and xenobiotic metabolism (Clarke et al., 2019). Vanillin, a commonly used major food additive, possesses antimicrobial, antioxidative, and flavoring properties (Fitzgerald et al., 2004; Ngarmsak et al., 2006). Metabolism of vanillin was delineated in the human body (Muskiet and Groen, 1979) where the liver metabolized it as vanillic acid and finally it was excreted as a free metabolite or in conjugate form through the urogenital system (Sayavongsa et al., 2007). Though the human gut microbiome plays a key metabolic component in food digestion, the role of the human gut microbiome in vanillin metabolism has never been studied. Additionally, there is a lack of information about microbial survival strategies toward antimicrobial properties of vanillin. The present study encompasses an integrative approach wherein the human gut microbiome has been shown to delineate the process of vanillin catabolism to counter its antimicrobial properties.

The studied human gut microbiome is primarily composed of Bacteroidetes, Firmicutes, and Proteobacteria, while Actinobacteria and other microbial groups contribute less to the total gut bacterial diversity. Efforts to analyze the human gut microbial diversity in a similar population also revealed the matching outcome wherein Bacteroidetes is the predominant

TABLE 2 | List of statistically significant ($p < 0.05$) metabolites associated with vanillin metabolism from the microbial pellet incubated with 5 mM vanillin at 37°C for 24 h.

Metabolite	Rf value	m/z value	*p*-value
Protocatechuate	6.26	153.019	0.0315
Catechol	6.26	109.030	0.0470
Beta-carboxy-cis,cis-muconate	6.38	181.986	0.0001
Beta-ketoadipate	16.68	159.030	0.0339

bacteria within the human gut (Human Microbiome Project Consortium, 2012; MetaHIT Consortium (additional members) et al., 2011). Additionally, *Prevotella* is the predominant microbial group within the Bacteroidetes and *Ruminococcaceae* and *Lachnospiraceae* among Firmicutes. These observations are in line with human gut microbial diversity studies highlighted by our group (Chauhan et al., 2018), as well as by other studies in Indian populations (Bhute et al., 2016). SSU rRNA gene amplification followed by their sequencing could introduce biases during the exploration of microbial diversity (Poussin et al., 2018). Hereby, the current study also assesses the microbial diversity through shotgun sequenced datasets that are considered more precise and accurate approach (Ranjan et al., 2016). The metagenomic diversity revealed through RNA and protein feature analysis indicated the abundance of Bacteroidetes followed by Firmicutes and Proteobacteria along with traces of archaea, viruses, fungi, and higher eukaryotes. These observations are in line with human gut microbial profiles generated from various global populations in the current study, as well as in other studies (MetaHIT Consortium (additional members) et al., 2011). Despite it, variability in microbial taxonomic distribution and abundance profile was observed across various populations. These variations could be attributed to diverse food habits, ethnicity, and lifestyle (Chauhan et al., 2018). Functional annotation of human gut metagenomic protein features shows an enrichment of the carbohydrate metabolism associated protein features. Harvesting energy from non-conventional carbohydrates might be allowing the human gut microbes to avoid any conflict with the host to meet their energy requirement (Flint et al., 2012). These interactions might be playing an active role in developing commensalism with the host toward the successful commensalism of the human gut microbiome (Kumar Mondal et al., 2017). In addition to the CAzyme associated protein features, a diverse array of the proteins associated with microbial growth and sustenance were identified (Kurokawa et al., 2007). This variability could be explained in terms of their evolutionary adaptations to meet up environmental requirements (Bradley and Pollard, 2017).

Protein features potentially associated with the vanillin metabolism were identified from the human gut metagenome dataset. Protein features like membrane-bound vanillin transport systems (VanK), vanillin dehydrogenase (ligV), and vanillin-O-demethylase (ligM) indicate the cellular process of vanillin metabolism in the human gut microbes. As characterized in *Acinetobacter* sp., VanK feature might be allowing the human gut microbes for the cellular transport of vanillin and Protocatechuate (D'Argenio et al., 1999). Similarly, ligV and ligM as characterized in *Sphingomonas paucimobilis* SYK-6, *Pseudomonas putida* (Abe et al., 2005; Masai et al., 2007) indicate vanillin catabolism into protocatechuate. The current metagenomic dataset also represents the presence of almost all genes associated with *pca* operon. These gene clusters were characterized for protocatechuate metabolism to TCA cycle intermediates through the beta-ketoadipate pathway in the free-living microbes (Iwagami et al., 2000). Similarly, cat operon genes *catA* (Catechol-1,2-dioxygenase), *catB* (Muconate cycloisomerase), and *catC* (Muconolactone-D-isomerase) have been characterized in free-living microbes for catabolizing catechol through the beta-ketoadipate intermediate of the central aromatic intermediate metabolic pathway (Cámara et al., 2007). Metabolic mapping of all these human gut microbiome protein features indicates a probable pathway for vanillin metabolism.

Presences of the vanillin catabolic features across diverse populations with varied age, sex, and geography indicates their omnipresence. The gut metagenome of Europe, United States, Venezuela and Malaysian population showed a relative higher enrichment of vanillin specific (Phase I) catabolic features in comparison to Japan and Malawi population. This varied enrichment of vanillin catabolic features could be an outcome of differential exposure to the vanillin supplemented foods; however the lack of vanillin consumption dataset across the global population limits the validation of this hypothesis.

However, the presence of genetic features does not confirm their functioning (Langille, 2018), hereby a translation approach needs to be implemented to confirm their function in the gut microbes (Zhang et al., 2019). Metabolomics approach was used for validating the functioning of vanillin catabolic features. It has shown statistical enrichment of metabolites associated with the proposed pathway. Additionally, a reciprocal relationship among the disappearance of vanillin with enrichment of protocatechuate and catechol also confirms the vanillin protocatechuate-mediated vanillin metabolism.

Phylogenetic affiliation analysis of protein features indicates that the vanillin specific catabolic features were selectively enriched in gammaproteobacteria group microbes, while protein features associated with protocatechuate metabolism showed omnipresence in the human gut microbial groups belonging to Firmicutes, Bacteroidetes, Proteobacteria, and Actinobacteria. This segregated distribution indicates either vanillin catabolism is the only function in proteobacteria microbial groups or there is a division of labor as well as stratified functioning in the gut ecosystem (Sichertz, 2011). Additionally, the majority of these identified genetic features shared homology with genetic features of the free-living microbes (Kumar Mondal et al., 2017). It indicates a possible transfer of the genes in the human gut microbiome through horizontal gene transfer for a better adaptation within the human gut environment (Lerner et al., 2017).

Though the current study helps to explain the mechanism of vanillin catabolism, it raises the scientific query as to whether the host microbiome is already enriched with such metabolic

machinery or exposure of these xenobiotics has modulated the human gut microbes to evolve (Maurice et al., 2013). Progressive evolution is a prominent feature of the microbes, which allows them to adapt and colonize in extreme environments (Li et al., 2014). It strongly favors the possibility that the continuous exposure of a xenobiotic has put an evolutionary pressure on the human gut microbes to enrich their genetic machinery to either protect from their antimicrobial nature (Sarmiento et al., 2019) or to harness energy from it (Dantas et al., 2008).

The current study is the first study to catalog human gut microbial gene clusters and the protein features involved in vanillin catabolism. Additionally, the current study has used the strength of multi-omics approach to rationalize the role of human gut microbiome composition in vanillin catabolism. This study strengthens the hypothesis of gut microbiome evolution with respect to dietary composition, as well as explains how microbes accustom to the changing gut environment for successful colonization.

DATA AVAILABILITY STATEMENT

Metagenomic DNA sequences can be found in MG-RAST server with "ab6d97f3c66d676d343633383135322e33id and 9a02e1b94c6d676d343633383135332e33" (https://www.mg-rast.org/mgmain.html?mgpage=token&token=aujodAvGtxRPyZ11oYYVeBW4Zno1J0LQuAT66Q6XSCWmKTBtow).

ETHICS STATEMENT

The studies involving human participants were reviewed and approved by the M. D. University, Rohtak, Haryana, India. The patients/participants provided their written informed consent to participate in this study.

AUTHOR CONTRIBUTIONS

NC designed the study and experiments and analyzed the data. NC, MY, and RP wrote the manuscript. MY carried out the experiments. All authors edited the manuscript and approved the final draft of the manuscript.

FUNDING

MY was thankful to the University Grants Commission for Junior Research Fellowship. The authors would like to thank MDU RKF Fund minor research project (Sanctioned amount: Rs. 50,000).

ACKNOWLEDGMENTS

We acknowledge Mitali Mukerji, CSIR-IGIB, New Delhi, India for DNA sequencing and Seema Kapoor, Maulana Azad Medical College, New Delhi, India for LC-MS analysis.

SUPPLEMENTARY MATERIAL

The Supplementary Material for this article can be found online at: https://www.frontiersin.org/articles/10.3389/fmicb.2020.588545/full#supplementary-material

Supplementary Figure 1 | Phylogenetic affiliation of SSU rRNA sequences derived from human feces metagenomic DNA. Taxonomic of SSU rRNA sequences affiliated with Bacteroidetes **(A)** and Firmicutes **(B)**.

Supplementary Figure 2 | Principle component analysis plots at different taxonomic levels [domain **(A)**, phylum **(B)**, and class **(C)** taxonomic levels].

Supplementary Figure 3 | Heatmap showing correlation of representative ribosomal features among metagenomic datasets at different taxonomic levels [domain **(A)**, phylum **(B)**, and class **(C)** taxonomic levels].

Supplementary Figure 4 | The functional assessment of vanillin catabolism using LC-MS analysis.

Supplementary Table 1 | Human gut metagenome datasets used for comparative analysis.

Supplementary Table 2 | Statistics of the current human gut metagenome dataset.

Supplementary Table 3 | Relative abundance of the sodium benzoate catabolic features across various gut metagenomes.

Supplementary Table 4 | Abundance profile of the Cluster of orthologous groups (COGs) identified in current metagenomic datasets.

Supplementary Table 5 | Correlation among the ribosomal features of the current metagenomic dataset with other datasets at different taxonomic levels.

Supplementary Table 6 | Abundance profile of vanillin catabolic features across gut metagenome datasets.

Supplementary Method 1 | Sample processing and chromatographic separation.

Supplementary Method 2 | Mass spectrometric detection of metabolites.

REFERENCES

Abe, T., Masai, E., Miyauchi, K., Katayama, Y., and Fukuda, M. (2005). A Tetrahydrofolate-dependent O-demethylase, LigM, is crucial for catabolism of vanillate and syringate in sphingomonas paucimobilis SYK-6. *JB* 187, 2030–2037. doi: 10.1128/JB.187.6.2030-2037.2005

Bhute, S., Pande, P., Shetty, S. A., Shelar, R., Mane, S., Kumbhare, S. V., et al. (2016). Molecular characterization and meta-analysis of gut microbial communities illustrate enrichment of prevotella and *Megasphaera* in Indian subjects. *Front. Microbiol.* 7:660. doi: 10.3389/fmicb.2016.00660

Bradley, P. H., and Pollard, K. S. (2017). *Proteobacteria* drive significant functional variability in the human gut microbiome. *Microbiome* 5:36. doi: 10.1186/s40168-017-0244-z

Cámara, B., Bielecki, P., Kaminski, F., dos Santos, V. M., Plumeier, I., Nikodem, P., et al. (2007). A gene cluster involved in degradation of substituted salicylates via ortho cleavage in *Pseudomonas* sp. strain MT1 encodes enzymes specifically adapted for transformation of 4-methylcatechol and 3-methylmuconate. *J. Bacteriol.* 189, 1664–1674. doi: 10.1128/JB.01192-06

Chaudhry, M. T., Huang, Y., Shen, X.-H., Poetsch, A., Jiang, C.-Y., and Liu, S.-J. (2007). Genome-wide investigation of aromatic acid transporters in

Corynebacterium glutamicum. *Microbiology* 153, 857–865. doi: 10.1099/mic.0.2006/002501-0

Chauhan, N. S., Pandey, R., Mondal, A. K., Gupta, S., Verma, M. K., Jain, S., et al. (2018). Western indian rural gut microbial diversity in extreme prakriti endophenotypes reveals signature microbes. *Front. Microbiol.* 9:118. doi: 10.3389/fmicb.2018.00118

Chen, H.-P., Chow, M., Liu, C.-C., Lau, A., Liu, J., and Eltis, L. D. (2012). Vanillin catabolism in *Rhodococcus jostii* RHA1. *Appl. Environ. Microbiol.* 78, 586–588. doi: 10.1128/AEM.06876-11

Chen, P., Yan, L., Wu, Z., Li, S., Bai, Z., Yan, X., et al. (2016). A microbial transformation using *Bacillus subtilis* B7-S to produce natural vanillin from ferulic acid. *Sci. Rep.* 6:20400. doi: 10.1038/srep20400

Clarke, G., Sandhu, K. V., Griffin, B. T., Dinan, T. G., Cryan, J. F., and Hyland, N. P. (2019). Gut Reactions: breaking down xenobiotic–microbiome interactions. *Pharmacol. Rev.* 71, 198–224. doi: 10.1124/pr.118.015768

Dantas, G., Sommer, M. O. A., Oluwasegun, R. D., and Church, G. M. (2008). Bacteria subsisting on antibiotics. *Science* 320, 100–103. doi: 10.1126/science.1155157

D'Argenio, D. A., Segura, A., Coco, W. M., Bünz, P. V., and Ornston, L. N. (1999). The physiological contribution of Acinetobacter PcaK, a transport system that acts upon protocatechuate, can be masked by the overlapping specificity of VanK. *J. Bacteriol.* 181, 3505–3515. doi: 10.1128/jb.181.11.3505-3515.1999

Durant, S., and Karran, P. (2003). Vanillins – A novel family of DNA-PK inhibitors. *Nucleic Acids Res.* 31, 5501–5512. doi: 10.1093/nar/gkg753

Endo, A., Nakamura, T., and Shima, J. (2009). Involvement of ergosterol in tolerance to vanillin, a potential inhibitor of bioethanol fermentation, in *Saccharomyces cerevisiae*. *FEMS Microbiol. Lett.* 299, 95–99. doi: 10.1111/j.1574-6968.2009.01733.x

Fitzgerald, D. J., Stratford, M., Gasson, M. J., Ueckert, J., Bos, A., and Narbad, A. (2004). Mode of antimicrobial action of vanillin against *Escherichia coli*, *Lactobacillus plantarum* and *Listeria innocua*. *J. Appl. Microbiol.* 97, 104–113. doi: 10.1111/j.1365-2672.2004.02275.x

Flint, H. J., Scott, K. P., Duncan, S. H., Louis, P., and Forano, E. (2012). Microbial degradation of complex carbohydrates in the gut. *Gut Microbes* 3, 289–306. doi: 10.4161/gmic.19897

Furuya, T., Miura, M., Kuroiwa, M., and Kino, K. (2015). High-yield production of vanillin from ferulic acid by a coenzyme-independent decarboxylase/oxygenase two-stage process. *New Biotechnol.* 32, 335–339. doi: 10.1016/j.nbt.2015.03.002

Gerischer, U., Segura, A., and Ornston, L. N. (1998). PcaU, a transcriptional activator of genes for protocatechuate utilization in Acinetobacter. *J. Bacteriol.* 180, 1512–1524. doi: 10.1128/jb.180.6.1512-1524.1998

Grant, D. J. W., and Patel, J. C. (1969). The non-oxidative decarboxylation ofp-hydroxybenzoic acid, gentisic acid, protocatechuic acid and gallic acid byKlebsiella aerogenes (Aerobacter aerogenes). *Antonie Van Leeuwenhoek* 35, 325–343. doi: 10.1007/BF02219153

Guo, J., Han, X., Zhan, J., You, Y., and Huang, W. (2018). Vanillin alleviates high fat diet-induced obesity and improves the gut microbiota composition. *Front. Microbiol.* 9:2733. doi: 10.3389/fmicb.2018.02733

Gupta, S., Kumar, M., Kumar, J., Ahmad, V., Pandey, R., and Chauhan, N. S. (2017). Systemic analysis of soil microbiome deciphers anthropogenic influence on soil ecology and ecosystem functioning. *Int. J. Environ. Sci. Technol.* 14, 2229–2238. doi: 10.1007/s13762-017-1301-7

Hooper, L. V. (2001). Commensal host-bacterial relationships in the gut. *Science* 292, 1115–1118. doi: 10.1126/science.1058709

Human Microbiome Project Consortium (2012). Structure, function and diversity of the healthy human microbiome. *Nature* 486, 207–214. doi: 10.1038/nature11234

Iwagami, S. G., Yang, K., and Davies, J. (2000). Characterization of the protocatechuic acid catabolic gene cluster from Streptomyces sp. strain 2065. *Appl. Environ. Microbiol.* 66, 1499–1508. doi: 10.1128/aem.66.4.1499-1508.2000

Jourova, L., Anzenbacher, P., and Anzenbacherova, E. (2016). Human gut microbiota plays a role in the metabolism of drugs. *Biomed. Pap. Med. Fac. Univ. Palacky Olomouc Czech. Repub.* 160, 317–326. doi: 10.5507/bp.2016.039

Kamimura, N., Takahashi, K., Mori, K., Araki, T., Fujita, M., Higuchi, Y., et al. (2017). Bacterial catabolism of lignin-derived aromatics: new findings in a recent decade: update on bacterial lignin catabolism: bacterial catabolism of lignin-derived aromatics. *Environ. Microbiol. Rep.* 9, 679–705. doi: 10.1111/1758-2229.12597

Kapono, C. A., Morton, J. T., Bouslimani, A., Melnik, A. V., Orlinsky, K., Knaan, T. L., et al. (2018). Creating a 3D microbial and chemical snapshot of a human habitat. *Sci. Rep.* 8:3669. doi: 10.1038/s41598-018-21541-4

Kent, W. J. (2002). BLAT—The BLAST-like alignment tool. *Genome Res.* 12, 656–664. doi: 10.1101/gr.229202

Koch, C. M., Chiu, S. F., Akbarpour, M., Bharat, A., Ridge, K. M., Bartom, E. T., et al. (2018). A Beginner's guide to analysis of RNA sequencing data. *Am. J. Respir. Cell Mol. Biol.* 59, 145–157. doi: 10.1165/rcmb.2017-0430TR

Kumar, J., Kumar, M., Gupta, S., Ahmed, V., Bhambi, M., Pandey, R., et al. (2016). An improved methodology to overcome key issues in human fecal metagenomic DNA extraction. *Genom. Proteom. Bioinform.* 14, 371–378. doi: 10.1016/j.gpb.2016.06.002

Kumar Mondal, A., Kumar, J., Pandey, R., Gupta, S., Kumar, M., Bansal, G., et al. (2017). Comparative genomics of host–symbiont and free-living oceanobacillus species. *Genome Biol. Evol.* 9, 1175–1182. doi: 10.1093/gbe/evx076

Kurokawa, K., Itoh, T., Kuwahara, T., Oshima, K., Toh, H., Toyoda, A., et al. (2007). Comparative metagenomics revealed commonly enriched gene sets in human gut microbiomes. *DNA Res.* 14, 169–181. doi: 10.1093/dnares/dsm018

Langille, M. G. I. (2018). Exploring linkages between taxonomic and functional profiles of the human microbiome. *mSystems* 3:e00163-17. doi: 10.1128/mSystems.00163-17

Lerner, A., Matthias, T., and Aminov, R. (2017). Potential effects of horizontal gene exchange in the human gut. *Front. Immunol.* 8:1630. doi: 10.3389/fimmu.2017.01630

Li, S.-J., Hua, Z.-S., Huang, L.-N., Li, J., Shi, S.-H., Chen, L.-X., et al. (2014). Microbial communities evolve faster in extreme environments. *Sci. Rep.* 4:6205. doi: 10.1038/srep06205

Masai, E., Yamamoto, Y., Inoue, T., Takamura, K., Hara, H., Kasai, D., et al. (2007). Characterization of *ligV* essential for catabolism of vanillin by *Sphingomonas paucimobilis* SYK-6. *Biosci. Biotechnol. Biochem.* 71, 2487–2492. doi: 10.1271/bbb.70267

Maurice, C. F., Haiser, H. J., and Turnbaugh, P. J. (2013). Xenobiotics shape the physiology and gene expression of the active human gut microbiome. *Cell* 152, 39–50. doi: 10.1016/j.cell.2012.10.052

Menon, S., and Nayeem, N. (2013). *Vanilla planifolia*: a review of a plant commonly used as flavouring agent. *Int. J. Pharm. Sci. Rev. Res.* 20, 225–228.

Menzel, P., Ng, K. L., and Krogh, A. (2016). Fast and sensitive taxonomic classification for metagenomics with Kaiju. *Nat. Commun.* 7:11257. doi: 10.1038/ncomms11257

MetaHIT Consortium (additional members), Arumugam, M., Raes, J., Pelletier, E., Le Paslier, D., Yamada, T., et al. (2011). Enterotypes of the human gut microbiome. *Nature* 473, 174–180. doi: 10.1038/nature09944

Meyer, F., Paarmann, D., D'Souza, M., Olson, R., Glass, E. M., Kubal, M., et al. (2008). The metagenomics RAST server – a public resource for the automatic phylogenetic and functional analysis of metagenomes. *BMC Bioinformatics* 9:386. doi: 10.1186/1471-2105-9-386

Milanese, A., Mende, D. R., Paoli, L., Salazar, G., Ruscheweyh, H.-J., Cuenca, M., et al. (2019). Microbial abundance, activity and population genomic profiling with mOTUs2. *Nat. Commun.* 10:1014. doi: 10.1038/s41467-019-08844-4

Morowitz, M. J., Denef, V. J., Costello, E. K., Thomas, B. C., Poroyko, V., Relman, D. A., et al. (2011). Strain-resolved community genomic analysis of gut microbial colonization in a premature infant. *Proc. Natl. Acad. Sci. U.S.A.* 108, 1128–1133. doi: 10.1073/pnas.1010992108

Muskiet, F. A., and Groen, A. (1979). Urinary excretion of conjugated homovanillic acid, 3,4-dihydroxyphenylacetic acid, p-hydroxyphenylacetic acid, and vanillic acid by persons on their usual diet and patients with neuroblastoma. *Clin. Chem.* 25, 1281–1284. doi: 10.1093/clinchem/25.7.1281

Ngarmsak, M., Delaquis, P., Toivonen, P., Ngarmsak, T., Ooraikul, B., and Mazza, G. (2006). Antimicrobial activity of vanillin against spoilage microorganisms in stored fresh-cut mangoes. *J. Food Prot.* 69, 1724–1727. doi: 10.4315/0362-028x-69.7.1724

Nishimura, M., Kawakami, S., and Otsuka, H. (2018). Molecular cloning and characterization of vanillin dehydrogenase from *Streptomyces* sp. NL15-2K. *BMC Microbiol.* 18, 154. doi: 10.1186/s12866-018-1309-2

O'Leary, N. A., Wright, M. W., Brister, J. R., Ciufo, S., Haddad, D., McVeigh, R., et al. (2016). Reference sequence (RefSeq) database at NCBI: current status, taxonomic expansion, and functional annotation. *Nucleic Acids Res.* 44, D733–D745. doi: 10.1093/nar/gkv1189

Oliphant, K., and Allen-Vercoe, E. (2019). Macronutrient metabolism by the human gut microbiome: major fermentation by-products and their impact on host health. *Microbiome* 7:91. doi: 10.1186/s40168-019-0704-8

Overbeek, R. (2005). The subsystems approach to genome annotation and its use in the project to annotate 1000 genomes. *Nucleic Acids Res.* 33, 5691–5702. doi: 10.1093/nar/gki866

Parke, D. (1995). Supraoperonic clustering of pca genes for catabolism of the phenolic compound protocatechuate in *Agrobacterium tumefaciens*. *J. Bacteriol.* 177, 3808–3817. doi: 10.1128/JB.177.13.3808-3817.1995

Parker, A., Lawson, M. A. E., Vaux, L., and Pin, C. (2018). Host-microbe interaction in the gastrointestinal tract. *Environ. Microbiol.* 20, 2337–2353. doi: 10.1111/1462-2920.13926

Plaggenborg, R., Overhage, J., Steinbüchel, A., and Priefert, H. (2003). Functional analyses of genes involved in the metabolism of ferulic acid in *Pseudomonas* putida KT2440. *Appl. Microbiol. Biotechnol.* 61, 528–535. doi: 10.1007/s00253-003-1260-4

Poussin, C., Sierro, N., Boué, S., Battey, J., Scotti, E., Belcastro, V., et al. (2018). Interrogating the microbiome: experimental and computational considerations in support of study reproducibility. *Drug Discovery Today* 23, 1644–1657. doi: 10.1016/j.drudis.2018.06.005

Qin, J., Li, R., Raes, J., Arumugam, M., Burgdorf, K. S., Manichanh, C., et al. (2010). A human gut microbial gene catalogue established by metagenomic sequencing. *Nature* 464, 59–65. doi: 10.1038/nature08821

Ramachandra Rao, S., and Ravishankar, G. (2000). Vanilla flavour: production by conventional and biotechnological routes. *J. Sci. Food Agric.* 80, 289–304. doi: 10.1002/1097-0010(200002)80:3and<289::AID-JSFA543and<3.0.CO;2-2

Ranjan, R., Rani, A., Metwally, A., McGee, H. S., and Perkins, D. L. (2016). Analysis of the microbiome: advantages of whole genome shotgun versus 16S amplicon sequencing. *Biochem. Biophys. Res. Commun.* 469, 967–977. doi: 10.1016/j.bbrc.2015.12.083

Rho, M., Tang, H., and Ye, Y. (2010). FragGeneScan: predicting genes in short and error-prone reads. *Nucleic Acids Res.* 38:e191. doi: 10.1093/nar/gkq747

Romero-Steiner, S., Parales, R. E., Harwood, C. S., and Houghton, J. E. (1994). Characterization of the pcaR regulatory gene from *Pseudomonas* putida, which is required for the complete degradation of p-hydroxybenzoate. *J. Bacteriol.* 176, 5771–5779. doi: 10.1128/jb.176.18.5771-5779.1994

Sarmiento, M. R. A., de Paula, T. O., Borges, F. M., Ferreira-Machado, A. B., Resende, J. A., Moreira, A. P. B., et al. (2019). Obesity, xenobiotic intake and antimicrobial-resistance genes in the human gastrointestinal tract: a comparative study of eutrophic, overweight and obese individuals. *Genes (Basel)* 10:349. doi: 10.3390/genes10050349

Sayavongsa, P., Cooper, M. L., Jackson, E. M., Harris, L., Ziegler, T. R., and Hibbert, J. M. (2007). Vanillic acid excretion can be used to assess compliance with dietary supplements. *e-SPEN Eur. e-J. Clin. Nutr. Metab.* 2, e134–e137. doi: 10.1016/j.eclnm.2007.08.003

Shyamala, B. N., Naidu, M., Sulochanamma, G., and Srinivas, P. (2007). Studies on the antioxidant activities of natural vanilla extract and its constituent compounds through in vitro models. *J. Agr. Food. Chem.* 55, 7738–7743. doi: 10.1021/jf071349%2B

Sichertz, P T. (2011). Metatranscriptomics of the human gut microbiome. *Genome Biol.* 12:I15. doi: 10.1186/gb-2011-12-s1-i15

Sinha, A. K., Sharma, U. K., and Sharma, N. (2008). A comprehensive review on vanilla flavor: extraction, isolation and quantification of vanillin and other constituents. *Int. J. Food Sci. Nutr.* 59, 299–326. doi: 10.1080/09687630701539350

Tatusov, R. L. (2000). The COG database: a tool for genome-scale analysis of protein functions and evolution. *Nucleic Acids Res.* 28, 33–36. doi: 10.1093/nar/28.1.33

Tian, R.-M., Zhang, W., Cai, L., Wong, Y.-H., Ding, W., and Qian, P.-Y. (2017). Genome reduction and microbe-host interactions drive adaptation of a sulfur-oxidizing bacterium associated with a cold seep sponge. *mSystems* 2:e00184-16. doi: 10.1128/mSystems.00184-16

Vemuri, R., Gundamaraju, R., Shastri, M. D., Shukla, S. D., Kalpurath, K., Ball, M., et al. (2018). Gut Microbial changes, interactions, and their implications on human lifecycle: an ageing perspective. *BioMed Res. Int.* 2018, 1–13. doi: 10.1155/2018/4178607

Yadav, M., Verma, M. K., and Chauhan, N. S. (2018). A review of metabolic potential of human gut microbiome in human nutrition. *Arch. Microbiol.* 200, 203–217. doi: 10.1007/s00203-017-1459-x

Yan, X., Liu, D.-F., Zhang, X.-Y., Liu, D., Xu, S.-Y., Chen, G.-X., et al. (2017). Vanillin protects dopaminergic neurons against inflammation-mediated cell death by inhibiting ERK1/2, P38 and the NF-κB signaling pathway. *Int. J. Mol. Sci.* 18:389. doi: 10.3390/ijms18020389

Yatsunenko, T., Rey, F. E., Manary, M. J., Trehan, I., Dominguez-Bello, M. G., et al. (2012). Human gut microbiome viewed across age and geography. *Nature* 486, 222–227. doi: 10.1038/nature11053

Yu, C. L., Louie, T. M., Summers, R., Kale, Y., Gopishetty, S., and Subramanian, M. (2009). Two distinct pathways for metabolism of theophylline and caffeine are coexpressed in *Pseudomonas* putida CBB5. *JB* 191, 4624–4632. doi: 10.1128/JB.00409-09

Zhang, X., Li, L., Butcher, J., Stintzi, A., and Figeys, D. (2019). Advancing functional and translational microbiome research using meta-omics approaches. *Microbiome* 7:154. doi: 10.1186/s40168-019-0767-6

Zimmermann, M., Zimmermann-Kogadeeva, M., Wegmann, R., and Goodman, A. L. (2019). Mapping human microbiome drug metabolism by gut bacteria and their genes. *Nature* 570, 462–467. doi: 10.1038/s41586-019-1291-3

Conflict of Interest: The authors declare that the research was conducted in the absence of any commercial or financial relationships that could be construed as a potential conflict of interest.

frontiers in Microbiology

ORIGINAL RESEARCH
published: 20 November 2020
doi: 10.3389/fmicb.2020.590877

Effect of Menopausal Hormone Therapy on the Vaginal Microbiota and Genitourinary Syndrome of Menopause in Chinese Menopausal Women

*Lulu Geng†, Wenjun Huang†, Susu Jiang, Yanwei Zheng, Yibei Zhou, Yang Zhou, Jiangshan Hu, Ping Li and Minfang Tao**

Department of Gynaecology and Obstetrics, Shanghai Jiao Tong University Affiliated Sixth People's Hospital, Shanghai, China

OPEN ACCESS

Edited by:
Teresa Nogueira, Instituto Nacional Investigaciao Agraria e Veterinaria (INIAV), Portugal

Reviewed by:
Ana Cristina Ferreira, Instituto Nacional Investigaciao Agraria e Veterinaria (INIAV), Portugal
Jeremy Wilkinson, Harvard University, United States

***Correspondence:**
Minfang Tao
taomf@sjtu.edu.cn

† These authors have contributed equally to this work

Specialty section:
This article was submitted to Microbial Symbioses, a section of the journal Frontiers in Microbiology

Received: *03 August 2020*
Accepted: *28 October 2020*
Published: *20 November 2020*

Citation:
Geng L, Huang W, Jiang S, Zheng Y, Zhou Y, Zhou Y, Hu J, Li P and Tao M (2020) Effect of Menopausal Hormone Therapy on the Vaginal Microbiota and Genitourinary Syndrome of Menopause in Chinese Menopausal Women. Front. Microbiol. 11:590877. doi: 10.3389/fmicb.2020.590877

Genitourinary syndrome of menopause (GSM) is a chronic and progressive condition with a series of vulvovaginal, sexual, and lower urinary tract discomforts, mainly due to hypoestrogenism. Menopausal hormone therapy (MHT) has generally been considered as the most effective treatment for GSM. In addition, vaginal microbiota is of particular significance to gynecological and reproductive illnesses and potentially has some intimate connections with GSM. Consequently, we sought to evaluate how MHT impacts the composition and structure of vaginal microbiota while alleviating GSM in Chinese menopausal women aged 45–65 years, which has not been investigated previously. 16S rRNA gene sequencing was performed to analyze microbial diversity and composition using vaginal swabs obtained from 100 menopausal women, classified as MHT women who have been taking tibolone regularly (n = 50) and non-treated women who never received any treatment (n = 50). Vaginal Health Index Score (VHIS) and GSM symptoms inquiry were also performed. We found that the vaginal microbial diversity decreased and that the abundance of *Lactobacillus* increased to be the dominant proportion significantly in the MHT group, in considerable contrast to vaginal microbiota of the non-treated group, which significantly comprised several anaerobic bacteria, namely, *Gardnerella*, *Prevotella*, *Escherichia-Shigella*, *Streptococcus*, *Atopobium*, *Aerococcus*, *Anaerotruncus*, and *Anaerococcus*. In this study, women without any MHT had significantly more severe GSM symptoms than those receiving tibolone, especially with regard to vulvovaginal dryness and burning, as well as decreased libido ($P < 0.01$). However, there was no significant difference in the severity of urological symptoms between the groups ($P > 0.05$). Furthermore, *Lactobacillus* was demonstrated to be associated with VHIS positively ($r = 0.626$, $P < 0.001$) and with GSM negatively ($r = -0.347$, $P < 0.001$). We also identified *Chlamydia* ($r = 0.277$, $P < 0.01$) and

Streptococcus (r = 0.270, P < 0.01) as having a prominent association with more serious GSM symptoms. Our study provided an elucidation that MHT could notably alleviate GSM and conspicuously reshape the composition of the vaginal microbiota, which is of extreme importance to clinical practice for the management of GSM.

Keywords: menopause, vaginal microbiota, genitourinary syndrome of menopause, menopausal hormone therapy, 16S rRNA gene sequencing, tibolone

INTRODUCTION

Genitourinary syndrome of menopause (GSM), previously known as vulvovaginal atrophy or atrophic vaginitis, is reported in approximately half of perimenopausal and postmenopausal women worldwide (Portman and Gass, 2014; Geng et al., 2018) and characterized by bothersome disorders interfering with quality of life. It is a collection of symptoms and signs associated with low circulating estrogen levels, commonly including vaginal dryness; dyspareunia; frequent, urgent, and painful urination; recurrent urinary tract infection; incontinence; etc. (Portman and Gass, 2014). However, GSM has not received enough attention from health care providers and patients, causing a delay in management. It is reported that only 25% of patients in Asia were willing to seek medical assistance, and only 24% of them had access to treatment (Chua et al., 2017). Menopausal hormone therapy (MHT) previously has been shown to be the most effective management for GSM (Gandhi et al., 2016; Faubion et al., 2017). As estrogen receptors distribute in diverse tissues and organs of our body, women in the menopausal stage tend to manifest various types of symptoms requiring treatment due to estrogen deficiency. We found that systemic hormone replacement therapy is suitable for a great many cases in our practical clinical work. The human microbiota inhabiting the vagina alter dynamically across different reproductive stages (Gajer et al., 2012). After menopause, endocrine level and vaginal environment change gradually accompanied by changes in vaginal microbial community structure. In general, vaginal dominant colonization with *Lactobacillus* is infrequent compared to premenopausal women (Muhleisen and Herbst-Kralovetz, 2016; Kaur et al., 2020). However, the correlation between menopausal related genitourinary symptoms and vaginal flora is still full of ambiguity. Some studies reported that women with examination findings of atrophy had lower proportion of *Lactobacillus* (Shen et al., 2016; Brotman et al., 2018), whereas other studies did not show this significant association (Mitchell et al., 2017, 2018). While there is evidence of associations between different types of hormone therapy and increased detection of *Lactobacillus* in vaginal environment (Devillard et al., 2004; Mitchell et al., 2018; Gliniewicz et al., 2019), relatively little is known about effects of MHT on the overall vaginal microbial composition and symptoms and signs of GSM, especially in Chinese women.

In this cross-sectional study, we sought to explore vaginal microbial structure and severity of GSM in women who received regular and uniform MHT in comparison with those who did not by using 16S rRNA gene amplicon sequencing to identify microbial taxa. Moreover, we evaluated the severity of common symptoms in GSM, confirmed a transformation in abundance and diversity of vaginal bacteria after MHT, and elucidated particular associations among vaginal microbiota, MHT, and clinical characteristics.

MATERIALS AND METHODS

Subjects' Data and Sample Collection

Menopausal women were recruited and selected from patients attending the menopause clinic in the Shanghai Jiao Tong University Affiliated Sixth People's Hospital in China, from February 2017 to December 2018. These participants were divided into two groups of 50 subjects each, according to whether they have received regular MHT (tibolone, a synthetic steroid, 2.5 mg orally per day, was selected as the uniform treatment in this study) at least in the past year. Women were included in the study if they were 45–65 years old and did not have menstruation in the past 60 days. In addition, women were excluded if they had any contraindications of MHT; irregular menstrual bleeding due to disease; induced menopause caused by drug, operation, or chemoradiotherapy; a history of diabetes or severe chronic diseases; or they were pregnant or lactating. Moreover, women receiving intravaginal operation such as gynecological examination within the past 24 h, systemic or vaginal topical antibiotic treatment in the past 30 days, or those with no sexual partner were also excluded from this study. All study subjects signed an informed consent form before participation.

Participants responded to one-on-one questionnaires conducted by trained investigators. Demographic characteristics were first assessed by a questionnaire including age, height, weight, reproductive history, menstruation, employment status, economic level, and years of education. Height and weight were measured to calculate body mass index (BMI). In addition, serum estradiol (E_2) and follicular stimulating hormone (FSH) levels were abstracted from medical records archived at the Shanghai Jiao Tong University Affiliated Sixth People's Hospital with participants' permission. Common menopausal genitourinary symptoms, such as (1) vulvovaginal symptoms including dryness, itching, and burning; (2) urological symptoms including frequent, urgent, and painful urination; recurrent urinary tract infection; and incontinence; and (3) sexual symptom including only decreased libido, were also evaluated by asking women if they had bothersome symptoms described above on a five-point scale ranging from 0 to 4, corresponding to "asymptomatic," "mild," "moderate," "severe," and "extremely severe," respectively. Objectively, the severity of GSM was represented by the sum of scores for all seven symptoms.

Then, women underwent a gynecological examination by an experienced gynecologist, during which the Vaginal Health Index Score (VHIS) was measured. The VHIS evaluates the condition of vaginal mucosa through elasticity, vaginal discharge, pH, mucosal integrity, and moisture. A lower VHIS means a worse vaginal physical condition, and if the score is less than 15, it indicates the status of vaginal atrophy (Arêas et al., 2019). Also during this visit, two sterile swabs were used to obtain vaginal secretions samples from the posterior vaginal fornix while avoiding touching the cervix and vulva to avert contamination. One swab was used to detect vaginal pH by a pH test strip (Merck, Darmstadt, Germany) from 4.0 to 7.0 (Huang et al., 2010), and the other was immediately placed in a cryopreservation tube and stored in a −80℃ freezer until processed.

DNA Extraction, Polymerase Chain Reaction Amplification, and Sequencing

Before the DNA extraction, frozen swabs containing vaginal secretions were thawed on the ice in a decontaminated environment. The bacterial genomic DNA was isolated from each specimen using the FastDNA® SPIN Kit for Soil (MP Biomedicals, Irvine, CA, United States), according to the standard manufacturer's protocol, and stored at −20°C prior to subsequent detection. DNA concentrations and purities were quantified by the NanoDrop® ND-2000 UV-Vis spectrophotometer (Thermo Fisher Scientific, Wilmington, DE, United States), and DNA quality was verified by 1% agarose gel electrophoresis.

The V3–V4 hypervariable region of the bacterial 16S ribosomal RNA gene was amplified using primers (Ling et al., 2017) 338F (5′-ACTCCTACGGGAGGCAGCA-3′) and 806R (5′-GACTACHVGGGTWTCTAAT-3′) under the following thermal-cycling parameters: an initial temperature of 95℃ for 3 min, followed by 28 cycles of 95℃ for 30 s, 55℃ for 30 s, and 72℃ for 45 s, and a final extension at 72°C for 10 min. The polymerase chain reaction (PCR) reactions were performed in a mixture in volume of 20 μL, containing 4 μL of 5 × FastPfu Buffer, 2 μL of 2.5 mM dNTPs, 0.8 μL of forward/reverse primer (5 μM), 0.4 μL of FastPfu Polymerase, 10 ng of template DNA, and 10 μL of ddH_2O. The PCR products were checked on a 2% agarose gel, extracted from the gel, and further purified using the AxyPrep DNA Gel Extraction Kit (Axygen Biosciences, Union City, CA, United States) and then quantified using QuantiFluor™-ST (Promega, Madison, WI, United States). Subsequently, purified amplicons were pooled in equal amounts and were sent for paired-end sequencing (2 * 300) on an Illumina MiSeq platform.

Bioinformatics and Statistical Analysis

Bioinformatics analysis was conducted in QIIME (v 1.9.0) or using R project (v 3.6.3) basically. Raw 16S rRNA gene sequences were analyzed using the Quantitative Insights into Microbial Ecology (QIIME) pipeline (v 1.9.0) as previously described (Caporaso et al., 2010). Briefly, raw sequences were assigned to respective samples based on the sample specific barcode sequences and trimmed through removal of both barcode and primer sequences for further quality filtering. Criteria used to filter the low-quality sequence reads were mainly as follows: sequences with a length less than 150 bp, sequences with an average quality score less than 20, sequences with mononucleotide repeats greater than 8, and sequences containing one or more ambiguous base (Huang et al., 2018). Retained high-quality sequences were clustered into distinct operational taxonomic units (OTUs) at a 97% similarity threshold using QIIME's UCLUST program (Edgar, 2010), and chimeric sequences were detected and removed with ChimeraSlayer implemented in QIIME (Haas et al., 2011). Finally, representative sequences were aligned against the SILVA database (Quast et al., 2013)[1] using the Ribosomal Database Project (RDP)[2] Bayesian classifier that was retrained to assign taxonomy to each OTU at a 70% confidence threshold. Vaginal microbial taxa were confirmed at the phylum, class, order, family, and genus levels in this portion of the study analysis. In order to eliminate the difference of sequencing depth among samples and to minimize the sequencing errors caused by different library sizes, an average and uniform OTUs table was generated by subsampling under the minimum sequencing depth for downstream analysis.

Based on the OTU information, alpha and beta diversities were utilized to examine vaginal microflora structure. Alpha diversity (de la Cuesta-Zuluaga et al., 2019) (considered as "within" sample diversity) indices were calculated using the vegan package in R (v 3.6.3), including Shannon diversity index, Ace richness index, Chao estimator, Simpson diversity index, and Good's coverage. Beta diversity (Chu et al., 2017) (known as "between" sample diversity) was analyzed using the Bray–Curtis and weighted UniFrac distance matrices. Then the principal coordinate analysis (PCoA) was plotted using R package ggplot with significant clustering in the intergroup Adonis test. The hierarchically clustered heatmap was generated to visualize microbial taxonomy composition and abundance by the R package pheatmap. Briefly, some relevant tables reflecting community structures were generated to reinforce argument explicitly. In addition, the linear discriminant analysis (LDA) effect size (LEfSe) (Segata et al., 2011) modeling was applied for the identification of significantly differential genera between groups based on relative abundance performed in the online Galaxy tools[3]. To define multivariate correlations of clinical characteristics and microbial community structure, Pearson correlation coefficient between them was calculated, and canonical correlation analysis (CCA) (Guo et al., 2016) was implemented in the R package vegan.

Further statistical analysis was performed using SPSS software (v 22.0). For continuous variables, data with a normal distribution were expressed as mean ± standard deviation; otherwise, data were shown as median (lower quartile, upper quartile). For categorical variables, the percentage was used to describe information. To judge differences between groups, independent-samples *t*-test (normal distribution and homogeneity of variance), Mann-Whitney *U*-test (non-normal distribution), χ^2-test, or Fisher exact test (comparison of rate)

[1]https://www.arb-silva.de/

[2]http://rdp.cme.msu.edu/

[3]http://huttenhower.sph.harvard.edu/galaxy/

was applied. Differences were considered statistically significant with $P < 0.05$.

RESULTS

Study Cohorts and the Severity of GSM Symptoms

A total of 100 vaginal samples from 100 menopausal women were available for analysis in this study and classified into two groups: non-treated women without any MHT ($n = 50$) and women on MHT over the past year ($n = 50$, tibolone was selected as the unified medication regimen for MHT in our study). **Table 1** describes the main demographic characteristics of each group, and no significant difference was observed between groups except for years since menopause that was longer in women with MHT than in non-treated women.

Table 2 shows common symptoms of GSM by severity, from asymptomatic to extremely severe, and **Figure 1** demonstrates intuitively the mean score for main symptoms by group. Scores of vaginal symptoms and sexual symptom, as well as GSM, were higher in the non-treated group, indicating that a majority of

TABLE 1 | Demographic characteristics of participants.

Demographics		Non-treated group	MHT group	*P*-values
		(*n* = 50)	(*n* = 50)	
Age (y, mean ± SD)		53.34 ± 3.33	54.76 ± 4.27	0.067[a]
BMI (kg/m^2, mean ± SD)		22.50 ± 3.54	21.85 ± 2.50	0.291[a]
E_2 [pg/mL, median (Q1–Q3)]		26.5 (17.00–33.25)	28.5 (17.75–37.75)	0.909[b]
FSH [mIU/mL, median (Q1–Q3)]		68.16 (51.29–80.08)	59.14 (47.52–68.29)	0.107[b]
No. of parity (*n*, %)	≤ 1	43 (86.0%)	43 (86.0%)	1.000[c]
	≥ 2	7 (14.0%)	7 (14.0%)	
No. of abortion (*n*, %)	≤ 1	29 (58.0%)	31 (62.0%)	0.683[c]
	≥ 2	21 (42.0%)	19 (38.0%)	
Occupational status (*n*, %)	In work	23 (46.0%)	21 (42.0%)	0.687[c]
	Retired/ unemployed	27 (54.0%)	29 (58.0%)	
Educational length (y, *n*, %)	≤ 6	2 (4.0%)	1 (2.0%)	0.638[d]
	6–9	9 (18.0%)	12 (24.0%)	
	9–12	19 (38.0%)	22 (44.0%)	
	> 12	20 (40.0%)	15 (30.0%)	
Economic state (monthly income, yuan, *n*, %)	≤ 3,000	17 (34.0%)	21 (42.0%)	0.533[c]
	3,000–5,000	15 (30.0%)	16 (32.0%)	
	> 5,000	18 (36.0%)	13 (26.0%)	

BMI, body mass index; E_2, estradiol; FSH, follicular stimulating hormone. [a]Independent-samples t-test. [b]Mann-Whitney U-test. [c]Pearson χ^2-test. [d]Fisher exact test.

TABLE 2 | Common symptoms of GSM.

Common symptoms	Non-treated group (*n* = 50)						MHT group (*n* = 50)						*P*-values
	Asymptomatic	Mild	Moderate	Severe	Extremely severe	Mean ± SD (Mean)	Asymptomatic	Mild	Moderate	Severe	Extremely severe	Mean ± SD (Mean)	
Vulvovaginal symptom						2.32 ± 0.36 (2)						1.06 ± 0.18 (1)	**< 0.01**
Dryness	30.00%	36.00%	20.00%	10.00%	4.00%	1.22 ± 0.16 (1)	58.00%	26.00%	16.00%	0.00%	0.00%	0.58 ± 0.11 (0)	**<0.005**
Itching	62.00%	20.00%	6.00%	12.00%	0.00%	0.68 ± 0.15 (0)	68.00%	22.00%	10.00%	0.00%	0.00%	0.42 ± 0.10 (0)	0.366
Burning	78.00%	10.00%	4.00%	8.00%	0.00%	0.42 ± 0.13 (0)	96.00%	2.00%	2.00%	0.00%	0.00%	0.06 ± 0.04 (0)	**< 0.01**
Urological symptom						0.94 ± 0.19 (0)						0.52 ± 0.16 (0)	0.051
Frequent, urgent, and painful urination	70.00%	18.00%	10.00%	2.00%	0.00%	0.44 ± 0.11 (0)	84.00%	14.00%	2.00%	0.00%	0.00%	0.18 ± 0.06 (0)	0.072
Recurrent urinary tract infection	90.00%	2.00%	8.00%	0.00%	0.00%	0.18 ± 0.08 (0)	96.00%	0.00%	4.00%	0.00%	0.00%	0.08 ± 0.06 (0)	0.436
Incontinence	74.00%	20.00%	6.00%	0.00%	0.00%	0.32 ± 0.08 (0)	84.00%	10.00%	2.00%	4.00%	0.00%	0.26 ± 0.10 (0)	0.305
Sexual symptom						2.58 ± 0.17 (3)						1.62 ± 0.20 (1)	**< 0.005**
Decreased libido	8.00%	8.00%	32.00%	22.00%	30.00%	2.58 ± 0.17 (3)	77.80%	24.00%	20.00%	14.00%	14.00%	1.62 ± 0.20 (1)	**<0.005**
GSM						5.84 ± 0.49 (5)						3.20 ± 0.41 (2.5)	**< 0.005**

P-value in bold indicates statistical difference is significant.

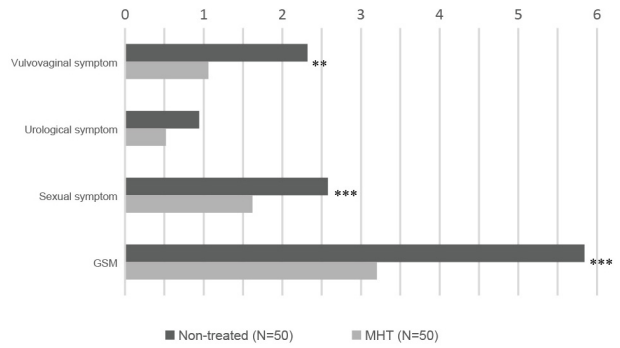

FIGURE 1 | Severity of GSM main symptoms in each group: non-treated vs. MHT. Higher score means more severe symptom; statistical differences are shown in this figure: $^{**}P < 0.01$, $^{***}P < 0.005$.

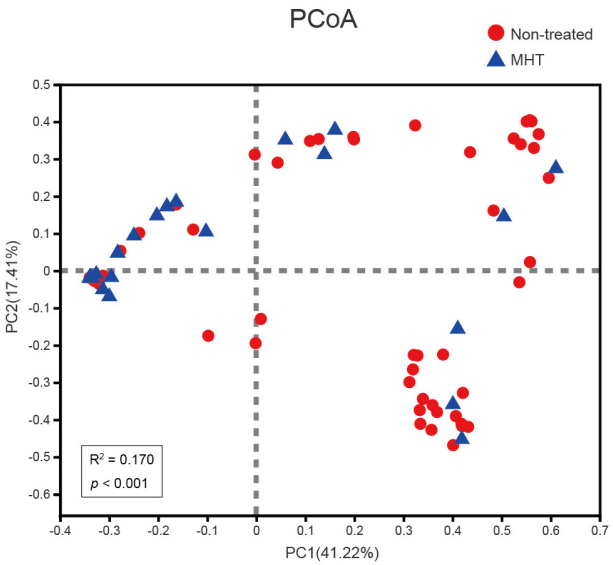

FIGURE 2 | Comparing samples distributions belonging to the non-treated (red) or MHT (blue) group by using principal coordinate analysis (PCoA) on the Bray–Curtis dissimilarity. Each sample is shown as a dot.

GSM symptoms were significantly relieved in women treated with MHT ($P < 0.01$). However, there was no significant drop in the severity scores of urological symptoms between the groups ($P > 0.05$).

Sequencing Data, Microbial Distribution, and Abundance

In this work, a total of 3,965,265 sequence reads (range 30,214–72,367 reads per sample) were acquired after quality control, with an average length of 444 bp per sample. Then high-quality sequences were classified into 27 phyla, 52 classes, 103 orders, 176 families, and 356 genera through bioinformatics processing.

The alpha diversity indices differed significantly between the non-treated group and MHT group as shown in **Table 3**. Shannon diversity index, Ace richness index, and Chao estimator were greater in the non-treated samples, whereas Simpson diversity index was lower in the non-treated samples relative to the MHT samples ($P < 0.005$). These results reflected a higher microbial diversity of vaginal environment in the non-treated women than in the MHT-treated women. However, there was no significant difference in Good's coverage value between two groups, and the value for each group was 1.00, suggesting that the sequencing depth was sufficient to saturate the taxa.

To examine how the vaginal microbiota varied between these two groups, beta diversity analysis was performed by PCoA on the Bray–Curtis dissimilarity. As illustrated in **Figure 2**, the community structure of MHT-treated women was mostly separated from non-treated women (Adonis $P < 0.001$), with an R^2-value (0.170) suggestive of this significant differentiation.

For more details on microbial community at the genus level, we analyzed the relative abundance of the top 50 classified genera in all samples, which was demonstrated as a hierarchically clustered heatmap (**Figure 3**). **Table 4** lists the most abundant genera in two groups and included only the genera with abundance proportions greater than 0.005 in each sample; those failing to meet the condition were expressed as "others." According to **Figure 3**, samples within the same group were more interrelated. Furthermore, microbial community profiles from the two groups were markedly different (**Figure 3** and **Table 4**), which was also verified by PCoA results. *Lactobacillus* was the most representative bacterial genus in both groups, but was dominant only in the MHT group (*Lactobacillus* proportion of 29.1% in the non-treated samples vs. 83.1% in the MHT samples). In the non-treated group, *Gardnerella*, *Prevotella*, *Streptococcus*, *Escherichia-Shigella*, *Atopobium*, *Sneathia*, *Bifidobacterium*, etc.,

TABLE 3 | Alpha diversity indices for vaginal microbiota.

Alpha diversity indices	Non-treated group (n = 50)			MHT group (n = 50)			P-values
	Median	Q1	Q3	Median	Q1	Q3	
Shannon	0.99	0.59	1.46	0.02	0.01	0.52	**< 0.005**
Simpson	0.48	0.30	0.70	1.00	0.70	1.00	**< 0.005**
Ace	51.53	24.43	111.52	30.58	12.54	63.07	**< 0.005**
Chao	35.13	21.75	107.00	22.10	10.75	30.44	**< 0.005**
Coverage	1.00	1.00	1.00	1.00	1.00	1.00	0.109

P-values were obtained from Mann-Whitney U-test. Bold value means there exists significant statistical difference.

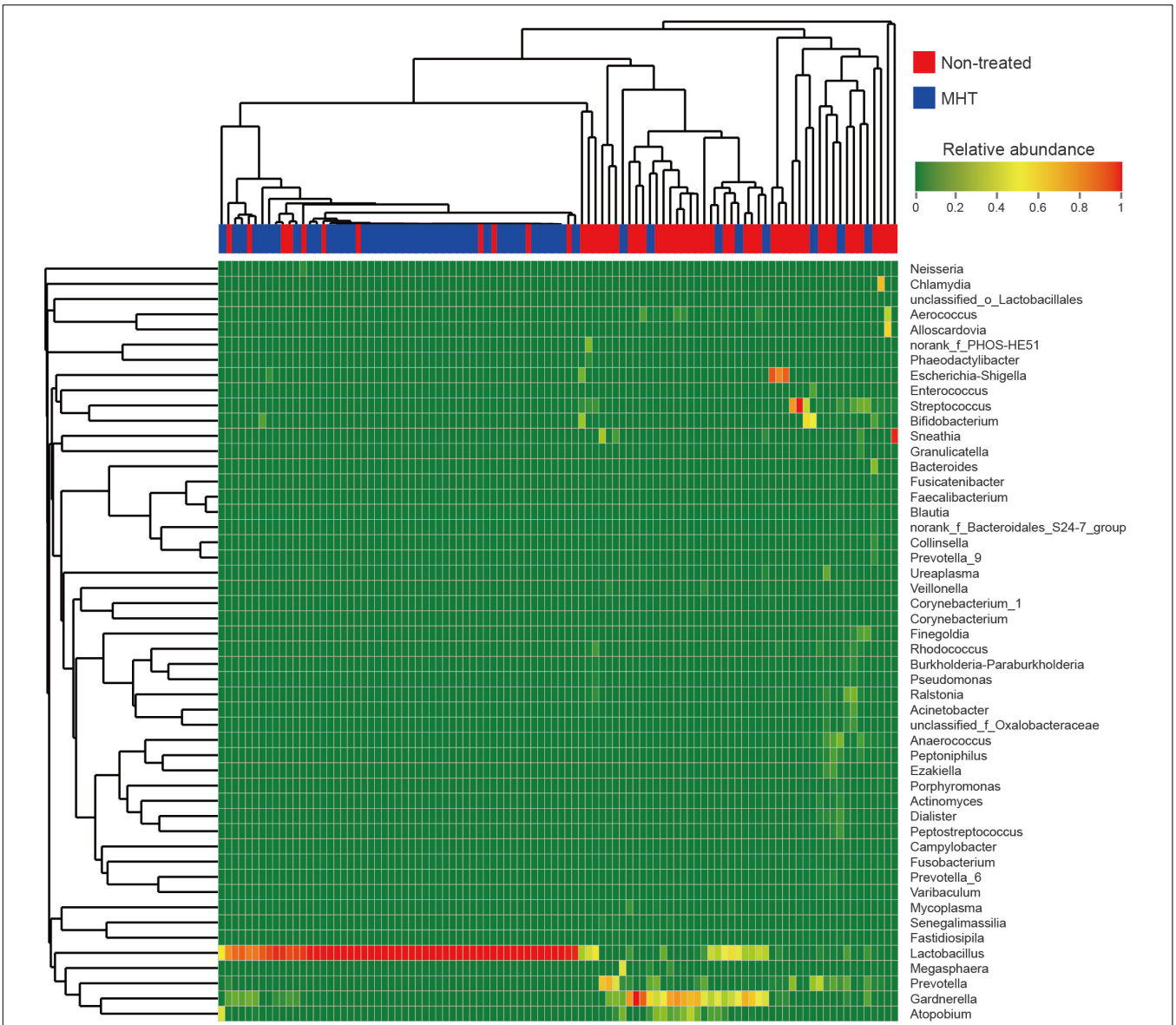

FIGURE 3 | Heatmap analysis of relative abundance of microbial taxa found in all vaginal samples at the genus level (top 50). Each sample is shown as vertical bar, and different color of each cell represents different relative abundance: the low abundance and high abundance are highlighted by green and red, respectively. The horizontal bar on the top indicates the non-treated (red) or MHT (blue) group; dendrograms reflect hierarchical clustering on Bray–Curtis dissimilarity (columns) or Euclidean distance (rows) using average linkage.

made great contributions, which was demonstrated by both data and graphics.

Significant Differences in Microbial Communities

Subsequently, biomarker analysis was conducted to identify the special microbial taxa with significant abundance differences between non-treated and MHT samples using the LEfSe modeling. As seen in **Figure 4**, there were 49 bacterial clades presenting significant intergroup differences with a LDA threshold of 3.5, and most bacteria were enriched in non-treated samples. Focusing on the genus level, we found that there were as many as eight significantly different genera in the non-treated group, namely, *Gardnerella*, *Prevotella*, *Escherichia-Shigella*, *Streptococcus*, *Atopobium*, *Aerococcus*, *Anaerotruncus*, and *Anaerococcus* (all $P < 0.05$). In contrast, only *Lactobacillus* manifested the abundance advantage in the MHT group ($P < 0.05$).

Multivariate Analysis

Finally, the CCA was applied to reveal the potentially multivariate correlation of clinical characteristics and primary microbial community (**Figure 5**). In the CCA, the length of the vector is

TABLE 4 | Proportion of most abundant genera in vaginal microbiota of different groups.

Genus	Abundance proportion in non-treated group			Abundance proportion in MHT group		
	Mean	Max	Min	Mean	Max	Min
Lactobacillus	29.1%	100.0%	0.0%	83.1%	100.0%	0.0%
Gardnerella	22.7%	99.9%	0.0%	6.4%	55.5%	0.0%
Prevotella	7.4%	63.5%	0.0%	1.7%	31.4%	0.0%
Streptococcus	5.8%	97.4%	0.0%	0.7%	21.4%	0.0%
Escherichia-Shigella	5.1%	81.4%	0.0%	0.2%	9.2%	0.0%
Atopobium	4.4%	37.0%	0.0%	2.1%	46.0%	0.0%
Sneathia	3.1%	92.5%	0.0%	0.1%	6.6%	0.0%
Bifidobacterium	2.1%	54.1%	0.0%	1.4%	52.0%	0.0%
Aerococcus	1.8%	38.4%	0.0%	0.1%	1.9%	0.0%
Ralstonia	1.5%	22.2%	0.0%	0.1%	1.3%	0.0%
Anaerococcus	1.3%	15.1%	0.0%	0.6%	23.6%	0.0%
Chlamydia	1.2%	58.6%	0.0%	0.0%	0.0%	0.0%
Alloscardovia	1.1%	56.1%	0.0%	0.0%	0.2%	0.0%
Rhodococcus	0.8%	11.3%	0.0%	0.0%	0.8%	0.0%
Peptoniphilus	0.7%	13.2%	0.0%	0.2%	7.5%	0.0%
Finegoldia	0.6%	15.1%	0.0%	0.4%	17.6%	0.0%
Acinetobacter	0.6%	14.1%	0.0%	0.0%	0.1%	0.0%
Ezakiella	0.6%	12.3%	0.0%	0.0%	2.1%	0.0%
Dialister	0.5%	5.4%	0.0%	0.3%	11.6%	0.0%
Ureaplasma	0.5%	18.0%	0.0%	0.2%	4.5%	0.0%
Megasphaera	0.2%	9.8%	0.0%	1.1%	46.4%	0.0%
Others	8.7%	72.9%	0.0%	1.4%	30.3%	0.0%

Others represent those genera with abundance proportion less than 0.005 in each sample. Mean, the average proportion of all samples in one group; Min, minimal proportion of a sample in one group; Max, maximal proportion of a sample in one group.

used to interpret this correlation (a longer vector means a greater correlation with bacterial distribution), and the angle between vectors could reflect associations of clinical variables (a positive association is plotted as an acute angle and a negative association as an obtuse angle). Additionally, a greater distance between samples indicates a stronger dissimilarity in microbial structure. According to **Figure 5**, we found that the dissimilarity between samples in the non-treated group was larger than that in the MHT group, this phenomenon was consistent with PCoA results. Moreover, the distribution of non-treated samples was generally in accordance with the GSM vector, whereas MHT samples were mostly distributed in the direction of the VHIS vector, which was similar to the comparison of the severity of GSM between these two groups. The first axis had a significantly positive correlation with VHIS ($P < 0.001$), as well as a negative correlation with GSM ($P < 0.005$); it was obvious that these two variables had an obtuse relationship. *Lactobacillus* was also associated with the first axis; similarly, it corrected with VHIS positively ($r = 0.626$, $P < 0.001$) and with GSM negatively ($r = -0.347$, $P < 0.001$). As for GSM, other vaginal genera had some connections with it as well, including *Chlamydia* ($r = 0.277$, $P < 0.01$), *Streptococcus* ($r = 0.270$, $P < 0.01$), *Enterococcus* ($r = 0.236$, $P < 0.05$), *Corynebacterium* ($r = 0.234$, $P < 0.05$), *Porphyromonas* ($r = 0.223$, $P < 0.05$), and *Escherichia-Shigella* ($r = 0.199$, $P < 0.05$), all of which increased with the GSM severity score. Additionally, the second axis only presented a significantly inverse relationship with BMI ($P < 0.001$), but age could not affect the microbial community distribution in our study ($P > 0.05$).

DISCUSSION

In the current study, we performed a cross-sectional survey to determine a vaginal microbial restoration and GSM-related symptom improvement with MHT application based on 16S rRNA gene sequencing and to demonstrate the salient relevance among them. Taking into account the possible impact of different MHT options on the outcome, we chose tibolone as the only unified treatment. The foremost reason is that the vast majority of women treated with tibolone had no menstrual period; in this way, effects of menstruation on vaginal flora could be eliminated. What needs to be explained was that in our study cohort, patients received tibolone treatment due to multiple systematic symptoms rather than genitourinary symptoms alone, in strict accordance with the medicine guidelines (Pinkerton, 2020). Tibolone, a synthetic steroid with estrogenic, progestogenic, and androgenic properties, has long been used worldwide for menopausal symptoms (Formoso et al., 2016). Obviously, we proved that women receiving tibolone had significantly milder GSM symptoms than non-treated women, especially for vulvovaginal dryness and burning, as well as decreased libido, which was similar to previously reported studies (Kenemans and Speroff, 2005). However, there was no significant distinction in vulvovaginal itching and all urological symptoms between the two populations. The underlying basis for these findings is presumably the medicinal property. Tibolone is rapidly metabolized into three metabolites that play diverse roles in target tissues in the body through binding with estrogen, progesterone, or androgen receptors and modulating enzymatic activity (Kloosterboer, 2004), which explains why the levels of serum E_2 and FSH were steady in all study participants. Tibolone itself and its $\Delta 4$ isomer have slight androgenic effects contributing to the increases in free testosterone and consequently to improving sexual desire (Laan et al., 2001). The female reproductive and lower urinary tracts share the same embryonic origin—urogenital sinus; furthermore, estrogen, and progesterone receptors have been identified in both tissues (Tincello et al., 2009). In theory, it could be anticipated that hormone therapy would help to ameliorate both genital and urinary symptoms, whereas the present researches still remain controversial about the effect of systemic estrogen on urinary symptoms (Robinson and Cardozo, 2011). We supposed that the urinary tract symptoms were mainly mild in the cohort, which to some extent may explain the lack of significant remission of symptoms after tibolone. Hence further clinical surveys and basic experiments should be carried out to clarify the management of postmenopausal lower urinary tract symptoms.

Herein, we demonstrated the vaginal microflora of women with MHT differed from that of non-treated women. First, the differences in all alpha diversity indices between groups

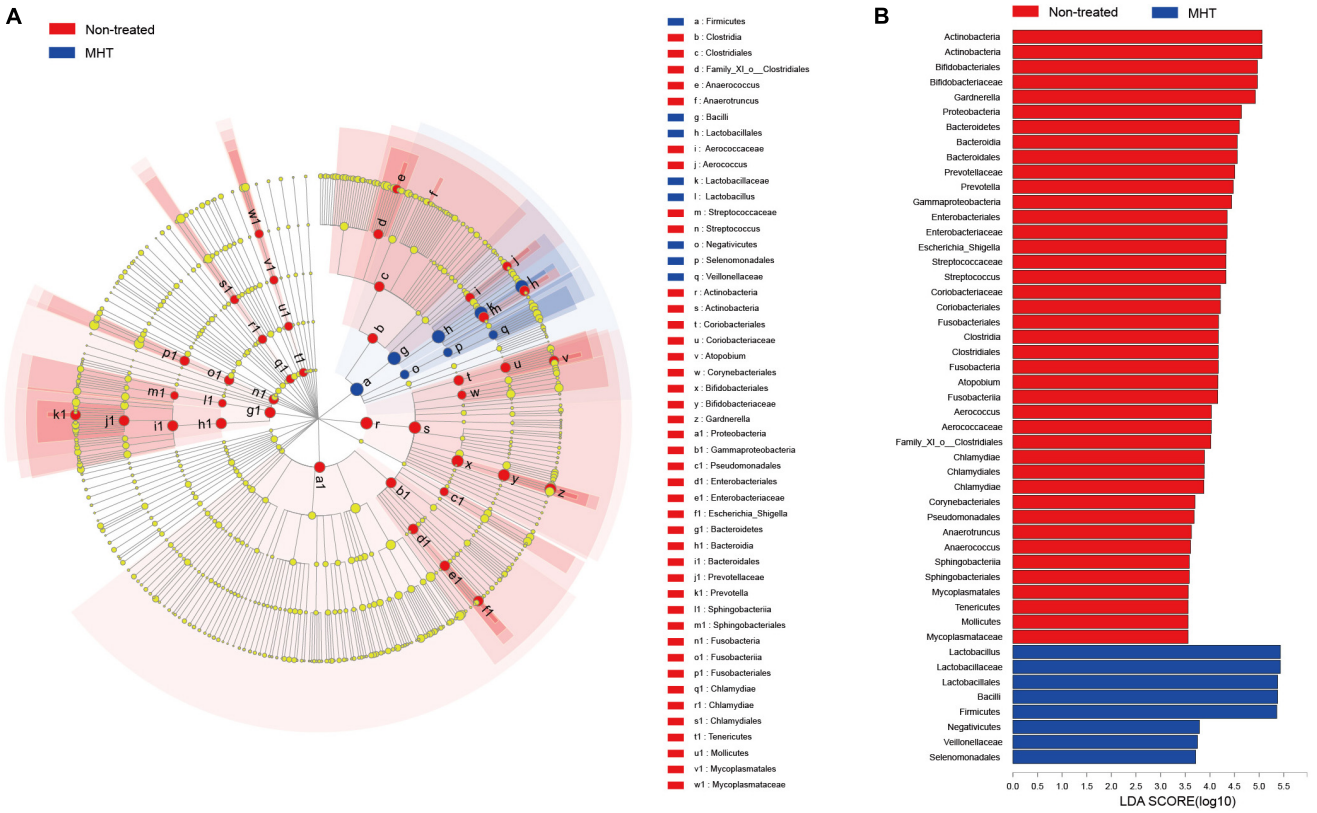

FIGURE 4 | Linear discriminant analysis (LDA) effect size (LEfSe) analysis for comparing microbial variations at the genus level between the non-treated (red) and MHT (blue) group. **(A)** LEfSE cladogram of microbial taxa in different group ($P < 0.05$). **(B)** LDA score identifying effect size of difference between groups with a threshold value of 3.5, a higher score represents a greater contribution to the observed intergroup difference, indicating this taxon is a more important biomarker.

implied a higher microbial diversity in samples of non-treated women, which suggested that there might be no definitely preponderant bacteria in these samples. Then, the analysis results revealed distinct vaginal microbial signatures in each group. *Lactobacillus* accounted for the highest proportion in both of them, but it was only dominant in the vaginal community of women with MHT. We also found it correlated positively with a healthier vaginal condition as well as negatively with more severe GSM, corresponding to the findings of previous studies (Muhleisen and Herbst-Kralovetz, 2016; Mitchell et al., 2018; Gliniewicz et al., 2019). However, it is pertinent to note that the non-treated vaginal microflora significantly included several anaerobic bacteria, namely, *Gardnerella*, *Prevotella*, *Escherichia-Shigella*, *Streptococcus*, *Atopobium*, *Aerococcus*, *Anaerotruncus*, and *Anaerococcus*. Interestingly, *Prevotella* has been shown to promote the growth of *Gardnerella* by producing polyamines during metabolism, in the same way, the existence of biofilm in *Gardnerella* could stimulate the growth of *Prevotella* (Randis and Ratner, 2019). Additionally, not only *Gardnerella* and *Prevotella* but also *Streptococcus* and *Atopobium* were strongly associated with bacterial vaginosis (Onderdonk et al., 2016). Numerous studies have affirmed that *Escherichia coli*, as the primary pathogen of urinary tract infections, could adhere to or even invade into vaginal epithelial cells prior to inducing an ascending infection (Brannon et al., 2020). Likewise, a few particular species of *Aerococcus* were also believed to involve in urinary tract infections (Rasmussen, 2016). One previous research detected that *Anaerotruncus* in the female reproductive tract might contribute to the development of endometrial cancer (Walther-António et al., 2016). Moreover, *Anaerococcus* was reported to be correlated with cervical intraepithelial neoplasia disease progression (Mitra et al., 2015). Taken together, these findings hint that ecological interactions are meaningful for vaginal environment and reproductive health; however, the potential interactions are far from definitive.

Our work specifically addressed relationships between the severity of GSM and vaginal microbiota, and except for a strikingly negative correlation between *Lactobacillus* and GSM, we demonstrated that other taxa correlated with GSM positively, including *Chlamydia* and *Streptococcus*, with high correlation coefficients. It has been suggested that a distinct bacterial community state characterized by *Streptococcus* was associated with vulvovaginal atrophy (Brotman et al., 2018), and our results were consistent with this finding. Moreover, it is well known that *Chlamydia* infection could result in acute and chronic reproductive disorders. Nevertheless, a few cross-sectional studies found that women in menopause were not susceptible to *Chlamydia* (Jackson et al., 2015; Stemmer et al.,

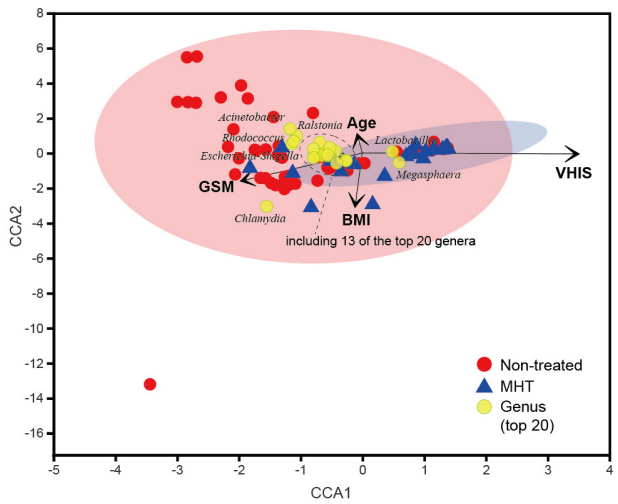

FIGURE 5 | Canonical correlation analysis (CCA) of the above vaginal microbiota and clinical characteristics. Red and blue points represent non-treated and MHT samples, respectively, the 95% confidence intervals of samples' distribution are visualized by ellipses, and the top 20 microbial genera are colored with yellow. Clinical characteristic variables (age, BMI, VHIS, GSM) are indicated by vectors in black.

2018). Notably, there was probably a complex mutual mechanism underlying the definite association between *Chlamydia* and more severe symptoms of GSM, as shown in our findings. Infection with *Chlamydia* in the female genital tract could drive increased expression of TLR2 and TLR4 accompanied by upregulation of cytokines, such as tumor necrosis factor α, interleukin 1α (IL-1α), and IL-6; these cytokines together trigger the inflammatory response during which tissue damage occurs (Agrawal et al., 2009). Unfortunately, our study did not involve immune-relevant research, so there was no way to directly provide an explicit conclusion of the interaction mechanism between vaginal bacteria and the local immune response. This aspect was one of limitations in the present study. However, based on the available evidence, we may speculate that the composition and stability of the vaginal microbiota play an essential part in determining the mucosal immune response and susceptibility to infection. Other limitations included that sample sizes were relatively small and participants included in this study were only from outpatients in one clinical center, which might lead to the issue that our results only partly reflected the situation of menopausal women in Shanghai, China. In this regard, additional studies with larger sample sizes and multicenter are required to further investigate the latent microbes associated with GSM and the microbiological mechanism in the occurrence and development of GSM.

In conclusion, GSM emerges with a decline in circulating estrogen levels, which may worsen gradually without intervention. Understanding the microbiological effect of MHT on GSM could help to improve novel strategies for GSM treatment and prevent discomfort. Our study demonstrated that *Lactobacillus* was distinctly abundant in the vagina and that symptoms of GSM were notably alleviated after regular hormone therapy. Furthermore, several special anaerobic bacteria were found to be significantly enriched in menopausal women without any treatment, and these bacteria were bound up with gynecological and reproductive diseases. Women infected with *Chlamydia* or *Streptococcus* in the vagina may be prone to suffer from GSM, which is necessary to be taken into account by medical staff. These findings are of great importance to clinical practice for the management of GSM, although the microbiological mechanism in the progression of GSM remains to be explored and perfected further.

DATA AVAILABILITY STATEMENT

The datasets presented in this study have been deposited in an online repository. The name of the repository and accession number can be found below: https://www.ncbi.nlm.nih.gov/, PRJNA669119.

ETHICS STATEMENT

The studies involving human participants were reviewed and approved by the Ethics Committee of Shanghai Sixth People's Hospital. The participants provided their written informed consent to participate in this study. Written informed consent was obtained from the individuals for the publication of any potentially identifiable images or data included in this article.

AUTHOR CONTRIBUTIONS

MT conceived, directed and coordinated all aspects of this study. LG, WH, SJ, YanwZ, and PL participated in sample collection, the data collation, and result analysis. YiZ, YangZ, and JH contributed to DNA extraction and PCR amplification from samples. LG and MT prepared and edited the manuscript. All authors contributed to the article and approved the submitted version.

FUNDING

This work was supported by the Shanghai Health and Family Planning Commission (20184Y0362) and the Science and Technology Commission of Shanghai Municipality (15411950202).

ACKNOWLEDGMENTS

We gratefully acknowledge participants in this study and sincerely thank colleagues at the Obstetrics and Gynecology Department of Shanghai Jiao Tong University Affiliated Sixth People's Hospital for the questionnaire survey, vaginal samples collection, and data arrangement.

REFERENCES

Agrawal, T., Vats, V., Salhan, S., and Mittal, A. (2009). The mucosal immune response to Chlamydia trachomatis infection of the reproductive tract in women. *J. Reprod. Immunol.* 83, 173–178. doi: 10.1016/j.jri.2009.07.013

Arêas, F., Valadares, A. L. R., Conde, D. M., and Costa-Paiva, L. (2019). The effect of vaginal erbium laser treatment on sexual function and vaginal health in women with a history of breast cancer and symptoms of the genitourinary syndrome of menopause: a prospective study. *Menopause* 26, 1052–1058. doi: 10.1097/GME.0000000000001353

Brannon, J. R., Dunigan, T. L., Beebout, C. J., Ross, T., Wiebe, M. A., Reynolds, W. S., et al. (2020). Invasion of vaginal epithelial cells by uropathogenic *Escherichia coli*. *Nat. Commun.* 11:2803. doi: 10.1038/s41467-020-16627-5

Brotman, R. M., Shardell, M. D., Gajer, P., Fadrosh, D., Chang, K., Silver, M. I., et al. (2018). Association between the vaginal microbiota, menopause status, and signs of vulvovaginal atrophy. *Menopause* 25, 1321–1330. doi: 10.1097/GME.0000000000001236

Caporaso, J. G., Kuczynski, J., Stombaugh, J., Bittinger, K., Bushman, F. D., Costello, E. K., et al. (2010). QIIME allows analysis of high-throughput community sequencing data. *Nat. Methods* 7, 335–336. doi: 10.1038/nmeth.f.303

Chu, D. M., Ma, J., Prince, A. L., Antony, K. M., Seferovic, M. D., and Aagaard, K. M. (2017). Maturation of the infant microbiome community structure and function across multiple body sites and in relation to mode of delivery. *Nat. Med.* 23, 314–326. doi: 10.1038/nm.4272

Chua, Y., Limpaphayom, K. K., Cheng, B., Ho, C. M., Sumapradja, K., Altomare, C., et al. (2017). Genitourinary syndrome of menopause in five Asian countries: results from the Pan-Asian revive survey. *Climacteric* 20, 367–373. doi: 10.1080/13697137.2017.1315091

de la Cuesta-Zuluaga, J., Kelley, S. T., Chen, Y., Escobar, J. S., Mueller, N. T., and Ley, R. E. (2019). Age- and sex-dependent patterns of gut microbial diversity in human adults. *mSystems* 4:e00261-19. doi: 10.1128/mSystems.00261-19

Devillard, E., Burton, J. P., Hammond, J. A., Lam, D., and Reid, G. (2004). Novel insight into the vaginal microflora in postmenopausal women under hormone replacement therapy as analyzed by PCR-denaturing gradient gel electrophoresis. *Eur. J. Obstet. Gynecol. Reprod. Biol.* 117, 76–81. doi: 10.1016/j.ejogrb.2004.02.001

Edgar, R. C. (2010). Search and clustering orders of magnitude faster than BLAST. *Bioinformatics* 26, 2460–2461. doi: 10.1093/bioinformatics/btq461

Faubion, S. S., Sood, R., and Kapoor, E. (2017). Genitourinary syndrome of menopause: management strategies for the clinician. *Mayo Clin. Proc.* 92, 1842–1849. doi: 10.1016/j.mayocp.2017.08.019

Formoso, G., Perrone, E., Maltoni, S., Balduzzi, S., Wilkinson, J., Basevi, V., et al. (2016). Short-term and long-term effects of tibolone in postmenopausal women. *Cochrane Database. Syst. Rev.* 10:CD008536. doi: 10.1002/14651858.CD008536.pub3

Gajer, P., Brotman, R. M., Bai, G., Sakamoto, J., Schütte, U. M., Zhong, X., et al. (2012). Temporal dynamics of the human vaginal microbiota. *Sci. Transl. Med.* 4:132ra52. doi: 10.1126/scitranslmed.3003605

Gandhi, J., Chen, A., Dagur, G., Suh, Y., Smith, N., Cali, B., et al. (2016). Genitourinary syndrome of menopause: an overview of clinical manifestations, pathophysiology, etiology, evaluation, and management. *Am. J. Obstet. Gynecol.* 215, 704–711. doi: 10.1016/j.ajog.2016.07.045

Geng, L., Zheng, Y., Zhou, Y., Li, C., and Tao, M. (2018). The prevalence and determinants of genitourinary syndrome of menopause in Chinese mid-life women: a single-center study. *Climacteric* 21, 478–482. doi: 10.1080/13697137.2018.1458832

Gliniewicz, K., Schneider, G. M., Ridenhour, B. J., Williams, C. J., Song, Y., Farage, M. A., et al. (2019). Comparison of the vaginal microbiomes of premenopausal and postmenopausal women. *Front. Microbiol.* 10:193. doi: 10.3389/fmicb.2019.00193

Guo, Y., Ding, X., Liu, C., and Xue, J. H. (2016). Sufficient canonical correlation analysis. *IEEE Trans. Image Process* 25, 2610–2619. doi: 10.1109/TIP.2016.2551374

Haas, B. J., Gevers, D., Earl, A. M., Feldgarden, M., Ward, D. V., Giannoukos, G., et al. (2011). Chimeric 16S rRNA sequence formation and detection in Sanger and 454-pyrosequenced PCR amplicons. *Genome Res.* 21, 494–504. doi: 10.1101/gr.112730.110

Huang, A. J., Moore, E. E., Boyko, E. J., Scholes, D., Lin, F., Vittinghoff, E., et al. (2010). Vaginal symptoms in postmenopausal women: self-reported severity, natural history, and risk factors. *Menopause* 17, 121–126. doi: 10.1097/gme.0b013e3181acb9ed

Huang, X., Li, C., Li, F., Zhao, J., Wan, X., and Wang, K. (2018). Cervicovaginal microbiota composition correlates with the acquisition of high-risk human papillomavirus types. *Int. J. Cancer* 143, 621–634. doi: 10.1002/ijc.31342

Jackson, J. A., McNair, T. S., and Coleman, J. S. (2015). Over-screening for chlamydia and gonorrhea among urban women age ≥25 years. *Am. J. Obstet. Gynecol.* 212, 40.e1–40.e6. doi: 10.1016/j.ajog.2014.06.051

Kaur, H., Merchant, M., Haque, M. M., and Mande, S. S. (2020). Crosstalk between female gonadal hormones and vaginal microbiota across various phases of women's gynecological Lifecycle. *Front. Microbiol.* 11:551. doi: 10.3389/fmicb.2020.00551

Kenemans, P., and Speroff, L. (2005). Tibolone: clinical recommendations and practical guidelines. A report of the international tibolone consensus group. *Maturitas* 51, 21–28. doi: 10.1016/j.maturitas.2005.02.011

Kloosterboer, H. J. (2004). Tissue-selectivity: the mechanism of action of tibolone. *Maturitas* 48(Suppl. 1), S30–S40. doi: 10.1016/j.maturitas.2004.02.012

Laan, E., van Lunsen, R. H., and Everaerd, W. (2001). The effects of tibolone on vaginal blood flow, sexual desire and arousability in postmenopausal women. *Climacteric* 4, 28–41. doi: 10.1080/713605033

Ling, Z., Liu, F., Shao, L., Cheng, Y., and Li, L. (2017). Dysbiosis of the urinary microbiota associated with urine levels of proinflammatory chemokine interleukin-8 in female Type 2 diabetic patients. *Front. Immunol.* 8:1032. doi: 10.3389/fimmu.2017.01032

Mitchell, C. M., Srinivasan, S., Plantinga, A., Wu, M. C., Reed, S. D., Guthrie, K. A., et al. (2018). Associations between improvement in genitourinary symptoms of menopause and changes in the vaginal ecosystem. *Menopause* 25, 500–507. doi: 10.1097/GME.0000000000001037

Mitchell, C. M., Srinivasan, S., Zhan, X., Wu, M. C., Reed, S. D., Guthrie, K. A., et al. (2017). Vaginal microbiota and genitourinary menopausal symptoms: a cross-sectional analysis. *Menopause* 24, 1160–1166. doi: 10.1097/GME.0000000000000904

Mitra, A., MacIntyre, D. A., Lee, Y. S., Smith, A., Marchesi, J. R., Lehne, B., et al. (2015). Cervical intraepithelial neoplasia disease progression is associated with increased vaginal microbiome diversity. *Sci. Rep.* 5:16865. doi: 10.1038/srep16865

Muhleisen, A. L., and Herbst-Kralovetz, M. M. (2016). Menopause and the vaginal microbiome. *Maturitas* 91, 42–50. doi: 10.1016/j.maturitas.2016.05.015

Onderdonk, A. B., Delaney, M. L., and Fichorova, R. N. (2016). The human microbiome during bacterial vaginosis. *Clin. Microbiol. Rev.* 29, 223–238. doi: 10.1128/CMR.00075-15

Pinkerton, J. V. (2020). Hormone therapy for postmenopausal women. *N. Engl. J. Med.* 382, 446–455. doi: 10.1056/NEJMcp1714787

Portman, D. J., and Gass, M. L. (2014). Genitourinary syndrome of menopause: new terminology for vulvovaginal atrophy from the international society for the study of women's sexual health and the North American menopause society. *Climacteric* 17, 557–563. doi: 10.3109/13697137.2014.946279

Quast, C., Pruesse, E., Yilmaz, P., Gerken, J., Schweer, T., Yarza, P., et al. (2013). The SILVA ribosomal RNA gene database project: improved data processing and web-based tools. *Nucleic Acids Res.* 41, D590–D596. doi: 10.1093/nar/gks1219

Randis, T. M., and Ratner, A. J. (2019). Gardnerella and prevotella: co-conspirators in the pathogenesis of bacterial vaginosis. *J. Infect. Dis.* 220, 1085–1088. doi: 10.1093/infdis/jiy705

Rasmussen, M. (2016). Aerococcus: an increasingly acknowledged human pathogen. *Clin. Microbiol. Infect.* 22, 22–27. doi: 10.1016/j.cmi.2015.09.026

Robinson, D., and Cardozo, L. (2011). Estrogens and the lower urinary tract. *Neurourol. Urodyn.* 30, 754–757. doi: 10.1002/nau.21106

Segata, N., Izard, J., Waldron, L., Gevers, D., Miropolsky, L., Garrett, W. S., et al. (2011). Metagenomic biomarker discovery and explanation. *Genome Biol.* 12:R60. doi: 10.1186/gb-2011-12-6-r60

Shen, J., Song, N., Williams, C. J., Brown, C. J., Yan, Z., Xu, C., et al. (2016). Effects of low dose estrogen therapy on the vaginal microbiomes of women with atrophic vaginitis. *Sci. Rep.* 6:24380. doi: 10.1038/srep24380

Stemmer, S. M., Mordechai, E., Adelson, M. E., Gygax, S. E., and Hilbert, D. W. (2018). *Trichomonas vaginalis* is most frequently detected in women at the age of peri-/premenopause: an unusual pattern for a sexually transmitted pathogen. *Am. J. Obstet. Gynecol.* 218, 328.e1–328.e13. doi: 10.1016/j.ajog.2017.12.006

Tincello, D. G., Taylor, A. H., Spurling, S. M., and Bell, S. C. (2009). Receptor isoforms that mediate estrogen and progestagen action in the female lower urinary tract. *J. Urol.* 181, 1474–1482. doi: 10.1016/j.juro.2008.10.104

Walther-António, M. R., Chen, J., Multinu, F., Hokenstad, A., Distad, T. J., Cheek, E. H., et al. (2016). Potential contribution of the uterine microbiome in the development of endometrial cancer. *Genome Med.* 8:122. doi: 10.1186/s13073-016-0368-y

Conflict of Interest: The authors declare that the research was conducted in the absence of any commercial or financial relationships that could be construed as a potential conflict of interest.

frontiers in Microbiology

ORIGINAL RESEARCH
published: 08 January 2021
doi: 10.3389/fmicb.2020.588986

Effects of Dietary Isomaltooligosaccharide Levels on the Gut Microbiota, Immune Function of Sows, and the Diarrhea Rate of Their Offspring

*Longlin Zhang[1,2], Xueling Gu[1,2], Jie Wang[1,2], Shuang Liao[1,2], Yehui Duan[3], Hao Li[1,2], Zehe Song[1,2], Xi He[1,2] and Zhiyong Fan[1,2]**

[1] College of Animal Science and Technology, Hunan Agricultural University, Changsha, China, [2] Hunan Co-Innovation Center of Animal Production Safety, Hunan Agricultural University, Changsha, China, [3] Hunan Provincial Key Laboratory of Animal Nutritional Physiology and Metabolic Process, Key Laboratory of Agro-ecological Processes in Subtropical Region, Institute of Subtropical Agriculture, Chinese Academy of Sciences, Hunan Provincial Engineering Research Center for Healthy Livestock and Poultry Production, Scientific Observing and Experimental Station of Animal Nutrition and Feed Science in South-Central, Ministry of Agriculture, National Engineering Laboratory for Pollution Control and Waste Utilization in Livestock and Poultry Production, Changsha, China

OPEN ACCESS

Edited by:
Joao Inacio,
University of Brighton,
United Kingdom

Reviewed by:
Xia Xiong,
Institute of Subtropical Agriculture,
Chinese Academy of Sciences, China
Seungha Kang,
University of Queensland, Australia
Wenkai Ren,
South China Agricultural University,
China

***Correspondence:**
Zhiyong Fan
fzyong04@163.com

Specialty section:
This article was submitted to Systems Microbiology, a section of the journal Frontiers in Microbiology

Received: 03 August 2020
Accepted: 11 December 2020
Published: 08 January 2021

Citation:
Zhang LL, Gu XL, Wang J, Liao S, Duan YH, Li H, Song ZH, He X and Fan ZY (2021) Effects of Dietary Isomaltooligosaccharide Levels on the Gut Microbiota, Immune Function of Sows, and the Diarrhea Rate of Their Offspring. Front. Microbiol. 11:588986. doi: 10.3389/fmicb.2020.588986

To investigate the effects of dietary isomaltooligosaccharide (IMO) levels on the gut microbiota, immune function of sows, and the diarrhea rate of their offspring, 120 multiparous gestating pig improvement company (PIC) sows with similar body conditions were selected and fed 1 of 6 diets: a basal diet with no supplement (control, CON), or a diet supplemented with 2.5 g/kg, 5.0 g/kg, 10.0 g/kg, 20.0 g/kg, or 40.0 g/kg IMO (IMO1, IMO2, IMO3, IMO4, or IMO5 group, respectively). Results showed that dietary treatments did not affect the reproductive performance and colostrum composition of sows ($P > 0.05$). However, compared to the CON, IMO reduced the diarrhea rate of suckling piglets ($P < 0.05$) and improved the concentrations of colostrum IgA, IgG, and IgM ($P < 0.05$). Moreover, IMO decreased the concentrations of serum D-lactate (D-LA) and lipopolysaccharides (LPS) at farrowing and day 18 of lactation (L18) ($P < 0.05$). High-throughput pyrosequencing of the 16S rRNA demonstrated that IMO shaped the composition of gut microbiota in different reproductive stages (day 107 of gestation, G107; day 10 of lactation, L10) ($P < 0.05$). At the genus level, the relative abundance of g_*Parabacteroides* and g_*Slackia* in G107 and g_*Unclassified_Peptostreptococcaceae*, g_*Turicibacter,* g_*Sarcina*, and g_*Coprococcus* in L10 was increased in IMO groups but the g_*YRC22* in G107 was decreased in IMO groups relative to the CON group ($P < 0.05$). Furthermore, the serum D-LA and LPS were negatively correlated with the genus g_*Akkermansia* and g_*Parabacteroides* but positively correlated with the genus g_*YRC22* and g_*Unclassified_Peptostreptococcaceae*. Additionally, the colostrum IgA, IgG, and IgM of sows were positively correlated with the genus g_*Parabacteroides*, g_*Sarcina,* and

g_*Coprococcus* but negatively correlated with the genus g_*YRC22*. These findings indicated that IMO could promote the immune activation and had a significant influence in sows' gut microbiota during perinatal period, which may reduce the diarrhea rate of their offspring.

Keywords: reproductive performance, diarrhea, gut microbiota, sows, isomaltooligosaccharide

INTRODUCTION

The perinatal period of sows is the transition stage from gestation to lactation, which generally refers to the combined period of late gestation and early lactation (10 days before after delivery). And sows are the core of modern large-scale pig production; their health and reproductive performance are the key to the economic benefits of pig farms. There were massive researches which suggest that the gut microbiota homeostasis of sow is important for the healthy gut development of their offspring during perinatal period (Zambrano et al., 2016; Grześkowiak et al., 2020). In addition, the physiological condition of suckling piglets is closely connected with the sows in the first weeks of life, including energy and nutrient supply (Klobasa et al., 1987; Gao et al., 2020), immunological protection (Salmon et al., 2009) and the microbial colonization of the gastrointestinal tract. So far, there are increasingly studies on the sow-piglet-axis, but there are not many systematic research literatures in this field.

Previous studies have demonstrated that a probiotic treatment of sows altered the composition of the gut microbiota in their offspring (Mori et al., 2011; Baker et al., 2013; Starke et al., 2013). Isomaltooligosaccharides (IMO), as a functional oligosaccharide, is considered to act as a prebiotic, since it can modulate the composition and metabolic activity of the gut microbiota, which might potentially enhance the health of the host organism (Ketabi et al., 2011). In particular, previous studies have shown that *Bifidobacterium* and *Lactobacillus* were increased in fecal microbiota, when different doses of IMO were supplemented to the diets (Ketabi et al., 2011; Yen et al., 2011; Likotrafiti et al., 2014). Besides, IMO is also known for its potential to activate the immune system and to enhance the host's resistance to diseases and oxidation (Wu et al., 2017). However, no studies have been conducted to evaluate the effects of dietary IMO in gestating and lactating sows, although dietary IMO supplementation directly improved immune status and diarrhea of piglets (Wang et al., 2016; Wu et al., 2017). This aspect might be interesting, as a modulation of the gut microbiota of the sows might also influence the structure and composition of bacteria in the intestinal tract of their piglets. In addition, few studies have evaluated the potential of prebiotics in the sow-piglet-axis up to now, particular IMO. Therefore, it is necessary to study on the mechanism of IMO supplementation with respect to sow-piglet-axis.

Consequently, the purpose of this study was to study the effects of dietary IMO levels on reproductive performance, colostrum composition, immune index and gut microbiota of sows and diarrhea of offspring.

MATERIALS AND METHODS

Animal, Diets and Experimental Design

The protocol of this study was approved by the Institution Animal Care and Use Committee of college of Animal Science and Technology, Hunan Agricultural University (Changsha, China), and was conducted in accordance with the National Institutes of Health (Changsha, China) guidelines for the care and use of experimental animals. The IMO (IMO-900; purity $\geq$ 90%, with total isomaltose, panose, and isomaltotriose contents $>$ 45%) was provided by the Baolingbao Biology Company (Shandong, China).

One hundred and twenty late pregnant sows (day 85 of gestation, PIC) with an initial body weight of 253.36 $\pm$ 14.30 kg and parity of 5.27 $\pm$ 1.58 were randomly allocated to 1 of 6 dietary treatments with 20 replicates based on body weight, parity and back fat. The treatments are: 1) a basal diet from late gestation to farrowing (CON group), 2) a basal diet plus 2.5g/kg, 5.0g/kg, 10.0g/kg, 20.0g/kg or 40.0g/kg IMO (IMO1, IMO2, IMO3, IMO4, or IMO5 groups). The composition of basal diets (**Supplementary Table 1**) was formulated in compliance with NRC (1998) nutrient requirements.

Sows were housed in 2.0 m $\times$ 0.6 m concrete-floored farrowing pen during day 85 to day 107 of gestation. The average amount fed to sows in each group was half provided at each feeding for a total of 2.6–2.8 kg, twice a day (08:00 am and 15:00 pm). During gestation day 108 to lactation, the sows were housed indoors in 2.13 m $\times$ 0.66 m concrete-floored delivery room pen. The average amount fed to sows in each group was half provided at each feeding for a total of 3.2 kg, twice a day (08:00 am and 16:30 pm). Before farrowing days 1–2, the average feeding amount dropped to 2.0 kg d^{-1}. On the farrowing day (day 0 of lactation), the sows initially received a total of 1.0 kg day^{-1} of their lactation diets, which was then increased by 0.8 kg day^{-1} on days 1 and 2 and by 1.0 kg day^{-1} on days 3 and 4 until arriving at their maximum feed intake. To feed sows diets *ad libitum* to ensure that the sow's trough has surplus fodder from day 5 of lactation to weaning. Sows were provided *ad libitum* access to water during the experimental period. The experiment was carried out in Hunan Xinguangan Agriculture and Animal Husbandry Co., Ltd. Pingjiang Branch (Xinguangan, Inc., Hunan, China), and the feeding management and immunization procedure were carried out in accordance

with the company's standard of breeding management. The trial lasted for 60 days.

Sample Collection

Seven sows per group were randomly selected for sample collection. Fresh feces were collected directly by massaging the rectum of sow on G107 and L10. Then, 60 samples stored in dry ice were transported to the laboratory and then stored at -80°C until analysis. A 10-mL blood sample of sow from the ear vein was collected on farrowing day within 2 h after delivery and L18 after an overnight fasting period of 16–18 h. Serum samples were obtained by centrifuging at 3,000 × *g* for 15 min at 4°C after standing for 1 h at 4°C. Then the samples were immediately stored at −80°C for the next analysis. Within two hours after farrowing, seven sows in each group were randomly selected for milk sample collection by hand-milking of four to six teats.

Reproductive Performance and Diarrhea Rate of Piglets

The total number of born, born alive, born robust (weight greater than 800 g), stillborn, and mummy number was recorded, so were average piglet birth weight (BW) at farrowing and lactation as well as average daily feed intake (ADFI) during lactation. On this basis, the survival rate of piglets, litter weight gain (from day 3 after birth to weaning) and total milk yield [(weaning litter weight-initial litter weight)/4] were calculated. In addition, from birth to weaning, the fecal score of piglets of each litter was recorded daily and their diarrhea rate during days 1–3, 1–7, 1–14, and 1–21 after birth were also be calculated.

Sow's Milk Composition and Immunity, and Serum D-Lactate and Lipopolysaccharides

The milk samples of sows in each group were separately analyzed for the concentrations of fat, protein, lactose, urea nitrogen, fatting dry matter, and total dry matter using a Milko-Scan FT 120 (Foss Electric, Hillerford, Denmark). Colostrum and serum concentrations of immunoglobulin G (IgG), immunoglobulin A (IgA), and immunoglobulin M (IgM) were determined by the radial immunodiffusion method using a commercial kit (Wuhan Biological Engineering Co., Ltd, Wuhan, China). Besides, the serum D-lactate (D-LA) and lipopolysaccharides (LPS) were assessed by ELISA using commercially available kits (Wuhan Biological Engineering Co., Ltd, Wuhan, China).

DNA Extraction 16S rDNA Amplification and 16S rRNA Sequencing

DNA was extracted from fecal samples of sows (G107 and L10) using a Stool DNA Isolation Kit (Tiangen Biotech Co., Ltd., Beijing, China). The V3–V4 hypervariable region of the bacterial 16S rRNA gene was amplified using universal primers (338F and 806R). For each fecal sample, a 10-digit barcode sequence was added to the 5' end of the forward and reverse primers (provided by Allwegene Company, Beijing, China). The PCR components contained 5 μL of Q5 reaction buffer (5×), 5 μL of Q5 High-Fidelity GC buffer (5×), 0.25 μL of Q5 high-fidelity

TABLE 1 | Effects of different doses of IMO on the reproductive performance of sows.

Items	CON	IMO[a]				*P*-value			
		2.5 g/kg	5.0 g/kg	10.0 g/kg	20.0 g/kg	40.0 g/kg	IMO1/CON	IMO2/CON	IMO3/CON	IMO4/CON	IMO5/CON
Total pigs born, *n*	12.68 ± 0.89	11.52 ± 0.60	13.00 ± 0.58	12.35 ± 0.51	12.61 ± 0.63	12.52 ± 0.52	0.084	0.577	0.216	0.695	0.087
Pigs born alive, *n*	11.58 ± 0.86	11.00 ± 0.55	11.94 ± 0.59	11.94 ± 0.52	11.80 ± 0.64	11.85 ± 0.53	0.085	0.290	0.561	0.712	0.120
Pigs born robust, *n*	11.26 ± 0.82	10.74 ± 0.56	11.46 ± 0.60	11.40 ± 0.52	11.51 ± 0.64	11.61 ± 0.54	0.254	0.530	0.659	0.205	0.200
Stillbirth number, *n*	1.08 ± 0.25	0.50 ± 0.22	1.07 ± 0.27	0.41 ± 0.24	0.80 ± 0.29	0.68 ± 0.24	0.553	0.147	0.410	0.139	0.494
Mummy number, *n*	0.15 ± 0.14	0.26 ± 0.13	0.22 ± 0.16	0.21 ± 0.14	0.20 ± 0.17	0.12 ± 0.14	0.037	0.124	0.049	0.012	0.917
Average piglet BW, kg	1.43 ± 0.05	1.43 ± 0.04	1.49 ± 0.05	1.44 ± 0.05	1.53 ± 0.06	1.42 ± 0.05	0.140	0.060	0.315	0.156	0.606
Survival rate,	0.95 ± 0.02	0.94 ± 0.02	0.97 ± 0.02	0.97 ± 0.02	0.95 ± 0.02	0.96 ± 0.02	0.722	0.124	0.120	0.306	0.613
Litter weight gain, kg	32.90 ± 2.03	35.04 ± 1.90	34.34 ± 2.04	34.91 ± 2.00	33.85 ± 2.20	31.71 ± 2.24	0.295	0.978	0.922	0.816	0.719
Lactation ADFI, kg	5.97 ± 0.15	5.90 ± 0.14	6.04 ± 0.15	5.95 ± 0.15	6.04 ± 0.16	5.87 ± 0.16	0.011	0.154	0.055	0.346	0.013

The results were expressed as mean ± SEM.

[a]*IMO: IMO1, 2.5 g/kg IMO group; IMO2, 5.0 g/kg IMO group; IMO3, 10.0 g/kg IMO group, IMO4, 20.0 g/kg IMO group, IMO5, 40.0 g/kg IMO group. BW, birth weight; ADFI, average daily feed intake.*

DNA polymerase (5 U/μL), 2 μL (2.5 mM) of dNTPs, 1 μL (10 uM) of each forward and reverse primer, 1 μL of DNA template, and 9.75 μL of ddH_2O. Cycling parameters were 98℃ for 5 min, followed by 25 cycles at 98℃ for 30 s, 52℃ for 30 s, and 72℃ for 1 min, and a final extension at 72℃ for 5 min. PCR amplicons were purified with Agencourt AMPure beads (Beckman Coulter, Indianapolis, IN, United States) and quantified using the PicoGreen dsDNA Assay Kit (Invitrogen, Carlsbad, CA, United States). After the individual quantification step, amplicons were pooled in equal amounts, and pair-end 2 × 300 bp sequencing was performed using the Illlumina MiSeq platform with MiSeq Reagent Kit v3 at Shanghai Personal Biotechnology Co., Ltd (Shanghai, China). The sequences were clustered into operational taxonomic units (OTUs) at a similarity level of 97% to generate rarefaction curves and to calculate the richness and diversity indices. OTUs representing <0.005% of the population were removed and taxonomy was assigned by the Ribosomal Database Project (RDP) classifier.

The Qiime[1] software (Caporaso et al., 2010) was employed to process the sequencing data and perform cluster analysis, ACE abundance indexing, and Simpson diversity indexing of the analysis results. In addition, USEARCH[2] was used to exclude chimeric sequences. Beta diversity analysis was used to investigate the structural variation of microbial communities across samples using UniFrac distance metrics. The Spearman's rho nonparametric correlations between the gut microbiota and immune-related indexes were determined using R packages (v3.5.2).

Statistical Analysis

An individual sow served as the experimental unit. All statistical analyses were performed using SPSS 20.0 software (SPSS Inc., Chicago, IL, United States). The differences among groups were compared using covariance analysis, one-way ANOVA and Duncan multiple range test. In addition, the reproductive performance and colostrum composition of sows were compared with use of independent-samples *T*-test, and the diarrhea rates of suckling piglets were compared with use of chi-square analysis. Significance was set at $P < 0.05$.

[1]V1.8.0, http://qiime.org/

[2]v5.2.236, http://www.drive5.com/usearch/

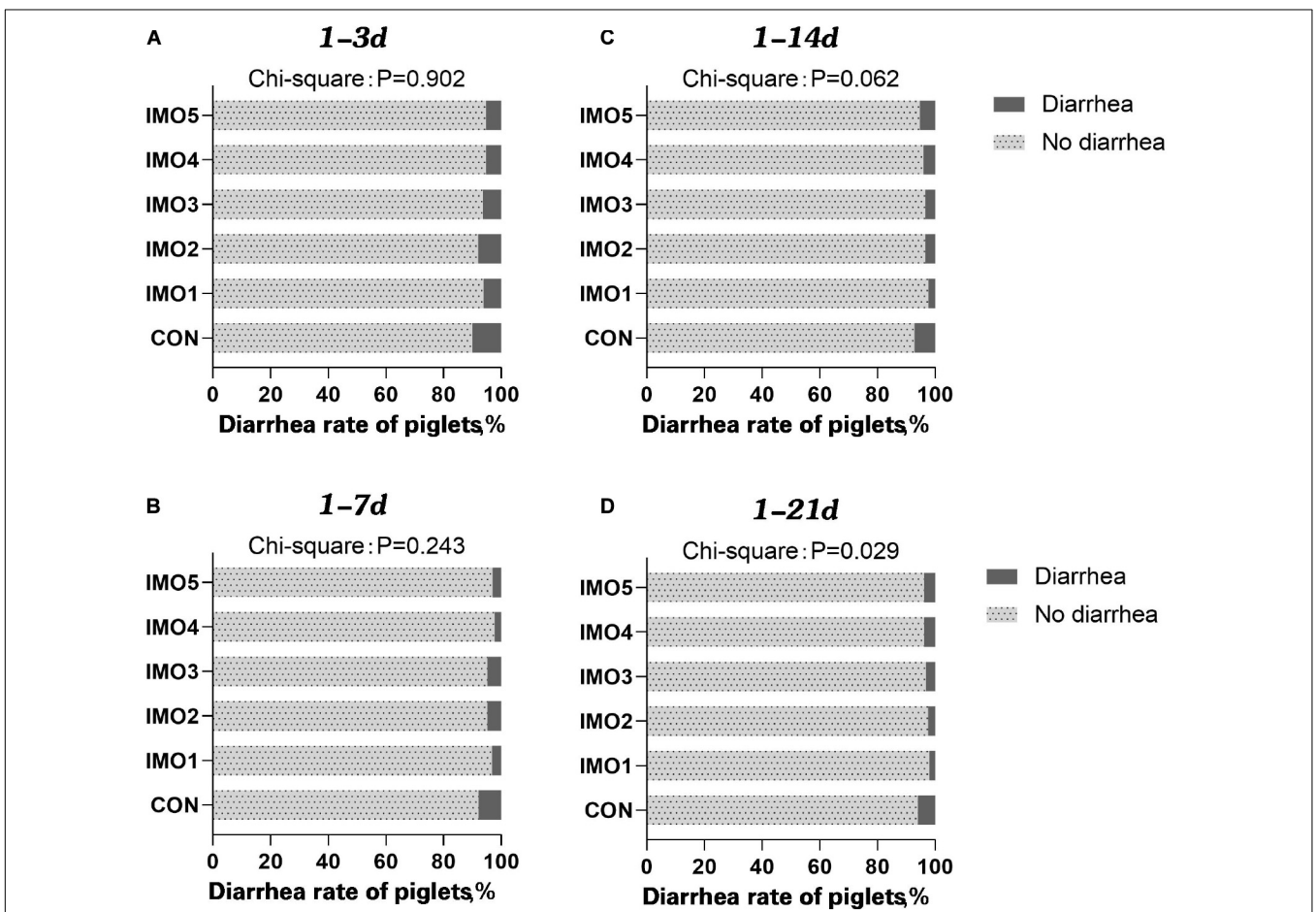

FIGURE 1 | Effects of different doses of IMO on the diarrhea of suckling piglets in a different stage [**(A)**, 1–3 days; **(B)** 1–7 days; **(C)** 1–14 days; **(D)** 1–21 days]. Data were compared with use of chi-square analysis ($P < 0.10$).

RESULTS

Reproductive Performance on Sows

The effects of dietary IMO levels on reproductive performance of sows were shown in **Table 1**. There were also no effects of IMO treatment on mainly reproductive performance of sows ($P > 0.05$), in addition to mummy number and lactation ADFI ($P < 0.05$).

The Diarrhea Rate of Suckling Piglets

The results of dietary IMO levels on diarrhea rate of piglets were shown in **Figure 1**. The diarrhea rate of piglets was awfully high at days 1 to 14 of lactation (1–14 days) and days 1 to 21 of lactation (1–21 days), whereas dietary IMO reversed the diarrhea rate of piglets in a dose-dependent manner ($P < 0.05$, **Figures 1C,D**).

The Colostrum Composition and Immunity of Sows

Effects of dietary IMO levels on colostrum composition and immunity were shown in **Table 2** and **Figure 2**. The results displayed that dietary IMO had no marked effect on the colostrum composition of sows ($P > 0.05$, **Table 2**). However, sows fed the IMO had a higher IgA, IgG, and IgM concentration in colostrum, with the highest values observed in IMO3 and IMO4 groups ($P < 0.001$, **Figure 2**).

The Serum Immunity of Sows

As shown in **Figure 3**, sows in the IMO5 group exhibited the highest concentrations of serum IgA, IgG, and IgM ($P < 0.05$) at farrowing. Besides, the IMO4 significantly increased the serum IgG concentration compared with CON, IMO1, and IMO2 groups ($P < 0.05$, **Figure 3B**).

The Serum Biomarker of Sows

At farrowing, the D-LA concentration in IMO1 group and LPS concentration in IMO1, IMO3, IMO4 and IMO5 groups were lower than those in the CON group (Linear, $P < 0.05$, **Figures 4A,C**). In addition, sows fed the diets containing IMO5 had a higher concentration of serum D-LA compared to IMO1 and IMO2 in L18 (Linear, $P < 0.05$), but the lower concentration of serum LPS was shown in IMO4 and IMO5 groups (Linear, $P < 0.05$, **Figures 4B,D**).

The Gut Microbiota Diversity and Composition of Sows

Isomaltooligosaccharide changed the gut microbiota diversity of sows in G107 and L10 but the trend was different. The Chao 1 and ACE diversity indices were significantly reduced by dietary IMO supplementation in sows (expect IMO1 group) compared with the CON group in G107 (Linear, $P < 0.05$, **Figure 5A**). The Simpson and Shannon diversity indices were increased in all IMO groups, and the significantly difference was observed among the CON group and IMO3 and IMO4 groups in L10 (Quadratic, $P < 0.05$, **Figure 5B**).

All 60 fecal samples were subjected to 16S rRNA gene sequencing. Illumina Miseq sequencing of the V3-V4

TABLE 2 | Effects of different doses of IMO on colostrum composition of sows.

Items	CON	IMO[a]				*P*-value			
		2.5 g/kg	5.0 g/kg	10.0 g/kg	20.0 g/kg	40.0 g/kg	IMO1/CON	IMO2/CON	IMO3/CON	IMO4/CON	IMO5/CON
Milk fat, %	0.92 ± 0.07	0.88 ± 0.10	0.79 ± 0.08	0.78 ± 0.05	0.77 ± 0.06	0.81 ± 0.12	0.601	0.660	0.382	0.700	0.279
Milk protein, %	2.99 ± 0.19	2.65 ± 0.22	3.06 ± 0.10	2.98 ± 0.13	3.05 ± 0.15	2.82 ± 0.19	0.228	0.171	0.303	0.676	0.798
Milk lactose, %	0.67 ± 0.02	0.69 ± 0.02	0.69 ± 0.02	0.69 ± 0.03	0.65 ± 0.02	0.70 ± 0.02	0.684	0.915	0.712	0.911	0.918
Milk urea nitrogen, mg·dL^{-1}	10.70 ± 0.28	9.72 ± 0.85	9.58 ± 0.68	9.38 ± 0.39	10.15 ± 0.53	9.10 ± 0.74	0.296	0.515	0.320	0.772	0.749
Milk total dry matter, %	5.93 ± 0.20	5.62 ± 0.26	5.89 ± 0.14	5.80 ± 0.12	5.81 ± 0.17	5.72 ± 0.26	0.192	0.348	0.282	0.077	0.832
Milk somatic cell count, ml^{-1}	135.50 ± 15.4	173.50 ± 25.8	139.00 ± 25.8	162.00 ± 27.7	128.00 ± 2.74	179.00 ± 15.98	0.060	0.067	0.704	0.216	0.084

The results were expressed as mean ± SEM.

[a]*IMO: IMO1, 2.5 g/kg IMO group; IMO2, 5.0 g/kg IMO group; IMO3, 10.0 g/kg IMO group, IMO4, 20.0 g/kg IMO group, IMO5, 40.0 g/kg IMO group.*

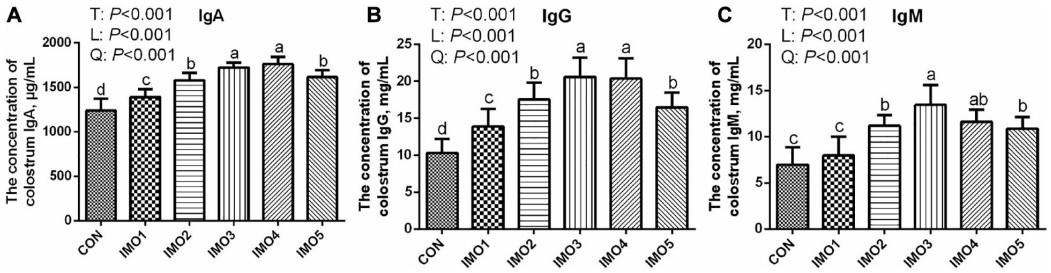

FIGURE 2 | Effects of dietary isomaltooligosaccharide (IMO) levels on the concentrations of colostrum IgA **(A)**, IgG **(B)**, and IgM **(C)**. Data are presented as means ± SD (n = 7). (a–d) Significant effects of treatment ($P < 0.05$; values with different lowercase letters are significantly different; T, total; L, linear; Q, quadratic).

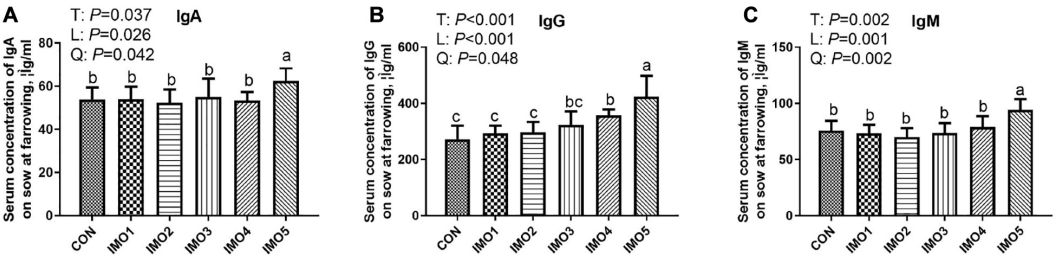

FIGURE 3 | Effects of dietary isomaltooligosaccharide (IMO) levels on the concentrations of serum IgA **(A)**, IgG **(B)**, and IgM **(C)**. Data are presented as means ± SD (n = 7). (a–c) Significant effect of treatment ($P < 0.05$; values with different lowercase letters are significantly different; T, total; L, linear; Q, quadratic).

regions of bacterial 16S rRNA genes generated 1,094,499 and 1,132,136 high-quality sequences in G107 and L10, respectively (**Supplementary Table 2**). On the basis of 97% sequence similarity, we obtained 7,806 and 7,969 OTUs in G107 and L10, respectively. Further, variations in the microbial composition of all groups were explored. LEfSe analysis of the bacterial community was used to filter the significantly different OTUs among groups and the results showed that there exist dramatic differences in microbial composition between the treatment groups and the CON group (**Supplementary Figure 1**). There were no significant difference in the relative abundance of bacterial p_*Firmicutes* and p_*Bacteroidet*es and its ratio (F/B) among the all treatment groups in G107 and L10 ($P > 0.05$, **Figures 6A–C**, **7A,B**). g_*Lactobacillus* increased but g_*YRC22* showed a remarkable reduction in IMO4 group compared with the CON group in G107 (Linear, $P < 0.05$, **Figures 6D,E**). Sows in IMO3 group had a highest relative abundance of g_*Unclassified_Coriobacteriaceae* and g_*Slackia*, and it significantly differ from IMO2, IMO4, and IMO5 groups in the relative abundance of g_*Unclassified_Coriobacteriaceae* and CON group, IMO1,IMO2, IMO4, and IMO5 groups in the relative abundance of g_*Slackia* (Total, $P < 0.05$, **Figures 6F,H**). Besides, the relative abundance of g_*Parabacteroides* was enhanced in IMO2 and IMO3 groups (Quadratic, $P < 0.05$, **Figure 6G**) and the relative abundance of g_*Bifidobacterium* was increased in IMO4 and IMO5 groups ($P > 0.05$, **Figure 6I**). At the genus level, the relative abundances of g_*Unclassified_Ruminococcaceae* and g_*Coprococcus* were the highest (Total, $P < 0.05$, **Figures 7C,E**) but the g_*Unclassified_Peptostreptococcaceae* and g_*Sarcina* was the lowest in IMO4 group in L10 ($P < 0.05$, **Figures 7D,G**). In addition, the relative abundances of g_*Unclassified_Peptostreptococcaceae*, g_*Turicibacter* and g_*Sarcina* were the highest in IMO2 group (Quadratic, $P < 0.05$, **Figures 7D,F,G**) and the relative abundance of g_*Akkermansia* was the highest in IMO1 group ($P > 0.05$, **Figure 7H**). Furthermore, IMO increased the relative abundance of g_*Bifidobacterium* compared with the CON ($P > 0.05$, **Figure 7I**). Therefore, the above results indicated that the gut microbiota composition of sows was profoundly altered during late pregnancy and lactation.

Correlations Between Gut Microbiota and Serum Biomarker and Colostric Immunoglobulin

A Spearman's correlation analysis was performed to evaluate the potential link between alterations in gut microbiota composition in G107 and L10 and serum D-LA, LPS, IgA, IgG, and IgM of sows at farrowing and L18 or IgA, IgG, and IgM in colostrum of sows at farrowing (**Figure 8**). The serum D-LA and LPS at farrowing was negatively correlated with the genus g_*Akkermansia* and g_*Parabacteroides* in L10 ($P < 0.05$), respectively. However, the serum LPS in L18 was positively correlated with the genus g_*YRC22* in G107 and the genus g_*Unclassified_Peptostreptococcaceae* in L10 ($P < 0.05$). Moreover, the IgA, IgG, and IgM in colostrum of sows at farrowing was positively correlated with the genus g_*Parabacteroides* and g_*Slackia* in G107 and g_*Coprococcus* in L10 but negatively correlated with the genus g_*YRC22* in G107 ($P < 0.05$).

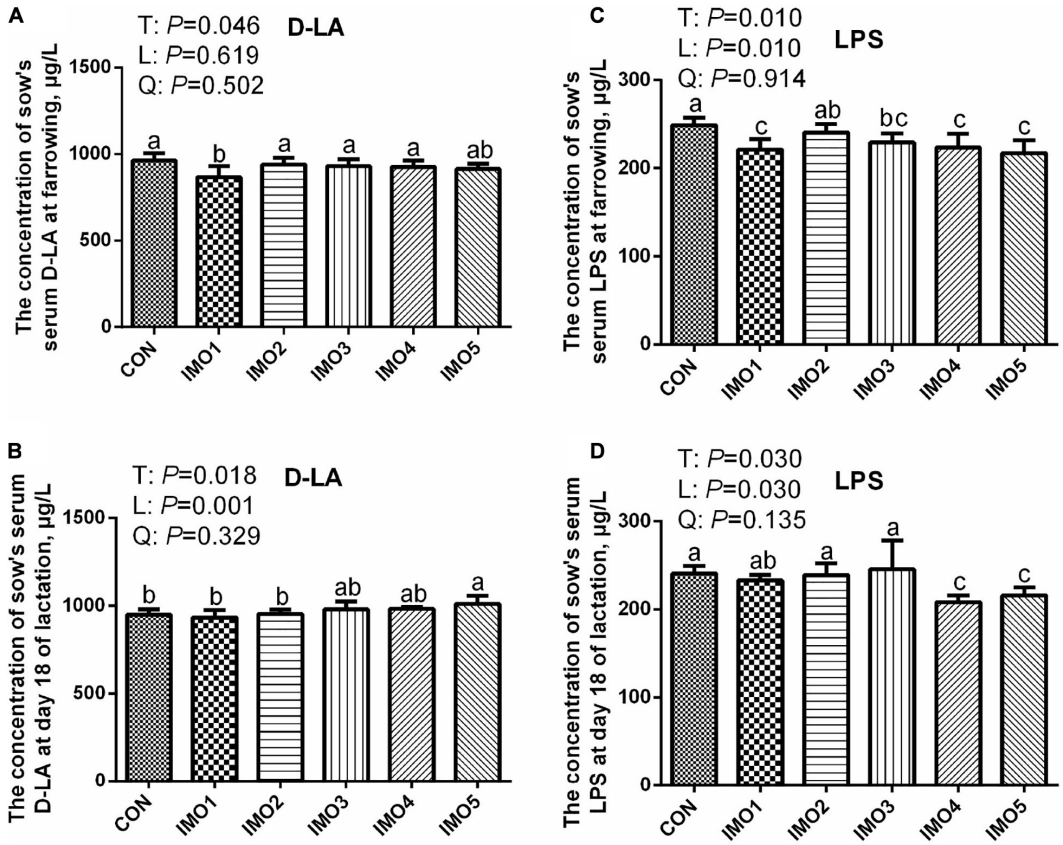

FIGURE 4 | Effects of dietary isomaltooligosaccharide (IMO) levels on the concentrations of sows' serum D-LA **(A)** and LPS **(C)** at farrowing as well as serum D-LA **(B)** and LPS **(D)** at day 18 of lactation. Data are presented as means ± SD (n = 7). (a–c) Significant effect of treatment ($P < 0.05$; values with different lowercase letters are significantly different; T, total; L, linear; Q, quadratic).

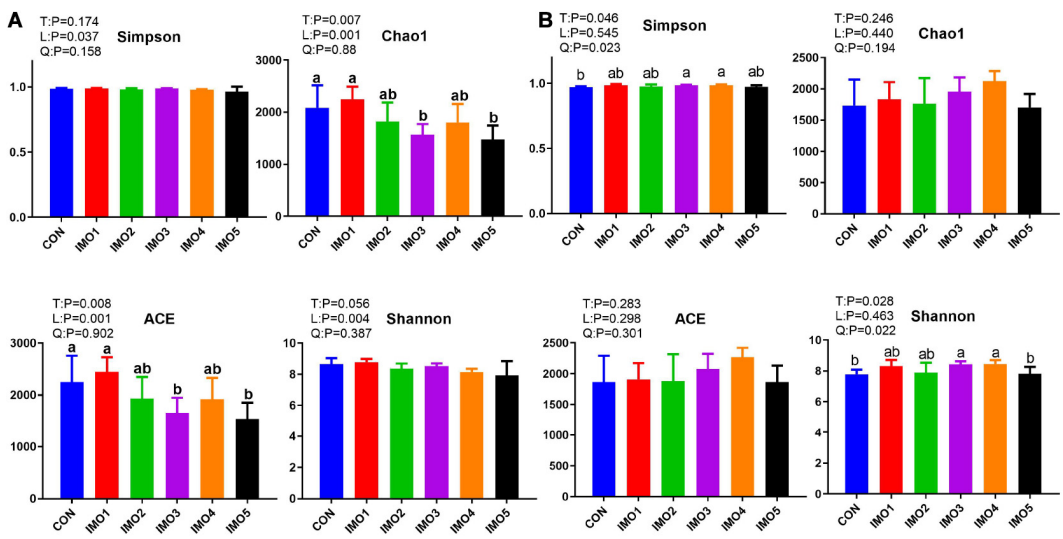

FIGURE 5 | Effects of dietary isomaltooligosaccharide (IMO) levels on the α-diversity of gut microbiota at day 107 of gestation **(A)** and at day 10 of lactation **(B)** of sows. Simpson index, Chao1 index, ACE index, and Shannon index. Data are presented as means ± SD (n = 5). (a–c) Significant effect of treatment ($P < 0.05$; values with different lowercase letters are significantly different; T, total; L, linear; Q, quadratic).

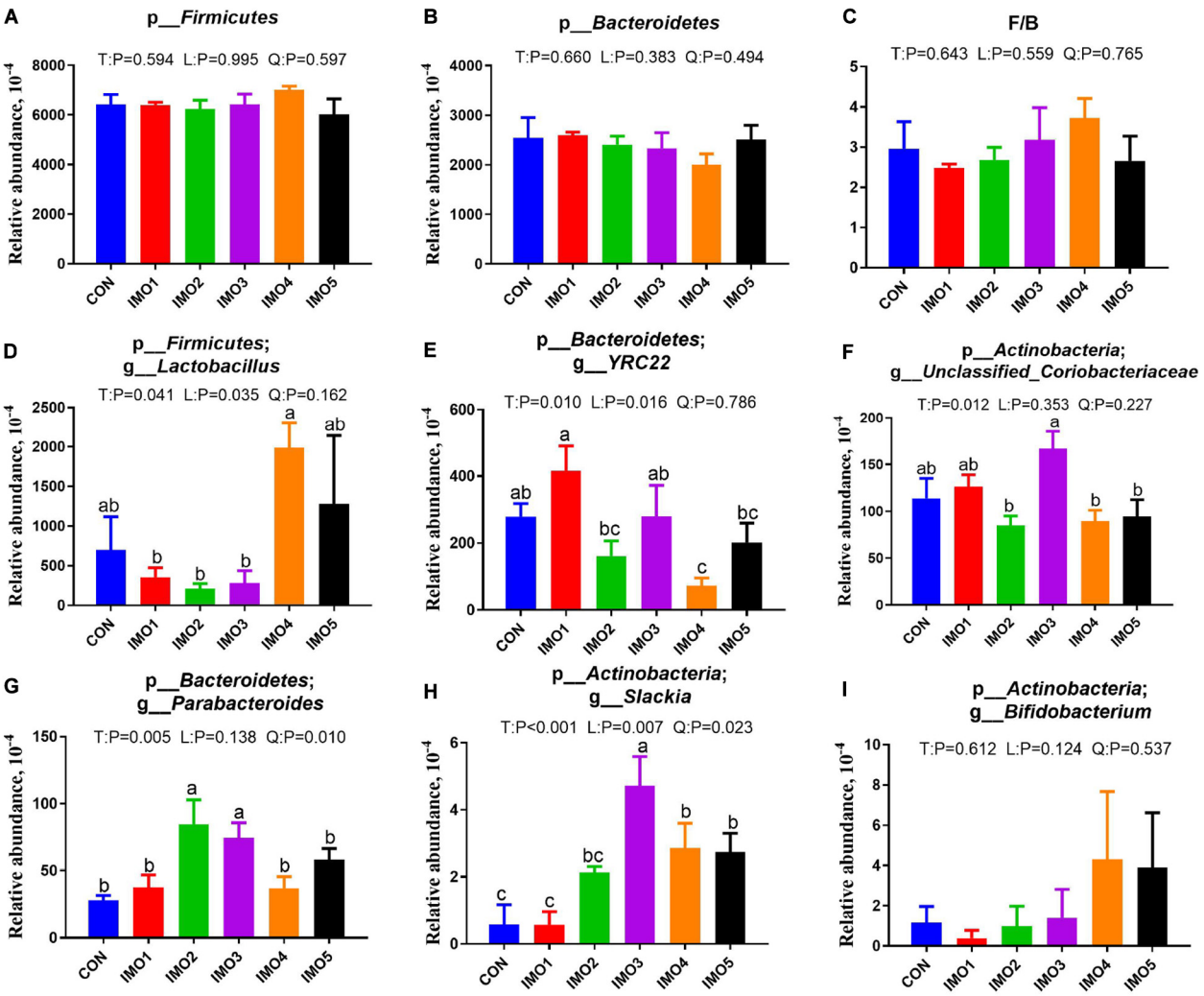

FIGURE 6 | Effects of dietary isomaltooligosaccharide (IMO) levels on the gut microbiota compositions at the phylum level in sows. **(A)** p_*Firmicutes*, **(B)** p_*Bacteroidetes*, **(C)** F/B, *Firmicutes/Bacteroidetes*, **(D)** p_*Firmicutes*; g_*Lactobacillus*, **(E)** p_*Bacteroidetes*;g_*YRC22*, **(F)** p_*Actinobacteria*; g_*Unclassified_Coriobacteriaceae*, **(G)** p_*Bacteroidetes*; g_*Parabacteroides*, **(H)** p_*Actinobacteria*; g_*Slackia*, **(I)** p_*Actinobacteria*; g_*Bifidobacterium*. Data are presented as means ± SEM (n = 5). (a–c) Significant effect of treatment (P < 0.05; values with different lowercase letters are significantly different; T, total; L, linear; Q, quadratic).

DISCUSSION

The health of sow plays a crucial role in the pig production, and sows' reproductive performance is an important index of economic benefit of pig farm. However, sows in the late gestation due to rapid fetal growth caused by insulin resistance and the body's metabolic syndrome will lead to gut microbiota disorder, which will affect the reproductive performance of the sows and the growth and health of their offspring (Tan et al., 2016; Cheng et al., 2020). IMO is one of the oligosaccharides which produced by enzymatic conversion of starch and widely used in the food and feed industry, which has a wide spectrum of biological activities (Ketabi et al., 2011). Previous studies have shown that dietary oligosaccharides supplementation in sows improves sows' performance by regulating the homeostasis of gut microbiota (Li et al., 2012; Duan et al., 2019). Contrary to these results, our current study showed that IMO supplementation exerted no effects on the mainly reproductive performance of sows. This discrepancy could be attributed to the time phase of IMO supplementation and different polymerization degree of commercial IMO (Hu et al., 2013).

Interestingly, we found that dietary IMO supplementation in sows significantly reduced the diarrhea rate of piglets during lactation, especially for low dose. Consistently, Wang et al. (2016) reported that the diarrhea rate of piglets linearly declined as the IMO level increased, and the beneficial effects may be due to enhanced immune status of pigs. During lactation, milk is one of the most important ways that the sows connect with its offspring (Wu et al., 2020). Moreover, the breast milk is the only source of the energy and immunity

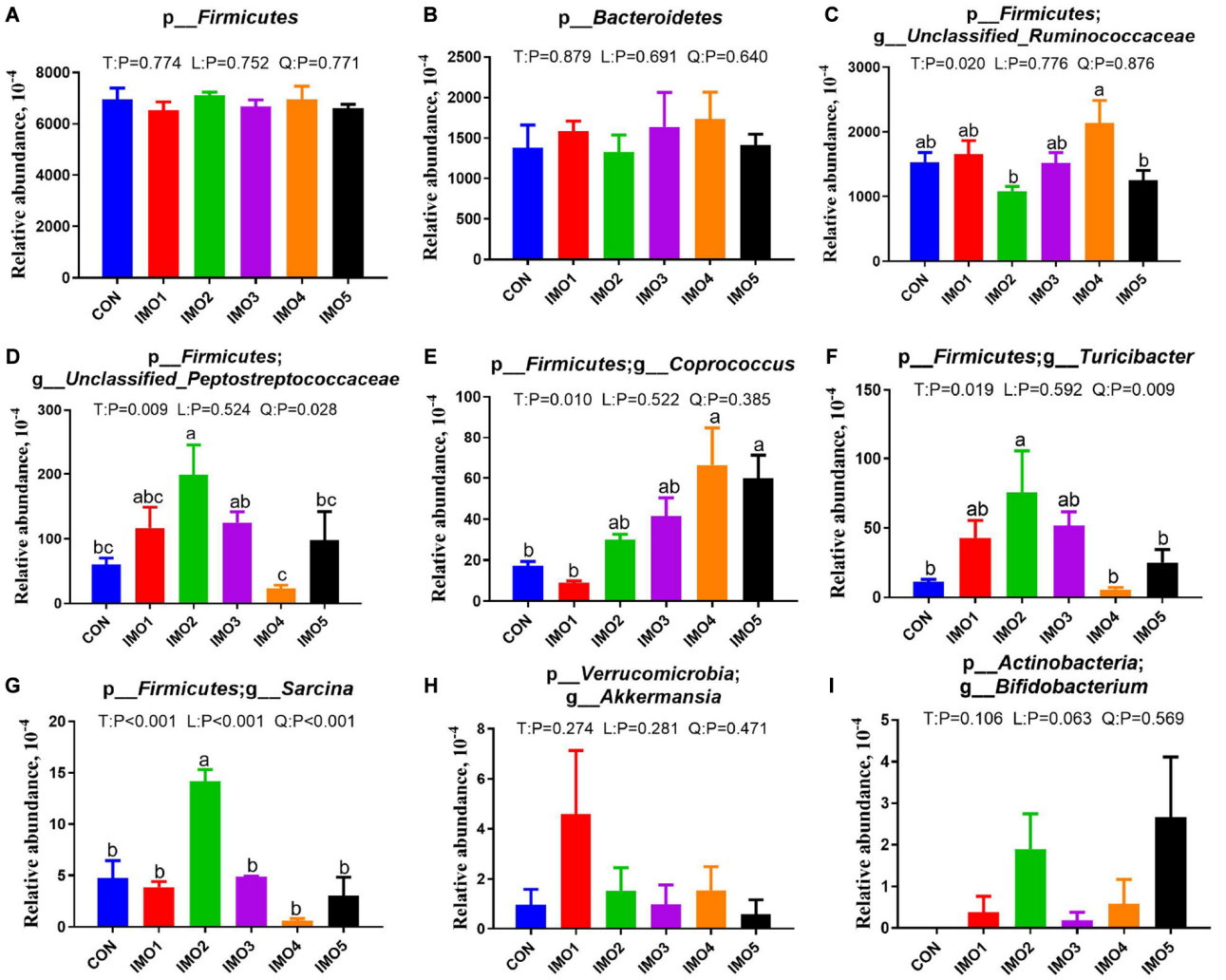

FIGURE 7 | Two major bacterial phyla and the changes in the seven distinct genera in gut microbiota composition of sows at day 10 of lactation. **(A)** p_*Firmicutes*, **(B)** p_*Bacteroidetes*, **(C)** p_*Firmicutes*; g_*Unclassified_Ruminococcaceae*, **(D)** p_*Firmicutes*; g_*Unclassified_Peptostreptococcaceae*, **(E)** p_*Firmicutes*; g_*Coprococcus*, **(F)** p_*Firmicutes*; g_*Turicibacter*, **(G)** p_*Firmicutes*; g_*Sarcina*, **(H)** p_*Verrucomicrobia*; g_*Akkermansia*, **(I)** p_*Actinobacteria*; g_*Bifidobacterium*. Data are presented as means ± SEM ($n = 5$). (a–c) Significant effect of treatment ($P < 0.05$; values with different lowercase letters are significantly different; T, total; L, linear; Q, quadratic).

of the piglets (Xie et al., 2015), which contributes to immune system maturation, organ development, and healthy microbial colonization (Parigi et al., 2015). Many studies have showed that the milk composition and its immuneglobulin concentration play key roles in the healthy growth and development of piglets (Lonnroth et al., 1988; Charneca et al., 2015), which is closely related to the gut microbiota (Solís et al., 2010; Burton et al., 2017) and may affect the growth and development of the piglets (Kirmiz et al., 2018). A recent study indicated that chitooligosaccharides supplementation modified milk composition (Cheng et al., 2015). Similarly, previous studies have also shown that the sows fed mannanoligosaccharides improved the colostrum and milk IgA IgG, IgM, and the serum IgG level in the suckling piglets (Newman and Newman, 2001). Especially during early lactation, the diarrhea of piglets occurred due to the colostrum immunoglobulin. Therefore, we measured the colostrum composition and immunoglobulin (IgA, IgG, and IgM) of sows. We found that IMO supplementation did not affect colostrum composition of sows, but improved the concentrations of colostrum IgA, IgG, and IgM, which may explain why the diarrhea rate of piglets decreased.

In addition, the injury of gut barrier function is also closely related to the milk quality. Perez et al. (2007) found that intestinally derived bacterial components are transported to the lactating breast within mononuclear cells, which affected the milk quality and the offspring health. Bacterial translocation usually caused by the destruction of gut barrier (MacFie, 2000). The concentrations of serum LPS and D-LA can be used to give expression to the gut barrier function, and if its concentration improved in serum, the gut barrier have been

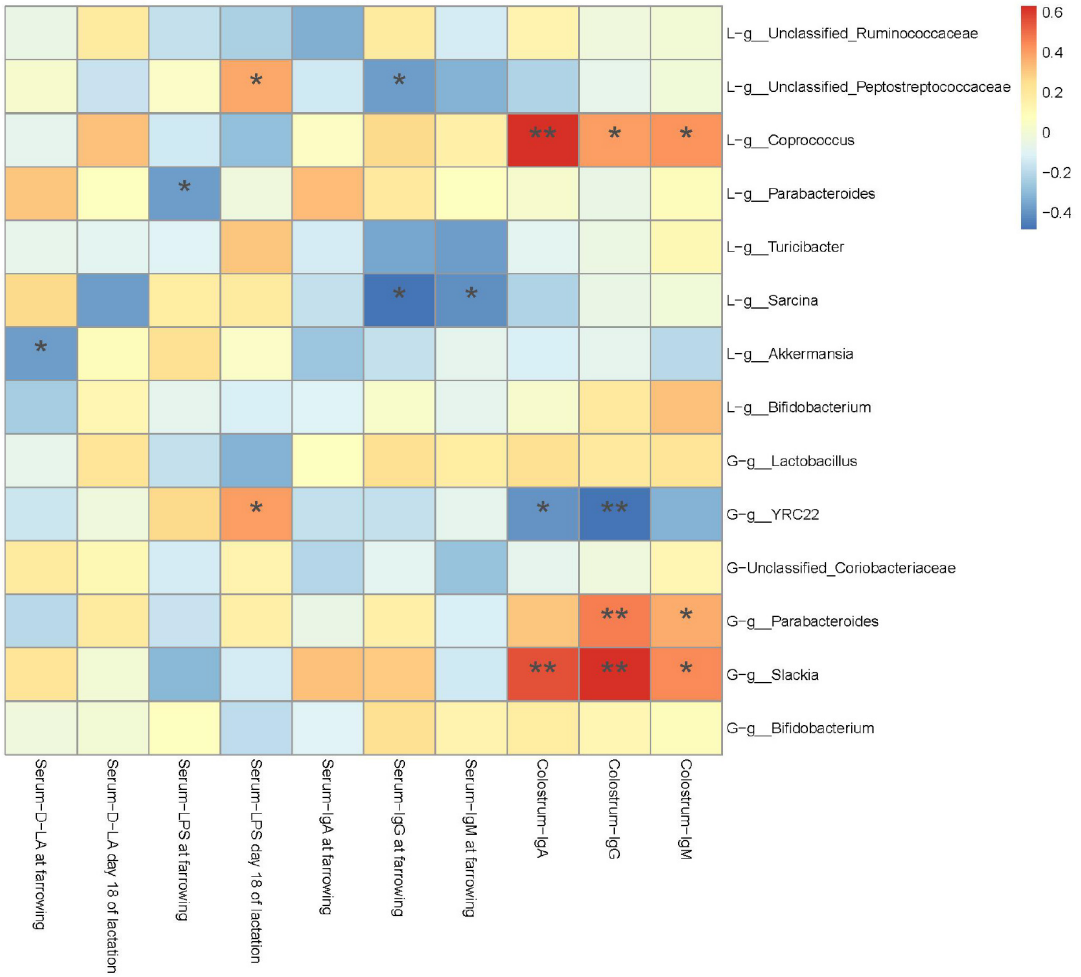

FIGURE 8 | Heatmap of the Spearman's *r* correlations between the gut microbiota significantly modified by different dietary treatments and period of sows. Data are presented as means ± SEM (n = 5 or 7). *$P < 0.05$; **$P < 0.01$ (following the Spearman's correlation analysis). G, at day 107 of gestation; L, at day 10 of lactation.

destroyed (Xu et al., 2018). In the present study, the diets of sows containing IMO especially at low and high doses have lower concentrations of serum LPS and D-LA at farrowing and L18, which reflected that the function of IMO protected the intestinal barriers.

The gut microbiota is one of the most important intestinal barriers, whose homeostasis will also affect the body immunity, including the milk immunity (Rooks and Garrett, 2016). As we know, the level of immunoglobulin expression in serum of sows can immediately reflect the body immunity, which will also cause the changes of gut bacteria. In the present study, we found that IMO with different doses changed the concentrations of serum IgA, IgG, and IgM, especially IMO5 was very significant increased the immunoglobulin expression in serum of sows. To some extent, this suggests that IMO can increase the immunity of perinatal sows, which influence the structure of gut microbiota in sows. Furthermore, the establishment of gut microbiota of piglets was influenced by sow's gut microbiota, which has already been demonstrated after a probiotic treatment of mother sows (Mori et al., 2011; Baker et al., 2013; Starke et al., 2013). Recent studies have suggested that diarrhea is strongly related to the dysbiosis of gut microbiota (Shrivastava et al., 2017; The et al., 2018). In addition, the disorderliness of gut microbiota during perinatal period of sows will affect its milk quality and gut microbiota of piglets, which may lead to diarrhea in piglets. Therefore, the functional pro(e)biotic supplementation to the diets of sows during perinatal period may improve the diarrhea of piglets by regulating sow's gut microbiota.

In the present study, we found that IMO with different doses changed the composition and structure of the gut microbiota of perinatal sows, especially G107 and L10. Except for the numbers of g_*YRC22*, the bacterial groups in the feces of the sows were increased with varying degrees by the dietary inclusion of IMO. In G107, dietary supplementation of IMO increased the abundance of g_*Parabacteroides*, belonging to p_*Bacteroidetes*, which were comprises anti-inflammatory bacteria (Ishioka et al., 2017). The relative abundance of bacterial g_*Slackia*, belonging to p_*Actinobacteria*, was also increased. It can produce some

bioactive substances to play a protective role and correlated with immunity. The same as our result, g_*Parabacteroides* and g_*Slackia* were closely correlated with colostrum IgA, IgG, and IgM, which may influence the diarrhea of piglets by this way.

Moreover, dietary supplementation of IMO in L10 can also significantly enhanced the relative abundance of bacterial g_*Unclassified_Peptostreptococcaceae*, g_*Coprococcus*, g_*Turicibacter* and g_*Sarcina*, which both belong to the p_*Firmicutes*. g_*Unclassified_Peptostreptococcaceae* was the dominant bacteria genus to produce the volatile fatty acids (VFAs), which contributed to the energy metabolism of host (Li et al., 2018). g_*Coprococcus* have been found to play beneficial roles in maintaining intestinal stability, also reported as the butyrate-producing genus (Nishino et al., 2018). g_*Turicibacter* and g_*Sarcina* are also in connection with intestinal barrier function and inflammation (Liu et al., 2014; Le Sciellour et al., 2019). It systematically enhancing effect of dietary IMO on the numbers of beneficial bacterium in sows can be assumed.

CONCLUSION

In conclusion, IMO could reduce the diarrhea rate of their offspring, the effects might be attributed to the enhanced immune system of piglets. This suggests that the reduced rate of diarrhea in piglets is mainly because of the role of immunoglobulin in the sows' milk, although the IMO still had a significant influence in sows' gut microbiota, which was significantly correlated with immunoglobulin in milk. In our studies, it has evaluated the potential of IMO with regard to the sow-piglet-axis, but the concrete mechanism needs to be further researched.

DATA AVAILABILITY STATEMENT

The original contributions presented in the study are publicly available. This data can be found here: https://www.ncbi.nlm.nih.gov/bioproject/PRJNA681971.

ETHICS STATEMENT

The animal study was reviewed and approved by the National Institutes of Health (Changsha, China) guidelines for the care and use of experimental animals.

AUTHOR CONTRIBUTIONS

ZYF, ZHS, and XH conceived and designed the experiment. LLZ, XLG, JW, and SL performed the experiments. LLZ, XLG, and HL analyzed the data and wrote the manuscript. YHD and ZYF revised the manuscript. All authors contributed to the article and approved the submitted version.

FUNDING

This study was jointly supported by funding from National Natural Science Foundation of China (U20A2054), the National Key R&D Program of Intergovernmental Key Projects of China (2018YFE0101700), Double first-class construction project of Hunan Agricultural University (SYL201802015 and SYL201802009), and Support project for Scientific and Technical Talents in Hunan Province (2020TJ-Q02).

ACKNOWLEDGMENTS

The authors extend their gratitude to the staff of Hunan Agricultural University and Hunan Xinguangan Agriculture and Animal Husbandry Co., Ltd., Pingjiang Branch (Xinguangan, Inc., Hunan, China) and to their graduate students for their assistance in this study.

SUPPLEMENTARY MATERIAL

The Supplementary Material for this article can be found online at: https://www.frontiersin.org/articles/10.3389/fmicb.2020.588986/full#supplementary-material

REFERENCES

Baker, A. A., Davis, E., Spencer, J. D., Moser, R., and Rehberger, T. (2013). The effect of a bacillus-based direct-fed microbial supplemented to sows on the gastrointestinal microbiota of their neonatal piglets. *J. Anim. Sci.* 91, 3390–3399. doi: 10.2527/jas.2012-5821

Burton, K. J., Rosikiewicz, M., Pimentel, G., Bütikofer, U., von Ah, U., et al. (2017). Probiotic yogurt and acidified milk similarly reduce postprandial inflammation and both alter the gut microbiota of healthy, young men. *Br. J. Nutr.* 117, 1312–1322. doi: 10.1017/S0007114517000885

Caporaso, J. G., Kuczynski, J., Stombaugh, J., Bittinger, K., Bushman, F. D., Costello, E. K., et al. (2010). Qiime allows analysis of high-throughput community sequencing data. *Nat. Methods* 7, 335–336. doi: 10.1038/nmeth.f.303

Charneca, R., Vila-Viçosa, M. J., Infante, P., Nunes, J., and Le Dividich, J. (2015). Colostrum production of alentejano and large-white × landrace sows: consumption, passive immunity and mortality of piglets. *Spanish J. Agric. Res.* 13, e611. doi: 10.5424/sjar/2015134-7537

Cheng, C., Wu, X., Zhang, X., Zhang, X., and Peng, J. (2020). Obesity of sows at late pregnancy aggravates metabolic disorder of perinatal sows and affects performance and intestinal health of piglets. *Animals* 10, 49. doi: 10.3390/ani10010049

Cheng, L. K., Wang, L. X., Xu, Q. S., Huang, L. J., Zhou, D. S., Li, Z., et al. (2015). Chitooligosaccharide supplementation improves the reproductive performance and milk composition of sows. *Livest. Sci.* 174, 74–81. doi: 10.1016/j.livsci.2015.02.003

Duan, X., Tian, G., Chen, D., Huang, L., Zhang, D., Zheng, P., et al. (2019). Mannan oligosaccharide supplementation in diets of sow and (or) their offspring improved immunity and regulated intestinal bacteria in piglet1. *J. Anim. Sci.* 97, 4548–4556. doi: 10.1093/jas/skz318

Gao, L. M., Liu, Y. L., Zhou, X., Zhang, Y., Wu, X., and Yin, Y. L. (2020). Maternal supplementation with uridine influences fatty acid and amino acid constituents

of offspring in a sow-piglet model. *Br. J. Nutr.* doi: 10.1017/S0007114520003165 [Epub ahead of print].

Grześkowiak, A., Teske, J., Zentek, J., and Vahjen, W. (2020). Distinct patterns of microbial metabolic fingerprints in sows and their offspring: a pilot study. *Arch. Microbiol.* 202, 511–517. doi: 10.1007/s00203-019-01766-1

Hu, Y., Ketabi, A., Buchko, A., and Ganzle, M. G. (2013). Metabolism of isomalto-oligosaccharides by *Lactobacillus reuteri* and bifidobacteria. *Lett. Appl. Microbiol.* 57, 108–114. doi: 10.1111/lam.12076

Ishioka, M., Miura, K., Minami, S., Shimura, Y., and Ohnishi, H. (2017). Altered gut microbiota composition and immune response in experimental steatohepatitis mouse models. *Digest. Dis. Sci.* 62, 396–406. doi: 10.1007/s10620-016-4393-x

Ketabi, A., Dieleman, L. A., and Ganzle, M. G. (2011). Influence of isomalto-oligosaccharides on intestinal microbiota in rats. *J. Appl. Microbiol.* 110, 1297–1306. doi: 10.1111/j.1365-2672.2011.04984.x

Kirmiz, N., Robinson, R. C., Shah, I. M., Barile, D., and Mills, D. A. (2018). Milk glycans and their interaction with the infant-gut microbiota. *Annu. Rev. Food Sci. Technol.* 9, 429–450. doi: 10.1146/annurev-food-030216-030207

Klobasa, F., Werhahn, E., and Butler, J. E. (1987). Composition of sow milk during lactation. *J. Anim. Sci.* 64, 1458–1466. doi: 10.2527/jas1987.6451458x

Le Sciellour, M., Zemb, O., Hochu, I., Riquet, J., Gilbert, H., Giorgi, M., et al. (2019). Effect of chronic and acute heat challenges on fecal microbiota composition, production, and thermoregulation traits in growing pigs1,2. *J. Anim. Sci.* 97, 3845–3858. doi: 10.1093/jas/skz222

Li, M., Bauer, L. L., Chen, X., Wang, M., Kuhlenschmidt, T. B., Kuhlenschmidt, M. S., et al. (2012). Microbial composition and in vitro fermentation patterns of human milk oligosaccharides and prebiotics differ between formula-fed and sow-reared piglets. *J. Nutr.* 142, 681–689. doi: 10.3945/jn.111.154427

Li, X., Liu, G., Liu, S., Ma, K., and Meng, L. (2018). The relationship between volatile fatty acids accumulation and microbial community succession triggered by excess sludge alkaline fermentation. *J. Environ. Manag.* 223, 85–91. doi: 10.1016/j.jenvman.2018.06.002

Likotrafiti, E., Tuohy, K. M., Gibson, G. R., and Rastall, R. A. (2014). An in vitro study of the effect of probiotics, prebiotics and synbiotics on the elderly faecal microbiota. *Anaerobe* 27, 50–55. doi: 10.1016/j.anaerobe.2014.03.009

Liu, J., Xu, T., Zhu, W., and Mao, S. (2014). High-grain feeding alters caecal bacterial microbiota composition and fermentation and results in caecal mucosal injury in goats. *Br. J. Nutr.* 112, 416–427. doi: 10.1017/S0007114514000993

Lonnroth, I., Martinsson, K., and Lange, S. (1988). Evidence of protection against diarrhoea in suckling piglets by a hormone-like protein in the sow's milk. *Zentralbl Veterinarmed B* 35, 628–635. doi: 10.1111/j.1439-0450.1988.tb00537.x

MacFie, J. (2000). Enteral versus parenteral nutrition: the significance of bacterial translocation and gut-barrier function. *Nutrition* 16, 606–611. doi: 10.1016/s0899-9007(00)00249-5

Mori, K., Ito, T., Miyamoto, H., Ozawa, M., Wada, S., Kumagai, Y., et al. (2011). Oral administration of multispecies microbial supplements to sows influences the composition of gut microbiota and fecal organic acids in their post-weaned piglets. *J. Biosci. Bioeng.* 112, 145–150. doi: 10.1016/j.jbiosc.2011.04.009

Newman, K. E., and Newman, K. C. (2001). Evaluation of mannanoligosaccharides on the microflora and immunoglobulin status of sows and piglet performance. *J. Anim. Sci. Biotechnol.* 79, 189. doi: 10.1186/s40104-020-00480-z

Nishino, K., Nishida, A., Inoue, R., Kawada, Y., Ohno, M., Sakai, S., et al. (2018). Analysis of endoscopic brush samples identified mucosa-associated dysbiosis in inflammatory bowel disease. *J. Gastroenterol.* 53, 95–106. doi: 10.1007/s00535-017-1384-4

Parigi, S. M., Eldh, M., Larssen, P., Gabrielsson, S., and Villablanca, E. J. (2015). Breast milk and solid food shaping intestinal immunity. *Front. Immunol.* 6:415. doi: 10.3389/fimmu.2015.00415

Perez, P. F., Dore, J., Leclerc, M., Levenez, F., Benyacoub, J., Serrant, P., et al. (2007). Bacterial imprinting of the neonatal immune system: lessons from maternal cells? *Pediatrics* 119, e724–e732. doi: 10.1542/peds.2006-1649

Rooks, M. G., and Garrett, W. S. (2016). Gut microbiota, metabolites and host immunity. *Nat. Rev. Immunol.* 16, 341–352. doi: 10.1038/nri.2016.42

Salmon, H., Berri, M., Gerdts, V., and Meurens, F. (2009). Humoral and cellular factors of maternal immunity in swine. *Dev. Comp. Immunol.* 33, 384–393. doi: 10.1016/j.dci.2008.07.007

Shrivastava, A. K., Kumar, S., Mohakud, N. K., Suar, M., and Sahu, P. S. (2017). Multiple etiologies of infectious diarrhea and concurrent infections in a pediatric outpatient-based screening study in Odisha, India. *Gut Pathog.* 9, 16. doi: 10.1186/s13099-017-0166-0

Solís, G., de Los Reyes-Gavilan, C. G., Fernández, N., Margolles, A., and Gueimonde, M. (2010). Establishment and development of lactic acid bacteria and bifidobacteria microbiota in breast-milk and the infant gut. *Anaerobe* 16, 307–310. doi: 10.1016/j.anaerobe.2010.02.004

Starke, I. C., Pieper, R., Neumann, K., Zentek, J., and Vahjen, W. (2013). Individual responses of mother sows to a *Probioticenterococcus faecium* strain lead to different microbiota composition in their offspring. *Beneficial Microbes* 4, 345–356. doi: 10.3920/BM2013.0021

Tan, C., Wei, H., Ao, J., Long, G., and Peng, J. (2016). Inclusion of konjac flour in the gestation diet changes the gut microbiota, alleviates oxidative stress, and improves insulin sensitivity in sows. *Appl. Environ. Microbiol.* 82, 5899–5909. doi: 10.1128/AEM.01374-16

The, H. C., Florez, D. S. P., Jie, S., Pham, T. D., Thompson, C. N., Minh, C. N. N., et al. (2018). Assessing gut microbiota perturbations during the early phase of infectious diarrhea in vietnamese children. *Gut Microbes* 9, 38–54. doi: 10.1080/19490976.2017.1361093

Wang, X. X., Song, P. X., Wu, H., Xue, J. X., Zhong, X., and Zhang, L. Y. (2016). Effects of graded levels of isomaltooligosaccharides on the performance, immune function and intestinal status of weaned pigs. *Asian Aust. J. Anim. Sci.* 29, 250–256. doi: 10.5713/ajas.15.0194

Wu, X., Gao, L.-M., Liu, Y.-l, Xie, C., Cai, L., Xu, K., et al. (2020). Maternal dietary uridine supplementation reduces diarrhea incidence in piglets by regulating the intestinal mucosal barrier and cytokine profiles. *J. Sci. Food Agric.* 100, 3709–3718. doi: 10.1002/jsfa.10410

Wu, Y., Pan, L., Shang, Q. H., Ma, X. K., Long, S. F., Xu, Y. T., et al. (2017). Effects of isomalto-oligosaccharides as potential prebiotics on performance, immune function and gut microbiota in weaned pigs. *Anim. Feed Sci. Technol.* 230, 126–135. doi: 10.1016/j.anifeedsci.2017.05.013

Xie, C., Guo, X., Long, C., Fan, Z., Xiao, D., Ruan, Z., et al. (2015). Supplementation of the sow diet with chitosan oligosaccharide during late gestation and lactation affects hepatic gluconeogenesis of suckling piglets. *Anim. Reprod. Sci.* 159, 109–117. doi: 10.1016/j.anireprosci.2015.06.004

Xu, J., Liu, Z., Zhan, W., Jiang, R., Yang, C., Zhan, H., et al. (2018). Recombinant tsp53 modulates intestinal epithelial barrier integrity via upregulation of zo1 in lpsinduced septic mice. *Mol. Med. Rep.* 17, 1212–1218. doi: 10.3892/mmr.2017.7946

Yen, C., Tseng, Y., Kuo, Y., Lee, M., and Chen, H. (2011). Long-term supplementation of isomalto-oligosaccharides improved colonic microflora profile, bowel function, and blood cholesterol levels in constipated elderly people—a placebo-controlled, diet-controlled trial. *Nutrition* 27, 445–450. doi: 10.1016/j.nut.2010.05.012

Zambrano, E., Ibáñez, C., Martínez-Samayoa, P. M., Lomas-Soria, C., Durand-Carbajal, M., Rodríguez-González, G. L., et al. (2016). Maternal obesity: lifelong metabolic outcomes for offspring from poor developmental trajectories during the perinatal period. *Arch. Med. Res.* 47, 1–12. doi: 10.1016/j.arcmed.2016.01.004

Conflict of Interest: The authors declare that the research was conducted in the absence of any commercial or financial relationships that could be construed as a potential conflict of interest.

The reviewer XX declared a shared affiliation with one of the authors YHD, to the handling editor at the time of the review.

frontiers in Microbiology

ORIGINAL RESEARCH
published: 03 February 2021
doi: 10.3389/fmicb.2020.617696

Temporal Characteristics of the Oropharyngeal and Nasal Microbiota Structure in Crewmembers Stayed 180 Days in the Controlled Ecological Life Support System

Yanwu Chen[1†], Chong Xu[2†], Chongfa Zhong[2], Zhitang Lyu[3], Junlian Liu[2], Zhanghuang Chen[2], Huanhuan Dun[2], Bingmu Xin[1,2] and Qiong Xie[2*]*

[1] Space Science and Technology Institute (Shenzhen), Shenzhen, China, [2] China Astronaut Research and Training Center, Beijing, China, [3] Key Laboratory of Microbial Diversity Research and Application of Hebei Province, College of Life Science, Baoding, China

OPEN ACCESS

Edited by:
Teresa Nogueira, Instituto Nacional Investigaciao Agraria e Veterinaria (INIAV), Portugal

Reviewed by:
Ebrahim Kouhsari, Iran University of Medical Sciences, Iran
Gaosen Zhang, Chinese Academy of Sciences, China

***Correspondence:**
Bingmu Xin
xin_bm@163.com
Qiong Xie
xieqio@sina.com

[†]These authors have contributed equally to this work and share first authorship

Specialty section:
This article was submitted to Microbial Symbioses, a section of the journal Frontiers in Microbiology

Received: *15 October 2020*
Accepted: *16 December 2020*
Published: *03 February 2021*

Citation:
Chen Y, Xu C, Zhong C, Lyu Z, Liu J, Chen Z, Dun H, Xin B and Xie Q (2021) Temporal Characteristics of the Oropharyngeal and Nasal Microbiota Structure in Crewmembers Stayed 180 Days in the Controlled Ecological Life Support System. Front. Microbiol. 11:617696. doi: 10.3389/fmicb.2020.617696

Confined experiments are carried out to simulate the closed environment of space capsule on the ground. The Chinese Controlled Ecological Life Support System (CELSS) is designed including a closed-loop system supporting 4 healthy volunteers surviving for 180 days, and we aim to reveal the temporal characteristics of the oropharyngeal and nasal microbiota structure in crewmembers stayed 180 days in the CELSS, so as to accumulate the information about microbiota balance associated with respiratory health for estimating health risk in future spaceflight. We investigated the distribution of microorganisms and their dynamic characteristics in the nasal cavity and oropharynx of occupants with prolonged confinement. Based on the 16S rDNA v3–v4 regions using Illumina high-throughput sequencing technology, the oropharyngeal and nasal microbiota were monitored at eight time points during confinement. There were significant differences between oropharyngeal and nasal microbiota, and there were also individual differences among the same site of different volunteers. Analysis on the structure of the microbiota showed that, in the phylum taxon, the nasal bacteria mainly belonged to Actinobacteria, Firmicutes, Proteobacteria, Bacteroidetes, etc. In addition to the above phyla, in oropharyngeal bacteria Fusobacterial accounted for a relatively high proportion. In the genus taxon, the nasal and oropharyngeal bacteria were independent. *Corynebacterium* and *Staphylococcus* were dominant in nasal cavity, and *Corynebacterium*, *Streptococcus*, and *Neisseria* were dominant in oropharynx. With the extension of the confinement time, the abundance of *Staphylococcus* in the nasal cavity and *Neisseria* in the oropharynx increased, and the index Chao fluctuated greatly from 30 to 90 days after the volunteers entered the CELSS.

Conclusion: The structure and diversity of the nasal and oropharyngeal microbiota changed in the CELSS, and there was the phenomenon of migration between occupants, suggesting that the microbiota structure and health of the respiratory tract could be affected by living in a closed environment for a long time.

Keywords: controlled ecological life support system, microbial community, space flight, oropharynx, nasal cavity, microbiota

INTRODUCTION

In the human respiratory tract, there is a complex microbiota and microecological balance, and the disruption of the balance at specific sites may lead to the overgrowth of pathogens and the increased susceptibility to infection. Infection is generally associated with altered microbial diversity and microbiota structure and that had been reported in a variety of respiratory diseases, including upper respiratory tract infection accompanied by acute otitis media (AOM) (Chonmaitree et al., 2017), pharyngitis (González-Andrade et al., 2017), asthma (Katsoulis et al., 2019), and pneumonia (Morinaga et al., 2019). Nasal cavity and oropharynx locate the entrance of the upper respiratory tract, which serve as the physical barrier to the invasion of the pathogens and also important habitats colonized by a large number of conditional pathogen. Clinical pathogenic bacterium, such as *Staphylococcus aureus*, *Streptococcus pneumoniae*, *Haemophilus influenzae*, and *Moraxella catarrhalis* are generally colonized in the nasal cavity. Thus, it is also a main position of the viral infection (de Steenhuijsen Piters et al., 2015; Brugger et al., 2016; Bomar et al., 2018). The oropharynx is an important site for the colonization of pathogenic bacteria. Metagenomic sequencing has proved that the pharynx of a healthy adult is colonized by pathogenic bacteria such as *Streptococcus*, *Haemophilus* and *Neisseria* (Segata et al., 2012; Ver Heul et al., 2019). Normally, these pathogenic microorganisms live in the host as part of the microecosystem, occupying an ecological niche and even resisting the infection of other exogenous pathogenic bacteria. However, in a few cases, they cause respiratory diseases, which need to be triggered by various exogenous or endogenous stimuli (Bogaert et al., 2004). Dynamic surveillance of oropharyngeal and nasal microbiota structure may be crucial in predicting inflammatory lung disease and guiding medical treatment (Lee et al., 2019).

During space flight, the astronauts will have to live in the spacecraft for a long time. Factors like confined living environment, lifestyle changes, stress, and biological rhythm changes may have a significant impact on the physiological environment and the body's immune function. On the other hand, the changes of environmental stress factors, such as oxygen, pH, humidity, and nutrient, may cause the dynamic response of symbiotic bacteria. The uncontrollable increase of pathogenic bacteria in the bacterial community may lead to infection. The experience of the manned space flight of the United States and Russia has proved that with the extension of flight time, the accumulation of microorganisms in the cockpit became more and more serious, and the increase of pathogens in the living environment was more likely to cause infection and allergy and affect human health. Dynamic studies of microbes in confined spaces have shown that harmful bacteria accumulated in the environment with prolonged confined time and it weakened the immune system of humans exposed to stress and extreme environmental conditions during space flight, leading to increased susceptibility. In aerospace health events, upper respiratory symptoms (0.97 per flight year) and other (non-respiratory) infectious events are among the most prevalent, second only to rashes (1.12 per flight year) (Crucian et al., 2016a).

Detection and analysis of on-orbit microorganisms can provide a comprehensive understanding of the microbial composition and changes in pathogenic microorganisms on the space station, which is conducive to the prevention of infectious diseases (Ichijo et al., 2016; Blachowicz et al., 2017; Lang et al., 2017).

In this study, the CELSS was used to simulate space environment on the ground, and four crewmembers were confined for 180 days in the experiment. With Illumina 16S rDNA V3–V4 high-throughput sequencing technologies, the systemic research of human source bacteria microbiota was carried out, in order to research microbial characteristics of the upper respiratory tract of the crew living in a closed environment for a long time. The risk of suffering from respiratory disease for humans living in an airtight environment was assessed, and we aimed to provide reference basis for infection control on orbit.

MATERIALS AND METHODS

Volunteers

The crewmembers consisted of 3 males and 1 female (age 34.2 ± 6.6 years, weight 64.5 ± 6.1 kg, height 169.3 ± 5.1 cm) that were selected from 2,110 volunteers through qualification examination and physical and psychological examinations. In this study, infectious disease including chronic pharyngitis, asthma, and pneumonia would be causes for rejection. Crewmembers were adequately trained to perform the related test tasks before the experiment.

The research program was approved by the Ethical Committee of the ACC (China Astronaut Research and Training Center, Beijing, China) and complied with all the guidelines in the Declaration of Helsinki. Each volunteer was informed of the content and schedule of the study, and the informed consent form was signed. Participants can withdraw from the study at any time.

Research Design

The CELSS platform consists of six interconnected modules and eight compartments, including two crew pods, four greenhouses, a resource pod, and a recovery and purification system to treat waste (feces, urine, plant residues, wastewater, exhaust gas) and produce CO_2 for plants, as well as a life support pod for storing and processing food. The crew cabin consists of a single bedroom, a working area, a medical monitoring area, a cafeteria, and a gym. The life support system is controlled by an automatic feedback network.

The four crewmembers follow a strict diet and working schedule. Meanwhile, they control water treatment units, plant culture, garbage disposal, life support, and air control systems, and they perform cleaning and maintenance tasks (Yuan et al., 2019). In addition, they actively engage in scientific experiments in which they are the subjects of many psychological and physical tests. The project described in this paper is one of these experiments, named "Confined Habitat and Microbial Ecology of Human Health" experiment, which aims to obtain detailed data on microbiota changes in human from confined environments. Nasal and oropharyngeal samples were taken from four crew

members during the experiment which lasted 180 days. Monthly sampling was conducted on the same day or one day before the delivery so that all the samples could be treated within 48 h. After sampling, the samples were marked, sealed, and put into the cold storage device for inspection.

Sample Collection

The samples were collected during the 180-days experiment, which was conducted in the CELSS platform located in Space Science and Technology Institute (Shenzhen), Shenzhen, Guangdong Province, China. The four crewmembers were quarantined for 180 days swabs. Sterile swabs were used for sampling from oropharynx and nasal cavity eight times. The swabs (155C conventional swab, Copan, Italy; ethylene oxide sterilization) were held on the handle and gently inserted into the oropharynx or nasal cavity, gently rotated 3–5 times, and then were removed slowly. Put the extracted samples into the sample collection tubes, break the handles, seal them and store them in the −80°C refrigerator to complete the sampling. Samples were taken 7 days before the confined experiment and 15, 30, 60, 90, 120, 150, and 180 days during the confined experiment. On a manned space station, in order to ensure that samples could truly reflect the growth of human microorganisms, on-orbit microbial samples were generally collected 1–2 days before the separation of the spacecraft and the space station (Novikova et al., 2006). So, nasal and oropharyngeal samples were collected on the same day or one day before delivery. Delivery modules happened once a month, and the samples were delivered from the capsule on that day. After sampling, the samples were marked, sealed, and stored in the cold storage device. The time between sampling and detection should not exceed 48 h. Then, DNA was extracted from samples, and microbiota analysis was carried out by using the molecular biological and genomics method.

Illumina MiSeq Amplicon Sequencing

DNA Extraction

DNA was extracted with QIAGEN PowerSoil DNA Isolation Kit. DNA quality was determined by 1% agarose gel electrophoresis. The concentration of the extracted DNA was detected and adjusted. The DNA working solution was stored at 4°C, and the storage solution was stored at −20°C.

16S rRNA Gene Amplicons for Sequencing

PCR amplification was performed on the V3–V4 regions of the 16S rRNA gene of samples. The PCR reaction (30 μl) was in triplets, including 22.4 μl ultra-pure water and 6 μl Taq&Go™ Mastermix (Biomedmix, Heidelburg MP, Germany), a forward and reverse primer of 0.3 μl, respectively (10 μM), and a 1-μl extracted DNA template. Amplification was performed in 35 cycles on the PCR instrument, which was set as follows: 95°C 45 s, 55°C, 45 s, 72°C 90 s, including initial denaturation at 95°C for 5 min and final elongation at 72°C for 10 min. Gel recovery and purification: the target strip was recovered by cutting, and purified samples were obtained. Quantification of each sample: a Qubit fluorescence quantitative analyzer was used to quantify each sample. Illumina TruSeq DNA Sample Preparation Guide was used to construct DNA library. Illumina MiSeq PE300 was used for sequencing.

Sequencing Analysis

Sequence reads were analyzed with QIIME 1.9.1 (Caporaso et al., 2010) according to tutorials provided by the QIIME developers. After quality checking with Fastqc, the reads were assigned to each sample according to barcodes. Reads were merged to tags, and they are clustered into OTUs at 97% similarity. Based on OTUs and annotation results, composition difference analysis and microbial diversity were analyzed.

Statistical Analysis

The comparisons of the microbial diversity were performed using R software (version 3.6.3). The Kruskal–Wallis test was used to compare the mean values of different groups, and $p < 0.05$ was considered statistically significant. The vegan package of R software was used to make principal coordinate analysis and draw the PCoA analysis chart.

RESULTS

The 64 swab samples were collected from the oropharynx and nasal cavity of the four crew members during isolation in the CELSS at eight time points over a 180-days period. The implementation of the whole experiment conforms to the design of the experiment (Yuan et al., 2019). The schematic diagram of the research experiment design is shown in **Figure 1**. The outline of the CELSS and the living and working places of the volunteers are shown in **Supplementary Figure 1**.

Microbial Diversity Analysis of Nasal and Oropharyngeal Samples Under Confined Conditions

A total of 1,050,859 sequence readings were obtained from the nasal sample, and the median number of reads in the nasal sample was 31,266. A total of 666,675 sequence readings were obtained from oropharyngeal samples, and the median number of reads in oropharyngeal samples was 18,830.

The overall structure of microbial community composition was characterized by principal coordinate analysis (PCoA) of diversity differences. The results showed that the largest factor affecting the differences between samples was the sampling site (**Supplementary Figure 2A**). The microbial composition in the nasal cavity and oropharynx was distinctly different at the taxon of phylum (**Supplementary Figure 2B**). The nasal bacteria mainly belonged to Actinobacteria, Firmicutes, Proteobacteria, and Bacteroidetes, while Fusobacterial occupied a relatively high proportion in oropharyngeal microbiota in addition to the above-mentioned phyla. The microbiota of the same site had an individual difference in relative numbers (**Supplementary Figures 2D,E**). The index Chao of the oropharyngeal microbial community was higher than the nasal cavity, and it fluctuated more wildly in the nasal microbial community, but there was no statistical difference ($P = 0.63$) (**Supplementary Figure 2C**).

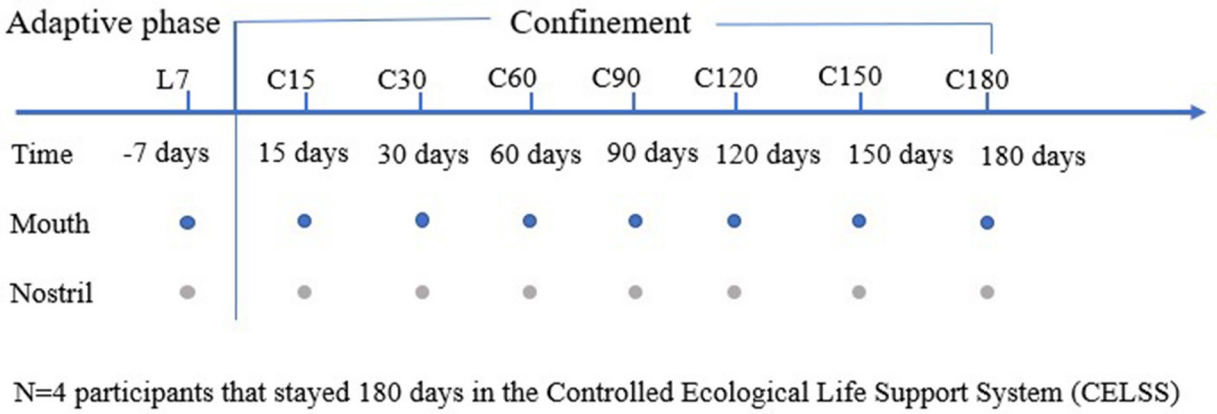

FIGURE 1 | Schematic diagram of research design. The sampling time point is shown at the top. The numbers represent the number of days before (L-) and during (C-) confinement, and−7 days represents the 7th day before the confinement experiment. The colored circles represent the time points that were used to collect the sample specified on the left side of the figure.

Temporal Characteristics of Nasal and Oropharyngeal Microbiota Under Confined Conditions

QIIME 1.9.1 was used to generate the species abundance distribution diagram of multiple samples. According to the classification results, bacteria in the top six positions of richness detected in the nose samples mainly belong to *Corynebacterium*, *Staphylococcus*, *Alloiococcus*, *Peptoniphilus*, *Propionibacterium*, and *Acinetobacter*. Analysis results of nasal bacterial composition (**Figure 2A**, **Supplementary Figure 3**) showed that *Corynebacterium* and *Staphylococcus* were dominant, and with the extension of confined time, the relative abundance of *Corynebacterium* showed a downward trend ($P = 0.083$), and *Staphylococcus* and *Alloiococcus* increased ($P = 0.48$, $P = 0.92$).

The analysis results of the oropharyngeal microbial composition showed that (**Figure 2B**, **Supplementary Figure 3**) the dominant bacteria in oropharyngeal samples belonged to *Corynebacterium*, *Streptococcus*, *Neisseria*, *Rothia*, *Prevotella*, *Leptotrichia*, *Haemophilus*, *Capnocytophaga*, etc. The evenness of oropharyngeal dominant bacteria was higher than that of nasal dominant bacteria. On the whole, *Prevotella* showed a decreasing trend ($P = 0.18$), *Neisseria* showed an increasing trend ($P = 0.34$), *Capnocytophaga* decreased at first and then increased, while *Leptotrichia* showed little change.

The index Chao showed no obvious trend (**Figures 2C,D**), but it fluctuated greatly over time, especially at the time points of C30, C60, and C90. The index was relatively stable at the beginning and end of confinement.

It is worth mentioning that at the time point of C60, *Corynebacterium* has increased in the nasal cavity and oropharynx synchronously, the index Chao reduced and *Staphylococcus* in the nasal cavity and *Streptococcus* in oropharynx reduced.

Dynamic Analysis of Individual Bacterial Community Structure During Confinement Time

There is some microbial specificity between individuals, so we analyzed the changes of individual bacterial community over time (**Supplementary Figure 4**). With the extension of the isolation time, as a whole, the nasal microbiota showed a decreasing trend of *Corynebacterium* ($P = 0.083$) and an increasing trend of *Staphylococcus* ($P = 0.48$), which was very obvious in volunteer 3 and 4. It should be noted that the abundance of *Alloiococcus* was higher and increased in the nasal cavity of volunteer 1, but it was rare in other volunteers. *Acinetobacter* was characterized abnormally high periodically in the nasal cavity of volunteer 4. *Propionibacterium* occupied a relatively low proportion in these dominant bacteria. *Staphylococcus* was very rarely in the nasal bacterial community of volunteers 2 and 4 before the confined experiment, while it was higher in the nasal bacterial community of volunteers 1 and 3. An interesting higher proportion of *Staphylococcus* was detected in the nasal bacterial community of all the volunteers during the confined experiment. The DNA extraction of nasal samples from volunteer 2 on day 180 and volunteer 4 on day 60 failed.

Neisseria in oropharyngiae (except occupant 1) showed an increased trend in the study (**Supplementary Figure 5**). An outbreak of *Rossella* happened 1–2 months after isolation and then returned to normal level. DNA was failed to be extracted from the oropharyngeal samples of volunteer 1 at day 60 and 90 and volunteer 4 at day 60.

With 97% similarity, the OTU number of each sample was obtained. The Venn diagram was used to show the number of common and unique OTU numbers of multiple samples, and the OTU overlap among samples was visually displayed to reflect the microbial crossover between samples. We selected two time points of pre-confinement (L7) and confinement time 180 days (C180) for the Venn diagram analysis. Since it was

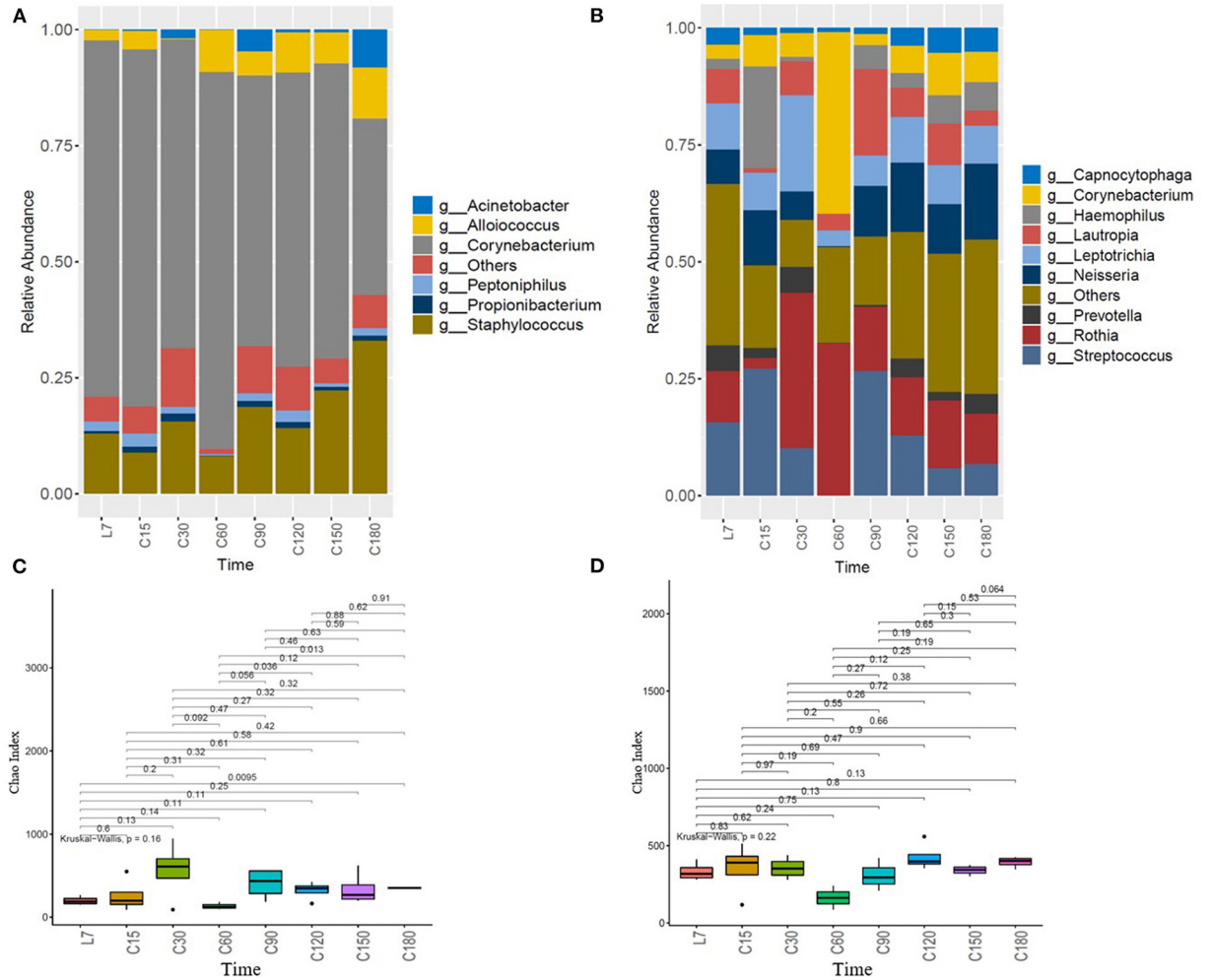

FIGURE 2 | Dynamic analysis of the changes in the structure of microbiota over time. **(A)** Temporal characteristic of nasal microbiota, **(B)** temporal characteristic of oropharyngeal microbiota, **(C)** changes of nasal microbial index Chao with time, and **(D)** changes of oropharyngeal microbial index Chao with time. The horizontal axis represents the time point. L7 represents 7 days before the confined experiment, and C15, C30, C60, C90, C120, C150, and C180, respectively represent 15, 30, 60, 90, 120, 150, and 180 days during the confined experiment. The vertical axis represents the relative abundance of the genera.

failed to extract the DNA of nasal sample C180 from Volunteer 2, we chosed the nasal sample of confinement time 150 days (C150) instead of C180 for analysis (**Figure 3**). The number of common and unique OTU numbers of oropharyngeal samples was consistent before and after confinement. The common OTU numbers of nasal samples increased after confinement, which indicated that the nasal microbiota had the dynamic characteristic of evolving in the same direction after confinement, and the reason may be that airtight environmental factors caused the change of microbiota, while some microorganisms in the nasal cavity spread through the air and transfered between individuals in an airtight space.

Distribution of Opportunistic Pathogens Before and After Confinement

Some genera of the dominant bacteria in the oropharyngeal and nasal microbial community contain pathogenic or opportunistic pathogens. According to the literature reports (Chonmaitree et al., 2017; González-Andrade et al., 2017; Katsoulis et al., 2019; Morinaga et al., 2019), several genera were selected from the dominant bacteria, which contained opportunistic pathogens. For example, *Staphylococcus* contains *staphylococcus aureus*, which produces enterotoxins that are harmful to health. *Neisseria* contains *N. meningitidis* which is a pathogenic bacterium of epidemic cerebrospinal meningitis, and it is mainly transmitted through the respiratory tract. *S. pyogenes* attached to *Streptococcus* can cause a variety of suppurative inflammation and hypersensitivity diseases, and *S. pneumoniae* can cause respiratory infections in human beings. The *A. otitis* attached to *Alloiococcus* is a pathogenic factor in adult secretome otitis media. *P. acnes* in *Propionibacterium* can cause skin inflammation and is the pathogen of acne.

To reveal the changes of the above opportunistic pathogens in the human body in an isolation environment, we

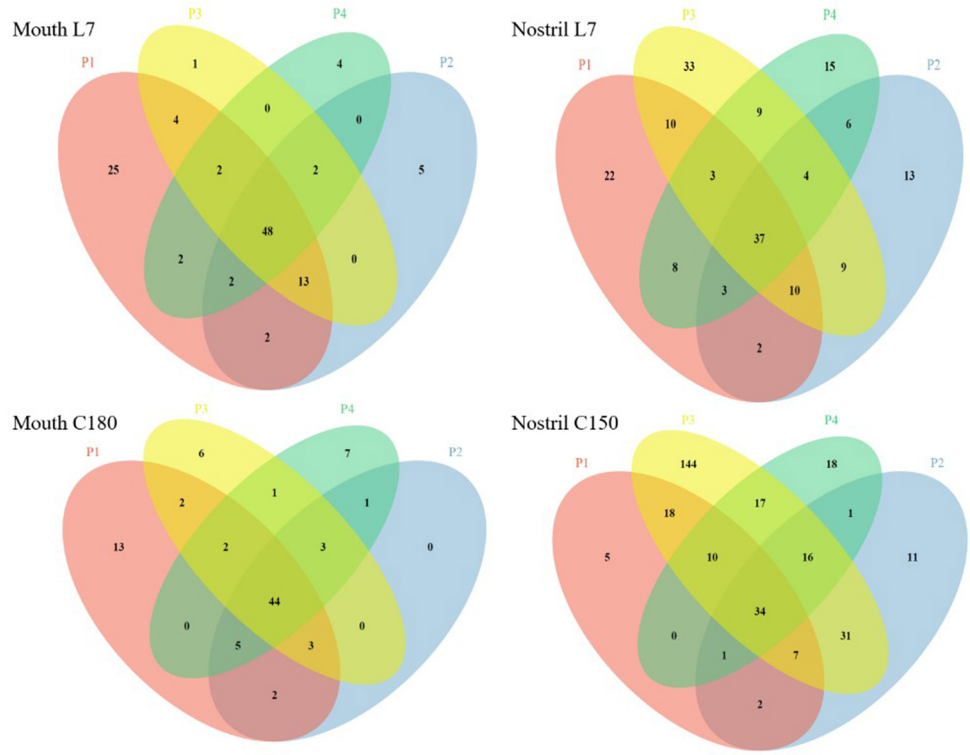

FIGURE 3 | Venn diagram of oropharyngeal and nasal samples before and after confinement. Mouth L7 and Mouth C180 represent oropharyngeal samples taken 7 days before and 180 days after confinement, and Nostril L7 and Nostril C150 represent nasal samples taken 7 days before and 150 days after confinement, respectively. P1, P2, P3, and P4 are the numbers of four volunteers. Circles of different colors are used to represent different individual samples, and the numbers of overlapping areas represent the numbers of common OTUs among samples. The common OUT numbers increase after confinement in Nostril samples Nostril L7 and Nostril C150.

tried to compare the difference of the genera containing pathogen bacteria before and after the isolation (**Figure 4**, **Supplementary Table 2**). It was worth mentioning that the sequencing sequence of the 16s rRNA gene V3–V4 area could not distinguish the species level; however, the genera containing potentially pathogenic bacteria that we had listed could reflect the increased risk of infection by opportunistic pathogens from the side. It was failed to extract DNA from the nasal sample of C180 of Volunteer 2, and C150 was used for alternative analysis. The figure showed obvious increase in *Staphylococcus* of the nasal cavity and in *Neisseria* of the oropharynx after confinement, suggesting an increased risk of infection.

DISCUSSION

In space, the special environmental factors may change bacterial community structure in the human body of astronauts, and break the microbiota balance. Working on-orbit results in decreased immunity and increases the risk of pathogenic infections. These infections may occur in the respiratory tract, the digestive tract, urinary tract, and skin, affecting the individual health and subjective experience. At the same time, these could affect other individuals, even the whole crew, through the migration of bacteria. Therefore, the study of the human bacterial community structure in the confined environment is of great significance for the prevention of infectious diseases during long-term flight on-orbit in the future. In our study, the temporal characteristics of the oropharyngeal and nasal microbiota structure in crewmembers were researched, in order to provide reference for revealing possible effects of microbiota balance on respiratory health in a closed environment.

The culture method is the most commonly used method for studying microbes on the space station, and although there have been attempts to sequence them on-orbit, conditions on the space station have limited the use of sequencing technology on-orbit. Currently, on-orbit microbial samples are returned to the earth for high-throughput sequencing and analysis for microbiota studies on space station. However, due to the limitation of return time, dynamic analysis of microbiota cannot be carried out immediately, and long-term preservation and space transportation may lead to the risk of analysis error. Therefore, many scholars simulate the space environment on the ground to dynamically study the changes of environment and human microbiota. In order to monitor the microbial characteristics of the closed system on the ground in real time, the researchers designed different experiments and simulated buildings to conduct research. Russia conducted a confined Mars500 habitat, and simulated flight and landing on Mars, using

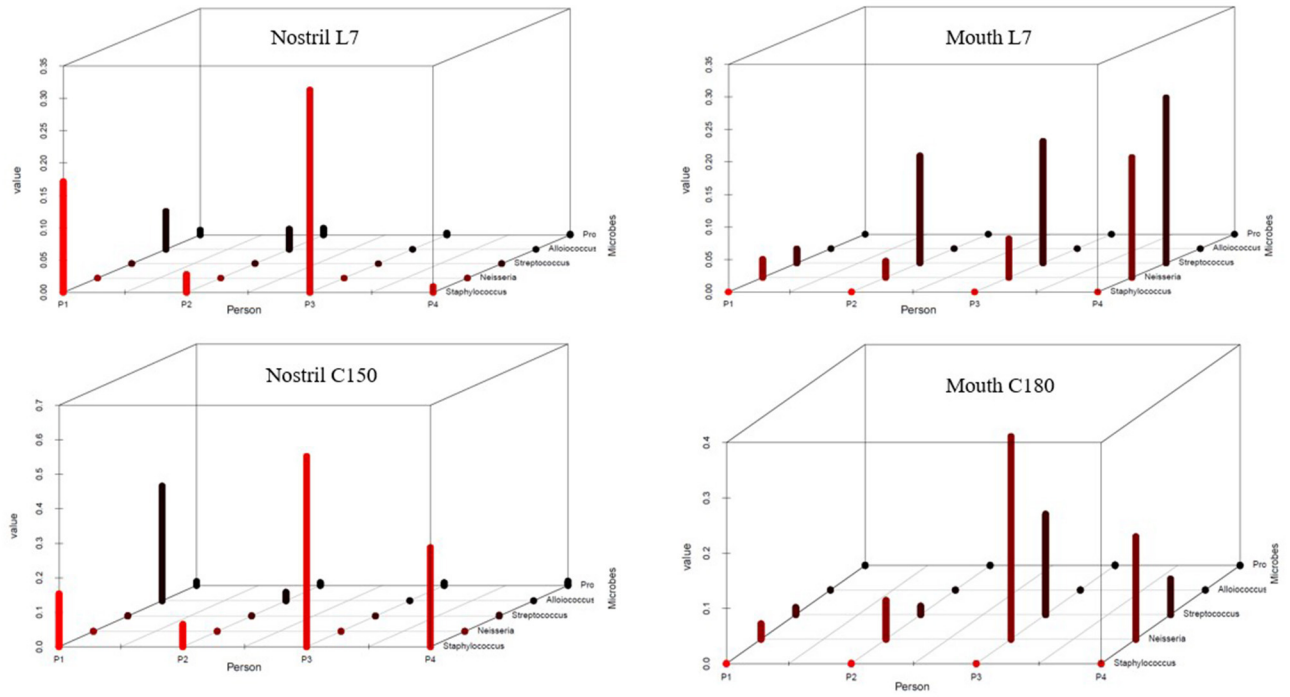

FIGURE 4 | Changes in the content of potential pathogenic bacteria before and after confinement. The bacterial distribution 7 days before confinement (L7) and 180 days after confinement (C180) in different individuals was statistically analyzed. The horizontal axis P1, P2, P3, and P4 represented volunteers, the vertical axis represented the content value of bacteria, and the oblique axis represents the names of the bacterial genera. Nostril L7 and Nostril C180 represented the nasal samples taken 7 days before and 180 days after confinement. It was failed to extract in which the DNA of 180 days' nasal sample of Volunteer 2 and it was replaced by 150 days' nasal sample of Volunteer 2. Mouth L7 and Mouth C180 represented oropharyngeal samples taken 7 days before and 180 days after confinement, respectively. Note that the scale values used on the vertical axis were different and need to be distinguished.

high-throughput sequencing technology to study the dynamic changes of the intestinal microbiota structure over time in six volunteers (Schwendner et al., 2017). Then, in the expansion of the lunar/Mars habitat simulation test was carried out, high-throughput sequencing technology was used to survey bacterial community in the air, and the results showed that in closed habitats, bacterial structure of air had a close relationship with human existence (Mayer et al., 2016).

The CELSS system is an excellent platform to simulate the closed environment of the space capsule on the ground. The confined experiment of four people for 180 days provided an opportunity to dynamically track the changes of the crews' own microbiota and the microbiota of others living in close proximity for a long time. During the 180-days confinement simulation experiment, human respiratory tract microbial samples were collected at eight time points, and the microbiota were continuously observed over time. This is the first time to study the changes of respiratory microbiota over time through CELSS.

This study aimed to reveal the effect of long-term confinement on the composition and diversity of nasal and oropharyngeal microbiota. We found that nasal cavity and oropharynx were independent in terms of microbiota structure and diversity (**Supplementary Figures 2A,B**), and this independence did not disappear with the extension of confinement time, indicating that the physiological environment and microecological environment of the growth site of the microbiota were the most important influential factors on the microbiota. Studies had investigated the temporal stability and diversity of skin microbiota, regardless of the sampling interval, and despite the skin community's constant exposure to external factors, the stability of the microbiota still existed, while the nature and degree of this stability was highly individualized (Oh et al., 2014).

In terms of bacterial composition, the nasal bacteria mainly belong to Actinobacteria, Firmicutes, Proteobacteria, Bacteroidetes, etc. In addition to the abovementioned phyla, the Fusobacterial occupies a relatively high proportion in oropharyngeal bacteria. At the level of genus, the dominant bacteria of nasal cavity are *Corynebacterium*, *Staphylococcus*, *Diaphylococcus*, *Propionibacterium*, etc., while the dominant bacteria of oropharynx are *Corynebacterium, Streptococcus, Neisseria*, and *Prevotella*. Previous studies have shown that the main members of the microbial ecosystem in the nasal cavity are usually Actinobacteria (containing *Corynebacterium* and *Propionibacterium*) and Firmicutes (*Streptococcus* in children and *Staphylococcus* in adults), while the abundance of anaerobic

bacteria in Bacteroidetes is low (Camarinha-Silva et al., 2014; Oh et al., 2014). At the generic level, *Corynebacterium, Propionibacterium*, and *Staphylococcus* are the most common genera in the nasal cavity (Zhou et al., 2014). Previous studies have shown that bacterial biodiversity and uniformity vary greatly in the upper respiratory tract; thus, the oropharynx and oral cavity have the highest biodiversity and uniformity (Charlson et al., 2010; Zhou et al., 2013). On the contrary, similar to other areas covered by human skin epithelium, the nasal cavity shows low biodiversity (Grice and Segre, 2011).

During 30–90 days of confinement, the structure of nasal and oropharyngeal microbiota changed (**Figures 2A,B**), and the index Chao of the microbiota fluctuated greatly (**Figures 2C,D**). The confinement environment disturbed the nasal and oropharyngeal microbiota, especially after 30 days of confinement. In addition, the oropharyngeal microbial diversity was higher than the nasal cavity, and the index Chao of nasal cavity fluctuated more, but there was no statistical difference ($P = 0.63$) (**Supplementary Figure 2C**). The results of behavioral monitoring and psychological state assessment in this project showed that after 1 month of detention, behavioral flow reflecting global activity decreased 1.5- to 2-fold. Psychological questionnaires revealed a decrease in hostility and negative emotions but an increase in emotional adaptation suggesting boredom and monotony (Biesbroek et al., 2014). Physiological and psychological changes in volunteers in the isolation environment may trigger a series of physiological stress changes, such as immunity and secretion of respiratory antibacterial substances, which may affect the respiratory microbiota. According to NASA's research data, the exchange or migration of pathogenic microorganisms between passenger groups occurred in flight missions over 18 days (Crucian et al., 2016a). This is another explanation for the change in the microbiota after 30 days of confinement.

Dynamic analysis of the microbiota structure over time found that *Staphylococcus* and *Alloiococcus* showed an upward trend, while *Corynebacterium* showed a downward trend (**Figure 2A**). *Neisseria* showed an upward trend in oropharyngeal microbiota, while *Corynebacterium* showed a large fluctuation (**Figure 2B**). Early nasopharyngeal microbial studies showed that high abundance ratios of *Corynebacterium* and *Moraxella* marked a more stable structure, and poor stability was characterized by high abundance of *Streptococcus* and acquired *H. influenzae*, and the microbiota characteristics were correlative with reported higher incidence of respiratory tract infections and asthma in the early stages of life (Stubbendieck et al., 2019). Microbial communities characterized by high abundance of *Corynebacterium* and lack of the presence of *H. influenzae* and *S. pneumoniae*, suggesting colonization resistance to these potential pathogens. In this study, the abundance of *Corynebacterium* was the highest, indicating that the structure of the bacterial community was stable. However, during the confined period, *Corynebacterium* showed a downward trend, while *Staphylococcus* showed an increasing trend, suggesting that confinement had an adverse effect on the structural stability of the nasal bacterial community.

Worth noting is that although *Corynebacterium* showed a trend of decrease in the nasal cavity, but at the C60 time point, there was a dramatic rise of *Corynebacterium* in nasal and oropharyngeal microbiota collaboratively (**Figures 2A,B**), together with much lower index Chao (**Figures 2C,D**), at the same time *Staphylococcus* in the nasal cavity and *Streptococcus* in oropharynx greatly reduced. Studies have shown that *Corynebacterium* competes for limited iron resources in the nasal cavity by producing the iron-chelating vector, which is related to the ability to inhibit *Staphylococcus*. At the same time, the lipase secreted by *Corynebacterium* can lyse the triacylglycerol in the nasal cavity and produce the free fatty acid which is resistant to microorganisms, thus inhibiting the growth of *Streptococcus in vitro* (Marik, 2001).

Oropharynx connects the mouth, nasopharynx, larynx, lower respiratory tract, and gastrointestinal tract and it is exposed to exogenous and endogenous microorganisms. Thus, the species pool contained in oropharyngeal microecology is usually large and a highly diverse of bacterial community can be observed in adults. The oropharynx is also the niche of potentially pathogenic bacteria that may cause local (pharyngitis) or diffuse (lung) diseases (Mermel, 2013). *Neisseria* contains *N. meningitidis* which is a pathogenic bacterium of epidemic cerebrospinal meningitis, and it is mainly transmitted through the respiratory tract. *Rothia* is a class of symbiotic bacteria that is widespread in the mouth. In this study, *Neisseria* in the oropharynx (except volunteer 1) showed an increasing trend. An outbreak of *Rossella* happened 1–2 months after confinement, then it returned to normal (**Supplementary Figure 5**). Disturbance of the microbiota may lead to increased risk of infection. The analysis suggests that it may be related to the inadaptability to the confined environment at the initial stage of experiment, the insufficient proficiency of each item, the tension of the volunteers, and the great physical and mental pressure.

We respectively analyzed the changes in the microbiota of four volunteers over time and compared them crosswise. Nasal *Staphylococcus* in volunteers 2 and 4 makes up only a very small percentage, while in volunteers 1 and 3 they makes up a bigger percentage before confined experiment. Nasal *Staphylococcus* accounted for a bigger percentage in all volunteers after 180 days confined experiment (**Supplementary Figure 4**). To explore this phenomenon, we used the Venn diagram to show the common and unique OTU numbers of samples before and after confinement, and there is a tendency of convergence in the nasal cavity (**Figure 3**), so we speculated that four volunteers had a long and close contact in a confined space, resulting in a microbial transfer between them. The microorganisms carried on the surface of the volunteers are in direct contact with the environment and can have an impact on the environment and then can be transferred. According to NASA's research data, the exchange or migration of pathogenic microorganisms between the crew takes place in a flight mission of more than 18 days (Crucian et al., 2016a). The understanding of the population status of the nasal cavity and oropharyngeal microorganisms is beneficial to the prediction and prevention of the occurrence of on-orbit infectious diseases. Studies have shown that the microbiota on the internal surface of the

International Space Station is similar to the microbiota on the crew's skin. These data provide reference for future microbial monitoring work of the ISS and crew and the control of microbial contamination of manned spacecraft (Avila-Herrera et al., 2020).

To reveal the changes of pathogenic bacteria over time during confinement, considering our sequencing method could not accurately locate the level of species, so we chose genera for symbolic judgment (**Figure 4**). It could be seen that *Staphylococcus* in the nasal cavity and *Neisseria* in the oropharynx increases and spread with the extension of the confinement time. Venn diagrams also reflected a similar situation (**Figure 3**), and common OTU numbers of nasal samples increased after confinement. Nasal microbiota had the same direction of evolutionary dynamic characteristic, and the reason may be that closed environmental factors caused the change of bacterial community; some nasal microorganisms in airtight space spread through the air and transferred between individuals.

The results of the bacterial census of the International Space Station showed that *Staphylococcus*, *Bacillus*, and *Corynebacterium* were among the top three in the detection rate of environmental microbial samples from International Space Station (Venkateswaran et al., 2014). *Staphylococcus* are a bacteria of human origin, and it is also pathogen that induce infectious diseases. *Staphylococcus aureus* are a conditional pathogenic bacterium that NASA attaches great importance to, and crew need medical treatment whose naval *S. aureus* is resistant to drugs in preflight medical examination. The purpose is to reduce infectious diseases caused by migration and exchange of conditional pathogenic bacteria between susceptible people (individual difference) during long-term living closely (Ramakrishnan et al., 2013). A large number of studies have found that chronic nasosinusitis in the upper respiratory tract of patients is associated with higher abundance of *Staphylococcus* accompanied by decreased bacterial diversity (Feazel et al., 2012; Jervis Bardy and Psaltis, 2016; Muluk et al., 2018), and *Staphylococcus* is also positively correlated with other respiratory diseases (such as allergic rhinitis and asthma) (Voorhies et al., 2019). Although other factors experienced by ISS crew members may play a role in the development of upper respiratory symptoms, the increased relative abundance of *Staphylococcus* in the nasal bacterial community is consistent with these symptoms (Crucian et al., 2016; Paetzold et al., 2019).

The bacterial index Chao did not show an obvious trend (**Figures 2C,D**), but it fluctuated greatly over time, especially at the time points of C30, C60, and C90. The index Chao was relatively stable at the beginning of confinement and before confinement ended, showing a certain stability. Host state and complex interactions of the disturbance of environment may influence the local change of bacterial community, and some species could flow in some individuals and parts and influence the structure and function of the microbiota in the short term, while microbiota maintain certain stability in the long run. As with the study of skin microbiota, the most typical example is that the human use probiotics to improve skin health (Oh et al., 2016), but skin microbiota seem to have inherent stability (Crucian et al., 2016).

Two respiratory sites were detected in this study; in another article, we also discussed the changes of the skin microbiota (Bingmu et al., 2018). According to the on-orbit disease investigation and analysis, intestinal tract, urinary tract, and eye are also common sites of infectious disease, in addition to the respiratory disease, diarrhea, urinary tract infection with aeruginosa, and eye sty caused by *S. aureus* also happened on-orbit (Hurlbert et al., 2010; Hodkinson et al., 2017). These infectious diseases prompted us to analyze microbial microbiota of these parts and carry out astronaut individualized microbiota characteristic analysis, especially for long-term orbits. Some research directions such as real-time acquisition and detect microbial samples observe the change of environmental and the astronaut's microbiota, prevent infectious disease, also have important research value for future long-term orbit, and these works still need to continue to explore.

CONCLUSION

In this study, 16S rDNA Illumina Miseq high-throughput sequencing was used to analyze the effects of nasal and oropharyngeal microbiota from crewmembers' long-term confined in the CELSS. The results showed that the structure of the nasal and oropharyngeal microbiota varied greatly, the individual bacterial community structure and the diversity changed with time. *Staphylococcus* in the nasal cavity increased and showed the characteristics of inter-individual transfer, suggesting that the microbiota structure and health of the respiratory tract could be affected by living in a closed environment for a long time.

The imbalance of the respiratory microbial community and the increase of opportunistic pathogens may be the inducement of respiratory diseases, but it does not mean that the increase of opportunistic pathogens will cause diseases; in addition, it is closely related to individual immune function. In the future, we will continue to carry out relevant studies on opportunistic pathogens. In the following work, we will also use a higher-resolution sequencing method to locate the species level and conduct in-depth analysis on pathogenic bacteria that may cause respiratory diseases.

DATA AVAILABILITY STATEMENT

The datasets presented in this article are not readily available because of the data confidentiality clause of the project sponsor. Requests to access the datasets should be directed to Space Science and Technology Institute (Shenzhen, http://www.szsisc.com/).

ETHICS STATEMENT

The research program was approved by the Ethical Committee of the ACC (China Astronaut Reasearch and Training Center Beijing, China) and complied with all the guidelines in the

Declaration of Helsinki. Each volunteer was informed of the content and schedule of the study and signed an informed consent form. Participants can withdraw from the study at any time.

AUTHOR CONTRIBUTIONS

YC and CX: experimental design. YC, BX, and CZ: methodology. ZL, ZC, and JL: investigation. YC and BX: writing—original draft. CX, QX, and ZL: writing—review and editing. BX and QX: funding acquisition. All authors agree to be accountable for the content of the work.

FUNDING

This work was supported by the Key Program of Logistics Research of China. Grant number BWS17J030, Advanced space medico-engineering research project of China. Grant number 010101, and National Science and Technology Major Project for Major New Drugs Innovation and Development. Grant number 2015zx09j15102-002.

ACKNOWLEDGMENTS

We are grateful to Cheng Zhang who checked for language errors. We thank Bin Xiao for graph processing and valuable advice. We thank Bin Wu, Zhiqi Fan, and Ying Chen for help during the experiments, as well as other members of the microbiology lab for suggestions.

SUPPLEMENTARY MATERIAL

The Supplementary Material for this article can be found online at: https://www.frontiersin.org/articles/10.3389/fmicb.2020.617696/full#supplementary-material

REFERENCES

Avila-Herrera, A., Thissen, J., Urbaniak, C., Be, N. A., Smith, D. J., Karouia, F., et al. (2020). Crewmember microbiome may influence microbial composition of ISS habitable surfaces. *PLoS ONE* 15:e0231838. doi: 10.1371/journal.pone.0231838

Biesbroek, G., Tsivtsivadze, E., Sanders, E. A., Montijn, R., Veenhoven, R. H., Keijser, B. J., et al. (2014). Early respiratory microbiota composition determines bacterial succession patterns and respiratory health in children. *Am. J. Respir. Crit. Care Med.* 190, 1283–1292. doi: 10.1164/rccm.201407-1240OC

Bingmu, X., Heng, W., Yuanliang, W., Chongfa, Z., Junlian, L., Zhanghuang, C., et al. (2018). Analysis on body microbiota of people surviving in controlled ecological life support system of 180 days experiment. *Space Med. Med. Eng.* 31, 282–288.

Blachowicz, A., Mayer, T., Bashir, M., Pieber, T. R., De León, P., and Venkateswaran, K. (2017). Human presence impacts fungal diversity of inflated lunar/mars analog habitat. *Microbiome* 5:62. doi: 10.1186/s40168-017-0280-8

Bogaert, D., De Groot, R., and Hermans, P. W. (2004). *Streptococcus pneumoniae* colonisation: the key to pneumococcal disease. *Lancet Infect. Dis.* 4, 144–154. doi: 10.1016/S1473-3099(04)00938-7

Bomar, L., Brugger, S. D., and Lemon, K. P. (2018). Bacterial microbiota of the nasal passages across the span of human life. *Curr. Opin. Microbiol.* 41, 8–14. doi: 10.1016/j.mib.2017.10.023

Brugger, S. D., Bomar, L., and Lemon, K. P. (2016). Commensal-pathogen interactions along the human nasal passages. *PLoS Pathog.* 12:e1005633. doi: 10.1371/journal.ppat.1005633

Camarinha-Silva, A., Jáuregui, R., Chaves-Moreno, D., Oxley, A. P., Schaumburg, F., Becker, K., et al. (2014). Comparing the anterior nare bacterial community of two discrete human populations using illumina amplicon sequencing. *Environ. Microbiol.* 16, 2939–2952. doi: 10.1111/1462-2920.12362

Caporaso, J. G., Kuczynski, J., Stombaugh, J., Bittinger, K., Bushman, F. D., Costello, E. K., et al. (2010). QIIME allows analysis of high-throughput community sequencing data. *Nat. Methods* 7, 335–336. doi: 10.1038/nmeth.f.303

Charlson, E. S., Chen, J., Custers-Allen, R., Bittinger, K., Li, H., Sinha, R., et al. (2010). Disordered microbial communities in the upper respiratory tract of cigarette smokers. *PLoS ONE* 5:e15216. doi: 10.1371/journal.pone.0015216

Chonmaitree, T., Jennings, K., Golovko, G., Khanipov, K., Pimenova, M., Patel, J. A., et al. (2017). Nasopharyngeal microbiota in infants and changes during viral upper respiratory tract infection and acute otitis media. *PLoS ONE* 12:e0180630. doi: 10.1371/journal.pone.0180630

Crucian, B., Babiak-Vazquez, A., Johnston, S., Pierson, D. L., Ott, C. M., and Sams, C. (2016). Incidence of clinical symptoms during long-duration orbital spaceflight. *Int. J. Gen. Med.* 9, 383–391. doi: 10.2147/IJGM.S114188

de Steenhuijsen Piters, W. A., Sanders, E. A., and Bogaert, D. (2015). The role of the local microbial ecosystem in respiratory health and disease. *Philos. Trans. R. Soc. Lond. Series B Biol. Sci.* 370:20140294. doi: 10.1098/rstb.2014.0294

Feazel, L. M., Robertson, C. E., Ramakrishnan, V. R., and Frank, D. N. (2012). Microbiome complexity and *Staphylococcus aureus* in chronic rhinosinusitis. *Laryngoscope* 122, 467–472. doi: 10.1002/lary.22398

González-Andrade, B., Santos-Lartigue, R., Flores-Treviño, S., Ramirez-Ochoa, N. S., Bocanegra-Ibarias, P., Huerta-Torres, F. J., et al. (2017). The carriage of interleukin-1B-31*C allele plus *Staphylococcus aureus* and *Haemophilus influenzae* increases the risk of recurrent tonsillitis in a Mexican population. *PLoS ONE* 12:e0178115. doi: 10.1371/journal.pone.0178115

Grice, E. A., and Segre, J. A. (2011). The skin microbiome. *Nat. Rev. Microbiol.* 9, 244–253. doi: 10.1038/nrmicro2537

Hodkinson, P. D., Anderton, R. A., Posselt, B. N., and Fong, K. J. (2017). An overview of space medicine. *Br. J. Anaesth.* 119(Suppl.1), i143–i153. doi: 10.1093/bja/aex336

Hurlbert, K., Bagdigian, B., Carroll, C., et al. (2010). *DRAFT Human Health, Life Support, and Habitation System*. NASA Headquarters Washington, 2010:TA06-18.

Ichijo, T., Yamaguchi, N., Tanigaki, F., Shirakawa, M., and Nasu, M. (2016). Four-year bacterial monitoring in the international space station-japanese experiment module "Kibo" with culture-independent approach. *NPJ Microgr.* 2:16007. doi: 10.1038/npjmgrav.2016.7

Jervis Bardy, J., and Psaltis, A. J. (2016). Next generation sequencing and the microbiome of chronic rhinosinusitis: a primer for clinicians and review of current research, its limitations, and future directions. *Ann. Otol. Rhinol. Laryngol.* 125, 613–621. doi: 10.1177/0003489416641429

Katsoulis, K., Ismailos, G., Kipourou, M., and Kostikas, K. (2019). Microbiota and asthma: clinical implications. *Respir. Med.* 146, 28–35. doi: 10.1016/j.rmed.2018.11.016

Lang, J. M., Coil, D. A., Neches, R. Y., Brown, W. E., Cavalier, D., Severance, M., et al. (2017). A microbial survey of the international space station (ISS). *PeerJ* 5:e4029. doi: 10.7717/peerj.4029

Lee, J. T., Kim, C. M., and Ramakrishnan, V. (2019). Microbiome and disease in the upper airway. *Curr. Opin. Allergy Clin. Immunol.* 19, 1–6. doi: 10.1097/ACI.0000000000000495

Marik, P. E. (2001). Aspiration pneumonitis and aspiration pneumonia. *N. Engl. J. Med.* 344, 665–671. doi: 10.1056/NEJM200103013440908

Mayer, T., Blachowicz, A., Probst, A. J., Vaishampayan, P., Checinska, A., Swarmer, T., et al. (2016). Microbial succession in an inflated lunar/mars

analog habitat during a 30-day human occupation. *Microbiome* 4:22. doi: 10.1186/s40168-016-0167-0

Mermel, L. A. (2013). Infection prevention and control during prolonged human space travel. *Clin. Infect. Dis.* 56, 123–130. doi: 10.1093/cid/cis861

Morinaga, Y., Take, Y., Sasaki, D., Ota, K., Kaku, N., Uno, N., et al. (2019). Exploring the microbiota of upper respiratory tract during the development of pneumonia in a mouse model. *PLoS ONE* 14:e0222589. doi: 10.1371/journal.pone.0222589

Muluk, N. B., Altin, F., and Cingi, C. (2018). Role of superantigens in allergic inflammation: their relationship to allergic rhinitis, chronic rhinosinusitis, asthma, and atopic dermatitis. *Am. J. Rhinol. Allergy* 32, 502–517. doi: 10.1177/1945892418801083

Novikova, N., De Boever, P., Poddubko, S., Deshevaya, E., Polikarpov, N., Rakova, N., et al. (2006). Survey of environmental biocontamination on board the international space station. *Res. Microbiol.* 157, 5–12. doi: 10.1016/j.resmic.2005.07.010

Oh, J., Byrd, A. L., Deming, C., Conlan, S., NISC Comparative Sequencing Program, Kong, H. H., et al. (2014). Biogeography and individuality shape function in the human skin metagenome. *Nature* 514, 59–64. doi: 10.1038/nature13786

Oh, J., Byrd, A. L., Park, M., NISC Comparative Sequencing Program, Kong, H. H., and Segre, J. A. (2016). Temporal stability of the human skin microbiome. *Cell* 165, 854–866. doi: 10.1016/j.cell.2016.04.008

Paetzold, B., Willis, J. R., Pereira de Lima, J., Knödlseder, N., Brüggemann, H., Quist, S. R., et al. (2019). Skin microbiome modulation induced by probiotic solutions. *Microbiome* 7:95. doi: 10.1186/s40168-019-0709-3

Ramakrishnan, V. R., Feazel, L. M., Abrass, L. J., and Frank, D. N. (2013). Prevalence and abundance of *Staphylococcus aureus* in the middle meatus of patients with chronic rhinosinusitis, nasal polyps, and asthma. *Int. Forum Allergy Rhinol.* 3, 267–271. doi: 10.1002/alr.21101

Schwendner, P., Mahnert, A., Koskinen, K., Moissl-Eichinger, C., Barczyk, S., Wirth, R., et al. (2017). Preparing for the crewed mars journey: microbiota dynamics in the confined Mars500 habitat during simulated mars flight and landing. *Microbiome* 5:129. doi: 10.1186/s40168-017-0345-8

Segata, N., Haake, S. K., Mannon, P., Lemon, K. P., Waldron, L., Gevers, D., et al. (2012). Composition of the adult digestive tract bacterial microbiome based on seven mouth surfaces, tonsils, throat and stool samples. *Genome Biol.* 13:R42. doi: 10.1186/gb-2012-13-6-r42

Stubbendieck, R. M., May, D. S., Chevrette, M. G., Temkin, M. I., Wendt-Pienkowski, E., Cagnazzo, J., et al. (2019). Competition among nasal bacteria suggests a role for siderophore-mediated interactions in shaping the human nasal microbiota. *Appl. Environ. Microbiol.* 85, e02406–e02418. doi: 10.1128/AEM.02406-18

Venkateswaran, K., La Duc, M. T., and Horneck, G. (2014). Microbial existence in controlled habitats and their resistance to space conditions. *Microb. Environ.* 29, 243–249. doi: 10.1264/jsme2.ME14032

Ver Heul, A., Planer, J., and Kau, A. L. (2019). The human microbiota and asthma. *Clin. Rev. Allergy Immunol.* 57, 350–363. doi: 10.1007/s12016-018-8719-7

Voorhies, A. A., Mark Ott, C., Mehta, S., Pierson, D. L., Crucian, B. E., Feiveson, A., et al. (2019). Study of the impact of long-duration space missions at the international space station on the astronaut microbiome. *Sci. Rep.* 9:9911. doi: 10.1038/s41598-019-46303-8

Yuan, M., Custaud, M. A., Xu, Z., Wang, J., Yuan, M., Tafforin, C., et al. (2019). Multi-system adaptation to confinement during the 180-day controlled ecological life support system (CELSS) experiment. *Front. Physiol.* 10:575. doi: 10.3389/fphys.2019.00575

Zhou, Y., Gao, H., Mihindukulasuriya, K. A., La Rosa, P. S., Wylie, K. M., Vishnivetskaya, T., et al. (2013). Biogeography of the ecosystems of the healthy human body. *Genome Biol.* 14:R1. doi: 10.1186/gb-2013-14-1-r1

Zhou, Y., Mihindukulasuriya, K. A., Gao, H., La Rosa, P. S., Wylie, K. M., Martin, J. C., et al. (2014). Exploration of bacterial community classes in major human habitats. *Genome Biol.* 15:R66. doi: 10.1186/gb-2014-15-5-r66

Conflict of Interest: The authors declare that the research was conducted in the absence of any commercial or financial relationships that could be construed as a potential conflict of interest.

frontiers in Microbiology

ORIGINAL RESEARCH
published: 23 March 2021
doi: 10.3389/fmicb.2021.647119

Genetic Evolution and Implications of the Mitochondrial Genomes of Two Newly Identified *Taenia* spp. in Rodents From Qinghai-Tibet Plateau

Yao-Dong Wu[1], Li Li[1], Yan-Lei Fan[1,2], Xing-Wei Ni[1,3], John Asekhaen Ohiolei[1], Wen-Hui Li[1], Jian-Qiu Li[1], Nian-Zhang Zhang[1], Bao-Quan Fu[1], Hong-Bin Yan[1] and Wan-Zhong Jia[1,4]**

[1] State Key Laboratory of Veterinary Etiological Biology, National Professional Laboratory for Animal Echinococcosis, Key Laboratory of Veterinary Parasitology of Gansu Province, Lanzhou Veterinary Research Institute, Chinese Academy of Agricultural Sciences, Lanzhou, China, [2] School of Pharmaceutical Sciences, Tsinghua University, Beijing, China, [3] Animal Disease Prevention and Control Center of Guizhou Province, Guiyang, China, [4] Jiangsu Co-innovation Center for Prevention and Control of Important Animal Infectious Disease, Yangzhou, China

The larva of Taeniidae species can infect a wide range of mammals, causing major public health and food safety hazards worldwide. The Qinghai-Tibet Plateau (QTP), a biodiversity hotspot, is home to many species of rodents, which act as the critical intermediate hosts of many Taeniidae species. In this study, we identified two new larvae of *Taenia* spp., named *T. caixuepengi* and *T. tianguangfui*, collected from the plateau pika (*Ochotona curzoniae*) and the Qinghai vole (*Neodon fuscus*), respectively, in QTP, and their mitochondrial genomes were sequenced and annotated. Phylogenetic trees based on the mitochondrial genome showed that *T. caixuepengi* has the closest genetic relationship with *T. pisiformis*, while *T. tianguangfui* was contained in a monophyletic group with *T. crassiceps*, *T. twitchelli,* and *T. martis*. Biogeographic scenarios analysis based on split time speculated that the speciation of *T. caixuepengi* (∼5.49 Mya) is due to host switching caused by the evolution of its intermediate host. Although the reason for *T. tianguangfui* (∼13.11 Mya) speciation is not clear, the analysis suggests that it should be infective to a variety of other rodents following the evolutionary divergence time of its intermediate host and the range of intermediate hosts of its genetically close species. This study confirms the species diversity of Taeniidae in the QTP, and speculates that the uplift of the QTP has not only a profound impact on the biodiversity of plants and animals, but also that of parasites.

Keywords: mtDNA, Qinghai-Tibet Plateau, phylogeny, divergence time, *Taenia* spp.

OPEN ACCESS

Edited by:
Teresa Nogueira, Instituto Nacional Investigaciao Agraria e Veterinaria (INIAV), Portugal

Reviewed by:
Hamed Mirjalali, Shahid Beheshti University of Medical Sciences, Iran
Dennis Ken Bideshi, California Baptist University, United States

***Correspondence:**
Hong-Bin Yan
yanhongbin@caas.cn
Wan-Zhong Jia
jiawanzhong@caas.cn

Specialty section:
This article was submitted to Evolutionary and Genomic Microbiology, a section of the journal Frontiers in Microbiology

Received: *29 December 2020*
Accepted: *23 February 2021*
Published: *23 March 2021*

Citation:
Wu Y-D, Li L, Fan Y-L, Ni X-W, Ohiolei JA, Li W-H, Li J-Q, Zhang N-Z, Fu B-Q, Yan H-B and Jia W-Z (2021) Genetic Evolution and Implications of the Mitochondrial Genomes of Two Newly Identified Taenia spp. in Rodents From Qinghai-Tibet Plateau. Front. Microbiol. 12:647119. doi: 10.3389/fmicb.2021.647119

INTRODUCTION

The most recent molecular phylogenetic analysis has suggested that the family Taeniidae (Eucestoda: Cyclophyllidea) should be composed of four genera: *Taenia*, *Echinococcus*, *Hydatigera,* and *Versteria* (Nakao et al., 2013). Among them, *Taenia* and *Echinococcus* species pose a serious public health threat to humans and animals globally. Terrestrial mammals are crucial to the

life cycle of taeniids. Most adult tapeworms parasitize the intestines of carnivores while the intermediate hosts harbor the larva stage that develops from ingested eggs, causing severe health effects (Jia et al., 2012; Nakao et al., 2013; Lymbery, 2017; Deplazes et al., 2019).

Before the new classification recommendation of Nakao et al. (2013), two genera (*Taenia* and *Echinococcus*) were generally accepted. *Taenia* was constituted by about 42 valid species and three subspecies based on morphology (Hoberg et al., 2000; Hoberg, 2006; Nakao et al., 2013). As for *Echinococcus*, a total of 16 species and 13 subspecies were described based on morphology, but most of these taxa were subsequently invalidated following widespread application of molecular genetic methods (Lymbery, 2017). It is difficult to distinguish taeniid species according to their morphological characteristics at different stages of their life cycle, even by specialists (Flisser et al., 2005; Mathis and Deplazes, 2006; Jia et al., 2012). Sometimes, morphological characteristics are substantially influenced by the different intermediate host origins (Lymbery, 1998).

Mitochondrial (mt) DNA sequence has been recognized among the most suitable molecular markers of molecular ecology, population genetics, evolutionary biology and biological differentiation due to its high mutation rate and maternal inheritance (Hebert and Gregory, 2005; Will et al., 2005; Hajibabaei et al., 2007; Jia et al., 2012). In the last two decades, comparative analyses of taeniid mtDNAs have been increasingly applied in phylogenetic studies, for inferring evolutionary relationship, new species identification, species reclassification, phylogeography, genetic diversity, and tracing of evolutionary origins of related and identical species (Xiao et al., 2005; Nakao et al., 2007; Nakao et al., 2013; Terefe et al., 2014; Kinkar et al., 2018). Among the taeniid family, mt genomes of 36 species and genotypes have been sequenced and are available on GenBank[1], providing valuable data support for phylogenetic studies of Taeniidae.

The shrinkage and fragmentation of wildlife habitats due to human activities can lead to increased contact between humans or livestock and wildlife, which potentially increases the risk of transmission of natural focal disease (Suzán et al., 2008). Rodents, the largest (∼43% of all mammal species) and most widely distributed group of mammals, act as major vectors of human and domestic animal diseases (Singla et al., 2008; Wu et al., 2018). The Qinghai-Tibet Plateau (QTP), one of the biodiversity hotspots on earth, is habitat to a rich diversity of wild rodent species (Zhou and Ma, 2002), as well as many rodent-eating carnivores (Smith et al., 2019), creating the conditions for various taeniid species to complete their life cycles. The high altitude geographic isolation combined with the geological complexity of the QTP increases the opportunities for genetic variation and speciation, leading to the continuous discovery of new species of rodents and Taeniidae (Xiao et al., 2005; Dahal et al., 2017). However, few studies have involved the population structure and biodiversity of taeniid species in QTP, except for *Echinococcus*.

[1]https://www.ncbi.nlm.nih.gov/genbank/

As endangered or protected carnivores are difficult to sample, we collected metacestode samples of rodents to investigate the biodiversity and distribution of taeniid species in QTP. In this study, two new mt genomes of the metacestode samples were firstly sequenced and annotated. Through the phylogenetic analysis of mt genomes with species in the four different genera of taeniids, the validity of these two new *Taenia* spp., named *T. caixuepengi* and *T. tianguangfui* larvae, were confirmed and their phylogenetic relationship and evolutionary origin were analyzed.

MATERIALS AND METHODS

Ethics Statement

All animals were handled in strict accordance with good animal practice according to the Animal Ethics Procedures and Guidelines of the People's Republic of China, and the study was approved by the Animal Ethics Committee of Lanzhou Veterinary Research Institute, Chinese Academy of Agricultural Sciences (No. LVRIAEC2012-007).

Parasite Materials

Plateau pikas (*Ochotona curzoniae*) and Qinghai voles (*Neodon fuscus*) were trapped in Darlag county (33°43′N; 99°38′E; altitude at 4,068 m) and Jiuzhi county (33°19′N; 100°32′E; altitude at 3,832 m) of Qinghai province, the People's Republic of China in July 2013. Following ethical approval, all trapped pikas and voles were dissected regarding the enterocoelia, chest and cranial cavities. Many banded cysticerci were collected in the enterocoelia of Plateau pika (**Supplementary Figures S1A,B**) and numerous lenticular cysticerci were collected in the enterocoelia and chest of Qinghai vole (**Supplementary Figures S1C,D**). Detailed sample collection data can be found in **Supplementary Table S1**. After detaching the lesions, the cysticerci were put into 75% (v/v) ethanol for molecular and morphological identification. Cysticerci from pikas and voles were photographed by Thermo Scientific™ Apreo S SEM, and their hooks were hand-drawn using Point 3D of Microsoft.

DNA Isolation, Amplification, and Sequencing

Cysticercus DNA was extracted using a commercial kit as instructed by the manufacturer (Blood and Tissue Kit, Qiagen, Germany). The mt genomes of *Taenia* spp., whose intermediate hosts include rodents, downloaded from GenBank (**Supplementary Table S3**) were aligned by using MEGA 7.0. Nine overlapping primers targeting the complete mt genome were designed using Oligo 6.0 at relatively conserve regions observed on alignment of the mt genome sequences. The primer sequences (**Supplementary Table S2**) were synthesized by Genewiz Biotech (Beijing, China). A standard 50 μl PCR protocol was used to amplify the mtDNA fragments. PCR products were purified directly from an agarose gel (1%) using an Axy Prep™ DNA Gel Extraction Kit (AXVGEN, United States) and then sent to the company Genewiz Biotech for sequencing.

Mitochondrial Genome Annotation

These two mtDNAs were assembled manually, and annotated preliminarily by Geseq[2] with the reference of related species, *T. pisiformis* and *T. crassiceps*, identified by the *cox*1 gene alignment of Neighbor-Joining method in MEGA 7.0 (data not shown). Putative tRNA genes were identified using ARWEN[3] (Laslett and Canbäck, 2008). The positions of their open reading frames and rRNA genes were also further checked and modified based on alignment with the mt genomes annotation of *T. pisiformis* and *T. crassiceps*, respectively. SnapGene (v3.2.1) was used to translate the amino acid sequence of the protein-coding genes with Echinoderm, Flatworm Mitochondrial genetic code and map the annular diagram of the mt genomes.

Phylogenetic Analyses

To determine the phylogenetic status of these two Taenia spp., the phylogenetic trees were constructed using Bayesian methods in MrBayes v3 with the tandem DNA sequences and amino acid sequences of 12 encoding genes in their mt genomes and other 32 taeniid mt genome sequences downloaded from GenBank, while the sequences of *Schistosoma japonicum* was used as outgroup (**Supplementary Table S2**). For the amino acid data set, the mixed model was applied (prset aamodelpr = mixed); two chains (temp = 0.2) were run for 3,000,000 generations and sampled every 1,000 generations (Rota-Stabelli et al., 2009). For the nucleotide data set, Modeltest 3.7 maxX (Posada and Crandall, 1998) was used to estimate a suitable model for nucleotide substitution; this was equivalent to GTR + I + G and settings were nst = 6, rates = invgamma, ngammacat = 4. Four chains (temp = 0.2) were run for 1,000,000 generations and sampled every 1,000 generations. The first 25% of trees were omitted as burn-in and the remaining trees were used to calculate Bayesian posterior probabilities. The best Bayesian tree was then compiled and processed by FigTree.v1.4.4.

Divergence Times Analysis

The phylogenetic trees were used as a reference for species selection in divergence times analysis. *Echinococcus multilocularis* and *E. shiquicus* were also selected because the parasitism of their larvae is also found in Plateau pika (*O. curzoniae*) (Wang et al., 2018), besides *E. multilocularis* is the sister species of *E. shiquicus* (Lymbery, 2017). Divergence times were calculated from the concatenated CDS alignment of the 12 mitochondrial protein-coding genes by BEAST2 (v2.6.2). The Strict Clock model was chosen to ignore the rate differences between the branches in the mode. The gamma category count was set to 4, and HKY substitution model was selected with the empirical setting from the frequencies in site model. Other settings, such as substitution rate and shape, in the site model were evaluated in the analysis. The calibrated Yule model was used as the tree prior. Time calibration was calibrated with the previously estimated date between *T. saginata* and *T. asiatica* (∼1.14 Mya) (Michelet and Dauga, 2012; Wang et al., 2016). Samples from the posterior were drawn every 1,000 steps over a total of 10,000,000 steps per MCMC run. Other options were run on their default values. The convergence of likelihood values was determined by Tracer (v1.7.1). Trees were annotated by TreeAnnotator (v2.1.2) using maximum clade credibility tree and median heights settings with 50% burn-in. The evolutionary divergence time of the intermediate host, Qinghai vole (*N. fuscus*), was also calculated with the concatenated CDS alignment of 13 mt protein-coding genes of the rodents, and the species involved were selected from our previous report (Li et al., 2019; **Supplementary Table S3**). The time calibration was based on the divergence time of *Mus* and *Rattus* (11–13 Mya) (Wang et al., 2020), and other parameters were the same as above.

[2]https://chlorobox.mpimp-golm.mpg.de/geseq.html

[3]http://130.235.46.10/ARWEN/

RESULTS

General Features of the Mitochondrial Genome of Two Parasites

A total of 300 pika (125) and voles (175) were examined. Overall, 7.3% were infected with cysticerci (see **Supplementary Table S1** for more details). Amplification and sequencing of a fragment of the *cox*1 gene using the conserved JB3 and JB4.5 primers (Bowles et al., 1992) confirmed their identity. From both study sites, cysticerci from pikas were the same new species, named *T. caixuepengi* larva, meanwhile, the cysticerci from voles were morphologically different from *T. caixuepengi* larva and were named *T. tianguangfui* larva. Their complete mt genomes were sequenced and spliced, and were 13,747 bp (GenBank ID: MT882036) and 13,522 bp (GenBank ID: MT882037) in length, respectively. Both contain 2 rRNA genes [the small (*rrn*S) and large (*rrn*L) subunits of rRNA], 12 protein-encoding genes (*atp*6, *cyt*b, *nad*4L, *cox*1-3, and *nad*1-6) and 22 tRNA genes, but lack *atp*8 gene, which are typical of cestode mt genomes (**Figure 1**). The inferred gene boundaries and their lengths are shown in **Table 1**.

In accordance with other mtDNAs of flatworms sequenced to date (Jia et al., 2010; Liu et al., 2011), the nucleotide compositions are mostly biased toward T, while least favored toward C. AT-richness of mtDNAs in *T. caixuepengi* and *T. tianguangfui* are 71.96% (45.00% T, 26.97% A, 19.17% G, 8.87% C) and 73.48% (46.35% T, 27.13% A, 18.61% G, 7.91% C), respectively.

Flatworms use an unusual mt code to exert protein translation (Nakao et al., 2000; Telford et al., 2000). GTG was used as an alternative initiation codon in *cox*3 and *nad*3 genes of *T. caixuepengi* and *nad*5 gene of *T. tianguangfui*. Furthermore, the codon ATT was inferred as a more unusual start codon of *atp*6 gene in *T. caixuepengi*. The termination codon was mostly TAA, and the ending codon TGA was deprecated (**Table 1**).

Morphological Description

By gross observation and measurement, *T. caixuepengi* larva was translucent and stripped, 33-36 mm long, and contains cystic fluid (**Supplementary Figures S1A,B**); *T. tianguangfui* larva on the other hand was opaque, bean-shaped and about 4–10 mm in length (**Supplementary Figures S1C,D**). Scanning electron microscope observation of their scoleces showed that *T. caixuepengi* larva had four suckers, 16 large hooks and 18 small hooks, the average length of which was about 250 and 100 μm,

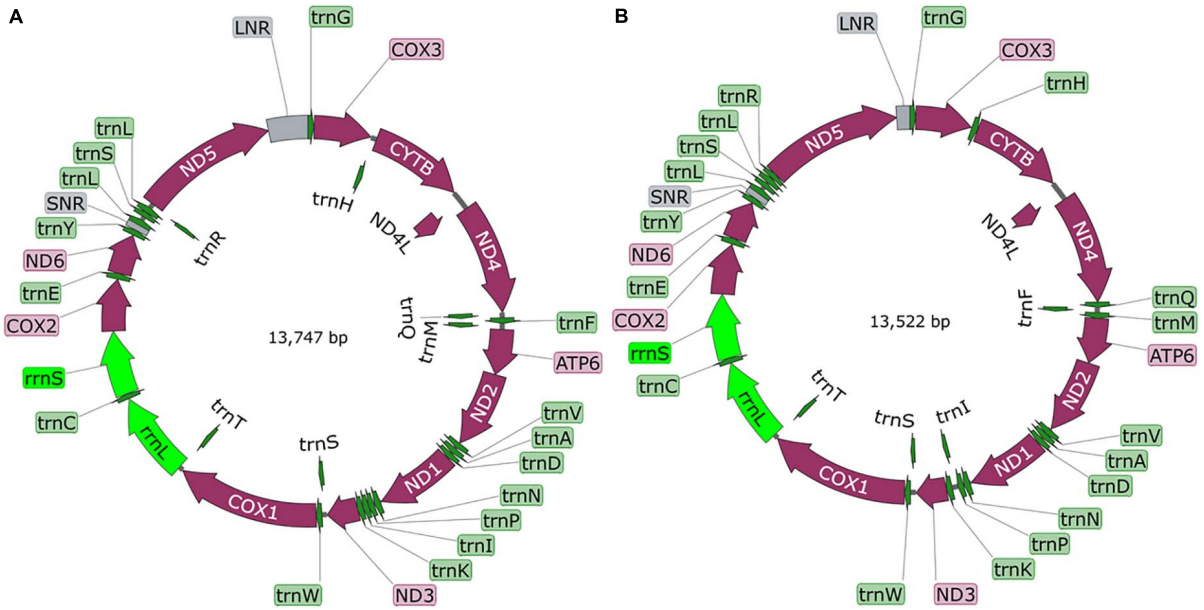

FIGURE 1 | The diagram of complete mitochondrial genome of *Taenia tianguangfui* **(A)** and *Taenia caixuepengi* **(B)**. The protein-encoding genes are depicted in plum, the tRNAs are depicted in green, the rRNAs are depicted in light green and the non-coding mitochondrial regions (NCRs including LNR and SNR) are depicted in gray. The inferred gene boundaries of them are shown in **Table 1**.

respectively (**Figures 2A–C**); *T. tianguangfui* larva also had four suction cups, and 31–33 large and small hooks of about 100 and 80 μm in length, respectively (**Figures 2D–F**).

Phylogenetic Relationships

Phylogenies inferred from both tandem amino acid sequences and DNA sequences of the 12 mt protein-encoding genes demonstrated *T. caixuepengi* in a monophyletic group with *T. pisiformis* and *T. laticollis*, with the closest genetic relative being *T. pisiformis*; *T. tianguangfui* was also found in a monophyletic group with *T. crassiceps*, *T. twitchelli*, and *T. martis*, and has a distant genetic relationship with *T. caixuepengi* (**Figure 3**).

Divergence Times Analyses

The divergence time analysis based on mitochondrial protein-coding genes suggested that *T. saginata* and *T. asiatica* should diverge at 1.10 Mya (0.80–1.41, 95% highest probability density) in the early Pleistocene period, which is consistent with the previous reports based on genomic genes (Michelet and Dauga, 2012; Wang et al., 2016); *T. caixuepengi* should diverge from *T. pisiformis* 5.49 Mya (3.87–7.19, 95% highest probability density) in the initial Pliocene period, which is close to the divergence time between *E. shiquicus* and *E. multilocularis* (4.12 Mya, 2.81–5.32, 95% highest probability density); *T. tianguangfui* on the other hand, originated 13.11 Mya (9.36–17.18, 95% highest probability density) in the middle Miocene period, which was earlier than the differentiation of its intermediate host, *N. fuscus* (4.98 Mya, 4.08–5.90, 95% highest probability density) (**Figure 4** and **Supplementary Figure S2**).

DISCUSSION

The discovery of these two new parasites, *T. caixuepengi* and *T. tianguangfui*, highlights the species diversity of the family Taeniide, and further proved the true biodiversity characteristic of the QTP. Given the lack of human intervention and the rich diversity of wild host species, the present understanding of the species diversity within this family in QTP is apparently just a tip of the iceberg. This is not surprising, given the appreciable cryptic diversity so far uncovered within the taeniid family in Africa and northern latitudes (Lavikainen et al., 2011, 2013; Terefe et al., 2014).

Morphological features traditionally used to distinguish the cysticerci, including the number of hooks, the length of large hooks and small hooks (Loos-Frank, 2000), are insufficient in inferring evolutionary lineages. This is because homoplasy of morphological characters can represent a serious obstacle in taxonomic investigation (Scholz et al., 2020). Here the whole mt genomes of both species were sequenced, and clearly different from all available *Taenia* mt genome sequences, verifying the validity of their species status. Their mt genomes were similar as those of other sequenced tapeworms with respect to length, nucleotide bias, and their tRNA, rRNA and protein-encoding genes composition (**Figure 1**; Le et al., 2000; Nakao et al., 2003; Jeon et al., 2005; Jeon et al., 2007). Furthermore, the codon ATT was inferred as a more unusual start codon for the *atp6* gene of *T. caixuepengi* (**Table 1**), which is a common start codon used by *Caenorhabditis elegans* and *Ascaris suum* (Okimoto et al., 1990).

T. caixuepengi larva is so far undetected in other animals, except plateau pika (*O. curzoniae*), meanwhile, no other

TABLE 1 | Positions and gene lengths in the mitochondrial genomes of *Taenia tianguangfui* (Tt), *T. caixuepengi* (Tc).

Genes	Positions (length, bp)		Initiation and termination codons		Anticodons
	Tt	Tc	Tt	Tc	
*trn*G	1–65 (65)	1–68 (68)			TCC
*cox*3	68–715 (648)	72–722 (651)	ATG/TAG	GTG/TAA	
*trn*H	724–792 (69)	716–786 (71)			GTG
*Cyt*b	796–1,863 (1,068)	790–1,857 (1,068)	ATG/TAG	ATG/TAA	
*nad*4L	1,865–2,125 (261)	1,857–2,117 (261)	ATG/TAG	ATG/TAA	
*nad*4	2,092–3,348 (1,257)	2,084–3,337 (1,254)	ATG/TAG	ATG/TAA	
*trn*Q	3,349–3,409 (61)	3,338–3,400 (63)			TTG
*trn*F	3,409–3,472 (64)	3,400–3,463 (64)			GAA
*trn*M	3,469–3,534 (66)	3,461–3,524 (64)			CAT
*atp*6	3,535–4,053 (519)	3,531–4,043 (513)	ATG/TAG	ATT/TAA	
*nad*2	4,058–4,930 (873)	4,045–4,917 (873)	ATG/TAA	ATG/TAG	
*trn*V	4,947–5,011 (65)	4,922–4,983 (62)			TAC
*trn*A	5,012–5,075 (64)	4,996–5,058 (63)			TGC
*trn*D	5,085–5,149 (65)	5,067–5,128 (62)			GTC
*nad*1	5,154–6,047 (894)	5,134–6,030 (897)	ATG/TAA	ATG/TAA	
*trn*N	6,064–6,131 (68)	6,044–6,109 (66)			GTT
*trn*P	6,141–6,205 (65)	6,118–6,180 (63)			TGG
*trn*I	6,205–6,267 (63)	6,181–6,244 (64)			GAT
*trn*K	6,273–6,338 (66)	6,246–6,309 (64)			CTT
*nad*3	6,342–6,689 (348)	6,310–6,657 (348)	ATG/TAA	GTG/TAA	
*trn*S	6,689–6,747 (59)	6,656–6,716 (61)			GCT
*trn*W	6,755–6,820 (66)	6,716–6,778 (63)			TCA
*cox*1	6,824–8,443 (1,620)	6,782–8,401 (1,620)	ATG/TAA	ATG/TAA	
*trn*T	8,429–8,495 (67)	8,387–8,451 (65)			TGT
*rrn*L	8,496–9,468 (973)	8,452–9,412 (961)			
*trn*C	9,469–9,529 (61)	9,418–9,475 (58)			GCA
*rrn*S	9,530–10,266 (737)	9,476–10,200 (725)			
*cox*2	10,267–10,844 (578)	10,201–10,785 (585)	ATG/TAA	ATG/TAA	
*trn*E	10,853–10,920 (68)	10,787–10,853 (67)			TTC
*nad*6	10,923–11,375 (453)	10,855–11,307 (453)	ATG/TAA	ATG/TAG	
*trn*Y	11,379–11,441 (63)	11,314–11,376 (63)			GTA
SNR	11,442–11,508 (67)	11,377–11,441 (65)			
*trn*L	11,509–11,574 (66)	11,443–11,512 (70)			TAG
*trn*S	11,604–11,661 (58)	11,550–11,609 (60)			TGA
*trn*L	11,673–11,738 (66)	11,612–11,680 (69)			TAA
*trn*R	11,744–11,802 (59)	11,680–11,734 (55)			TCG
*nad*5	11,803–13,371 (1,569)	11,729–13,303 (1,575)	GTG/TAA	ATG/TAA	
LNR	13,372–13,522 (151)	13,304–13,747 (444)			

cysticerci have been found in plateau pika hitherto. Lagomorph is the intermediate host of *T. pisiformis* and *T. laticollis* (Valdmann et al., 2004; Hallal-Calleros et al., 2016). Although similar in appearance and size to the vole, the plateau pika belongs to Lagomorpha (Smith et al., 2019). The close phylogenetic relatedness of these three *Taenia* species (**Figure 3**) is further highlighted by their high preference for lagomorphs as an intermediate host. Based on the divergence time and phylogeographic analyses, the extent pikas (genus *Ochotona*) originated on the QTP in the middle Miocene, ∼14 Mya (Wang et al., 2020). However, the rapid speciation of many *Ochotona* species, including *O. curzoniae*, occurred during the late Miocene and early Pliocene period (Wang et al., 2020), which almost coincided with the rapid uplift of the QTP (An et al., 2006; Li et al., 2007; Shi et al., 2015). Coincidentally, the evolutionary divergence time analysis in this study also suggests that both *T. caixuepengi* and *E. shiquicus* had evolved in the early Pliocene epoch, about 5.49 and 4.12 Mya, respectively (**Figure 4**). These almost synchronous events may not have happened by chance. Large-scale diversification of species is often provoked by abiotic factors, such as changes in the living environment and food supply (Benton, 2009). The uplift of the QTP from south to north provided climatic opportunities and food supply for the diversification of cold temperature-preferring pikas but led to

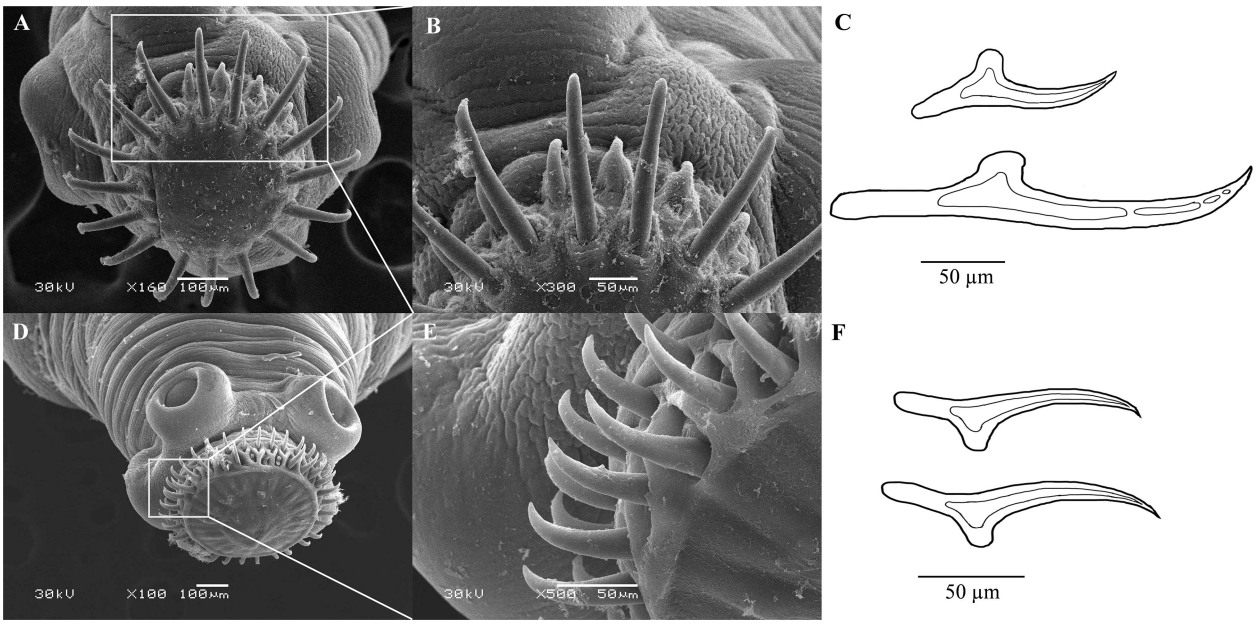

FIGURE 2 | Scanning electron micrographs of scoleces and line drawing of hooks of *Taenia tianguangfui* larva **(A–C)** and *Taenia caixuepengi* larva **(D–F)**.

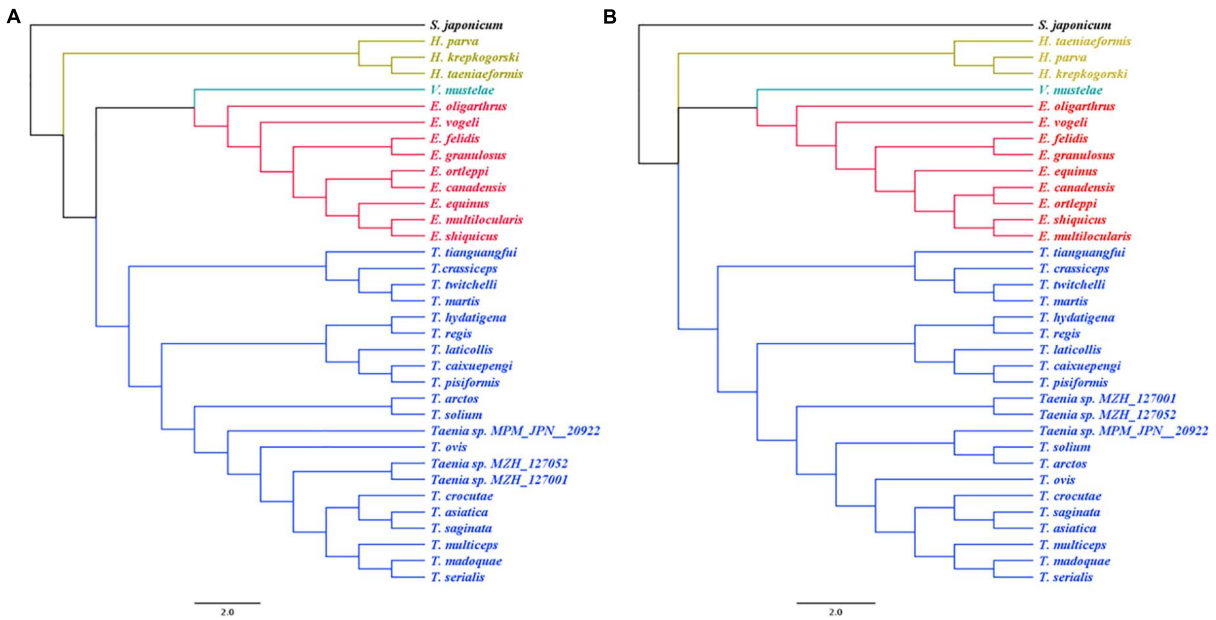

FIGURE 3 | The phylogenetic relationship of *Taenia tianguangfui* and *Taenia caixuepengi*, with other 32 tapeworm species inferred from a Bayesian method based on the concatenated amino acid **(A)** and CDS alignments **(B)** of mitochondrial 12 protein-encoding genes. The species' name corresponding to the GenBank ID is given in the **Supplementary Table S2**. The *Echinococcus* spp. are depicted in red, the *Taenia* spp. are depicted in blue, the *Hydatigera* spp. are depicted in yellow and the only one *Versteria* species, *Versteria mustelae*, is depicted in green. The *Schistosoma japonicum* depicted in black was chosen as outgroup.

the extinction of other warm temperature-preferring rodents (Wang et al., 2020).

For most free-living organisms, speciation is usually the result of genetic drift or adaptive differentiation between geographically separate populations (Turelli et al., 2001). For parasites, however, it has long been thought that sympatric speciation of parasites is common, mediated by ecological isolation caused by host switching within the same geographic region (de Meeûs et al., 1998; Paul, 2002; Huyse et al., 2005). Therefore, we speculate that *T. pisiformis* in the QTP (Li et al., 2013) may share a common ancestor with *T. caixuepengi*; the split of the pika population caused the ecological isolation between their ancestral

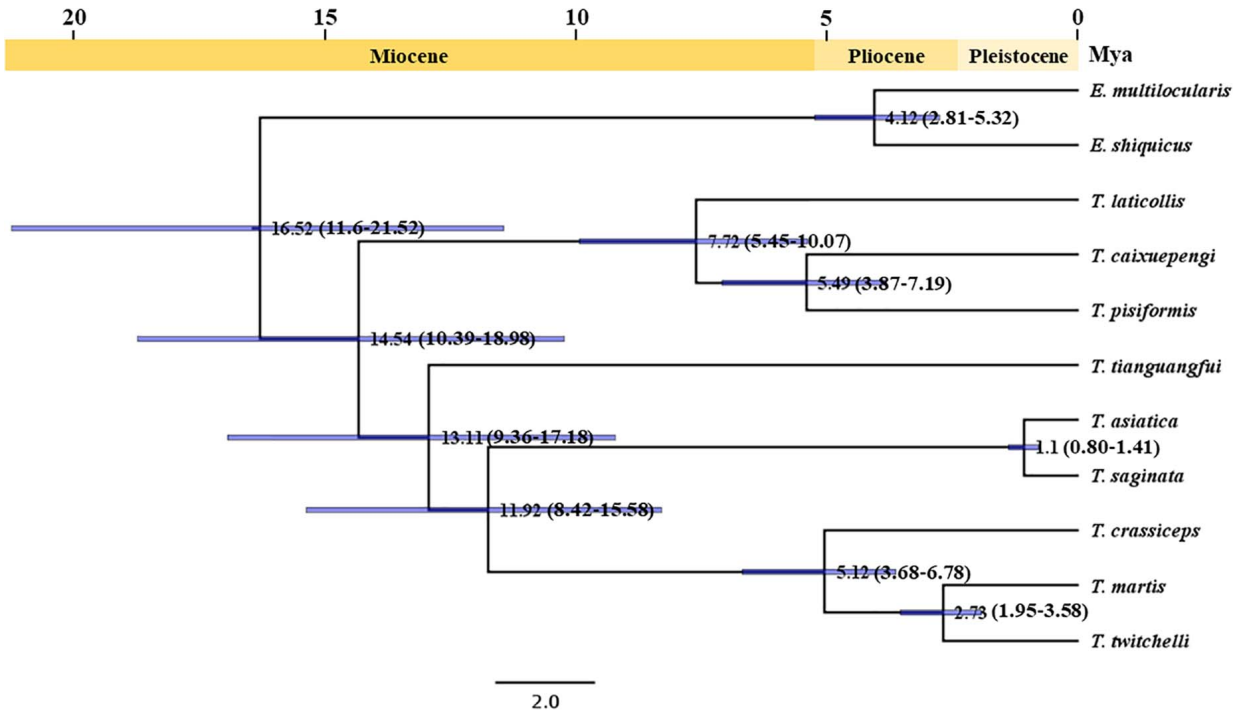

FIGURE 4 | Divergence times construction for *Taenia tianguangfui* and *Taenia caixuepengi* based on the concatenated CDS alignments of mitochondrial 12 protein-encoding genes. The number at the node represents the divergence time between two lineages. The blue bar represents interval of 95% highest probability density, and the number in brackets represents the detailed time interval of 95% highest probability density of divergence time between two lineages. A time scale shows the extent of the Miocene, Pliocene and Pleistocene period.

populations, which further resulted in the lack of gene flow between them due to intermediate host switching, and the eventual formation of two different species. It can also be speculated that the differentiation pattern between *E. shiquicus* and *E. multilocularis* is similar as that of *T. caixuepengi* and *T. pisiformis*.

Our evolutionary divergence time analysis suggests that the speciation of *T. tianguangfui* occurred in the middle Miocene period (∼13.11 Mya) (**Figure 4**) when the QTP was undergoing a slow uplift period (An et al., 2006). The timing of the divergence of *N. fuscus* evolved from ∼4.98 Mya (**Supplementary Figure S2**), which also coincided with the rapid uplift of the QTP (An et al., 2006; Li et al., 2007; Shi et al., 2015). As the species spread in the QTP and Himalaya (Pradhan et al., 2019), the evolutionary origin of the *Neodon* spp., like the plateau pika, may well be due to changes in climate and food supply caused by the uplift of the QTP and Himalaya. The speciation of *T. tianguangfui* was earlier than that of its intermediate host, indicating that *T. tianguangfui* did not differentiate into a new *Taenia* species in order to adapt to the intermediate host, rather, it suggests that *T. tianguangfui* larva might not be limited to *N. fuscus*. *Taenia crassiceps* and *T. martis* have similar intermediate hosts range, infecting a variety of rodents, even humans and other primates (Deplazes et al., 2019). Given the close relationship between *T. tianguangfui*, *T. crassiceps,* and *T. martis*, it also cannot be excluded that *T. tianguangfui* may be infective to a variety of rodents other than *N. fuscus*, as well as humans and other primates. So far, a clear understanding of their evolutionary origin from these clues is elusive, thus, more data and investigation are needed to provide further insight.

Adult worms of the *T. tianguangfui* and *T. caixuepengi* have not yet been collected due to the difficulty in sampling endangered or protected carnivores. However, nucleic acid from feces of wolves, foxes and dogs found at the sampling sites were examined, so far, no positive feces samples for these two species have been found. Plateau pikas and voles are the primary food source for wild canids across the QTP. Tibetan foxes are the obligate predator of plateau pikas, as their remains (plateau pikas) are often encountered in 99% of their feces (Smith et al., 2019). Wild canids, especially the red fox and the Tibetan fox, may well be important definitive hosts for *T. tianguangfui* and *T. caixuepengi*.

Adult or larval samples of tapeworm are easily damaged in the process of collection, freeze-thaw and processing, and the morphological features are mostly unidentifiable (Lavikainen et al., 2013). While mt genome data alone may not fully answer the scientific questions surrounding their evolutionary origins, it is the most cost-effective and accurate method. Recently, although laborious and costly, there have been an increasing whole genome sequencing and analyses for many tapeworm species. This kind of investigation, not only is it important to provide insights into their host adaptation and switching, evolution mechanisms through gene groups amplification, hosts-parasites interaction, immune regulation and nutrition, it also

provides urgently needed resources for the identification of drug target and diagnostic molecular markers (Wang et al., 2016; International Helminth and Genomes Consortium, 2019). In the future, a lot of genomic data will be needed to study this fascinating group.

In conclusion, the mitochondrial genome sequence data adequately confirm the validity of the two new *Taenia* species named *T. caixuepengi* and *T. tianguangfui*, we have previously reported. The phylogenetic trees and divergence times analyses suggest that *T. caixuepengi* evolve from its closest relative, *T. pisiformis*, in the initial Pliocene period (∼5.49 Mya), due to the intermediate host switching caused by the rapid uplift of the QTP; *T. tianguangfui* is probably parasitic in a wide variety of rodents, and share a common ancestor with *T. crassiceps*, *T. twitchelli* and *T. martis*, splitting in middle Miocene period (∼13.11 Mya).

DATA AVAILABILITY STATEMENT

The datasets presented in this study can be found in online repositories. The names of the repository/repositories and accession number(s) can be found below: https://www.ncbi.nlm.nih.gov/nucleotide.GenBankID:MT882036~and~MT882037.

ETHICS STATEMENT

The animal study was reviewed and approved by the Animal Ethics Procedures and Guidelines of the People's Republic of China and Animal Ethics Committee of Lanzhou Veterinary Research Institute, Chinese Academy of Agricultural Sciences (No. LVRIAEC2012-007).

AUTHOR CONTRIBUTIONS

Y-DW, LL, H-BY, and W-ZJ conceived and designed the experiments. Y-DW, Y-LF, and X-WN performed the experiments. Y-DW and Y-LF performed the data analyses. Y-DW prepared the figures and wrote the manuscript. JO provided improving paragraphs and language editing. W-HL, N-ZZ, and B-QF provided very constructive suggestions for revisions. All authors read and approved the final manuscript.

FUNDING

This work was funded by the National Key Research and Development Plan (2018YFC1602504 and 2017YFD0501301), Central Public-Interest Scientific Institution Basal Research Fund (1610312020016), and Cultivation of Achievements of State Key Laboratory of Veterinary Etiological Biology (SKLVEB2020CGPY01).

SUPPLEMENTARY MATERIAL

The Supplementary Material for this article can be found online at: https://www.frontiersin.org/articles/10.3389/fmicb.2021.647119/full#supplementary-material

Supplementary Figure 1 | The larvae of *Taenia caixuepengi* and *Taenia tianguangfui* were found in Plateau pikas *(Ochotona curzoniae)* and Qinghai voles (*Neodon fuscus*), respectively. The banded larvae of *T. caixuepengi* in the plate **(A)** were picked out from the enterocoelia of Plateau pikas **(B)**, and the granular larvae of *T. tianguangfui* in the plate **(C)** were picked out from the enterocoelia and chest of Qinghai voles **(D)**. The blue arrow indicates the parasitic larvae.

Supplementary Figure 2 | Divergence times construction for *Neodon fuscus* based on the concatenated CDS alignments of mitochondrial 13 protein-encoding genes. The number at the node represents the divergence time between two lineages. The blue bar represents interval of 95% highest probability density, and the number in brackets represents the detailed time interval of 95% highest probability density of divergence time between two lineages. A time scale shows the extent of the Miocene, Pliocene and Pleistocene period.

Supplementary Table 1 | Detailed sample collection data.

Supplementary Table 2 | The primers for amplifying the complete mitochondrial genomes of cysticercus.

Supplementary Table 3 | GenBank accession numbers of mitochondrial genome sequences used for phylogenetic analyses and divergence times analyses in this study.

REFERENCES

An, Z. S., Zhang, P. Z., Wang, E. Q., Wang, S. M., Qiang, X. K., Li, L., et al. (2006). Changes of the monsoon−arid environment in China and growth of the Tibetan Plateau since the Miocene. *Q. Sci.* 26, 678–693.

Benton, M. J. (2009). The Red Queen and the Court Jester: species diversity and the role of biotic and abiotic factors through time. *Science* 323, 728–732. doi: 10.1126/science.1157719

Bowles, J., Blair, D., and McManus, D. P. (1992). Genetic variants within the genus *Echinococcus* identified by mitochondrial DNA sequencing. *Mol. Biochem. Parasitol.* 54, 165–173. doi: 10.1016/0166-6851(92)90109-w

Dahal, N., Lissovsky, A. A., Lin, Z., Solari, K., Hadly, E. A., Zhan, X., et al. (2017). Genetics, morphology and ecology reveal a cryptic pika lineage in the Sikkim Himalaya. *Mol. Phylogenet. Evol.* 106, 55–60. doi: 10.1016/j.ympev.2016.09.015

de Meeûs, T., Michalakis, Y., and Renaud, F. (1998). Santa rosalia revisited: or why are there so many kinds of parasites in; the garden of earthly delights'? *Parasitol. Today* 14, 10–13. doi: 10.1016/s0169-4758(97)01163-0

Deplazes, P., Eichenberger, R. M., and Grimm, F. (2019). Wildlife-transmitted *Taenia* and *Versteria* cysticercosis and coenurosis in humans and other primates. *Int. J. Parasitol. Parasites Wildl.* 9, 342–358. doi: 10.1016/j.ijppaw.2019.03.013

Flisser, A., Correa, D., Avilla, G., and Marvilla, P. (2005). "Biology of *Taenia solium*, *Taenia saginata* and *Taenia saginata asiatica*," in *WHO/FAO/OIE Guidelines for the Surveillance, Prevention and Control of Taeniosis/Cysticercosis*, eds K. D. Murrell and Paris (Geneva: World Health Organization), 14–22.

Hajibabaei, M., Singer, G. A., Hebert, P. D., and Hickey, D. A. (2007). DNA barcoding: how it complements taxonomy, molecular phylogenetics and population genetics. *Trends Genet.* 23, 167–172. doi: 10.1016/j.tig.2007.02.001

Hallal-Calleros, C., Morales-Montor, J., Orihuela-Trujillo, A., Togno-Peirce, C., Murcia-Mejía, C., Bielli, A., et al. (2016). *Taenia pisiformis* cysticercosis induces decreased prolificacy and increased progesterone levels in rabbits. *Vet. Parasitol.* 229, 50–53. doi: 10.1016/j.vetpar.2016.09.015

Hebert, P. D., and Gregory, T. R. (2005). The promise of DNA barcoding for taxonomy. *Syst. Biol.* 54, 852–859. doi: 10.1080/10635150500354886

Hoberg, E. P., Jones, A., Rausch, R. L., Eom, K. S., and Gardner, S. L. (2000). A phylogenetic hypothesis for species of the genus *Taenia* (Eucestoda : Taeniidae). *J. Parasitol.* 86, 89–98. doi: 10.1645/0022-3395200 0086[0089:APHFSO]2.0.CO;2

Hoberg, E. P. (2006). Phylogeny of *Taenia*: Species definitions and origins of human parasites. *Parasitol. Int.* 55, S23–S30. doi: 10.1016/j.parint.2005.11.049

Huyse, T., Poulin, R., and Théron, A. (2005). Speciation in parasites: a population genetics approach. *Trends Parasitol.* 21, 469–475. doi: 10.1016/j.pt.2005. 08.009

International Helminth, and Genomes Consortium. (2019). Comparative genomics of the major parasitic worms. *Nat. Genet.* 51, 163–174. doi: 10.1038/s41588-018-0262-1

Jeon, H. K., Kim, K. H., and Eom, K. S. (2007). Complete sequence of the mitochondrial genome of *Taenia saginata*: comparison with *T. solium* and *T. asiatica*. *Parasitol. Int.* 56, 243–246. doi: 10.1016/j.parint.2007.04.001

Jeon, H. K., Lee, K. H., Kim, K. H., Hwang, U. W., and Eom, K. S. (2005). Complete sequence and structure of the mitochondrial genome of the human tapeworm. Taenia asiatica (Platyhelminthes; Cestoda). *Parasitology* 130, 717–726. doi: 10. 1017/s0031182004007164

Jia, W. Z., Yan, H. B., Guo, A. J., Zhu, X. Q., Wang, Y. C., Shi, W. G., et al. (2010). Complete mitochondrial genomes of *Taenia multiceps*, *T. hydatigena* and *T. pisiformis*: additional molecular markers for a tapeworm genus of human and animal health significance. *BMC Genomics* 11:447. doi: 10.1186/1471-2164-11-447

Jia, W., Yan, H., Lou, Z., Ni, X., Dyachenko, V., Li, H., et al. (2012). Mitochondrial genes and genomes support a cryptic species of tapeworm within *Taenia taeniaeformis*. *Acta Trop.* 123, 154–163. doi: 10.1016/j.actatropica.2012.04.006

Kinkar, L., Laurimäe, T., Acosta-Jamett, G., Andresiuk, V., Balkaya, I., Casulli, A., et al. (2018). Global phylogeography and genetic diversity of the zoonotic tapeworm *Echinococcus granulosus* sensu stricto genotype G1. *Int. J. Parasitol.* 48, 729–742. doi: 10.1016/j.ijpara.2018.03.006

Laslett, D., and Canbäck, B. (2008). ARWEN: a program to detect tRNA genes in metazoan mitochondrial nucleotide sequences. *Bioinformatics* 24, 172–175. doi: 10.1093/bioinformatics/btm573

Lavikainen, A., Haukisalmi, V., Deksne, G., Holmala, K., Lejeune, M., Isomursu, M., et al. (2013). Molecular identification of *Taenia* spp. in the Eurasian lynx (*Lynx lynx*) from Finland. *Parasitology* 140, 653–662. doi: 10.1017/ S0031182012002120

Lavikainen, A., Laaksonen, S., Beckmen, K., Oksanen, A., Isomursu, M., and Meri, S. (2011). Molecular identification of *Taenia* spp. in wolves (*Canis lupus*), brown bears (*Ursus arctos*) and cervids from North Europe and Alaska. *Parasitol. Int.* 60, 289–295. doi: 10.1016/j.parint.2011.04.004

Le, T. H., Blair, D., Agatsuma, T., Humair, P. F., Campbell, N. J., Iwagami, M., et al. (2000). Phylogenies inferred from mitochondrial gene orders-a cautionary tale from the parasitic flatworms. *Mol. Biol. Evol.* 17, 1123–1125. doi: 10.1093/ oxfordjournals.molbev.a026393

Li, D. P., Zhao, Y., Hu, J. M., Wan, J. L., Li, X. L., Zhou, X. K., et al. (2007). Fission track thermochronologic constraints on plateau surface and geomorphic relief formation in the northwestern margin of the Tibetan Plateau. *Acta Petrologica Sinica* 23, 900–910.

Li, J. Q., Li, L., Fu, B. Q., Yan, H. B., and Jia, W. Z. (2019). Complete mitochondrial genomes confirm the generic placement of the plateau vole. *Neodon fuscus*. *Biosci. Rep.* 39:BSR20182349. doi: 10.1042/BSR201 82349

Li, W., Guo, Z., Duo, H., Fu, Y., Peng, M., Shen, X., et al. (2013). Survey on helminths in the small intestine of wild foxes in Qinghai. *China. J. Vet. Med. Sci.* 75, 1329–1333. doi: 10.1292/jvms.13-0187

Liu, G. H., Lin, R. Q., Li, M. W., Liu, W., Liu, Y., Yuan, Z. G., et al. (2011). The complete mitochondrial genomes of three cestode species of *Taenia* infecting animals and humans. *Mol. Biol. Rep.* 38, 2249–2256. doi: 10.1007/s11033-010-0355-0

Loos-Frank, B. (2000). An up-date of Verster's (1969) 'Taxonomic revision of the genus *Taenia* Linnaeus' (Cestoda) in table format. *Syst. Parasitol.* 45, 155–183. doi: 10.1023/a:1006219625792

Lymbery, A. J. (1998). Combining data from morphological traits and genetic markers to determine transmission cycles in the tape worm, *Echinococcus granulosus*. *Parasitology* 117, 185–192. doi: 10.1017/s0031182098 002911

Lymbery, A. J. (2017). Phylogenetic Pattern, Evolutionary Processes and Species Delimitation in the Genus *Echinococcus*. *Adv. Parasitol.* 95, 111–145. doi: 10. 1016/bs.apar.2016.07.002

Mathis, A., and Deplazes, P. (2006). Copro-DNA tests for diagnosis of animal taeniid cestodes. *Parasitol. Int.* 55, S87–S90. doi: 10.1016/j.parint.2005.11.012

Michelet, L., and Dauga, C. (2012). Molecular evidence of host influences on the evolution and spread of human tapeworms. *Biol. Rev. Camb. Philos. Soc.* 87, 731–741. doi: 10.1111/j.1469-185X.2012.00217.x

Nakao, M., Lavikainen, A., Iwaki, T., Haukisalmi, V., Konyaev, S., Oku, Y., et al. (2013). Molecular phylogeny of the genus *Taenia* (Cestoda: Taeniidae): proposals for the resurrection of *Hydatigera* Lamarck, 1816 and the creation of a new genus *Versteria*. *Int. J. Parasitol.* 43, 427–437. doi: 10.1016/j.ijpara.2012. 11.014

Nakao, M., McManus, D. P., Schantz, P. M., Craig, P. S., et al. (2007). A molecular phylogeny of the genus *Echinococcus* inferred from complete mitochondrial genomes. *Parasitology* 134, 713–722. doi: 10.1017/S0031182006001934

Nakao, M., Sako, Y., and Ito, A. (2003). The mitochondrial genome of the tapeworm *Taenia solium*: a finding of the abbreviated stop codon U. *J. Parasitol.* 89, 633–635. doi: 10.1645/0022-3395(2003)089[0633:TMGOTT]2.0.CO;2

Nakao, M., Sako, Y., Yokoyama, N., Fukunaga, M., and Ito, A. (2000). Mitochondrial genetic code in cestodes. *Mol. Biochem. Parasitol.* 111, 415–424. doi: 10.1016/s0166-6851(00)00334-0

Okimoto, R., Macfarlane, J. L., and Wolstenholme, D. R. (1990). Evidence for the frequent use of TTG as the translation initiation codon of mitochondrial protein genes in the nematodes, *Ascaris suum* and *Caenorhabditis elegans*. *Nucleic Acids Res.* 18, 6113–6118. doi: 10.1093/nar/18.20.6113

Paul, R. (2002). Species concepts versus species criteria. *Trends Parasitol.* 18, 439–440. doi: 10.1016/s1471-4922(02)02319-x

Posada, D., and Crandall, K. A. (1998). MODELTEST: testing the model of DNA substitution. *Bioinformatics* 14, 817–818. doi: 10.1093/bioinformatics/14.9.817

Pradhan, N., Sharma, A. N., Sherchan, A. M., Chhetri, S., Shrestha, P., and Kilpatrick, C. W. (2019). Further assessment of the Genus *Neodon* and the description of a new species from Nepal. *PLoS One* 14:e0219157. doi: 10.1371/ journal.pone.0219157

Rota-Stabelli, O., Yang, Z., and Telford, M. J. (2009). MtZoa: A general mitochondrial amino acid substitutions model for animal evolutionary studies. *Mol. Phylogenet. Evol.* 52, 268–272. doi: 10.1016/j.ympev.2009.01.011

Scholz, T., Waeschenbach, A., Oros, M., Brabec, J., and Littlewood, D. T. J. (2020). Phylogenetic reconstruction of early diverging tapeworms (Cestoda: Caryophyllidea) reveals ancient radiations in vertebrate hosts and biogeographic regions [published online ahead of print, 2020 Dec 2]. *Int. J. Parasitol.* 2020:009. doi: 10.1016/j.ijpara.2020.09.009

Shi, Z. G., Liu, X. D., and Sha, Y. Y. (2015). Did northern Tibetan Plateau uplift during Pliocene? A modeling test. *J. Earth Env.* 6, 67–80.

Singla, L. D., Singla, N., Parshad, V. R., Juyal, P. D., and Sood, N. K. (2008). Rodents as reservoirs of parasites in India. *Integr. Zool.* 3, 21–26. doi: 10.1111/j.1749-4877.2008.00071.x

Smith, A. T., Badingqiuying, Wilson, M. C., and Hogan, B. W. (2019). Functional-trait ecology of the plateau pika *Ochotona curzoniae* in the Qinghai-Tibetan Plateau ecosystem. *Integr. Zool.* 14, 87–103. doi: 10.1111/1749-4877.1 2300

Suzán, G., Marcé, E., Giermakowski, J. T., Armién, B., Pascale, J., Mills, J., et al. (2008). The effect of habitat fragmentation and species diversity loss on hantavirus prevalence in Panama. *Ann. N. Y. Acad. Sci.* 1149, 80–83. doi: 10.1196/annals.1428.063

Telford, M. J., Herniou, E. A., Russell, R. B., and Littlewood, D. T. (2000). Changes in mitochondrial genetic codes as phylogenetic characters: two examples from the flatworms. *Proc. Natl. Acad. Sci. U. S. A.* 97, 11359–11364. doi: 10.1073/pnas. 97.21.11359

Terefe, Y., Hailemariam, Z., Menkir, S., Nakao, M., Lavikainen, A., Haukisalmi, V., et al. (2014). Phylogenetic characterisation of *Taenia* tapeworms in spotted hyenas and reconsideration of the "Out of Africa" hypothesis of *Taenia* in humans. *Int. J. Parasitol.* 44, 533–541. doi: 10.1016/j.ijpara.2014.03.013

Turelli, M., Barton, N. H., and Coyne, J. A. (2001). Theory and speciation. *Trends Ecol. Evol.* 16, 330–343. doi: 10.1016/s0169-5347(01)02177-2

Valdmann, H., Moks, E., and Talvik, H. (2004). Helminth fauna of Eurasian lynx (*Lynx lynx*) in Estonia. *J. Wildl. Dis.* 40, 356–360. doi: 10.7589/0090-3558-40.2.356

Wang, S., Wang, S., Luo, Y., Xiao, L., Luo, X., Gao, S., et al. (2016). Comparative genomics reveals adaptive evolution of Asian tapeworm in switching to a new intermediate host. *Nat. Commun.* 7:12845. doi: 10.1038/ncomms12845

Wang, X., Liang, D., Jin, W., Tang, M., Liu, S., and Zhang, P. (2020). Out of Tibet: Genomic Perspectives on the Evolutionary History of Extant Pikas. *Mol. Biol. Evol.* 37, 1577–1592. doi: 10.1093/molbev/msaa026

Wang, X., Liu, J., Zuo, Q., Mu, Z., Weng, X., Sun, X., et al. (2018). *Echinococcus multilocularis* and *Echinococcus shiquicus* in a small mammal community on the eastern Tibetan Plateau: host species composition, molecular prevalence, and epidemiological implications. *Parasit. Vectors* 11:302. doi: 10.1186/s13071-018-2873-x

Will, K. W., Mishler, B. D., and Wheeler, Q. D. (2005). The perils of DNA barcoding and the need for integrative taxonomy. *Syst. Biol.* 54, 844–851. doi: 10.1080/10635150500354878

Wu, Z., Lu, L., Du, J., Yang, L., Ren, X., Liu, B., et al. (2018). Comparative analysis of rodent and small mammal viromes to better understand the wildlife origin of emerging infectious diseases. *Microbiome* 6, 178. doi: 10.1186/s40168-018-0554-9

Xiao, N., Qiu, J., Nakao, M., Li, T., Yang, W., Chen, X., et al. (2005). *Echinococcus shiquicus* n. sp., a taeniid cestode from Tibetan fox and plateau pika in China. *Int. J. Parasitol.* 35, 693–701. doi: 10.1016/j.ijpara.2005.01.003

Zhou, L., and Ma, Y. (2002). Distribution patterns of rodent diversity in arid regions of West China. Biodiversity Science. *Chinese Biodiver.* 10, 44–48.

Conflict of Interest: The authors declare that the research was conducted in the absence of any commercial or financial relationships that could be construed as a potential conflict of interest.

frontiers in Microbiology

ORIGINAL RESEARCH
published: 31 March 2021
doi: 10.3389/fmicb.2021.594075

Domestication Shapes the Community Structure and Functional Metagenomic Content of the Yak Fecal Microbiota

Haibo Fu[1,2,3†], Liangzhi Zhang[1,2†], Chao Fan[1,2,3†], Chuanfa Liu[1,2], Wenjing Li[1,2], Jiye Li[4], Xinquan Zhao[1,2], Shangang Jia[5*] and Yanming Zhang[1,2*]*

[1] Key Laboratory of Adaptation and Evolution of Plateau Biota, Northwest Institute of Plateau Biology, Chinese Academy of Sciences, Xining, China, [2] Qinghai Provincial Key Laboratory of Animal Ecological Genomics, Xining, China, [3] University of Chinese Academy of Sciences, Beijing, China, [4] Datong Yak Breeding Farm of Qinghai Province, Datong, China, [5] College of Grassland Science and Technology, China Agricultural University, Beijing, China

Domestication is a key factor of genetic variation; however, the mechanism by which domestication alters gut microbiota is poorly understood. Here, to explore the variation in the structure, function, rapidly evolved genes (REGs), and enzyme profiles of cellulase and hemicellulose in fecal microbiota, we studied the fecal microbiota in wild, half-blood, and domestic yaks based on 16S rDNA sequencing, shotgun-metagenomic sequencing, and the measurement of short-chain-fatty-acids (SCFAs) concentration. Results indicated that wild and half-blood yaks harbored an increased abundance of the phylum *Firmicutes* and reduced abundance of the genus *Akkermansia*, which are both associated with efficient energy harvesting. The gut microbial diversity decreased in domestic yaks. The results of the shotgun-metagenomic sequencing showed that the wild yak harbored an increased abundance of microbial pathways that play crucial roles in digestion and growth of the host, whereas the domestic yak harbored an increased abundance of methane-metabolism-related pathways. Wild yaks had enriched amounts of REGs in energy and carbohydrate metabolism pathways, and possessed a significantly increased abundance of cellulases and endohemicellulases in the glycoside hydrolase family compared to domestic yaks. The concentrations of acetic, propionic, n-butyric, i-butyric, n-valeric, and i-valeric acid were highest in wild yaks. Our study displayed the domestic effect on the phenotype of composition, function in gut microbiota, and SCFAs associated with gut microbiota, which had a closely association with the growth performance of the livestock. These findings may enlighten the researchers to construct more links between economic characteristics and gut microbiota, and develop new commercial strains in livestock based on the biotechnology of gut microbiota.

Keywords: Yak, domestication, 16S rDNA, shotgun metagenomic sequencing, fecal microbiota

OPEN ACCESS

Edited by:
Joao Inacio, University of Brighton, United Kingdom

Reviewed by:
Mircea Podar, Oak Ridge National Laboratory (DOE), United States
Lifeng Zhu, Nanjing Normal University, China
Guoliang Li, Chinese Academy of Sciences (CAS), China

****Correspondence:***
Xinquan Zhao
xqzhao@nwipb.cas.cn
Shangang Jia
shangang.jia@cau.edu.cn
Yanming Zhang
zhangym@nwipb.cas.cn

† These authors have contributed equally to this work

Specialty section:
This article was submitted to Microbial Symbioses, a section of the journal Frontiers in Microbiology

Received: *12 August 2020*
Accepted: *05 March 2021*
Published: *31 March 2021*

Citation:
Fu H, Zhang L, Fan C, Liu C, Li W, Li J, Zhao X, Jia S and Zhang Y (2021) Domestication Shapes the Community Structure and Functional Metagenomic Content of the Yak Fecal Microbiota. Front. Microbiol. 12:594075. doi: 10.3389/fmicb.2021.594075

INTRODUCTION

Wildlife domestication is one of the most important events in the last 10,000 – 15,000 years of human history (Wendorf and Schild, 1998). Many types of wildlife, including insects, birds, and mammals, have been domesticated by humans to provide ample food and clothing, support large population sizes, and develop the expanse of civilization (Diamond, 2002; Boyazoglu et al., 2005). Artificial selection modifies not only the phenotypes of domestic animals, such as color, fur, body size, and personality, but also the genotypes, causing species divergence or the emergence of new species (Robison et al., 2006; Qiu et al., 2015; Pendleton et al., 2018). The gut microbiome, as the second genome of organisms, plays a crucial role in the growth and development of individuals (Grice and Segre, 2012; Shi et al., 2014). Recently, with developments in metagenome and hologenome sequencing, studies have reported the interdependence between the host and their symbionts, and that the microbial community aids the host in adapting to the challenges of varying environments (Mendoza et al., 2018). The gut microbiomes of mammals provide vital functions for their hosts, such as training the immune system throughout life, metabolism, and the biosynthesis of vitamins. This crucial relationship between mammals and their gut microbiota is the result of long-term coevolution (McFall-Ngai et al., 2013; Zeder, 2015; Alessandri et al., 2019). Although gut microbiota is a major research topic in microbial ecology, the effects of domestication on the gut microbiome of herbivorous mammals is still far from being fully understood (Metcalf et al., 2017). During wildlife domestication, gut microbes are influenced by diet (Mcknite et al., 2012), environment (Nicholson et al., 2012; Chevalier et al., 2015), and artificial breeding (Leamy et al., 2014). Anthropogenic forces may have reshaped the mammalian gut microbial composition and its subsequent metabolism, because natural habitats and host genetics are often greatly revised by such forces. However, the gut microbiota of domesticated species is also influenced by the current climate and vegetation (Chen C.Y. et al., 2018). Thus, it is difficult to distinguish the combined effects of genetics and ecological environments on the gut microbiota. Compared to readily digestible starch, fat and protein for most mammals, the cellulose and hemicellulose are indigestible substances (Gomez et al., 2015). Even in ruminants, it is difficult to digest completely in rumen for these indigestible substances (Lippke et al., 1986). As the auxiliary digestive organ of ruminants, the hindgut plays an important role in the utilization of indigestible substances, such as hemicellulose and pectin, which, largely, can reflect the influence of domestication on the utilization efficiency of food resources (Faichney, 1969; Hoover, 1978). Those individuals, who harbored strong capacity of digest indigestible substances in hindgut, may obtain more ecological advantages during utilization of food resources.

Yaks, a keystone species of the Qinghai Tibetan Plateau (QTP), are widely distributed on the QTP, numbering more than 14 million. They were domesticated by Tibetan people between 6,000 and 12,000 years ago (Guo et al., 2006; Wang et al., 2010). During the domestication of yaks, desirable traits, such as certain colors, fur types, and tameness, were chosen and strengthened by humans to breed appropriate yaks that satisfied anthropic needs for survival in the QTP (Qiu et al., 2015). Some studies reported that the phenotypic and behavioral characteristics of domestic yaks (*Bos grunniens*) are markedly different from those of their wild counter parts, wild yaks (*Bos mutus*), with changes in genetic variations and dwelling environments (Andersson and Georges, 2004; Rubin et al., 2010; Vigne, 2011; Larson and Burger, 2013). Geneticists have confirmed, that the host genes linked to specific phenotypes are advanced under selection, such as genes improving tameness, and a reduction in the copy number of sugar metabolism genes in the domestic yak (Qiu et al., 2015; Zhang X. et al., 2016). However, little is known about the gut microbiota under artificial selection.

The Qinghai Wild Yak Rescue Center was founded in 1,952, it is an organization that specializes in the rescue of wild yaks injured in the field, and in yak breeding by hybridization based on wild and domestic individuals, where wild yaks (*Bos mutus*), half-blood and domestic yaks (*Bos grunniens*) share the same environment. It provides ample opportunities to decouple the effects of host domestication.

To explore how host genetics reshaped the mammalian gut microbiota, we collected fecal samples from the Qinghai Wild Yak Rescue Center and analyzed the compositional and functional variations in fecal microbiota using 16S rDNA sequencing. Moreover, shotgun metagenomics based on the fecal samples from the three types of yaks were used to measure the variation in Kyoto Encyclopedia of Genes and Genomes (KEGG) pathways, rapidly evolved genes (REGs), and enzyme profiles of cellulase and hemicellulase. The results were further confirmed by surveying the short-chain fatty acid (SCFA) concentration yielded by the fecal microbiota. We focused on the following questions: (1) whether host genetic variation of domesticated mammals caused by anthropogenic forces could dramatically reshape the fecal microbiomes; (2) how domestication changes crucial metabolic pathways in bacteria that may be linked to nutrition metabolism; and (3) whether modifications in host genetics results in distinct profiles of the glycoside hydrolase (GH) family of cellulose and hemicellulose enzymes in the fecal microbiota of domesticated mammals, compared to their wild conspecifics.

Here, we investigated the variations in microbial community structure and function of wild, domesticated, and half-blood yaks, exposed to the same environmental conditions. We also examined the changes in the REGs and enzyme profiles of GH caused by domestication. Our results may assist to better understand the evolutionary associations between the host and their gut microbiota in herbivorous mammals under artificial selection.

MATERIALS AND METHODS

Animal Material and Sample Information

We collected fresh feces from three types of yaks (domestic, half-blood, and wild) at the Datong Yak Breeding Farm in Qinghai Province (37°15′N, 101°22.8′E, and 2,980 m above sea level). More than 60 offspring of wild yaks that were

injured by wolves (*Canis lupus Linnaeus*) or brown bears (*Ursus arctos*) were rescued by workers of the Datong Breeding Farm in Hoh Xil Region since the 1980s. Domestic yaks belonged to local individuals, and the half-blooded yaks are the F1 generation of male wild yaks and female domestic yaks (Jiang and Zhonglin, 2005).

The wild and half-blood yaks are raised on a small hillside of the farm, about 300 hectares, surrounded by a 2 m high iron fence to prevent them from escaping. We hid in the shelter, guided by local workers, and observed the excretion of feces of the target animals. After determining the identity of the wild or half-blood yak, we collected the samples within two hours. Samples of domestic yaks were taken within a 1 km radius of the breeding center. Under the guidance of farm workers, we followed the yaks, collected the samples, and stored them in liquid nitrogen.

Fresh fecal samples of 29 healthy adult yaks, including 10 wild yaks, 11 half-blood yaks, and eight domestic yaks were collected for 16S rDNA in September 2017. In addition, nine fecal samples were prepared for metagenome sequencing, each group contained three samples. All samples were immediately frozen in cryotubes in liquid nitrogen. Then, the samples were stored at −80°C for further analysis. In addition, we listed the nutrition composition of diet for yaks in **Supplementary Table 1**. We performed the animal experiments following the Administration of Laboratory Animals established by the Ministry of Science and Technology of the People's Republic of China.

DNA Extraction and 16S rDNA Gene Amplification Sequencing

We carried out the extraction and amplification of 16S rRNA gene based on the previous study (Fu et al., 2020). The amplification was conducted targeting the V3 and V4 regions of 16S rRNA gene using the primers 341F (5′-CCTAYGGGRBGCASCAG-3′) and 806R (5′-GGACTACNNGGGTATCTAAT-3′) (Claesson et al., 2010; Vilo and Dong, 2012). The quantification and purification of the polymerase chain reaction (PCR) products according to the previous study (Fu et al., 2020). To ensure that there was no contamination, a positive and negative control was used during PCR. Then, the sequencing libraries were prepared and measured following the method in previous study (Fu et al., 2020). Finally, the libraries were sequenced on the HiSeq 2,500 platform of Illumina (Illumina Inc., San Diego, CA, United States) to produce 250 bp paired-end reads.

We obtained the gut metagenomic DNA from nine fecal samples (three for each type of yak, respectively) according to the previous method (Fu et al., 2020). After that, we determined the DNA concentration using the proved method in other study (Fu et al., 2020).

Shotgun Metagenomic Sequencing

Qualifying DNA samples were randomly interrupted using a Covaris ultrasonic crusher and produced approximately 150 bp libraries (Bowers et al., 2015). The whole libraries were prepared using the steps of end repair with a 3′ A tail, ligation of adapters and purification (Bentley et al., 2008). After that, library quality was assessed and sequenced with 150 bp paired-end reads based on the previous methods (Tringe and Rubin, 2005; Fu et al., 2020). Finally, we obtained an average of 540 million metagenomic-jointed reads (12 Gb) per sample from the sequencing platform (Edgar, 2004).

OTU Clustering and Species Annotation

Raw forward-read sequences were analyzed using the quantitative insights into microbial ecology (QIIME) pipeline (Version 1.9.1) (Caporaso et al., 2010). Sequence analysis was performed with Uparse software (Uparse v7.0.1001[1]) (Edgar, 2013), and preprocessed sequences were conducted at a 97% cut-off of nucleotide sequence similarity level. Taxonomic information was annotated to the OTUs based on the Greengenes 13_8 reference database[2] (DeSantis et al., 2006). The sequences clustered into mitochondria and chloroplast were removed from the OTU table. The unclassified sequences at the Kindom level were discarded. A standard sequence number corresponding to the least sequences (89,510) of the samples was adopted to normalize the OTU abundance information.

Treatment of the Raw Metagenomic Data

We measured the quality of the raw data using the fastqc_v0.11.5, then filtered the low quality sequences using Trimmomatic v0.36 with the parameters of LEADING:20 TRAILING:20 SLIDINGWINDOW:3:15 MINLEN:140. After that, we measured the quality of sequences filtered by Trimmomatic v0.36 again using fastqc_v0.11.5 to ensure the quality of filtered sequences for the further analysis. Owing to the potential containment of host sequences in the metagenomic data, we searched against the host database using SoapAligner (soap2.21,[3]) based on the filtered data, and the parameters are as follows: identity ≥90%, −l 30, −v 7, −M 4, −m 200, and −x 400 (Law et al., 2013).

Glycoside Hydrolase Families Responsible for Cellulose and Hemicellulose Degradation

We predicted the open reading frames (ORFs) based on the trimmed metagenomic reads using the FragGeneScan v1.15 (Rho et al., 2010). Then, we searched against the complete, non-redundant sequences in the dbCAN database[4] using the basic local alignment search tool (BLASTp) best hits with a cut-off E-value of 1e-5 based on the predicted ORFs (Yin et al., 2012), the ORFs for candidate proteins that have sequence homologous with GH families were extracted (Yin et al., 2012). Next, all the clean DNA reads corresponding to GH families were aligned against the bacterial genome database for species assignment[5] using BLASTn. Lastly, a table with CAZy IDs and species assignments was made by running local perl scripts written by ourselves.

[1]http://drive5.com/uparse/

[2]http://greengenes.lbl.gov/cgi-bin/nph-index.cgi

[3]http://soap.genomics.org.cn/soapaligner.html

[4]http://csbl.bmb.uga.edu/dbCAN/download/CAZyDB.03172015.fa

[5]ftp://ftp.ncbi.nlm.nih.gov/genomes/all/

Gene Set Enrichment Analysis Based on the Metagenomic Data

Gene set Enrichment Analysis (GSEA) was performed to identify differential abundance of microbial gene pathways using the KEGG database. Microbial genes from all samples were represented as KOs, and a *p*-value was generated for each KO using either a gamma model or a mixture model (Schwimmer et al., 2019). The relative enrichment of KEGG pathways within KO rankings was calculated using the R piano package (Varemo et al., 2013). Positive and negative gene-level statistics belonging to a gene set were separated based on the direction of the normalized Wilcoxon signed-rank test statistic, and for each of the two subsets, the absolute sum was divided by the total number of genes in the set (Katoh and Standley, 2013). Significance was determined at $p < 0.05$ after FDR correction (Varemo et al., 2013; Schwimmer et al., 2019).

Calculation of One-to-One Orthologs and Identification of Rapidly Evolving Genes Based on the *Ka*/*Ks* in the Gut Microbiota

For any two types of yaks (a, b), the one-to-one orthologs in the gut microbiota were defined as homologous genes. Then, we conducted a two-way microbial protein alignment to identify the homologous genes using the BLAST software (*E*-value threshold was 1e-5) (Hulsen et al., 2006). Then, we carried out a microbial protein multiple sequence alignment using the software multiple alignment by fast Fourier transform (MAFFT) v7.402 with the default parameters (Katoh and Standley, 2013). The corresponding aligned DNA sequences were obtained using the pal2nal.pl script (version V4, [6]). Subsequently, non-synonymous-to-synonymous substitution rate (*Ka*/*Ks* ratio) was calculated using the pairwise model in the software phylogenetic analysis by maximum likelihood (PAML) v8.0 (Yang, 2007; Katoh and Standley, 2013). $Ka/Ks < 1$ indicates purifying selection, whereas $Ka/Ks > 1$ is the signature of positive selection (Hurst, 2002). Based on this definition, those identified orthologs with $Ka/Ks > 1$ (*FDR*-corrected $p < 0.05$) were considered as REGs (domestic yak vs. wild yak: 18,216 REGs with 191,852 orthologs; domestic yak vs. half-blood yak: 18,831 REGs with 194,930 orthologs; half-blood yak vs. wild yak: 19,765 REGs with 202,590 orthologs). Based on the KEGG annotation of homologous microbial genes results, we identified the enriched KEGG of accelerating evolution genes using Fisher's exact test in R. The formula was as follows: fisher.test {matrix [c (A, B, C, D), nc = 2], alternative = "two. Sided," conf.level = 0.99, simulate. *P*-value = false, *B* = 10000}. In the formula, A represents the number of rapidly evolving genes in a specific pathway; B represents the number of non-rapidly evolving-genes in a specific pathway; C represents the number of all homologous genes in a specific pathway; D represents the number of homologous genes in a non-specific pathway. The statistical threshold of multiple testing using the FDR corrections was $p < 0.05$.

[6]http://www.bork.embl.de/pal2nal/

Determination of SCFAs Concentration

The short-chain fatty acids in yak feces were determined using propyl chloroformate (PCF) derivatization followed by gas chromatography-mass spectrometry (GC-MS) (Zheng et al., 2013). The experimental procedures, instrument and reagent used during the operation were based on the previous methods (Fan et al., 2020).

Bioinformatics and Statistical Analyses

The taxa with significant differences between different types of yaks were measured using a Kruskal-Wallis test followed by Dunn's *post hoc* multiple-comparison test in GraphPad Prism v7.00. Alpha diversity (including Shannon-Wiener and Simpson) was calculated using Python scripts in QIIME (Version 1.9.1) in workflows *Alpha_rarefaction.py* (Shannon, 1948; Simpson, 1949; Chao, 1984; Chao and Lee, 1992; Lozupone et al., 2011; Parfrey et al., 2014), finally the alpha diversity was visualized in GraphPad Prism v7.00, and measured the differences using a Kruskal-Wallis test followed by Dunn's *post hoc* multiple-comparison test. The beta diversities were tested using permutational analysis of variance (PERMANOVA) with 999 permutations in R 3.2.2, using the function *adonis*. The significant level in this study was determined according to the common standard ($p > 0.05$, no significance; $p < 0.05$, *; $p < 0.01$, **; $p < 0.001$, ***). LEfSe was used to identify the different bacterial taxa among different groups using a common standard (*LDA* scores > 3, $p < 0.05$).

The read numbers of GH families associated with the cellulases and hemicellulases were visualized and measured the differences using the Welch *t*-test ($p < 0.05$) in GraphPad Prism v7.00. The SCFA results were analyzed using the Wilcoxon rank-sum test ($p < 0.05$).

Data Availability

The 16S rDNA as well as the whole-metagenome data in this study can be freely retrieved from the NCBI Sequence Read Archive with project accession Nos. PRJNA528194 and PRJNA529943, respectively.

RESULTS

Domestication Modified the Diversity and Community Structure of the Yak Fecal Microbiota

After sequences were subjected to quality filtering and assembly, 3,065,986 16S rRNA gene sequences were obtained. The composition of the fecal microbiota in yaks was dominated by the phyla *Firmicutes*, *Bacteroidetes*, *Verrucomicrobia*, *Proteobacteria*, and *Actinobacteria* (**Supplementary Table 2**). The results of alpha diversity showed that the Shannon-Wiener and Simpson indices were significantly higher in wild yaks than in domestic yaks (Shannon-Wiener: $\chi^2 = 8.099$, df = 2, $p = 0.0149$; Simpson: $\chi^2 = 7.369$, df = 2, $p = 0.0141$) (**Figures 1A,B**). However, there were no significant differences between the three types of yaks in both the Chao 1 index and observed species number (Chao

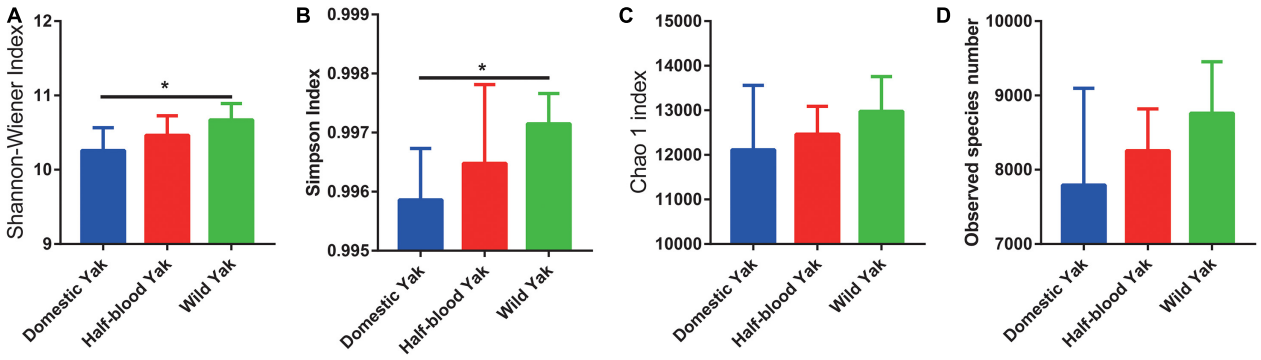

FIGURE 1 | The alpha diversity of gut microbial communities in three types of yaks, asterisks indicate significance level between groups ($p > 0.05$, no significance; $p < 0.05$, *; $p < 0.01$, **; $p < 0.001$, ***). **(A)** The Chao 1 index **(B)** and observed species number. **(C)** The Shannon-Wiener, **(D)** and Simpson indices.

1: $\chi^2 = 2.890$, df = 2, $p = 0.2358$; Observed species number: $\chi^2 = 4.411$, df = 2, $p = 0.1102$) (**Figures 1C,D**).

Characteristics of Fecal Microbial Composition in Different Types of Yaks

We used the principal-coordinate analysis (PCoA) based on the Bray-Curtis distance of the microbial community at the genus and phylum level to investigate the similarity of the gut microbial community structure for each individual between the three types of yak. We found that clear clustering of samples by host family (**Figure 2A** and **Supplementary Figure 1A**), and PERMANOVA, based on Bray-Curtis distance, revealed that significant differences among the three groups were observed at the genus and phylum level (genus: $F_{2,26} = 4.3$, $R^2 = 0.25$, $p = 0.002$, permutations = 999; phylum: $F_{2,26} = 6.3$, $R^2 = 0.32$, $p = 0.001$, permutations = 999) (**Figure 2A** and **Supplementary Figure 1A**). The distribution of individuals in the PCoA was mainly driven by dominant taxon at both genus and phylum level (**Figure 2A** and **Supplementary Figure 1A**). *Akkermansia*, family Pirellulaceae unclassified genus, family Victivallaceae unclassified genus, and family p-2534-18B5 unclassified genus were positively correlated and contributed significantly to the domestic group, while genus *Oscillospira*, family Ruminococcaceae unclassified genus were positively correlated and contributed significantly to the wild yaks. Furthermore, the heatmap of the relative abundance of the genera with the cluster of the groups shows that *Akkermansia*, family Pirellulaceae unclassified genus, family Victivallaceae unclassified genus, and family p-2534-18B5 unclassified genus, which were positively correlated to the domestic group, form a cluster in the hierarchical cluster; while genus *Oscillospira*, family Ruminococcaceae unclassified genus, which were positively correlated to wild yaks, form another cluster in the hierarchical cluster (**Figure 2B**). At the phylum level, the phylum *Verrucomicrobia* and Lentisphaerae were positively correlated and contributed significantly to the domestic yaks (**Supplementary Figure 1A**), and form a cluster in the hierarchical cluster of the heatmap (**Supplementary Figure 1B**); while the phylum *Firmicutes* was positively correlated and contributed significantly to the half-blood and wild yaks (**Supplementary Figure 1A**), and forms another cluster in the hierarchical cluster of the heatmap (**Supplementary Figure 1B**). Moreover, three types of yak shared 242 (68.9%) genera; the shared genus number between domestic and wild yak is 257 (73.2%), while the shared genus number between half-blood and wild yak is 290 (82.6%). At the phylum level, among 22 phyla, three types of yak share 19 phyla (86.4%), and the wild yaks have two unique phyla (9.1%), though two unique phyla (Thermi and SR1) are rare in the wild yaks (**Supplementary Table 2**). We further identified the significantly different genus based on the top 30 genera, as they spanned over 95% of the total microbial community. We found that genus *Akkermansia*, family Victivallaceae unclassified genus, family RFP12 unclassified genus, order YS2 unclassified family displayed significantly higher abundance in domestic yaks (**Figure 2C** and **Supplementary Table 3**), and the order Bacteroidales unclassified family, genus *Oscillospira*, family *Lachnospiraceae* unclassified genus, family RF16 unclassified genus, family *Coriobacteriaceae* unclassified genus, and genus *Dorea* displayed significantly higher abundance in wild yaks (**Figure 2C** and **Supplementary Table 3**). At the phylum level, the abundance of phylum *Verrucomicrobia*, Lentisphaerae, and *Cyanobacteria* are significantly higher in domestic yaks (**Supplementary Figure 1C** and **Supplementary Table 3**). The abundance of phylum *Firmicutes*, *Actinobacteria*, TM7, and Elusimicrobia are significantly higher in wild yaks (**Supplementary Figure 1C** and **Supplementary Table 3**).

To further illustrate the influence of domestication on the bacteria in yaks, we conducted a linear discriminant analysis (LDA) effect size (LEfSe) analysis based on the genus and phylum level for the different taxon with lineage classification (*LDA* scores > 3.0, $p < 0.05$) (**Figures 3A–C** and **Supplementary Figures 2A,B**). Domestic and wild yaks harbored the richest significantly different taxa (total: 48; wild > domestic: 24, domestic > wild: 24) (**Figure 3A**), domestic and half-blood yaks possessed a moderate number of significantly different taxa (total: 29; half-blood > domestic: 9, domestic > half-blood: 20) (**Figure 3B**). *Prevotella* was the only significantly different taxon between the half-blood and wild yaks (**Figure 3C**). At the phylum level, the *Firmicutes*,

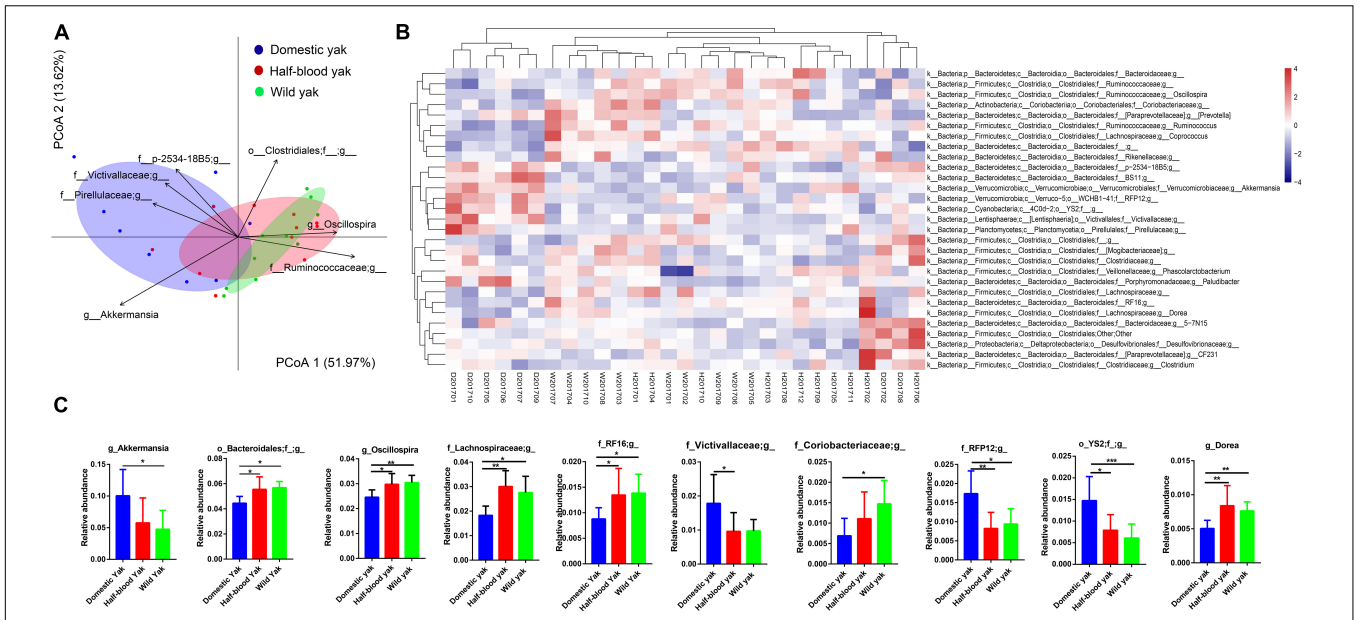

FIGURE 2 | Composition of fecal microbiota of the three types of yaks at the genus level, the letters "D," "H," and "W" represent domestic, half-blood, and wild yaks, respectively. **(A)** Bray-Curtis dissimilarity of gut microbial communities among the three types of yaks based on top 30 genera, ellipses with 95% confidence interval around the centroid of each group are displayed in PCoA, the genera which have significant correlation with the ordination in PCoA are displayed using the arrows (permutation test, $p < 0.01$), with the length of the arrow representing the goodness of fit statistic, squared correlation coefficient. **(B)** Heatmap of the top 30 genera based on the relative abundance of gut mcirobiota among the three types of yak, complete linkage clustering was used. **(C)** Relative abundance of the gut microbiota indicating the significantly discrepancies among the three types of yak at the genus level across 29 samples, asterisks indicate significance level between groups ($p > 0.05$, no significance; $p < 0.05$, *; $p < 0.01$, **; $p < 0.001$, ***).

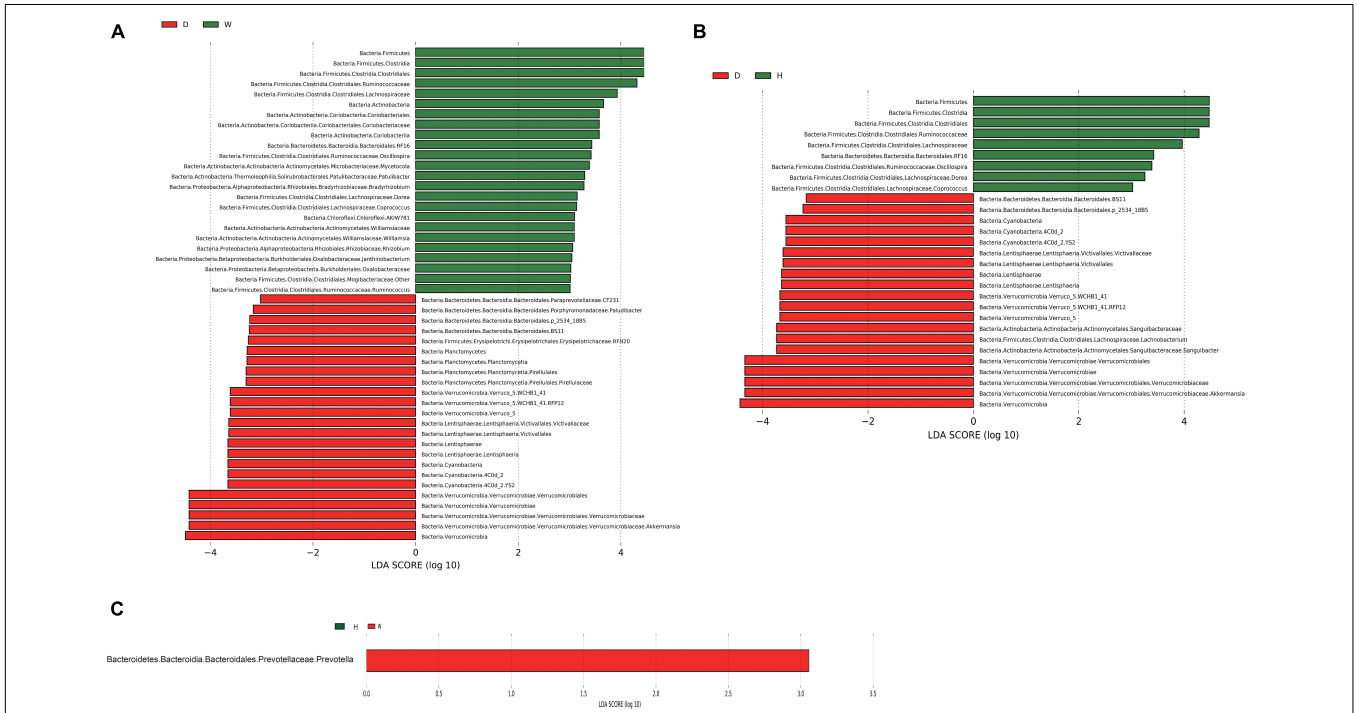

FIGURE 3 | The linear discriminant analysis effect size (LEfSe) shows the significantly different taxa of the gut microbiota between the different groups at the genus level (*LDA* scores > 3.0, $p < 0.05$); the letters "D," "H," and "W" represent domestic, half-blood, and wild yaks, respectively. **(A)** The significantly different taxa between domestic and wild yaks. **(B)** The significantly different taxa between domestic and half-blood yaks. **(C)** The significantly different taxon between half-blood and wild yaks.

Actinobacteria, Elusimicrobia, and TM7 displayed a significantly higher abundance in wild yaks than in domestic yaks, and the *Verrucomicrobia*, Lentisphaerae, *Cyanobacteria*, *Planctomycetes*, and Tenericutes were significantly higher in domestic yaks than in wild yaks (*LDA* scores > 2.0, $p < 0.05$) (**Supplementary Figure 2A**). Moreover, the *Firmicutes*, TM7, and Spirochetes displayed significantly higher abundances in half-blood yaks than in domestic yaks, and the *Verrucomicrobia*, Lentisphaerae, and *Cyanobacteria* were significantly higher in domestic yaks than in half-blood yaks (*LDA* scores > 2.0, $p < 0.05$) (**Supplementary Figure 2B**). No significantly different taxon was identified between half-blood yaks and wild yaks (*LDA* scores > 2.0, $p > 0.05$).

Gene Set Enrichment Analysis and REGs

Based on GSEA, 16 pathways were differentially abundant in one or more pairwise comparisons. The most striking differences were found in genes related to methane emission in domestic yaks (**Table 1**). GSEA also identified the insulin-signaling pathway, which contributed to the synthesis of glycogen, lipids, and proteins, as a highly enriched pathway with six upregulated KEGG orthologs (KOs) in the metagenome dataset from wild yaks (**Table 1**). Additionally, the mitogen-activated protein kinase (MAPK) signaling pathway associated with cell division was significantly enriched in wild yaks (**Table 1**).

Further, we obtained 191,852 one-to-one orthologs in the metagenomes of wild and domestic yaks, 194,930 for domestic and half-blood yaks, and 202,590 for wild and half-blood yaks. After FDR correction, 18,216 (9.5%), 18,831 (9.7%), and 19,765 (9.8%) REGs were detected, respectively (**Table 2**; $p < 0.05$, Fisher's exact test).

Enriched REGs among the wild, domestic, and half-blood yaks were significant in functional categories involved in energy, carbohydrate, and lipid metabolism, as well as glycan biosynthesis and metabolism (**Table 2**; $p < 0.05$, Fisher's exact test). REGs of wild and domestic yaks were significantly involved in sulfur metabolism, pentose and glucuronate interconversions, sphingolipid metabolism, lipopolysaccharide biosynthesis, pantothenate and CoA biosynthesis, thiamine metabolism, and nicotinate and nicotinamide metabolism (**Table 2**; $p < 0.05$, Fisher's exact test). Enriched REGs between half-blood and wild yaks were involved in lipopolysaccharide biosynthesis, folate biosynthesis, thiamine metabolism, and phenylalanine, tyrosine, and tryptophan biosynthesis (**Table 2**; $p < 0.05$, Fisher's exact test).

Profile of Enzymes Associated With Cellulose and Hemicellulose Degradation

We identified the GH family, which contains cellulases and hemicellulases, based on shotgun metagenome sequencing data. The results revealed that the total reads of GH families, which were responsible for hemicellulose degradation, were significantly higher in wild and half-blood yaks than in domestic yaks (Welch *t*-test, $p < 0.05$) (**Figure 4A**), and the total reads of GH families, which were responsible for cellulose degradation, were almost significant between wild and half-blood yak (Welch *t*-test, $p = 0.055$) (**Figure 4B**). To further investigate the relative contribution of bacteria encoding cellulases and hemicellulases, we choose GH10, GH28, and GH53 which degraded hemicellulose, and GH5 which degraded cellulose, and found that replacement or absence often occurred in the bacterial producer of the same enzyme (GH) between wild and domestic yaks (**Supplementary Table 4**).

SCFA Concentrations

We surveyed six dominant SCFAs, and the results showed that half-blood and wild yaks had significantly higher concentrations of acetic acid, propionic acid, n-butyric acid, i-butyric acid, n-valeric acid, and i-valeric acid than domestic yaks (Wilcoxon Rank-Sum test, $p < 0.05$) (**Figures 5 A–F**).

DISCUSSION

Domestication provides people important and stable food sources by modifying the genetic characters of wild animals, yet its influence on the gut microbiome is still poorly understood (Diamond, 2002; Boyazoglu et al., 2005). Here, we assessed the gut microbial community by comparing the wild, hybrid and domestic types of yaks in the same environment. We measured the diversity, difference of the gut microbial structure, and also explored the differences of metagenomic functions and SCFAs among three types of yaks. Most lineal wild ancestors of current domestic animals have been extinct (Hassanin and Ropiquet, 2004). However, we collected the wild, hybrid and domestic types of yaks at the same time, as the domestication of yaks is still in the early stage, and wild population still exists on QTP, though the population is small compared to the historical period (Shi et al., 2016). Thus, three types of yaks provided a rare opportunity to explore the domestic effects on the gut microbiota for us. We will discuss the domestic effects on the gut microbial structure, metagenomic functions, and SCFAs by comparing the three types of yaks in the following sections.

Recently, many studies have indicated that domestication decreases the diversity of the gut microbial community in horses, fruit fly larvae, and Eastern African cichlid fish, because of the loss of some taxa (Larson and Burger, 2013; Baldo et al., 2015; Deutscher et al., 2018). In this study, domestic yaks had a lower Shannon-Wiener index (**Figure 1A**), consistent with above results (Larson and Burger, 2013; Deutscher et al., 2018; Alessandri et al., 2019). Higher diversity of the gut microbiota is closely associated with adaptation to a diverse diet and expanding the breadth of the dietary niche of mammalian herbivores, which benefits the fitness of the host (Kohl et al., 2014; Li et al., 2019). Thus, higher Shannon-Wiener index of gut microbial community in wild yaks may imply that the wild individuals have evolved a broad dietary niche adaption to survive the harsh environment in the field.

Recently, there has been increasing evidence that the composition of gut microbiota in domesticated animals is substantially different from that of related wild species, such as domestic and wild horses, geese, and silkworms (Larson and Burger, 2013; Gao et al., 2016; Metcalf et al., 2017;

TABLE 1 | Metabolic pathways enriched in different types of yak.

	Enriched in Pathway	KEGG ID	KOs in pathway	KOs detected in study	GSEA statistic	*p*-value	*q*-value	KOs up in rank	KOs down in rank
Domestic yak	Photosynthesis	ko00195	63	21	0.743778489	0.00140056	0.058292697	19	2
	Ribosome biogenesis in eukaryotes	ko03008	82	20	0.701824916	0.002808989	0.058292697	15	5
	Methane metabolism	ko00680	167	118	0.555595404	0.001116071	0.058292697	104	14
	Microbial metabolism in diverse environments	ko01120	1057	465	0.322232731	0.006085193	0.083271058	366	99
Half-blood yak	Lipopolysaccharide biosynthesis	ko00540	40	35	0.540141042	0.001766784	0.022438541	29	6
	Bacterial secretion system	ko03070	74	52	0.537770079	0.001785714	0.022438541	41	11
Wild yak	Autophagy-animal	ko04140	100	11	0.811226568	0.005780347	0.073048687	5	6
	Tuberculosis	ko05152	131	10	0.769289429	0.005617978	0.073048687	5	5
	Autophagy-yeast	ko04138	77	16	0.757671878	0.007575758	0.073048687	9	7
	Insulin signaling pathway	ko04910	86	12	0.737158547	0.006289308	0.073048687	6	6
	Phagosome	ko04145	95	10	0.670552842	0.011235955	0.073048687	6	4
	Endocytosis	ko04144	178	11	0.668547332	0.005780347	0.073048687	6	5
	Spliceosome	ko03040	122	10	0.616286826	0.011235955	0.073048687	6	4
	Glucagon signaling pathway	ko04922	55	11	0.60784035	0.005780347	0.073048687	3	8
	Epstein-Barr virus infection	ko05169	164	17	0.592686653	0.007633588	0.073048687	9	8
	MAPK signaling pathway-yeast	ko04011	90	14	0.547305429	0.006802721	0.073048687	6	8

Metabolic pathways enriched in different types of yaks, gene set enrichment analysis (GSEA) results. Through the comparison among domestic, half-blood and wild yak, the metabolic pathways enriched in different types of yak were revealed.

TABLE 2 | Functional categories with significant enrichment in rapidly evolved genes (REGs).

	Enriched in pathway	KEGG ID	REG in pathway	REG detected in study	*p*-value	One-to-one orthologues	Number of REGs	Enriched REGs (proportion)
Wild yak vs domestic yak	Pentose and glucuronate interconversions	ko00040	399	2	2.16E-13			
	Sphingolipid metabolism	ko00600	474	2	2.96E-16			
	Pantothenate and CoA biosynthesis	ko00770	331	4	4.82E-09			
	Nicotinate and nicotinamide metabolism	ko00760	459	2	1.49E-15			
	Sulfur metabolism	ko00920	212	2	0.00000131			
	Thiamine metabolism	ko00730	456	4	2.28E-13			
	Lipopolysaccharide biosynthesis	ko00540	164	2	0.0000787			
	Total					191,852	18,216	9.5%
Wild yak vs half-blood yak	Phenylalanine, tyrosine and tryptophan biosynthesis	ko00400	525	5	2.2E-15			
	Lipopolysaccharide biosynthesis	ko00540	182	3	0.0000769			
	Folate biosynthesis	ko00790	263	2	1.42E-08			
	Thiamine metabolism	ko00730	410	4	4.32E-12			
	Total					202,590	19,765	9.8%
Domestic yak vs half-blood yak	Monobactam biosynthesis	ko00261	228	2	0.000000288			
	One carbon pool by folate	ko00670	420	3	2.25E-13			
	Carbon fixation in photosynthetic organisms	ko00710	370	2	1.42E-12			
	Pantothenate and CoA biosynthesis	ko00770	347	5	7.66E-09			
	Porphyrin and chlorophyll metabolism	ko00860	245	2	6.33E-08			
	Drug metabolism – other enzymes	ko00983	225	4	0.0000184			
	Nicotinate and nicotinamide metabolism	ko00760	459	3	1.17E-14			
	Pentose and glucuronate interconversions	ko00040	372	2	1.48E-12			
	Biofilm formation – Escherichia coli	ko02026	270	2	9.92E-09			
	Folate biosynthesis	ko00790	227	2	0.000000287			
	Citrate cycle (TCA cycle)	ko00020	399	2	1.49E-13			
	Fructose and mannose metabolism	ko00051	490	4	7.66E-15			
	Total					194,930	18,831	9.7%

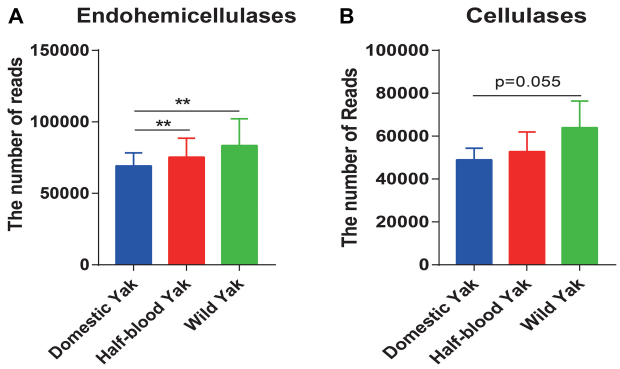

FIGURE 4 | (A,B) The total read number of the GH families encoding hemicellulases and cellulases across the three types of yaks, asterisks indicate significance level between groups ($p > 0.05$, no significance; $p < 0.05$, *; $p < 0.01$, **; $p < 0.001$, ***).

Chen B. et al., 2018). Li et al., 2017 found that wild musk deer possess a higher abundance of the phylum *Firmicutes*, and a lower abundance of the genus *Akkermansia* than captive individuals. Additionally, wild house mice harbored an increased abundance of *Firmicutes* and reduced abundance of *Akkermansia* (Kreisinger et al., 2014). These two taxa of gut microbiota are strongly associated with the efficient harvest of energy from the diet (Nicholson et al., 2012). Furthermore, the study of the core gut microbiome in obese and lean twins suggested that the phylum *Actinobacteria* yielded 75% of obesity-enriched genes, while *Firmicutes* yielded the other 25% (Turnbaugh et al., 2009), suggesting that *Actinobacteria* and *Firmicutes* were closely associated with growth and fat deposition. In this study, the wild and half-blood yaks harbored a significantly increased abundance of *Firmicutes* and *Actinobacteria* and a reduced abundance of *Akkermansia* (**Supplementary Figure 1C** and **Figure 2C**), similarly to wild musk deer and wild house mice (Kreisinger et al., 2014; Li et al., 2017). These results may imply that an efficiency microbial biomarker for food resources utilization in wild yaks than in domestic yaks.

Methane metabolism enriched in domestic yak rather than wild and half-blood yak might imply that domestic yaks had a higher methane emission level, and further cause energy loss (**Table 1**). In fact, low-altitude ruminants, such as cattle and ordinary sheep, which experienced longer and stronger domestication than yak, possessed an increased methane emission phenotype in comparison to related high-altitude

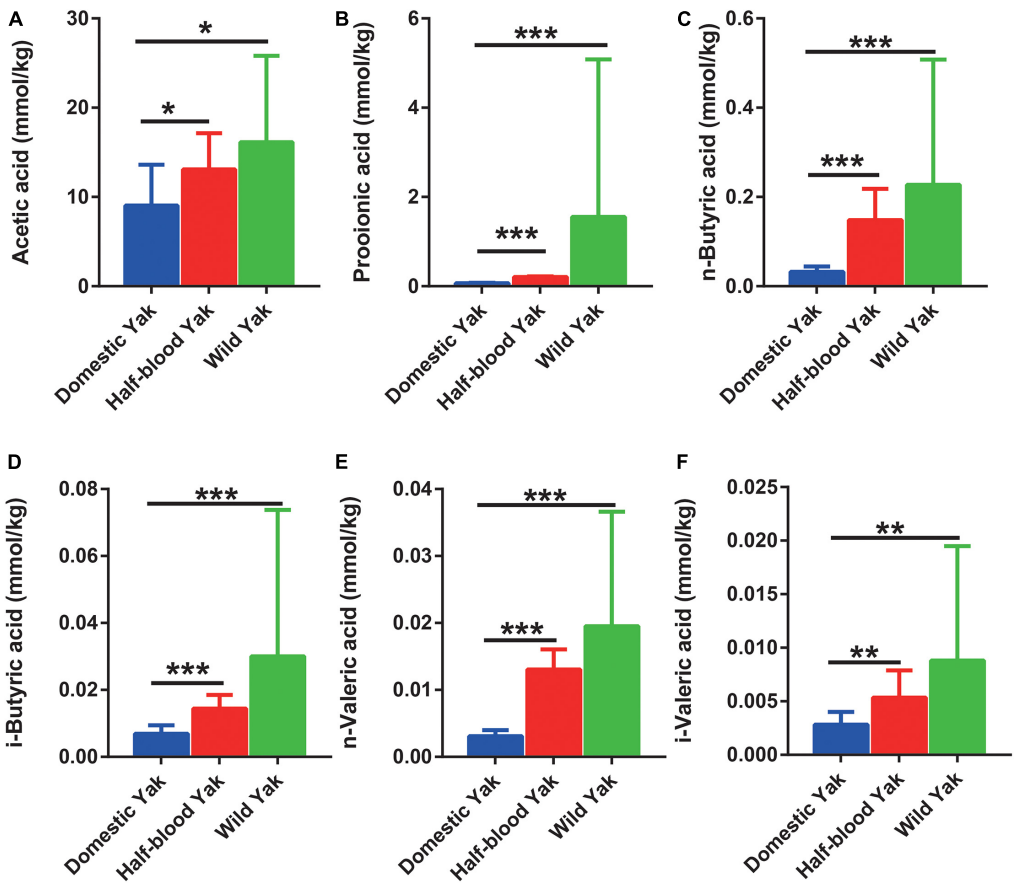

FIGURE 5 | The SCFAs concentration of gut microbiota in the three types of yaks, asterisks indicate significance level between groups ($p > 0.05$, no significance; $p < 0.05$, *; $p < 0.01$, **; $p < 0.001$, ***). **(A)** Acetic acid, **(B)** propionic acid, **(C)** n-butyric acid, **(D)** i-butyric acid, **(E)** n-valeric acid, and **(F)** i-valeric acid.

ruminants (yak and Tibetan sheep) (Zhang Z. et al., 2016). Additionally, the insulin-signaling pathway enriched in wild yaks might be a biomarker of assimilation (**Table 1**), as and may benefit growth by contributing to the repression of catabolism.

Adaptive divergence in the gene sequence may also contribute to the phenotypes of low-methane-yielding and high-SCFA organisms (Zhang Z. et al., 2016). The results showed the REGs of wild yaks were enriched in energy and carbohydrate metabolism pathways compared to domestic yaks, indicating that wild yaks potentially possessed the typical high-SCFA phenotype. The lower content of SCFAs in domestic yaks may further reflect changes in host biology compared to the wild yaks (**Figures 5A–F**). Conversely, the enrichment of REGs in domestic yaks showed that the pathways were associated with the methane emission pathway (**Tables 1**, **2**). These results illustrated that artificial selection may cause rapid gene evolution of the gut microbiome and weaken the feed efficiency in domestic yaks.

Metagenomic sequencing further confirmed that the wild and half-blood yaks harbored more reads for endohemicellulases in GH families (**Figure 4A**). These findings implied that wild yaks might harbor a stronger capacity for fiber digestion, which might potentially promote the ability of the host to acquire more calories from the diet. Similar results show that wild individuals harbor an increased abundance of cellulose- or hemicellulose-degrading bacteria in wild house mice (Kreisinger et al., 2014). Furthermore, the wild saiga has a higher digestibility than the related domestic species in the same territory (Abaturov et al., 2003), and wild asses achieve higher digestibility than domesticated asses (Hummel et al., 2017). These common features occurring in different, unrelated, domesticated animals suggest that domestication provides animals with plentiful food but may reduce their fermentation efficiency by reshaping the fecal microbiota, especially with regards to the efficiency of cellulose and hemicellulose degradation.

Generally, the fecal microbiota has higher diversity than the rumen microbiota (Meale et al., 2016), which may be due to the fact that the hindgut has to decompose the recalcitrant substances, as the digestible starch, fat, and protein have been almost digested in rumen. The residual substances were often recalcitrant to degrade for the rumen microbiota. Thus, the hindgut has to develop a more complex microbial structure to cope with the recalcitrant substances, for instance, higher microbial diversity, higher *Firmicutes*, lower *Bacteroidetes*, while the rumen microbiota has a lower diversity, predominant *Bacteroidetes* and lower *Firmicutes* (Meale et al., 2016; Andrade et al., 2020). Higher *Firmicutes* was often associated with degradation cellulose and hemicellulose and higher SCFAs content (Mao et al., 2012). Higher *Firmicutes/Bacteroidetes* was often considered as a biomarker of efficient energy extraction from diet (Turnbaugh et al., 2008). Thus, hindgut microbiota may focus on the degradation of recalcitrant substances compared to rumen microbiota.

Generally, the concentration of SCFAs was positively correlated with their gut microbial diversity and activity of fiber degradation (Li et al., 2018), represented a high energy harvest in plateau pikas and yaks (Zhang Z. et al., 2016; Li et al., 2018). The SCFAs verified the microbial activity in bears (Schwab et al., 2009). Yaks had a higher SCFAs content compared to cattle, which represented more effective metabolic pathways for hydrogen consumption and lower methane emission (Huang et al., 2012, 2016; Zhang Z. et al., 2016). In our study, the concentrations of six types of SCFAs (acetic, propionic, n-butyric, i-butyric, n-valeric, and i-valeric acid) were highest in wild yaks and lowest in domestic yaks (**Figures 5A–F**). Likewise, wild yaks have the largest body size, and domestic yaks have the smallest body size (**Supplementary Tables 5–7**). These scenes indicated that domestication might cause potential negative effects to the producing of SCFAs via dietary fermentation in yaks. The concentration of SCFAs corresponds to the reads of the GH family, which is responsible for encoding cellulases and endohemicellulases, and corresponds well with a previous report indicating that cellulolytic activity is positively correlated with the SCFA concentrations (Li et al., 2018). Therefore, the SCFA concentrations may further confirme that the cellulolytic activity in wild yaks was higher than that in domestic yaks, and that domestication weakened the digestive capacity in yaks.

The connections between the gut microbiome and SCFAs were consistent with the previous studies. For instance, the *Prevotella* spp. and *Ruminococcus* spp., which produce acetic acid from pyruvate via acetyl-CoA (Louis et al., 2014), were higher in wild yaks (**Figure 3A,C**). Correspondingly, the concentration of acetic acid was higher in wild yaks (**Figure 5A**). Likewise, the synchronization was also observed between propionic acid and the gut microbial producer. *Coprococcus* spp., which produce propionic acid and butyric acid (Louis et al., 2014), were higher in wild yaks (**Figure 3A**).

The domestication of animals is a long-term event; people preferred animals with less aggressiveness and more tameness rather than large-body in the early stage of domestication, as large-body individuals may hurt the people, especially in the domestication of large animals (Diamond, 2002; Jensen, 2014), this scene was also observed in yaks (Qiu et al., 2015). Modern genetic methods have been used to breed efficient and economical commercial lines of domesticated species only in recent years, while many local species have been domesticated by people living in less developed area (Zeder, 2015), including yaks (Qiu et al., 2015). The domestic yak is still in the early phase of domestication, without the experience of modern genetic breeding methods (Qiu et al., 2015). These locally domesticated animals in less developed area often exhibit bad growth performance with small body size compared to modern commercial lines, for example Landrace sows have a stronger capacity for fiber degradation and produce more SCFAs in the gut than Meishan and Jinhua sows (two local pigs in China) (Li et al., 2009; Ai et al., 2013).

The gut microbiota of hybrid offspring is different from their parents, as both the male and female parents gene expression in the hybrid offspring (Zhipeng et al., 2016). In this study, we collected three types of fecal samples in the same environment to exclude the influence of environment.

Here, hybrids were considered as intermediaries to explore the influence of domestication. In composition, diversity, functional pathway, network, enzyme system and SCFAs, the hybrids showed an intermediate type, implied that they may be influenced by both male parent and female parent, meanwhile it implied that stable characters have been fixed during domestication. Hybridization may partly recover the composition and function of gut microbiota and promote the energy harvest capacity of the host (Benis et al., 2015; Zhipeng et al., 2016). These results corresponded well with previous studies that indicated the gut microbiota experienced vertical transmission with host genetics during the process of hybridization and was affected by the heritable character of parents (Wang et al., 2015; Zhipeng et al., 2016).

CONCLUSION

In summary, our study provides novel insights into the effects of domestication and hybridization on the fecal microbiota, may further enlighten other researchers to investigate the role of fecal microbiota in livestock growth and development, and may provide a promising way to improve the growth performance of livestock by revising the fecal microbiota.

DATA AVAILABILITY STATEMENT

The 16S rDNA as well as the whole-metagenome data in this study can be freely retrieved from the NCBI Sequence Read Archive with project accession Nos. PRJNA528194 and PRJNA529943, respectively.

ETHICS STATEMENT

The animal study was reviewed and approved by the Animal Ethics Committee of Northwest Plateau Institute of Biology, Chinese Academy of Sciences. Written informed consent was obtained from the owners for the participation of their animals in this study.

AUTHOR CONTRIBUTIONS

YZ and XZ designed the research. HF, CL, LZ, CF, and WL collected the samples. JL provided the sampling site and live specimen. CL and CF measured the content of SCFAs. HF, SJ, LZ, and CF analyzed the data. HF and CL wrote the draft of manuscript. YZ, SJ, and LZ revised the final manuscript. All authors contributed to the article and approved the submitted version.

FUNDING

Our study was supported by the Second Tibetan Plateau Scientific Expedition and Research Program (No. 2019QZKK0501), the Recovery techniques and demonstration of degraded alpine ecosystems in the source region of three rivers under contract (No. 2016YFC0501900), the National Natural Science Foundation of China (No. 31670394), the project of western light for interdisciplinary teams, and the Science and Technology Department of Qinghai Province Major Project "Sanjiangyuan National Park Animal Genome Program."

SUPPLEMENTARY MATERIAL

The Supplementary Material for this article can be found online at: https://www.frontiersin.org/articles/10.3389/fmicb.2021.594075/full#supplementary-material

Supplementary Figure 1 | Composition of the fecal microbiota of the three types of yaks at the phylum level, the letters "D," "H," and "W" represent domestic, half-blood, and wild yaks, respectively. **(A)** Bray-Curtis dissimilarity of gut microbial communities among the three types of yaks at phylum level, Ellipses with 95% confidence interval around the centroid of each group are displayed in PCoA, the phyla which have significant correlation with the ordination in PCoA are displayed using the arrows (permutation test, $p < 0.01$), with the length of the arrow representing the goodness of fit statistic, squared correlation coefficient.

(B) Heatmap of phylum based on the relative abundance of gut microbiota among the three types of yak, and complete linkage clustering was used. **(C)** Relative abundance of the gut microbiota indicating the significantly discrepancies among the three types of yak at the phylum level across 29 samples.

Supplementary Figure 2 | The linear discriminant analysis effect size (LEfSe) shows the significantly different taxa of the gut microbiota between the different groups at phylum level (*LDA* scores > 2.0, $p < 0.05$); each line of the heatmap corresponds to the significantly different taxonomic result of each line in LEfSe on the left; the letters "D", "H" and "W" represent domestic, half-blood, and wild yaks, respectively.

Supplementary Table 1 | Nutrition composition of diet in Datong Breeding Farm (Zhang et al., 2014; Zhou et al., 2015).

Supplementary Table 2 | Average relative abundance of gut microbiota across the three types of yaks at the phylum level.

Supplementary Table 3 | Statistical differences of phyla and top 30 genera among three types of yaks.

Supplementary Table 4 | The proportion of bacteria encoding the GH families (GH10, GH28, GH53, and GH5) across the three types of yaks.

Supplementary Table 5 | Measurements of the Kunlun type of wild yak (Jiye et al., 2005).

Supplementary Table 6 | Variation in body weight with season and group (Hu, 2001). G1 (May 2000), G2 (October 2000), and G3 (April 2000). WY (wild yak), TZ (domestic yak living in Tianzhu, Gansu Province), and DT (Daton g yak, F1 generation of wild yak × domestic yak).

Supplementary Table 7 | Live weight and linear body measurements of domesticated and crossbred yaks at 6 and 18 months of age (Jialin et al., 1998).

REFERENCES

Abaturov, B. D., Kolesnikov, M. P., Nikonova, O. A., and Pozdnyakova, M. K. (2003). Experience of quantitative investigation of nutrition in free-ranging mammals in natural habitat. *Zool. Zhurnal* 82, 104–114.

Ai, L., Su, Y., and Zhu, W. (2013). A comparison of in vitro fermentation characteristics of eight fiber substrates by faecal microbiota from Meishan and Landrace sows. *Acta Prataculturae Sinica* 22, 99–107.

Alessandri, G., Milani, C., Mancabelli, L., Mangifesta, M., Lugli, G. A., Viappiani, A., et al. (2019). Metagenomic dissection of the canine gut microbiota: insights into taxonomic, metabolic and nutritional features. *Env. Microbiol.* *.

Andersson, L., and Georges, M. (2004). Domestic-animal genomics: deciphering the genetics of complex traits. *Nat. Rev. Genet.* 5, 202–212. doi: 10.1038/nrg1294

Andrade, B. G. N., Bressani, F. A., Cuadrat, R. R. C., Tizioto, P. C., and de Oliveira, P. S. N., et al. (2020). The structure of microbial populations in Nelore GIT reveals inter-dependency of methanogens in feces and rumen. *J. Animal Sci. Biotechnol.* 11. doi: 10.1186/s40104-019-0422-x

Baldo, L., Riera, J. L., Tooming-Klunderud, A., Alba, M. M., and Salzburger, W. (2015). Gut microbiota dynamics during dietary shift in Eastern African cichlid fishes. *PLoS One* 10:e0127462. doi: 10.1371/journal.pone.0127462

Benis, N., Schokker, D., Suarez-Diez, M., Dos Santos, V. A. P. M., Smidt, H., and Smits, M. A. (2015). Network analysis of temporal functionalities of the gut induced by perturbations in new-born piglets. *Bmc Genom.* 2015:16.

Bentley, D. R., Balasubramanian, S., Swerdlow, H. P., Smith, G. P., Milton, J., Brown, C. G., et al. (2008). Accurate whole human genome sequencing using reversible terminator chemistry. *Nature* 456, 53–59.

Bowers, R. M., Clum, A., Tice, H., Lim, J., Singh, K., Ciobanu, D., et al. (2015). Impact of library preparation protocols and template quantity on the metagenomic reconstruction of a mock microbial community. *Bmc Genomics* 2015:16.

Boyazoglu, J., Hatziminologlou, I., and Morand-Fehr, P. (2005). The role of the goat in society: Past, present and perspectives for the future. *Small Ruminant Res.* 60, 13–23. doi: 10.1016/j.smallrumres.2005.06.003

Caporaso, J. G., Kuczynski, J., Stombaugh, J., Bittinger, K., Bushman, F. D., Costello, E. K., et al. (2010). QIIME allows analysis of high-throughput community sequencing data. *Nature Methods* 7, 335–336.

Chao, A. (1984). Nonparametric-estimation of the number of classes in a population. *Scandinavian J. Stat.* 11, 265–270.

Chao, A., and Lee, S. M. (1992). Estimating the number of classes via sample coverage. *J. Am. Stat. Assoc.* 87, 210–217. doi: 10.1080/01621459.1992.10475194

Chen, B., Du, K., Sun, C., Vimalanathan, A., Liang, X., Li, Y., et al. (2018a). Gut bacterial and fungal communities of the domesticated silkworm (*Bombyx mori*) and wild mulberry-feeding relatives. *Isme J.* 2018:12.

Chen, C. Y., Huang, X. C., Fang, S. M., Yang, H., He, M. Z., Zhao, Y. Z., et al. (2018b). Contribution of host genetics to the variation of microbial composition of cecum lumen and feces in pigs. *Front. Microb.* 9:13.

Chevalier, C., Stojanovic, O., Colin, D. J., Suarez-Zamorano, N., Tarallo, V., Veyrat-Durebex, C., et al. (2015). Gut microbiota orchestrates energy homeostasis during cold. *Cell* 163, 1360–1374. doi: 10.1016/j.cell.2015.11.004

Claesson, M. J., Wang, Q. O., O'sullivan, O., Greene-Diniz, R., Cole, J. R., Ross, R. P., et al. (2010). Comparison of two next-generation sequencing technologies for resolving highly complex microbiota composition using tandem variable 16S rRNA gene regions. *Nucleic Acids Res.* 38:13.

DeSantis, T. Z., Hugenholtz, P., Larsen, N., Rojas, M., Brodie, E. L., Keller, K., et al. (2006). Greengenes, a chimera-checked 16S rRNA gene database and workbench compatible with ARB. *Appl. Env. Microb.* 72, 5069–5072. doi: 10.1128/aem.03006-05

Deutscher, A. T., Burke, C. M., Darling, A. E., Riegler, M., Reynolds, O. L., and Chapman, T. A. (2018). Near full-length 16S rRNA gene next-generation sequencing revealed Asaia as a common midgut bacterium of wild and domesticated Queensland fruit fly larvae. *Microbiome* 6:85.

Diamond, J. (2002). Evolution, consequences and future of plant and animal domestication. *Nature* 418, 700–707. doi: 10.1038/nature01019

Edgar, R. C. (2004). MUSCLE: multiple sequence alignment with high accuracy and high throughput. *Nucleic Acids Res.* 32, 1792–1797. doi: 10.1093/nar/gkh340

Edgar, R. C. (2013). UPARSE: highly accurate OTU sequences from microbial amplicon reads. *Nat. Methods* 10:996. doi: 10.1038/nmeth.2604

Faichney, G. J. (1969). Production of volatile fatty acids in sheep caecum. *Austr. J. Agricult. Res.* 20:491. doi: 10.1071/ar9690491

Fan, C., Zhang, L., Fu, H., Liu, C., and Zhang, Y. (2020). Enterotypes of the gut microbial community and their response to plant secondary compounds in plateau pikas. *Microorganisms* 8, 1311. doi: 10.3390/microorganisms8091311

Fu, H., Zhang, L., Fan, C., Liu, C., Li, W., Cheng, Q., et al. (2020). Environment and host species identity shape gut microbiota diversity in sympatric herbivorous mammals. *Micro. Biotechnol.* doi: 10.1111/1751-7915.13687

Gao, G. L., Zhao, X. Z., Li, Q., He, C., Zhao, W. J., Liu, S. Y., et al. (2016). Genome and metagenome analyses reveal adaptive evolution of the host and interaction with the gut microbiota in the goose. *Sci. Rep.* 6:11.

Gomez, A., Petrzelkova, K., Yeoman, C. J., Vlckova, K., Mrazek, J., Koppova, I., et al. (2015). Gut microbiome composition and metabolomic profiles of wild western lowland gorillas (*Gorilla gorilla gorilla*) reflect host ecology. *Mol. Ecol.* 24, 2551–2565. doi: 10.1111/mec.13181

Grice, E. A., and Segre, J. A. (2012). The human microbiome: our second genome. *Annu. Rev. Genom. Hum. Genet.* 13, 151–170. doi: 10.1146/annurev-genom-090711-163814

Guo, S. C., Savolainen, P., Su, J. P., Zhang, Q., Qi, D. L., Zhou, J., et al. (2006). Origin of mitochondrial DNA diversity of domestic yaks. *Bmc Evol. Biol.* 6:13.

Hassanin, A., and Ropiquet, A. (2004). Molecular phylogeny of the tribe Bovini (*Bovidae, Bovinae*) and the taxonomic status of the Kouprey, Bos sauveli Urbain 1937. *Mol. Phylogenet. Evol.* 33, 896–907. doi: 10.1016/j.ympev.2004.08.009

Hoover, W. H. (1978). Digestion and absorption in hindgut of ruminants. *J. Anim. Sci.* 46, 1789–1799. doi: 10.2527/jas1978.4661789x

Huang, X. D., Martinez-Fernandez, G., Padmanabha, J., Long, R. J., Denman, S. E., and Mcsweeney, C. S. (2016). Methanogen diversity in indigenous and introduced ruminant species on the Tibetan Plateau. *Archaea-An Int. Microb. J.* 2016:10.

Huang, X. D., Tan, H. Y., Long, R. J., Liang, J. B., and Wright, A. D. G. (2012). Comparison of methanogen diversity of yak (*Bos grunniens*) and cattle (*Bos taurus*) from the Qinghai-Tibetan plateau, China. *Bmc Microb.* 12:10.

Hu, J. (2001). *Study on the Biological Characteristics and Genetic Diversities of Wild Yak and Domestic Yak and Their Hybrid*. Lanzhou, China: Master's dissertation, Gansu Agriculture University.

Hulsen, T., Huynen, M. A., De Vlieg, J., and Groenen, P. M. A. (2006). Benchmarking ortholog identification methods using functional genomics data. *Genome Biol.* 7:12.

Hummel, J., Hammer, C., Hammer, S., Sudekum, K. H., Muller, D. W. H., and Clauss, M. (2017). Retention of solute and particle markers in the digestive tract of captive Somali wild asses (*Equus africanus somaliensis*). *Eur. J. Wildlife Res.* 63:5.

Hurst, L. D. (2002). The Ka/Ks ratio: diagnosing the form of sequence evolution. *Trends Genet.* 18, 486–487. doi: 10.1016/s0168-9525(02)02722-1

Jensen, P. (2014). "Behavior genetics and the domestication of animals," in *Annual Review of Animal Biosciences*, Vol. 2, eds H. A. Lewin and R. M. Roberts (Palo Alto: Annual Reviews), 85–104. doi: 10.1146/annurev-animal-022513-114135

Jialin, B., Mingqiang, W., Zhonglin, L., and Chesworth, J. M. (1998). Meat production from crossbred and domestic yaks in China. *Animal Sci.* 66, 465–469.

Jiang, H., and Zhonglin, L. (2005). Study on The Blood Physiological Indices of Wild Yak, Domestic Yak and Their Crossbreeds. *China Herbivores* 23:228.

Jiye, L., Xiaolin, H., Kexuan W., and Huan, L. (2005). Growth and development of the Kunlun Type of wild yak. *China Herbivores* 227–228.

Katoh, K., and Standley, D. M. (2013). MAFFT Multiple Sequence Alignment Software Version 7: Improvements in Performance and Usability. *Mole. Biol. Evol.* 30, 772–780. doi: 10.1093/molbev/mst010

Kohl, K. D., Weiss, R. B., Cox, J., Dale, C., and Dearing, M. D. (2014). Gut microbes of mammalian herbivores facilitate intake of plant toxins. *Ecol. Lett.* 17, 1238–1246. doi: 10.1111/ele.12329

Kreisinger, J., Cizkova, D., Vohanka, J., and Pialek, J. (2014). Gastrointestinal microbiota of wild and inbred individuals of two house mouse subspecies assessed using high-throughput parallel pyrosequencing. *Mole. Ecol.* 23, 5048–5060. doi: 10.1111/mec.12909

Larson, G., and Burger, J. (2013). A population genetics view of animal domestication. *Trends Genet.* 29, 197–205. doi: 10.1016/j.tig.2013.01.003

Law, J., Jovel, J., Patterson, J., Ford, G., O'keefe, S., Wang, W., et al. (2013). Identification of hepatotropic viruses from plasma using deep sequencing: A Next Generation Diagnostic Tool. *Plos One* 2013:8.

Leamy, L. J., Kelly, S. A., Nietfeldt, J., Legge, R. M., Ma, F., Hua, K., et al. (2014). Host genetics and diet, but not immunoglobulin A expression, converge to shape compositional features of the gut microbiome in an advanced intercross population of mice. *Genom. Biol.* 15:552.

Li, C. Y., Wu, C., Liu, J. X., Wang, Y. Z., and Wang, J. K. (2009). Spatial variation of intestinal skatole production and microbial community in Jinhua and Landrace pigs. *J. Sci. Food Agricult.* 89, 639–644. doi: 10.1002/jsfa.3494

Li, G. L., Li, J., Kohl, K. D., Yin, B. F., Wei, W. H., Wan, X. R., et al. (2019). Dietary shifts influenced by livestock grazing shape the gut microbiota composition and co-occurrence networks in a local rodent species. *J. Anim. Ecol.* 88, 302–314. doi: 10.1111/1365-2656.12920

Lippke, H., Ellis, W. C., and Jacobs, B. F. (1986). Recovery of indigestible fiber from feces of sheep and cattle on forage diets1. *J. Dairy Sci.* 69, 403–412. doi: 10.3168/jds.s0022-0302(86)80418-0

Li, H., Qu, J. P., Li, T. T., Wirth, S., Zhang, Y. M., Zhao, X. Q., et al. (2018). Diet simplification selects for high gut microbial diversity and strong fermenting ability in high-altitude pikas. *Appl. Microb. Biotechnol.* 102, 6739–6751. doi: 10.1007/s00253-018-9097-z

Li, Y., Hu, X., Yang, S., Zhou, J., Zhang, T., Qi, L., et al. (2017). Comparative analysis of the gut microbiota composition between captive and wild forest musk deer. *Front. Microbiol.* 8:1705.

Louis, P., Hold, G. L., and Flint, H. J. (2014). The gut microbiota, bacterial metabolites and colorectal cancer. *Nat. Rev. Microb.* 12, 661–672. doi: 10.1038/nrmicro3344

Lozupone, C., Lladser, M. E., Knights, D., Stombaugh, J., and Knight, R. (2011). UniFrac: an effective distance metric for microbial community comparison. *Isme J.* 5, 169–172. doi: 10.1038/ismej.2010.133

Mao, S. Y., Zhang, R. Y., Wang, D. S., and Zhu, W. Y. (2012). The diversity of the fecal bacterial community and its relationship with the concentration of volatile fatty acids in the feces during subacute rumen acidosis in dairy cows. *Bmc Veterinary Res.* 8:13. doi: 10.1186/1746-6148-8-237

McFall-Ngai, M., Hadfield, M. G., Bosch, T. C. G., Carey, H. V., Domazet-Loso, T., Douglas, A. E., et al. (2013). Animals in a bacterial world, a new imperative for the life sciences. *Proc. Natl. Acad. Sci. U S A.* 110, 3229–3236.

Mcknite, A. M., Elisa, P. M. M., Lu, L., Williams, E. G., Simon, B., Andreux, P. A., et al. (2012). Murine gut microbiota is defined by host genetics and modulates variation of metabolic traits. *PLoS One* 2012:7.

Meale, S. J., Li, S., Azevedo, P., Derakhshani, H., Plaizier, J. C., Khafipour, E., et al. (2016). Development of ruminal and fecal microbiomes are affected by weaning but not weaning strategy in dairy calves. *Front. Microbiol.* 7:582. doi: 10.3389/fmicb.2016.00582

Mendoza, M. L. Z., Xiong, Z. J., Escalera-Zamudio, M., Runge, A. K., Theze, J., Streicker, D., et al. (2018). Hologenomic adaptations underlying the evolution of sanguivory in the common vampire bat. *Nat. Ecol. Evol.* 2, 659–668. doi: 10.1038/s41559-018-0476-8

Metcalf, J. L., Song, S. J., Morton, J. T., Weiss, S., Seguinorlando, A., Joly, F., et al. (2017). Evaluating the impact of domestication and captivity on the horse gut microbiome. *Sci. Rep.* 7:15497.

Nicholson, J. K., Holmes, E., Kinross, J., Burcelin, R., Gibson, G., Jia, W., et al. (2012). Host-gut microbiota metabolic interactions. *Science* 336, 1262–1267. doi: 10.1126/science.1223813

Parfrey, L. W., Walters, W. A., Lauber, C. L., Clemente, J. C., Berg-Lyons, D., Teiling, C., et al. (2014). Communities of microbial eukaryotes in the mammalian gut within the context of environmental eukaryotic diversity. *Front. Microb.* 5:13.

Pendleton, A. L., Shen, F. C., Taravella, A. M., Emery, S., Veeramah, K. R., Boyko, A. R., et al. (2018). Comparison of village dog and wolf genomes highlights the role of the neural crest in dog domestication. *Bmc Biol.* 16:21.

Qiu, Q., Wang, L., Wang, K., Yang, Y., Ma, T., Wang, Z., et al. (2015). Yak whole-genome resequencing reveals domestication signatures and prehistoric population expansions. *Nat. Commun.* 6:10283.

Rho, M. N., Tang, H. X., and Ye, Y. Z. (2010). FragGeneScan: predicting genes in short and error-prone reads. *Nucleic Acids Res.* 38:12.

Robison, B. D., Drew, R. E., Settles, M., Churchill, E., Moretz, J., and Martins, E. P. (2006). Variation in gene expression among the brains of behaviorally distinct zebrafish strains. no evidence for parallel transcriptome evolution during domestication. *Integr. Comparat. Biol.* 46, E120–E120.

Rubin, C.-J., Zody, M. C., Eriksson, J., Meadows, J. R. S., Sherwood, E., Webster, M. T., et al. (2010). Whole-genome resequencing reveals loci under selection during chicken domestication. *Nature* 464, 587–U145.

Schwab, C., Cristescu, B., Boyce, M. S., Stenhouse, G. B., and Ganzle, M. (2009). Bacterial populations and metabolites in the feces of free roaming and captive grizzly bears. *Canad. J. Microbiol.* 55, 1335–1346. doi: 10.1139/w09-083

Schwimmer, J. B., Johnson, J. S., Angeles, J. E., Behling, C., Belt, P. H., Borecki, I., et al. (2019). Microbiome signatures associated with steatohepatitis and moderate to severe fibrosis in children with nonalcoholic fatty liver disease. *Gastroenterology* 157, 1109–1122.

Shannon, C. E. (1948). A mathematical theory of communication. *Bell Syst. Tech. J.* 27, 623–656.

Shi, Q. J., Guo, Y. Y., Engelhardt, S. C., Weladji, R. B., Zhou, Y., Long, M., et al. (2016). Endangered wild yak (*Bos grunniens*) in the Tibetan plateau and adjacent regions: Population size, distribution, conservation perspectives and its relation to the domestic subspecies. *J. Nat. Conserv.* 32, 35–43. doi: 10.1016/j.jnc.2016.04.001

Shi, W., Moon, C. D., Leahy, S. C., Kang, D., Froula, J., Kittelmann, S., et al. (2014). Methane yield phenotypes linked to differential gene expression in the sheep rumen microbiome. *Genome Res.* 1517–1525. doi: 10.1101/gr.168245.113

Simpson, E. H. (1949). Measurement of diversity. *Nat.* 163, 688–688.

Tringe, S. G., and Rubin, E. M. (2005). Metagenomics: DNA sequencing of environmental samples. *Nat. Rev. Genet.* 6, 805–814. doi: 10.1038/nrg1709

Turnbaugh, P. J., Baeckhed, F., Fulton, L., and Gordon, J. I. (2008). Diet-induced obesity is linked to marked but reversible alterations in the mouse distal gut microbiome. *Cell Host Microbe* 3, 213–223. doi: 10.1016/j.chom.2008.02.015

Turnbaugh, P. J., Hamady, M., Yatsunenko, T., Cantarel, B. L., Duncan, A., Ley, R. E., et al. (2009). A core gut microbiome in obese and lean twins. *Nature* 457, 480–U487.

Varemo, L., Nielsen, J., and Nookaew, I. (2013). Enriching the gene set analysis of genome-wide data by incorporating directionality of gene expression and combining statistical hypotheses and methods. *Nucleic Acids Res.* 41, 4378–4391. doi: 10.1093/nar/gkt111

Vigne, J. D. (2011). The origins of animal domestication and husbandry: A major change in the history of humanity and the biosphere. *Comptes Rendus Biol.* 334, 171–181. doi: 10.1016/j.crvi.2010.12.009

Vilo, C., and Dong, Q. (2012). Evaluation of the RDP classifier accuracy using 16S rRNA gene variable regions. *Metagenomics* 2012:1. doi: 10.4303/mg/235551

Wang, J., Kalyan, S., Steck, N., Turner, L. M., Harr, B., Kunzel, S., et al. (2015). Analysis of intestinal microbiota in hybrid house mice reveals evolutionary divergence in a vertebrate hologenome. *Nat. Commun.* 6:10.

Wang, Z. F., Shen, X., Liu, B., Su, J. P., Yonezawa, T., Yu, Y., et al. (2010). Phylogeographical analyses of domestic and wild yaks based on mitochondrial DNA: new data and reappraisal. *J. Biogeogr.* 37, 2332–2344. doi: 10.1111/j.1365-2699.2010.02379.x

Wendorf, F., and Schild, R. (1998). Nabta Playa and its role in northeastern African prehistory. *J. Anthropolog. Arch.* 17, 97–123. doi: 10.1006/jaar.1998.0319

Yang, Z. H. (2007). PAML 4: Phylogenetic analysis by maximum likelihood. *Mole. Biol. Evol.* 24, 1586–1591. doi: 10.1093/molbev/msm088

Yin, Y. B., Mao, X. Z., Yang, J. C., Chen, X., Mao, F. L., and Xu, Y. (2012). dbCAN: a web resource for automated carbohydrate-active enzyme annotation. *Nucleic Acids Res.* 40, W445–W451.

Zeder, M. A. (2015). The domestication of animals. *J. Anthropolog. Res.* 9, 321–327.

Zhang, H. B., Wang, Z. S., Peng, Q. H., Tan, C., and Zou, H. W. (2014). Effects of different levels of protein supplementary diet on gene expressions related to intramuscular deposition in early-weaned yaks. *Animal Sci. J.* 85, 411–419.

Zhang, X., Wang, K., Wang, L. Z., Yang, Y. Z., Ni, Z. Q., Xie, X. Y., et al. (2016a). Genome-wide patterns of copy number variation in the Chinese yak genome. *Bmc Genomics* 17:12.

Zhang, Z., Xu, D., Wang, L., Hao, J., Wang, J., Zhou, X., et al. (2016b). Convergent evolution of rumen microbiomes in high-altitude mammals. *Curr. Biol.* 26, 1873–1879. doi: 10.1016/j.cub.2016.05.012

Zheng, X. J., Qiu, Y. P., Zhong, W., Baxter, S., Su, M. M., Li, Q., et al. (2013). A targeted metabolomic protocol for short-chain fatty acids and branched-chain amino acids. *Metabolomics* 9, 818–827. doi: 10.1007/s11306-013-0500-6

Zhipeng, L., Ag, W., Si, H., Wang, X., Qian, W., Zhang, Z., et al. (2016). Changes in the rumen microbiome and metabolites reveal the effect of host genetics on hybrid crosses. *Env. Microb. Rep.* 8:1016. doi: 10.1111/1758-2229.12482

Zhou, A., Wang, W., Wang, Z., Zou, H., Peng, Q., Feng, Y., et al. (2015). Effect of different protein levels of supplementary diets on performance and gastrointestinal development in early-weaned yak calves. *Chinese J. Animal Nut.* 27, 918–925.

Conflict of Interest: The authors declare that the research was conducted in the absence of any commercial or financial relationships that could be construed as a potential conflict of interest.

frontiers in Microbiology

ORIGINAL RESEARCH
published: 31 May 2021
doi: 10.3389/fmicb.2021.683714

Gut Microbial SNPs Induced by High-Fiber Diet Dominate Nutrition Metabolism and Environmental Adaption of *Faecalibacterium prausnitzii* in Obese Children

Hui Li[1], *Liping Zhao*[1,2] *and Menghui Zhang*[1]*

[1] State Key Laboratory of Microbial Metabolism and Joint International Research Laboratory of Metabolic and Developmental Sciences, School of Life Sciences and Biotechnology, Shanghai Jiao Tong University, Shanghai, China, [2] Ministry of Education Key Laboratory for Systems Biomedicine, Shanghai Centre for Systems Biomedicine, Shanghai Jiao Tong University, Shanghai, China

OPEN ACCESS

Edited by:
Teresa Nogueira, Instituto Nacional Investigaciao Agraria e Veterinaria (INIAV), Portugal

Reviewed by:
Farzam Vaziri, Pasteur Institute of Iran (PII), Iran
Sandrine Auger, Le nouvel Institut national de recherche sur l'agriculture, l'alimentation et l'environnement en France INRAE, France

***Correspondence:**
Menghui Zhang
mhzhang@sjtu.edu.cn

Specialty section:
This article was submitted to Systems Microbiology, a section of the journal Frontiers in Microbiology

Received: 22 March 2021
Accepted: 23 April 2021
Published: 31 May 2021

Citation:
Li H, Zhao L and Zhang M (2021) Gut Microbial SNPs Induced by High-Fiber Diet Dominate Nutrition Metabolism and Environmental Adaption of Faecalibacterium prausnitzii in Obese Children. Front. Microbiol. 12:683714. doi: 10.3389/fmicb.2021.683714

Dietary intervention is effective in human health promotion through modulation of gut microbiota. Diet can cause single-nucleotide polymorphisms (SNPs) to occur in the gut microbiota, and some of these variations may lead to functional changes in human health. In this study, we performed a systematic SNP analysis based on metagenomic data collected from children with Prader–Willi syndrome (PWS, n = 17) and simple obese (SO) children (n = 19), who had better healthy conditions after receiving high-fiber diet intervention. We found that the intervention increased the SNP proportions of *Faecalibacterium*, *Bifidobacterium*, and *Clostridium* and decreased those of *Bacteroides* in all children. Besides, the PWS children had *Collinsella* increased and *Ruminococcus* decreased, whereas the SO had *Blautia* and *Escherichia* decreased. There were much more BiasSNPs in PWS than in SO (4,465 vs 303), and only 81 of them appeared in both groups, of which 78 were from *Faecalibacterium prausnitzii*, and 51 were nonsynonymous mutations. These nonsynonymous variations were mainly related to pathways of environmental adaptation and nutrition metabolism, particularly to carbohydrate and nucleotide metabolism. In addition, dominant strains carrying BiasSNPs in all children shifted from *F. prausnitzii* AF32-8AC and *F. prausnitzii* 942/30-2 to *F. prausnitzii* SSTS Bg7063 and *F. prausnitzii* JG BgPS064 after the dietary intervention. Furthermore, although the abundance of *Bifidobacterium* increased significantly by the intervention and became dominant strains responsible for nutrition metabolism, they had less BiasSNPs between the pre- and post-intervention group in comparison with *Faecalibacterium*. The finding of *F. prausnitzii* as important functional strains influenced by the intervention highlights the superiority of applying SNP analysis in studies of gut microbiota. This study provided evidence and support for the effect of dietary intervention on gut microbial SNPs, and gave some enlightenments for disease treatment.

Keywords: SNP, gut microbiota, high-fiber diet, non-synonymous, obese children, metagenome

INTRODUCTION

Single-nucleotide polymorphism (SNP) is the most common genetic variation in DNA sequence in order to better adapt to the external environment in the evolutionary process (Haraksingh and Snyder, 2013). SNPs in the coding region can be classified as nonsynonymous mutation and synonymous mutation. Nonsynonymous mutation changes the sequence of amino acids and then affects the genetic function, while the synonymous mutation does not affect the genetic function (Tennessen, 2008). There are huge amounts of microorganisms living in the human intestinal tract, and the diet is one of the most important factors shaping the structure and function of the gut microbiota (Goldsmith and Sartor, 2014; Shen, 2017). Environmental pressure caused by the change in the diet not only alter the structure of the gut microbiota but also led to genetic variations in the microbes (Truong et al., 2017). These variations can lead to different functions in strains, which, in turn, affect the health of the host.

Considering the taxonomic diversity of bacteria and the genetic variations in response to constant environmental change (Hofreiter et al., 2015), the analyses based on the abundance and composition of the gut microbiota are not enough to reflect changes in gene function or microbial transfer, which might not only omit some correlations but also infer wrong conclusions from this rough quantitative level. For instance, researchers had studied the gut metagenomes of 98 mothers and their infants over 1 year, used rare SNPs to reveal vertical transmission of strains, and found that the colonization with strains of infants mainly derived from the environment but not from their mothers, although the gut microbial composition of infants converged toward that of their mothers over time (Nayfach et al., 2016). This pattern might be missed in the analysis with the gut microbial composition, and it was mistakenly assumed that vertical bacterial transmission of infants from their mother was increased during the first year after birth.

Single-nucleotide polymorphisms, which refer to single-nucleotide variations in genes, are more able to reveal the differences between strains and between genes. The continuous expansion of gut metagenomic sample dataset and an increasing number of the bacterial reference genome have facilitated the studies of gut microbial SNPs. The flexible application of gut microbial SNPs can solve the complex problems that other analysis at species level cannot solve, obtain more accurate results at the strain- or gene-level, and provide new clues for the precision diagnosis and treatment of diseases (Galloway-Peña et al., 2012; Leonard et al., 2016; Zou et al., 2020). Patient-specific SNPs were found in the gut microbiota of both type 2 diabetes mellitus (T2D) and tuberculosis patients, which could separate the patients from the healthy individuals. The gene carrying T2D-specific SNPs encodes the alpha glucoside enzyme, which is a kind of important T2D drug target, and the researchers believed that these SNPs could be used as drug targets for the treatment of T2D (Chen et al., 2017). The tuberculosis-specific SNP genes were mainly involved in carbohydrate metabolism prevalently from *Bacteroides vulgatus*, suggesting that there were altered carbohydrate preference and different carbohydrate metabolism patterns in the gut of tuberculosis patients, and providing reference for the diagnosis and treatment of tuberculosis (Hu et al., 2019). Other researchers conducted gut microbial SNP studies on antibiotic resistance genes of individuals from different countries and found that the population-specific SNPs on antibiotic resistance genes were not related to the country, but might be attributed to the altered microbiota by differences in population structure or different antibiotic usage (Hu et al., 2013).

Many studies have proved the close relationship between the gut microbiota and obesity, but in-depth researches on the strain- or gene-level still need to be conducted (Turnbaugh et al., 2006; Flint, 2011; Baothman et al., 2016). Our previous study demonstrated that a high-fiber dietary intervention significantly improved the physiological conditions of the genetic (Prader–Willi syndrome, PWS) and simple obese (SO) children, and this promotion was found to be relevant to the change in the gut microbiota (Zhang et al., 2015). In order to better understand the underlying mechanism for this effective treatment, we performed a systemic SNP analysis based on high-throughput metagenomic sequencing data obtained from two longitudinal cohorts, children with PWS or SO. We first identified SNPs in each cohort affected by the intervention and screened out genes with significant change in SNP density. The species that carried these genes were then sourced and linked with relevant metabolic pathways. After that, we focused on BiasSNPs that occurred in both cohorts, particularly on those nonsynonymous mutations. Functional pathways and dominant strains with BiasSNPs influenced by the intervention were investigated further. Finally, PWS and SO-specific BiasSNP-affected strains and metabolic pathways were individually analyzed.

MATERIALS AND METHODS

Data Collection

The dietary intervention trial was approved by the Ethics Committee of the School of Life Sciences and Biotechnology, Shanghai Jiao Tong University, with No. 2012-016 and registered at the Chinese Clinical Trial Registry with No. ChiCTR-ONC-12002646. Written informed consent was obtained from the guardian of the obese children. The trial was performed as described in the previous study (Zhang et al., 2015). Briefly, 17 PWS and 19 SO children completed the dietary intervention in the hospital for 90 and 30 days, respectively. The diet used in the clinical trial for intervention mainly included whole grains, traditional Chinese medicinal foods, and prebiotics (WTP), incorporated certain amount of vegetables, fruits, and nuts (Xiao et al., 2014).

The fecal samples and physiological indexes of all obese children were collected at predefined time points (PWS: on intervention days 0, 30, 60, and 90; SO: days 0 and 30) (Zhang et al., 2015). Metagenomic sequencing of the extracted and purified DNA was performed on Illumina Hiseq 2000 platform at Shanghai Biotechnology Co., Ltd. All potential biologically hazardous materials in this study were properly handled according to Chinese biosafety laws and regulations.

The raw metagenome sequencing data was accessed at the NCBI SRA (Sequence Read Archive) database with accession number SRP045211 (Zhang et al., 2015).

Detection of Single-Nucleotide Polymorphisms

The data pre-processing was done as described in our previous study (Zhang et al., 2015). Briefly, the original sequencing data was quality controlled by FlexBar and Prinseq (Schmieder and Edwards, 2011; Dodt et al., 2012), and then aligned to the human genome reference (*Homo sapiens*, UCSC hg19) using Bowtie2 to remove the reads from human (Langmead and Salzberg, 2012). Each sample had 84.6 ± 21.2 million (mean ± SD) high-quality reads on average. Then BWA (Li and Durbin, 2009) was used to align the high-quality reads to the integrated gene catalog (IGC), which contained approximately 11 million high-quality human gut microbial reference genes (Li et al., 2014; Xie et al., 2016). Afterward, the SAMTools was used to detect, filter, sort, and merge SNPs (Li et al., 2009; Li, 2011).

To ensure the reliability of the detected SNPs, only SNPs with at least five supported sequencing reads were kept, and those with less than 60% coverage in a group were furtherly removed to achieve more representative SNPs. The downstream analyses were all performed with the SNPs resulting from this procedure.

Calculation of Single-Nucleotide Polymorphisms Density

Single-nucleotide polymorphism density reflected the number of SNPs per kilobase in a gene per million sequencing paired-end reads. For any sample S, the SNP density D_i of gene i was calculated as follows:

$$D_i = \frac{n_i}{T_S L_i}$$

where n_i is the number of SNPs in gene i, T_s is the sequencing amount of sample S, and L_i is the length of the gene i per kilobase in sequence.

Detection of BiasSNP

Detection of BiasSNP was performed through comparison of an SNP in a nucleotide base between two groups. A BiasSNP was the differential SNP that dominated between two groups (**Supplementary Figure 1**). Nonsynonymous BiasSNP, whose mutation in a gene caused the encoded amino acid to be changed, was furtherly identified by in-house Perl script.

Statistical Analysis

In this study, the significance of the difference was judged with Wilcoxon paired test for a cohort between before and after the dietary intervention or with Wilcoxon unpaired test for two cohorts in R software (version 3.5.3). The significance of the difference among multiple groups was tested with permutational multivariate analysis of variance (perMANOVA) in the "vegan" library of the R software. The phylogenetic and clustering trees based on BiasSNPs were constructed using the maximum likelihood model GTRGAMMA and 1,000 bootstrap replicates in RAxML (Stamatakis, 2014). Additionally, the R package "clusterProfiler" (version 3.8.1) was used to perform enrichment analysis of the SNP genes (Yu et al., 2012).

Data Visualization

Data visualization was mainly realized in the R software, "ggalluvial" (version 0.11.3), which was used to illustrate the alluvial diagram between strain and metabolic pathway, while dotplot, boxplot, and pieplot were displayed by means of "ggplot2" (version 3.2.0). In addition, the network charts were drawn using the Cytoscape software (version 3.7.2) (Shannon et al., 2003), and the optimization of the tree diagram was accomplished with the aid of the online tool EvolView[1].

RESULTS

The Overall Effect of High-Fiber Dietary Intervention on Gut Microbial Single-Nucleotide Polymorphisms in Obese Children

A total of 218,343 SNPs were detected in the gut microbiota of the 36 obese children. These SNPs were concentrated in 40,515 genes, and these genes could be sourced from 57 genera and 150 species. The high-fiber dietary intervention lessened the overall SNP numbers on the 30th intervention day; the SNPs in PWS children decreased to 85,769 from 109,139, while in SO children, they decreased to 36,247 from 80,773. Before the intervention, all children had the dominant SNPs at genus level, which were from *Faecalibacterium*, *Ruminococcus*, and *Bacteroides*. In addition, the SO children had SNPs from *Escherichia* with relatively higher proportion (33.76%). The intervention increased the SNP proportions of *Faecalibacterium*, *Bifidobacterium*, and *Clostridium* and decreased those of *Bacteroides* in all children. Meanwhile, the PWS children had *Collinsella* increased and *Ruminococcus* decreased, whereas the SO had *Blautia* and *Escherichia* decreased (**Figure 1A**).

The Altered Single-Nucleotide Polymorphism Density Structure in Prader–Willi Syndrome and Simple Obese Children

In our previous study, the PWS group had worse health conditions such as higher inflammation level than the SO group before the intervention. However, we did not detect significant difference between the two groups in gut microbial structure (Zhang et al., 2015). Interestingly, with the SNP density structure, a significant separation between the two groups before the intervention was observed (**Figure 1B**, PerMANOVA test, $P < 0.001$). The SNP density structure was altered significantly by the dietary intervention in both groups (**Figure 1B**, PerMANOVA test, $P < 0.001$). According to the changes that occurred in the PWS group, the structure alteration might occur mainly in the earlier stage of the intervention, as the shift on the 60th and 90th days was less that on the 30th day.

[1]https://www.evolgenius.info/evolview

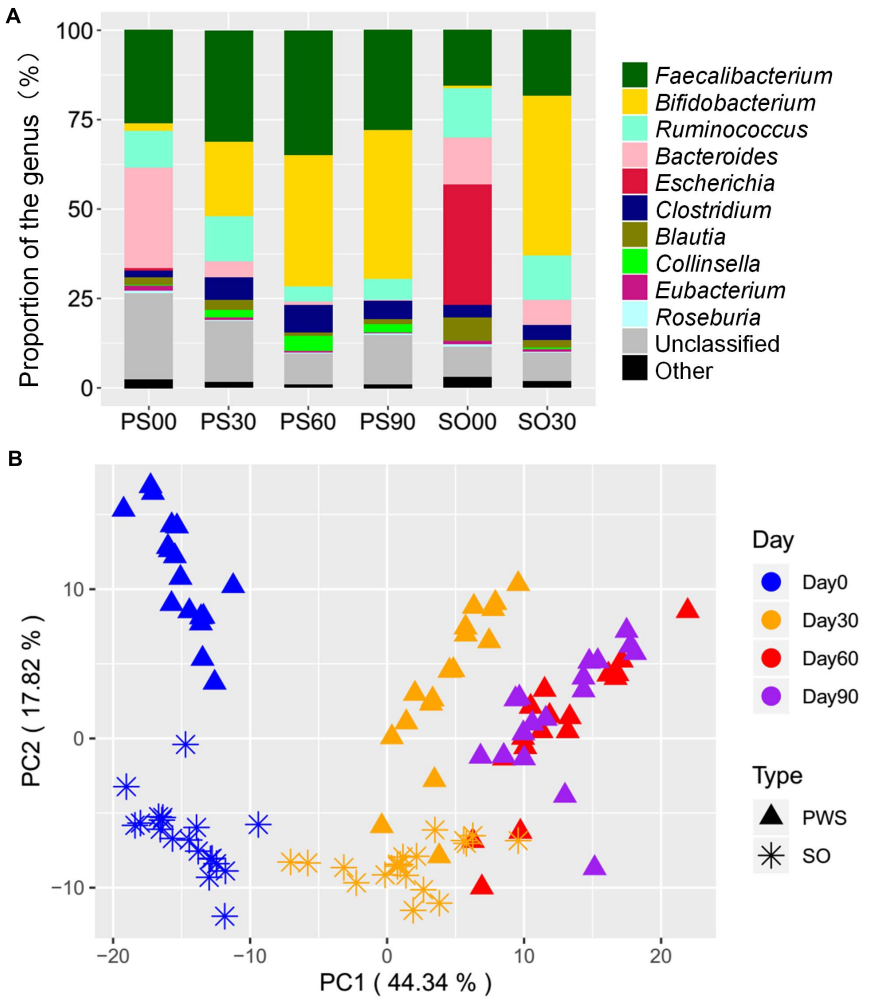

FIGURE 1 | High-fiber dietary intervention altered gut microbial single-nucleotide polymorphism (SNP) pattern in both Prader–Willi syndrome (PWS) (*n* = 17) and simple obese (SO) (*n* = 19) children. **(A)** The composition of SNPs at the genus level among different interventional time points. PWS on day 0 (PS00), 30 (PS30), 60 (PS60), and 90 (PS90); SO on day 0 (SO00) and day 30 (SO30). **(B)** PCA plot based on the SNP density of gut microbiota.

After 30 days of dietary intervention, the PWS children had 26,174 genes significantly changed in SNP density (Wilcoxon test, adjusted $P < 0.05$), and most of them (20,279) had fold changes lager than 8. Among these genes, 13,450 had higher SNP density before the intervention, which were distributed in 102 species and mainly concentrated in *Faecalibacterium prausnitzii* (20.27%), *Bacteroides stercoris* (15.63%), and *Bacteroides dorei* (12.49%). These genes were enriched in metabolic pathways for amino acid biosynthetic (ko01230), carbon metabolism (ko01200), two-component system (ko02020), and starch and sucrose metabolism (ko00500) (**Figure 2A**). After the intervention, 6,847 genes had higher SNP density. These genes were concentrated in 59 strains, mainly including butyrate-producing bacterium (24.65%), *Bifidobacterium catenulatum* (17.95%), and *Bifidobacterium longum* (10.60%). The corresponding metabolic pathways contained biosynthesis of amino acids (ko01230), carbon metabolism (ko01200), and starch and sucrose metabolism (ko00500) (**Figure 2B**). Notably, although the enriched metabolic pathways remain constant, their contributing strains changed after the intervention. For instance, the biosynthesis of amino acids (ko01230) was mainly from *F. prausnitzii* before the intervention, while the contributing strains of this function were replaced by butyrate-producing bacterium, *B. catenulatum*, and *B. longum* after the intervention.

The SO children had 17,427 genes significantly changed in SNP density (adjusted $P < 0.05$). The number of genes with fold change greater than 8 was 13,927. Among them, 10,409 genes with higher SNP density existed in the pre-intervention group, which were derived from 112 strains and mainly in *Escherichia coli* (37.53%), *F. prausnitzii* (16.88%), and *Ruminococcus* sp. 5_1_39BFAA (11.84%). Though the distribution of these strains in SO were different from that in PWS, these SNP density differential genes they carried also focused on biosynthesis of amino acids (ko01230), carbon metabolism (ko01200), and two-component system (ko02020) (**Figure 2C**), while 3,518

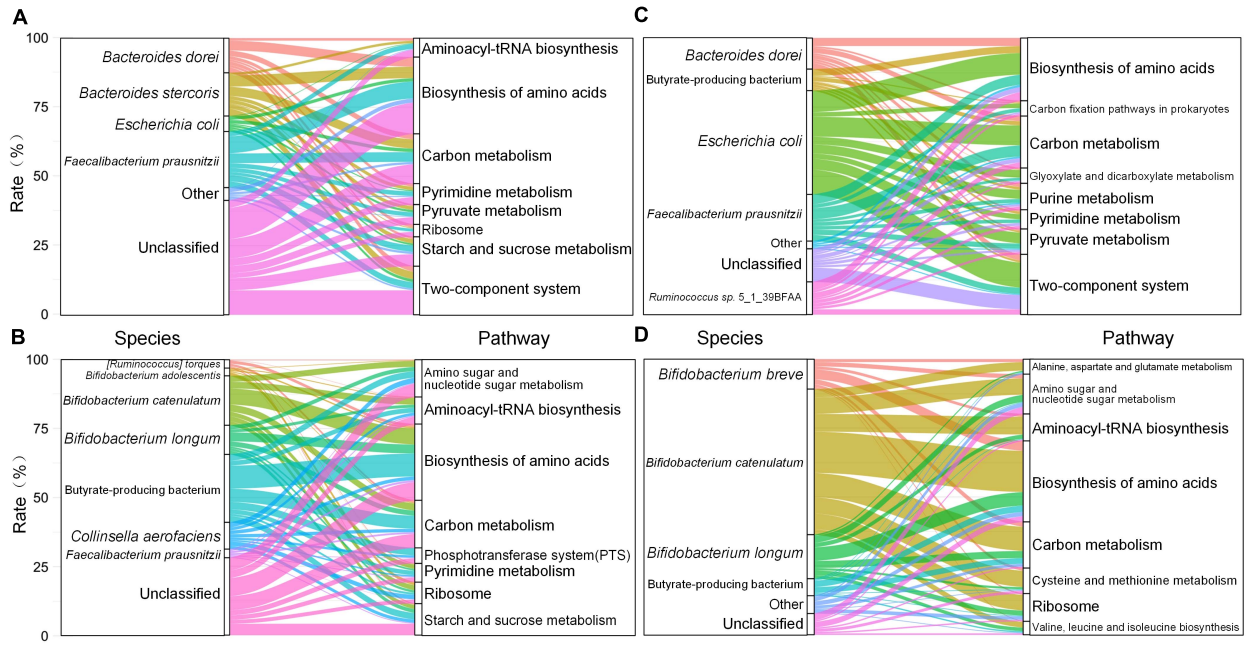

FIGURE 2 | Species and metabolic pathways corresponding to the genes with differential SNP density between before and after intervention in obese children. **(A)** The corresponding species and metabolic pathways of the genes with high SNP density in PWS before the intervention. **(B)** The corresponding species and metabolic pathways of the genes with high SNP density in PWS after the intervention. **(C)** The corresponding species and metabolic pathways of the genes with high SNP density in SO before the intervention. **(D)** The corresponding species and metabolic pathways of the genes with high SNP density in SO after the intervention.

genes with higher SNP density were detected in the post-intervention group, which were derived from 26 strains and mainly in *B. catenulatum* (52.84%), *B. longum* (15.98%), and *Bifidobacterium breve* (10.83%). These genes focused on biosynthesis of amino acids (ko01230), carbon metabolism (ko01200), and amino sugar and nucleoside sugar metabolism (ko00520) (**Figure 2D**). Similar to the PWS, the intervention also changed the relationships between the strains and the metabolic pathways. However, unlike in PWS, *E. coli* followed by *F. prausnitzii* were the main contributors in SO to the biosynthesis of amino acids before the intervention, while contributions from these two strains might be neglected, and *B. catenulatum* took dominant responsibilities after the dietary intervention.

Common BiasSNPs Before and After Intervention in Prader–Willi Syndrome and Simple Obese Children

With the interest in the differences of SNP between the groups in sequence, we furtherly screened BiasSNPs whose variation were dominant in one group/one time point among more than 60% of the individuals. Comparing with the SNPs before and after 30 days of intervention, the detected BiasSNPs in PWS was 4,465, larger than 303 in SO. The PWS and SO had only 81 BiasSNPs in common distributed in 69 genes. Source track indicated that 78 common BiasSNPs were from *F. prausnitzii*, and the remaining three were from *Streptococcus thermophilus*, suggesting that *F. prausnitzii* was the most affected under the intervention.

In order to identify the source of these BiasSNPs at genome level, 103 genomes of *F. prausnitzii* were downloaded from the GenBank database, and the nucleotide sites corresponding to common BiasSNPs were abstracted. Only nine out of the 103 *F. prausnitzii* strains had more than 70% coverage of BiasSNPs. Then, we constructed a phylogenetic tree of these nine *F. prausnitzii* and the corresponding strains from the pre- and post-intervention groups based on these 78 BiasSNPs. It was observed that *F. prausnitzii* AF32-8AC was closest to the pre-intervention group, followed by *F. prausnitzii* 942/30-2, *F. prausnitzii* APC942/18-1, and *F. prausnitzii* MGYG-HGUT-02545 in the phylogenetic tree (**Figure 3A**), while the closest to the post-intervention group was *F. prausnitzii* SSTS Bg7063, followed by *F. prausnitzii* JG BgPS064 and *F. prausnitzii* NZ FPSSTS7063 SV a2 mod. This suggested that the dominant strains of *F. prausnitzii* were converted from *F. prausnitzii* AF32-8AC and *F. prausnitzii* 942/30-2 to *F. prausnitzii* SSTS Bg7063 and *F. prausnitzii* JG BgPS064 after the dietary intervention.

Of the 81 common BiasSNPs, 53 were nonsynonymous mutations in which 51 were in *F. prausnitzii* and the remaining two were in *S. thermophilus*. These 53 nonsynonymous BiasSNPs existed in 49 genes, whose detailed information are listed in **Table 1**. The enriched KEGG metabolic pathways based on these 49 genes showed that these SNPs were mainly related to nutrition metabolism and environmental adaptation functions (**Figures 3B,C**). In detail, pathways related to nutrition metabolism included carbohydrate metabolism (ko00720), nucleotide metabolism (ko09104), amino acid metabolism (ko09105), lipid metabolism (ko09103),

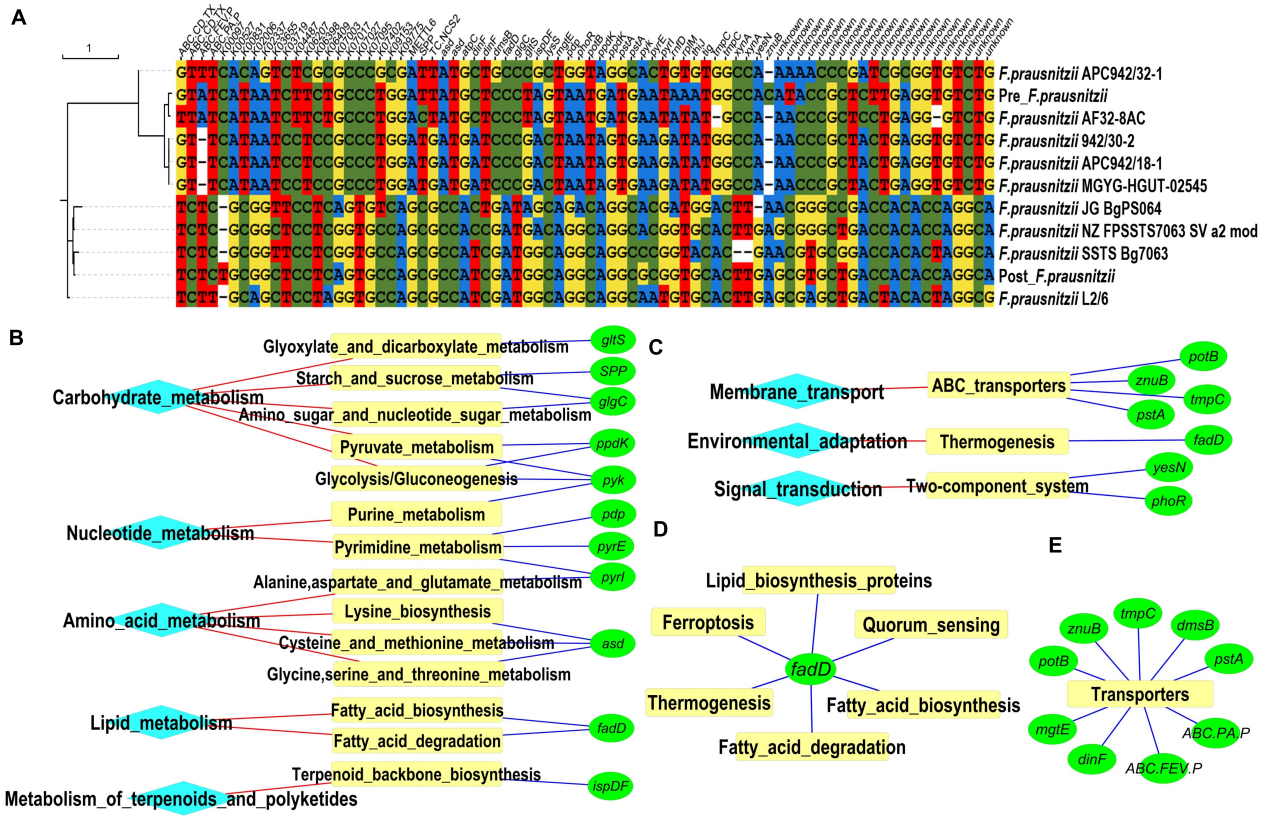

FIGURE 3 | Strains and metabolic pathways corresponding to common BiasSNPs. **(A)** Phylogenetic relationship of nine *Faecalibacterium prausnitzii* and the corresponding strains of pre- and post-intervention groups based on the common BiasSNPs. **(B)** Metabolic pathways related to nutrition metabolism. **(C)** Metabolic pathways associated with environmental adaptation. **(D)** Metabolic pathways associated with the gene *fadD*. **(E)** Genes encoding transporters.

and metabolism of terpenoids and polyketides (ko09109). Particularly, there were more genes related to carbohydrate and nucleotide metabolism (**Figure 3B**). Pathways associated with environmental information processing included membrane transport (ko09131), environmental adaptation (ko09159), and signal transduction (ko09132), which were mainly linked with ABC transporters (ko02010), thermogenesis (ko04714), and two-component system (ko02020), respectively (**Figure 3C**).

Notably, some genes, such as *pyk* and *fadD*, were involved in multiple metabolic pathways (**Figures 3B,D**), suggesting their important roles in the entire metabolic network. The gene *pyk* encodes pyruvate kinase (Gubler et al., 1994), mainly taking part in glycolysis/gluconeogenesis (ko00010), purine metabolism (ko00230), and pyruvate metabolism (ko00620). The gene *fadD* encodes long-chain acyl-CoA synthetase that can use long-chain fatty acids as carbon source and energy (Pech-Canul et al., 2020), and is mainly involved in fatty acid biosynthesis and degradation (ko00061 and ko00071), ferroptosis (ko04216), lipid biosynthesis proteins (ko01004), quorum sensing (ko02024), thermogenesis (ko04714), etc.

There were several gene-encoding transporters in enrichment pathways (**Figure 3E**). These transporters include a variety of proteins that are involved in signal transduction and various intracellular processes, such as cell proliferation and differentiation. In this study, the genes with common BiasSNPs encode a variety of transport system permease proteins, such as spermidine/putrescine transport system permease protein (*potB* encoding), phosphate transport system permease protein (*pstA* encoding), polar amino acid transport system permease protein (*ABC.PA.P* encoding), iron complex transport system permease protein (*ABC.FEV.P* encoding), zinc transport system permease protein (*znuB* encoding), etc. Besides, they also encode basic membrane protein A (*bmpA* encoding), multidrug resistance protein (*dinF* encoding), and anaerobic dimethyl sulfoxide reductase subunit B (*dmsB* encoding). These results indicated that these genes with nonsynonymous SNPs were closely related to the transporters under the dietary intervention.

Prader–Willi Syndrome-Specific BiasSNPs Affected by High-Fiber Dietary Intervention

PWS-specific BiasSNPs (4,384) were detected between the pre- and post-intervention groups, which were distributed in 2,039 genes and sourced from 34 strains. The distribution at strain level indicated that most of the BiasSNPs were derived from *F. prausnitzii* (82.0%) (**Figure 4A**).

TABLE 1 | Information of 49 genes with nonsynonymous BiasSNP.

GeneID	Name	Definition
SZEY-27A_GL0066464	*ABC.CD.TX*	HlyD family secretion protein
MH0423_GL0087716	*ABC.FEV.P*	Iron complex transport system permease protein
MH0204_GL0062877	*ABC.PA.P*	Polar amino acid transport system permease protein
O2.UC34-2_GL0007607	*ACSL, fadD*	Long-chain acyl-CoA synthetase
MH0094_GL0105570	*asd*	Aspartate-semialdehyde dehydrogenase
SZEY-58A_GL0041727	*ATPF1E, atpC*	F-type H+-transporting ATPase subunit epsilon
NOM017_GL0035853	*bmpA, bmpB, tmpC*	Basic membrane protein A and related proteins
SZEY-106A_GL0033468	*dmsB*	Anaerobic dimethyl sulfoxide reductase subunit B
MH0161_GL0016845	*E3.2.1.8, xynA*	Endo-1,4-beta-xylanase
MH0161_GL0083263	*glgC*	Glucose-1-phosphate adenylyltransferase
T2D-109A_GL0053344	*GLU, gltS*	Glutamate synthase (ferredoxin)
250twins_37179_GL0047337	*ispDF*	2-C-methyl-D-erythritol 4-phosphate Cytidylyltransferase/2-C-methyl-D-erythritol 2,4-Cyclodiphosphate synthase
BGI-28A_GL0080202	K07027	Glycosyltransferase 2 family protein
MH0260_GL0085944	K09153	Small membrane protein
MH0427_GL0005657	*KARS, lysS*	Lysyl-tRNA synthetase, class II
V1.FI16_GL0163211	*METTL6*	Methyltransferase-like protein 6
MH0089_GL0042766	*mgtE*	Magnesium transporter
NLM015_GL0035022	*pdp*	Pyrimidine-nucleoside phosphorylase
MH0222_GL0152632	*phoR*	Two-component system, OmpR family, phosphate regulon sensor histidine kinase PhoR
BGI-06A_GL0076090	*PK, pyk*	Pyruvate kinase
T2D-59A_GL0116703	*potB*	Spermidine/putrescine transport system permease protein
MH0251_GL0137853	*ppdK*	Pyruvate, orthophosphate dikinase
MH0055_GL0043341	*pstA*	Phosphate transport system permease protein
MH0069_GL0033002	*pyrE*	Orotate phosphoribosyltransferase
T2D-56A_GL0037409	*pyrI*	Aspartate carbamoyltransferase regulatory subunit
250twins_36674_GL0060378	*rnfD*	Na+-translocating ferredoxin:NAD+ oxidoreductase subunit D
SZEY-103A_GL0004639	*RP-L13, MRPL13, rplM*	Large subunit ribosomal protein L13
V1.CD6-0-PT_GL0047319	*SPP*	Sucrose-6-phosphatase
SZEY-90A_GL0013477	*TC.MATE, SLC47A, norM*	Multidrug resistance protein, MATE family
MH0176_GL0049322	*TC.NCS2*	Nucleobase:cation symporter-2, NCS2 family
MH0422_GL0084041	*thiJ*	Protein deglycase
160400887-stool1_196973	*tig*	Trigger factor
T2D-10A_GL0004234	*yesN*	Two-component system, response regulator YesN
763678604-stool1_204596	*znuB*	Zinc transport system permease protein
MH0136_GL0032411	K07003	Uncharacterized protein
N084A_GL0010742	K07017	Uncharacterized protein
V1.UC35-4_GL0167766	K07095	Uncharacterized protein
T2D-198A_GL0043098	K09775	Uncharacterized protein
V1.FI20_GL0181809	Unclassified	Unclassified
DOM026_GL0058508	Unclassified	Unclassified
MH0136_GL0100087	Unclassified	Unclassified
O2.UC34-2_GL0069427	Unclassified	Unclassified
V1.UC27-0_GL0047860	Unclassified	Unclassified
V1.CD2-0-PN_GL0116497	Unclassified	Unclassified
N051A_GL0048400	Unclassified	Unclassified
264199.stu_r17	Unclassified	Unclassified
MH0094_GL0121652	Unclassified	Unclassified
NLF010_GL0004489	Unclassified	Unclassified
MH0184_GL0028587	Unclassified	Unclassified

A network of the KEGG metabolic pathways, with the nonsynonymous BiasSNPs uniquely occurring in the PWS children, was constructed. This network showed that these BiasSNPs were mainly relevant to nutrition metabolism and environmental adaptation (**Figure 4B**). There were more BiasSNPs in PWS than in SO, and the metabolic functions of these PWS-specific BiasSNPs were similar to that of the common BiasSNPs, indicating that the gut microbial SNPs were more susceptible by dietary intervention in PWS. Nutrition metabolism mainly included carbohydrate metabolism, amino acid metabolism, metabolism of cofactors and vitamins, nucleotide metabolism, and lipid metabolism. Pathways of environmental adaptation mainly covered cellular community, membrane transport, and folding, sorting, and degradation. Genes (242) with nonsynonymous BiasSNPs in the pathway network of PWS children are listed in **Supplementary Table 1**.

Simple Obese-Specific BiasSNPs Affected by High-Fiber Dietary Intervention

There were 222 SO-specific BiasSNPs between before and after dietary intervention, far fewer than those in PWS. These BiasSNPs were distributed in 196 genes and sourced from 17 strains, also mainly from *F. prausnitzii* (74.8%) (**Figure 5A**). Among them, 104 BiasSNPs were nonsynonymous. The network of enriched KEGG metabolic pathways constructed with the genes carrying nonsynonymous BiasSNPs showed that these BiasSNPs were mainly related to nutrition metabolism, DNA replication and repair, and translation (**Figure 5B**). The nutrition metabolism included carbohydrate metabolism, amino

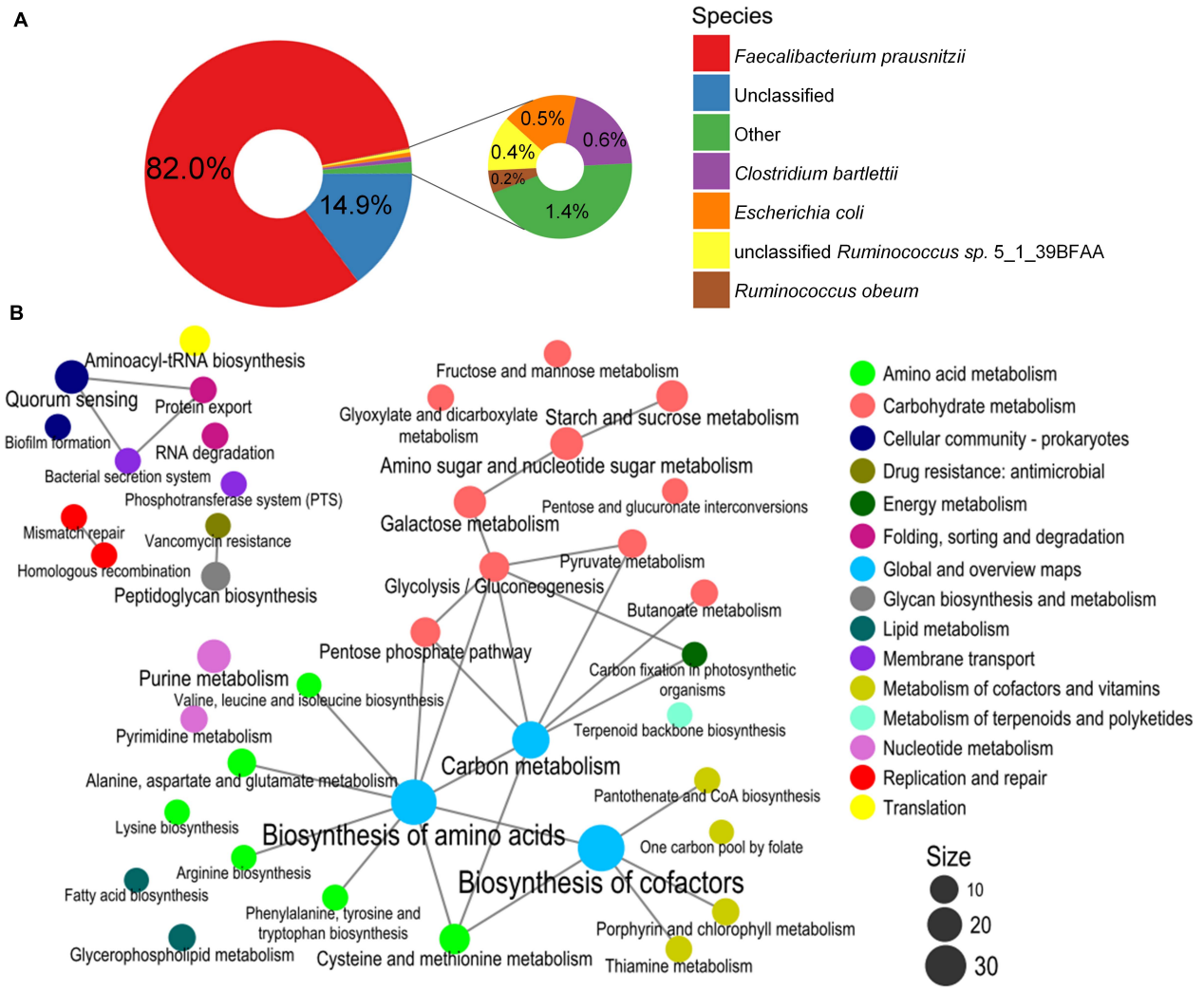

FIGURE 4 | Species composition and enrichment metabolic pathways carrying the BiasSNPs in PWS children. **(A)** Composition of species with BiasSNP in PWS children. Colors represent different species. **(B)** The relationship between the metabolic pathways of BiasSNP in PWS children. The line indicates that the metabolic pathways share the same gene, the dot represents the pathway, the size of the dot represents the number of genes with BiasSNP in the pathway, and the color represents the class of pathway.

acid metabolism, metabolism of cofactors and vitamins, and nucleotide metabolism. The SNPs related to DNA replication and repair may furtherly influence the genetic variation, including base excision repair, homologous recombination, mismatch repair, and nucleotide excision repair. In addition, a number of nonsynonymous BiasSNP existed in translation-related metabolic pathways, such as aminoacyl-tRNA biosynthesis and ribosome. Twenty-six genes with nonsynonymous BiasSNPs in the pathway network of SO children are presented in **Supplementary Table 2**.

DISCUSSION

Our previous study performed a dietary intervention trial on obese children with PWS and SO, and found that the high-fiber diet had improved significantly the physiological indexes of all the obese children and changed the composition and structure of the gut microbiota (Zhang et al., 2015). This study focused on the gut microbial SNP variations that occurred in genes, trying to figure out important genes and functional strains influenced by the intervention.

We found that the remarkable changes in gut microbial SNPs caused by the intervention were related to nutrition metabolism, including carbohydrate metabolism (e.g., gluconeogenesis and pyruvate metabolism), amino acid metabolism, and lipid metabolism in all obese children. This result was not surprising because the SNPs existed densely in strains to adapt to environmental changes. Compared with the normal diet, the WTP diet provides large quantities of whole-grain mix that is rich in starch, soluble and insoluble dietary fiber, protein, and amino acids, but contains a small amount of fat (Xiao et al., 2014). When

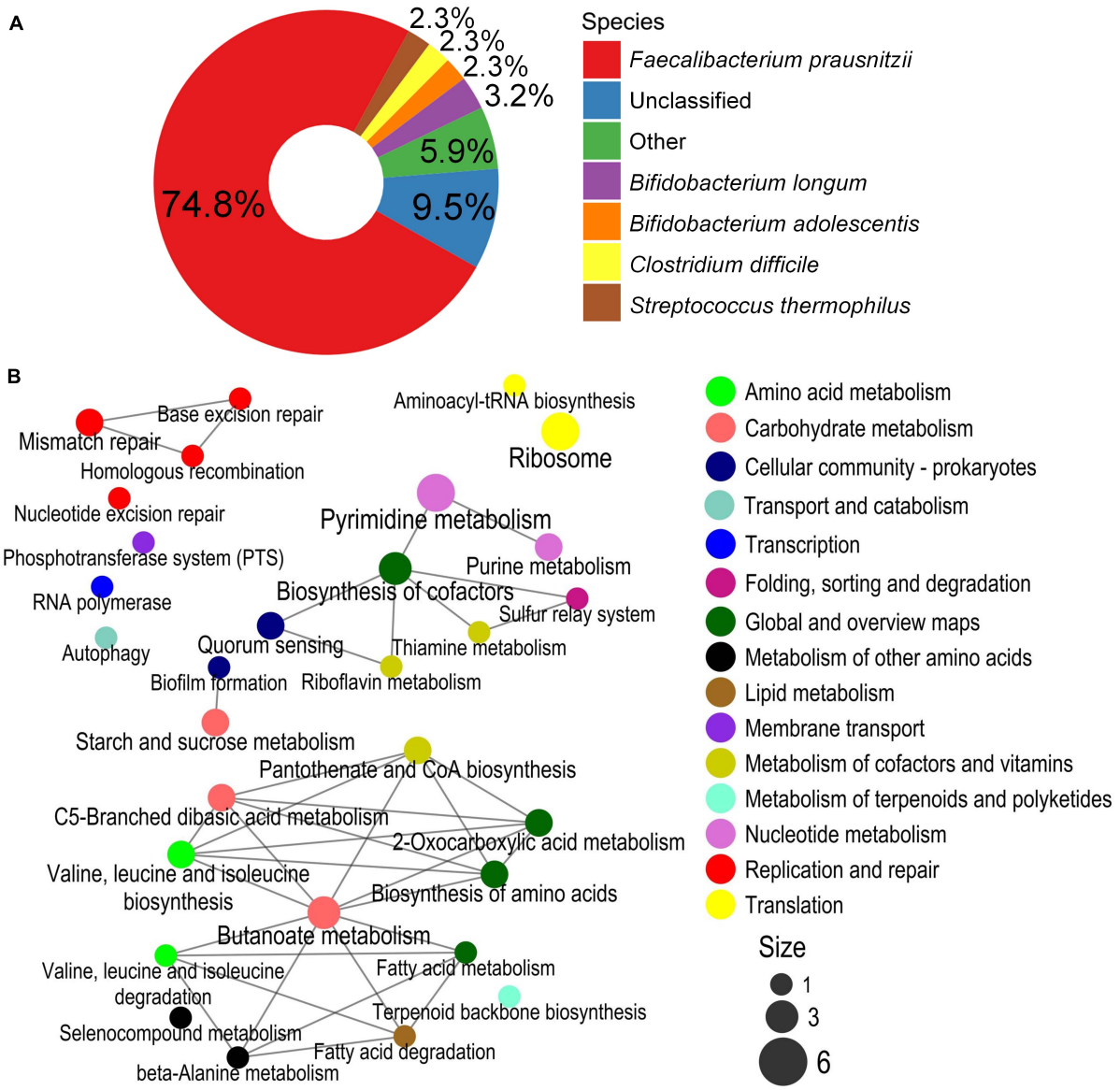

FIGURE 5 | Species composition and enrichment metabolic pathways carrying the BiasSNPs in SO children. **(A)** Composition of species with BiasSNP in PWS children. Colors represent different species. **(B)** The relationship between the metabolic pathways of BiasSNP in PWS children. The line indicates that the metabolic pathways share the same gene, the dot represents the pathway, the size of the dot represents the number of genes with BiasSNP in the pathway, and the color represents the class of pathway.

this excess and/or indigestible nutrition reached the colon, they brought environmental pressures to the microbiota that stayed there. This pressure could facilitate the utilization of indigestible nutrition by causing microbial SNPs and, thus, affecting the functions of the related genes (such as *pyk*, coding the pyruvate kinase). As a result, the metabolic efficiencies of indigestible nutrition substrates would be enhanced to adapt to the shifted environment better. Conversely, as the WTP diet is low in fat, the lower lipid substrate level in the intestinal environment might lead to SNPs in lipid metabolism-relevant genes (such as *fadD*, coding long-chain acyl-CoA synthetase) and, thus, would furtherly reduce the efficiencies of lipid nutrition substrates.

Meanwhile, SNPs also emerged in some pathways related to the adaptability to environmental changes and the virulence of bacteria, such as the two-component system, transport system, secretion system, and drug tolerance. The two-component system is a signal transduction system widely existing in bacteria, which plays an important role in responding to the constantly changing environment by means of protein phosphorylation (Wang et al., 2002; Zuniga et al., 2011). ABC transport system utilizes the energy released by ATP hydrolysis to transport various substrates across membranes, including amino acid, sugar, lipid, polypeptide, alcohol, metal, drug, etc. (Koster, 2001; Hollenstein et al., 2007). Additionally, the ABC transport system

is also involved in some other biological processes, such as RNA translation and DNA repair (Licht and Schneider, 2011). HlyD, a member of the membrane fusion proteins (MFP), links the inner and outer membranes in some way by spanning the periplasm and is necessary for the secretion of repeats in toxin (RTX) hemolytic toxins (Pimenta et al., 1999; Pimenta et al., 2005). RTX is a kind of high-molecular weight protein, heat-resistant, calcium-dependent toxin, secreted by a large class of Gram-negative pathogens, which can lysis various creatural target cells (Lally et al., 1999). Dietary changes brought drastic variations to the intestinal environment and intense evolutionary pressure on the gut microbiota in obese children. Though further validation is needed, our results implied that, in response to this environmental pressure, some gut microbial SNPs that occurred might affect the efficiency and function of metabolic pathways related to environmental adaptation, and might be relevant to the health promotion of the obese children.

Previous studies had observed that *Bifidobacterium* was the selectively promoted genera under the WTP intervention due to their outperforming ability to utilize carbohydrates (Xiao et al., 2014; Zhang et al., 2015; Zhao et al., 2018). Indeed, *Bifidobacterium* became dominant strains responsible for nutrition metabolism after the intervention in both PWS and SO children based on SNP density analysis. *Bifidobacterium* has been demonstrated to have various probiotic effects on the health of the host, involving protection of the intestinal barrier, modulation of the immune response, and effects of antimicrobial, anti-inflammatory, and anti-obesity (Marteau et al., 2001; Heuvelin et al., 2009; Turroni et al., 2014). However, when we turned to BiasSNP analysis, unexpectedly, it was *Faecalibacterium*, instead of *Bifidobacterium*, that had the most nonsynonymous SNPs, suggesting that the intervention mainly affected the functional mutations of *Faecalibacterium*, especially *F. prausnitzii*. *F. prausnitzii* can reduce the synthesis of colonic pro-inflammatory cytokines, induce the secretion of anti-inflammatory cytokines, and inhibit the activation of NF-κB and the production of IL-8 (Sokol et al., 2008; Miquel et al., 2015), and produce butyrate to make protective and anti-inflammatory effects (Ohira et al., 2017). In addition, the track to strains carrying BiasSNPs showed that the dominant strains, *F. prausnitzii* AF32-8AC and *F. prausnitzii* 942/30-2, converted to *F. prausnitzii* SSTS Bg7063 and *F. prausnitzii* JG BgPS064 after the dietary intervention, indicating that dietary intervention probably changed the dominant strains of *F. prausnitzii* by changing the intestinal environment. If the study only focuses on the composition or abundance of the gut microbiota as the mainstream used, the important information about *F. prausnitzii* would be neglected. A previous study of 31 *F. prausnitzii* genomes reported that the functional differences among these strains were mainly concentrated in the metabolism of carbohydrates and amino acids (Fitzgerald et al., 2018). However, we found that the functional differences of *F. prausnitzii* were not only on nutrition metabolism but also in response to environmental changes, such as signal transduction and membrane transport. This additional finding suggested that SNP analysis on gut microbiota could provide more details about the functions and characteristics at the strain level.

Some differences in the gut microbial SNP existed between PWS and SO children in response to the intervention. There were more BiasSNPs between before and after intervention in PWS children than in SO, suggesting that the influence of high-fiber diet on the gut microbial SNP may be greater in PWS than in SO. PWS-specific BiasSNPs were mainly related to nutrition metabolism, protein transport, and environmental adaptation. The phosphotransferase system (PTS) in bacteria can transport carbohydrates into cells by phosphorylation (Deutscher et al., 2007), and also perceive available carbohydrates and intracellular energy, regulate the decomposition of metabolites, and ensure the optimal utilization efficiency of carbohydrates in a complex environment (Lengeler, 1996; Kotrba et al., 2001). N-acetylgalactosamine-specific PTS, which correlated with the nonsynonymous BiasSNPs in PWS, is a common amino-sugar transport system in the gut microbiota, which can regulate and transport acetyl galactosamine (Brinkkotter et al., 2000; Ezquerro-Saenz et al., 2006). Additionally, PWS-specific BiasSNPs were also concentrated in two kinds of proteins translocation systems, general secretory (Sec) pathway and twin-arginine translocation (Tat) system. The Sec pathway is a common and universal protein translocation system, which could integrate synthetic proteins into bacterial cell membranes (Zhou et al., 2014; Tsirigotaki et al., 2017), while the Tat system can transport folded proteins efficiently across the cytoplasmic membranes (Palmer et al., 2010). Moreover, PWS-specific BiasSNPs were also related to spore formation, which is wrapped by a layer of complex macromolecular protein shell under special conditions to resist the hydrolysis of enzyme and protect the active molecules (Setlow, 2003; Kim et al., 2006). These differences in gut microbial SNPs between PWS and SO could not be discovered if only composition information was used, which emphasized the importance of SNP analysis again.

In this work, the identified non-synonymous SNPs were dominantly carried by *F. prausnitzii* strains. Though *F. prausnitzii* were well known for their biodiversity, we could not find functional reports about these SNPs. Future efforts are needed to verify/discern the specific effects of these SNPs on the encoded protein activity, their role on metabolism under high-fiber dietary intervention, and their potential beneficial or detrimental influences on host health. The verification/discernment could be done through combining molecular simulation or experimental design.

CONCLUSION

Our results demonstrated that the high-fiber dietary intervention altered the gut microbial SNP patterns in obese children, and intervened the efficiency and function of metabolic pathways in nutrition metabolism and environmental adaptation. *F. prausnitzii* had been screened out as the dominant strains by changing multiple functional SNPs under the intervention, which had the potential to improve obesity and could be used as a probiotic supplementary in the prevention and treatment of obesity. This bioinformatics study provided evidence for the influence of dietary intervention on gut microbial SNPs,

highlighted the importance of SNP analysis on searching differential genes and functional strains from complexed microbial ecosystem, and gave some enlightenment for obesity or other disease treatment.

DATA AVAILABILITY STATEMENT

The original contributions presented in the study are included in the article/**Supplementary Material**, further inquiries can be directed to the corresponding author/s.

ETHICS STATEMENT

The studies involving human participants were reviewed and approved by the Chinese Clinical Trial Registry. Written informed consent to participate in this study was provided by the participants' legal guardian/next of kin.

AUTHOR CONTRIBUTIONS

MZ, LZ, and HL contributed to conception and design of the study. HL performed the statistical analysis and wrote the first draft of the manuscript. All authors contributed to the manuscript revision and approved the submitted version.

ACKNOWLEDGMENTS

We would like to thank the members of the MOLECO Lab at Shanghai Jiao Tong University for comments and suggestions on the analysis.

SUPPLEMENTARY MATERIAL

The Supplementary Material for this article can be found online at: https://www.frontiersin.org/articles/10.3389/fmicb.2021.683714/full#supplementary-material

REFERENCES

Baothman, O. A., Zamzami, M. A., Taher, I., Abubaker, J., and Abu-Farha, M. (2016). The role of gut microbiota in the development of obesity and diabetes. *Lipids Health Dis.* 15:108. doi: 10.1186/s12944-016-0278-4

Brinkkotter, A., Kloss, H., Alpert, C., and Lengeler, J. W. (2000). Pathways for the utilization of N-acetyl-galactosamine and galactosamine in *Escherichia coli*. *Mol. Microbiol.* 37, 125–135. doi: 10.1046/j.1365-2958.2000.01969.x

Chen, Y. W., Li, Z. C., Hu, S. F., Zhang, J., Wu, J. Q., Shao, N. S., et al. (2017). Gut metagenomes of type 2 diabetic patients have characteristic single-nucleotide polymorphism distribution in *Bacteroides* coprocola. *Microbiome* 5:15. doi: 10.1186/s40168-017-0232-3

Deutscher, J., Francke, C., and Postma, P. W. (2007). How phosphotransferase system-related protein phosphorylation regulates carbohydrate metabolism in bacteria. *Microbiol. Mol. Biol. Rev.* 70, 939–1031. doi: 10.1128/Mmbr.00024-06

Dodt, M., Roehr, J. T., Ahmed, R., and Dieterich, C. (2012). FLEXBAR-Flexible barcode and adapter processing for next-generation sequencing platforms. *Biology (Basel)* 1, 895–905. doi: 10.3390/biology1030895

Ezquerro-Saenz, C., Ferrero, M. A., Revilla-Nuin, B., Lopez Velasco, F. F., Martinez-Blanco, H., and Rodriguez-Aparicio, L. B. (2006). Transport of N-acetyl-D-galactosamine in *Escherichia coli* K92: effect on acetyl-amino sugar metabolism and polysialic acid production. *Biochimie* 88, 95–102. doi: 10.1016/j.biochi.2005.06.011

Fitzgerald, C. B., Shkoporov, A. N., Sutton, T. D. S., Chaplin, A. V., Velayudhan, V., Ross, R. P., et al. (2018). Comparative analysis of *Faecalibacterium prausnitzii* genomes shows a high level of genome plasticity and warrants separation into new species-level taxa. *BMC Genomics* 19:931. doi: 10.1186/s12864-018-5313-6

Flint, H. J. (2011). Obesity and the gut microbiota. *J. Clin. Gastroenterol.* 45 Suppl, S128–S132. doi: 10.1097/MCG.0b013e31821f44c4

Galloway-Peña, J., Roh, J. H., Latorre, M., Qin, X., and Murray, B. E. (2012). Genomic and SNP analyses demonstrate a distant separation of the hospital and community-associated clades of *Enterococcus faecium*. *PLoS One* 7:e30187. doi: 10.1371/journal.pone.0030187

Goldsmith, J. R., and Sartor, R. B. (2014). The role of diet on intestinal microbiota metabolism: downstream impacts on host immune function and health, and therapeutic implications. *J. Gastroenterol.* 49, 785–798. doi: 10.1007/s00535-014-0953-z

Gubler, M., Jetten, M., Lee, S. H., and Sinskey, A. J. (1994). Cloning of the pyruvate kinase gene (pyk) of *Corynebacterium glutamicum* and site-specific inactivation of pyk in a lysine-producing *Corynebacterium lactofermentum* strain. *Appl. Environ. Microbiol.* 60, 2494–2500. doi: 10.1128/aem.60.7.2494-2500.1994

Haraksingh, R. R., and Snyder, M. P. (2013). Impacts of variation in the human genome on gene regulation. *J. Mol. Biol.* 425, 3970–3977. doi: 10.1016/j.jmb.2013.07.015

Heuvelin, E., Lebreton, C., Grangette, C., Pot, B., Cerf-Bensussan, N., and Heyman, M. (2009). Mechanisms involved in alleviation of intestinal inflammation by *Bifidobacterium breve* soluble factors. *PLoS One* 4:e5184. doi: 10.1371/journal.pone.0005184

Hofreiter, M., Paijmans, J. L., Goodchild, H., Speller, C. F., Barlow, A., Fortes, G. G., et al. (2015). The future of ancient DNA: technical advances and conceptual shifts. *Bioessays* 37, 284–293. doi: 10.1002/bies.201400160

Hollenstein, K., Dawson, R. J., and Locher, K. P. (2007). Structure and mechanism of ABC transporter proteins. *Curr. Opin. Struct. Biol.* 17, 412–418. doi: 10.1016/j.sbi.2007.07.003

Hu, Y., Feng, Y., Wu, J., Liu, F., Zhang, Z., Hao, Y., et al. (2019). The gut microbiome signatures discriminate healthy from pulmonary tuberculosis patients. *Front. Cell Infect. Microbiol.* 9:90. doi: 10.3389/fcimb.2019.00090

Hu, Y., Yang, X., Qin, J., Lu, N., Cheng, G., Wu, N., et al. (2013). Metagenome-wide analysis of antibiotic resistance genes in a large cohort of human gut microbiota. *Nat. Commun.* 4:2151. doi: 10.1038/ncomms3151

Kim, H., Hahn, M., Grabowski, P., McPherson, D. C., Otte, M. M., Wang, R., et al. (2006). The *Bacillus subtilis* spore coat protein interaction network. *Mol. Microbiol.* 59, 487–502. doi: 10.1111/j.1365-2958.2005.04968.x

Koster, W. (2001). ABC transporter-mediated uptake of iron, siderophores, heme and vitamin B12. *Res. Microbiol.* 152, 291–301. doi: 10.1016/s0923-2508(01)01200-1

Kotrba, P., Inui, M., and Yukawa, H. (2001). Bacterial phosphotransferase system (PTS) in carbohydrate uptake and control of carbon metabolism. *J. Biosci. Bioeng.* 92, 502–517. doi: 10.1263/jbb.92.502

Lally, E. T., Hill, R. B., Kieba, I. R., and Korostoff, J. (1999). The interaction between RTX toxins and target cells. *Trends Microbiol.* 7, 356–361. doi: 10.1016/s0966-842x(99)01530-9

Langmead, B., and Salzberg, S. L. (2012). Fast gapped-read alignment with Bowtie 2. *Nat. Methods* 9, 357–359. doi: 10.1038/nmeth.1923

Lengeler, J. W. (1996). "The Phosphoenolpyruvate-Dependent Carbohydrate: Phosphotransferase System (PTS) and Control of Carbon Source Utilization," in *Regulation of Gene Expression in Escherichia coli*, eds E. C. C. Lin, and A. Simon Lynch (Boston, MA: Springer US), 231–254.

Leonard, S. R., Mammel, M. K., Lacher, D. W., and Elkins, C. A. (2016). Strain-level discrimination of Shiga toxin-producing *Escherichia coli* in spinach using metagenomic sequencing. *PLoS One* 11:e0167870. doi: 10.1371/journal.pone.0167870

Li, H. (2011). A statistical framework for SNP calling, mutation discovery, association mapping and population genetical parameter estimation from sequencing data. *Bioinformatics* 27, 2987–2993. doi: 10.1093/bioinformatics/btr509

Li, H., and Durbin, R. (2009). Fast and accurate short read alignment with Burrows-Wheeler transform. *Bioinformatics* 25, 1754–1760. doi: 10.1093/bioinformatics/btp324

Li, H., Handsaker, B., Wysoker, A., Fennell, T., Ruan, J., Homer, N., et al. (2009). The sequence alignment/map format and SAMtools. *Bioinformatics* 25, 2078–2079. doi: 10.1093/bioinformatics/btp352

Li, J., Jia, H., Cai, X., Zhong, H., Feng, Q., Sunagawa, S., et al. (2014). An integrated catalog of reference genes in the human gut microbiome. *Nat. Biotechnol.* 32, 834–841. doi: 10.1038/nbt.2942

Licht, A., and Schneider, E. (2011). ATP binding cassette systems: structures, mechanisms, and functions. *Open Life Sci.* 6, 785–801.

Marteau, P. R., de Vrese, M., Cellier, C. J., and Schrezenmeir, J. (2001). Protection from gastrointestinal diseases with the use of probiotics. *Am. J. Clin. Nutr.* 73(2 Suppl), 430S–436S. doi: 10.1093/ajcn/73.2.430s

Miquel, S., Leclerc, M., Martin, R., Chain, F., Lenoir, M., Raguideau, S., et al. (2015). Identification of metabolic signatures linked to anti-inflammatory effects of *Faecalibacterium prausnitzii*. *mBio* 6:e00300-15. doi: 10.1128/mBio.00300-15

Nayfach, S., Rodriguez-Mueller, B., Garud, N., and Pollard, K. S. (2016). An integrated metagenomics pipeline for strain profiling reveals novel patterns of bacterial transmission and biogeography. *Genome Res.* 26, 1612–1625. doi: 10.1101/gr.201863.115

Ohira, H., Tsutsui, W., and Fujioka, Y. (2017). Are short chain fatty acids in gut microbiota defensive players for inflammation and atherosclerosis? *J. Atheroscler. Thromb.* 24, 660–672. doi: 10.5551/jat.RV17006

Palmer, T., Sargent, F., and Berks, B. C. (2010). The Tat protein export pathway. *EcoSal Plus* 4, 1–35. doi: 10.1128/ecosalplus.4.3.2

Pech-Canul, A. C., Rivera-Hernandez, G., Nogales, J., Geiger, O., Soto, M. J., and Lopez-Lara, I. M. (2020). Role of *Sinorhizobium meliloti* and *Escherichia coli* long-chain acyl-CoA synthetase FadD in long-term survival. *Microorganisms* 8:470. doi: 10.3390/microorganisms8040470

Pimenta, A. L., Racher, K., Jamieson, L., Blight, M. A., and Holland, I. B. (2005). Mutations in HlyD, part of the type 1 translocator for hemolysin secretion, affect the folding of the secreted toxin. *J. Bacteriol.* 187, 7471–7480. doi: 10.1128/jb.187.21.7471-7480.2005

Pimenta, A. L., Young, J., Holland, I. B., and Blight, M. A. (1999). Antibody analysis of the localisation, expression and stability of HlyD, the MFP component of the *E. coli* haemolysin translocator. *Mol. Gen. Genet.* 261, 122–132. doi: 10.1007/s004380050949

Schmieder, R., and Edwards, R. (2011). Quality control and preprocessing of metagenomic datasets. *Bioinformatics* 27, 863–864. doi: 10.1093/bioinformatics/btr026

Setlow, P. (2003). Spore germination. *Curr. Opin. Microbiol.* 6, 550–556. doi: 10.1016/j.mib.2003.10.001

Shannon, P., Markiel, A., Ozier, O., Baliga, N. S., Wang, J. T., Ramage, D., et al. (2003). Cytoscape: a software environment for integrated models of biomolecular interaction networks. *Genome Res.* 13, 2498–2504. doi: 10.1101/gr.1239303

Shen, T. D. (2017). Diet and gut microbiota in health and disease. *Nestle Nutr. Inst. Workshop Ser.* 88, 117–126. doi: 10.1159/000455220

Sokol, H., Pigneur, B., Watterlot, L., Lakhdari, O., Bermudez-Humaran, L. G., Gratadoux, J. J., et al. (2008). *Faecalibacterium prausnitzii* is an anti-inflammatory commensal bacterium identified by gut microbiota analysis of Crohn disease patients. *Proc. Natl. Acad. Sci. U.S.A.* 105, 16731–16736. doi: 10.1073/pnas.0804812105

Stamatakis, A. (2014). RAxML version 8: a tool for phylogenetic analysis and post-analysis of large phylogenies. *Bioinformatics* 30, 1312–1313. doi: 10.1093/bioinformatics/btu033

Tennessen, J. A. (2008). Positive selection drives a correlation between non-synonymous/synonymous divergence and functional divergence. *Bioinformatics* 24, 1421–1425. doi: 10.1093/bioinformatics/btn205

Truong, D. T., Tett, A., Pasolli, E., Huttenhower, C., and Segata, N. (2017). Microbial strain-level population structure and genetic diversity from metagenomes. *Genome Res.* 27, 626–638. doi: 10.1101/gr.216242.116

Tsirigotaki, A., De Geyter, J., Sostaric, N., Economou, A., and Karamanou, S. (2017). Protein export through the bacterial Sec pathway. *Nat. Rev. Microbiol.* 15, 21–36. doi: 10.1038/nrmicro.2016.161

Turnbaugh, P. J., Ley, R. E., Mahowald, M. A., Magrini, V., Mardis, E. R., and Gordon, J. I. (2006). An obesity-associated gut microbiome with increased capacity for energy harvest. *Nature* 444, 1027–1031. doi: 10.1038/nature05414

Turroni, F., Ventura, M., Buttó, L. F., Duranti, S., O'Toole, P. W., Motherway, M. O., et al. (2014). Molecular dialogue between the human gut microbiota and the host: a *Lactobacillus* and *Bifidobacterium* perspective. *Cell. Mol. Life Sci.* 71, 183–203. doi: 10.1007/s00018-013-1318-0

Wang, L., Sun, Y. P., Chen, W. L., Li, J. H., and Zhang, C. C. (2002). Genomic analysis of protein kinases, protein phosphatases and two-component regulatory systems of the cyanobacterium *Anabaena* sp. strain PCC 7120. *FEMS Microbiol. Lett.* 217, 155–165. doi: 10.1111/j.1574-6968.2002.tb11469.x

Xiao, S., Fei, N., Pang, X., Shen, J., Wang, L., Zhang, B., et al. (2014). A gut microbiota-targeted dietary intervention for amelioration of chronic inflammation underlying metabolic syndrome. *FEMS Microbiol. Ecol.* 87, 357–367. doi: 10.1111/1574-6941.12228

Xie, H., Guo, R., Zhong, H., Feng, Q., Lan, Z., Qin, B., et al. (2016). Shotgun metagenomics of 250 adult twins reveals genetic and environmental impacts on the gut microbiome. *Cell Syst.* 3, 572–584.e3. doi: 10.1016/j.cels.2016.10.004

Yu, G., Wang, L. G., Han, Y., and He, Q. Y. (2012). clusterProfiler: an R package for comparing biological themes among gene clusters. *OMICS* 16, 284–287. doi: 10.1089/omi.2011.0118

Zhang, C., Yin, A., Li, H., Wang, R., Wu, G., Shen, J., et al. (2015). Dietary modulation of gut microbiota contributes to alleviation of both genetic and simple obesity in children. *EBioMedicine* 2, 968–984. doi: 10.1016/j.ebiom.2015.07.007

Zhao, L., Zhang, F., Ding, X., Wu, G., Lam, Y. Y., Wang, X., et al. (2018). Gut bacteria selectively promoted by dietary fibers alleviate type 2 diabetes. *Science* 359, 1151–1156. doi: 10.1126/science.aao5774

Zhou, Z., Li, Y., Sun, N., Sun, Z., Lv, L., Wang, Y., et al. (2014). Function and evolution of two forms of SecDF homologs in *Streptomyces coelicolor*. *PLoS One* 9:e105237. doi: 10.1371/journal.pone.0105237

Zou, D., Pei, J., Lan, J., Sang, H., Chen, H., Yuan, H., et al. (2020). A SNP of bacterial blc disturbs gut lysophospholipid homeostasis and induces inflammation through epithelial barrier disruption. *EBioMedicine* 52:102652. doi: 10.1016/j.ebiom.2020.102652

Zuniga, M., Gomez-Escoin, C. L., and Gonzalez-Candelas, F. (2011). Evolutionary history of the OmpR/IIIA family of signal transduction two component systems in *Lactobacillaceae* and *Leuconostocaceae*. *BMC Evol. Biol.* 11:34. doi: 10.1186/1471-2148-11-34

Conflict of Interest: The authors declare that the research was conducted in the absence of any commercial or financial relationships that could be construed as a potential conflict of interest.

frontiers in Microbiology

ORIGINAL RESEARCH
published: 04 June 2021
doi: 10.3389/fmicb.2021.684233

Maternal Antibiotic Treatment Disrupts the Intestinal Microbiota and Intestinal Development in Neonatal Mice

Chung-Ming Chen[1,2], Hsiu-Chu Chou[3] and Yu-Chen S. H. Yang[4]*

[1]Department of Pediatrics, Taipei Medical University Hospital, Taipei, Taiwan, [2]Department of Pediatrics, School of Medicine, College of Medicine, Taipei Medical University, Taipei, Taiwan, [3]Department of Anatomy and Cell Biology, School of Medicine, College of Medicine, Taipei Medical University, Taipei, Taiwan, [4]Joint Biobank, Office of Human Research, Taipei Medical University, Taipei, Taiwan

OPEN ACCESS

Edited by:
Teresa Nogueira, Instituto Nacional Investigaciao Agraria e Veterinaria (INIAV), Portugal

Reviewed by:
Paulo Durao, Gulbenkian Institute of Science (IGC), Portugal
Axel Kornerup Hansen, University of Copenhagen, Denmark
Richard Agans, Independent Researcher, Dayton, OH, United States

***Correspondence:**
Chung-Ming Chen
cmchen@tmu.edu.tw

Specialty section:
This article was submitted to Microbial Symbioses, a section of the journal Frontiers in Microbiology

Received: *23 March 2021*
Accepted: *04 May 2021*
Published: *04 June 2021*

Citation:
Chen C-M, Chou H-C and Yang Y-CSH (2021) Maternal Antibiotic Treatment Disrupts the Intestinal Microbiota and Intestinal Development in Neonatal Mice. Front. Microbiol. 12:684233. doi: 10.3389/fmicb.2021.684233

Maternal antibiotic treatment (MAT) during prenatal and intrapartum periods alters the bacterial composition and diversity of the intestinal microbiota of the offspring. The effect of MAT during pregnancy on the intestinal microbiota and its relationship with intestinal development remain unknown. This study investigated the effects of MAT during pregnancy on intestinal microbiota, injury and inflammation, vascularization, cellular proliferation, and the intestinal barrier in neonatal mice. At timed intervals, we fed pregnant C57BL/6N mice sterile drinking water containing antibiotics (ampicillin, gentamicin, and vancomycin; all 1 mg/ml) from gestational day 15 to delivery. The control dams were fed sterile drinking water. Antibiotic administration was halted immediately after birth. On postnatal day 7, the intestinal microbiota was sampled from the lower gastrointestinal tract and the ileum was harvested for histology, Western blot, and cytokines analyses. MAT significantly reduced the relative abundance of *Bacteroidetes* and *Firmicutes* and significantly increased the relative abundance of *Proteobacteria* in the intestine compared with their abundances in the control group. MAT also significantly increased intestinal injury score and cytokine levels, reduced the number of intestinal goblet cells and proliferating cell nuclear antigen-positive cells, and reduced the expressions of vascular endothelial growth factor and tight junction proteins. Therefore, we proposed that maternal antibiotic exposure during pregnancy disrupts the intestinal microbiota and intestinal development in neonatal mice.

Keywords: microbiota, intestine, tight junction, proliferating cell nuclear antigen, vascular endothelial growth factor

INTRODUCTION

Approximately 25% of women receive a course of antibiotics during pregnancy, and antibiotics account for 80% of medications used by pregnant women (Broe et al., 2014). They receive antibiotics to treat various conditions, such as bacterial vaginosis, urinary tract infections, and upper respiratory tract infections (Bookstaver et al., 2015). Although antibiotics are necessary for treating infections during pregnancy, they have short- and long-term effects. Maternal antibiotic exposure during

pregnancy has been reported to be associated with lower rates of necrotizing enterocolitis and death in preterm infants and higher risks of asthma, atopic dermatitis, and hospitalization for infections in children (Blaser and Bello, 2014; Loewen et al., 2018; Miller et al., 2018; Reed et al., 2018; Alhasan et al., 2020).

The microbiota regulates inflammatory, infectious, and metabolic diseases and also causes, prevents, and sustains human diseases (Belkaid and Hand, 2014; Palm et al., 2015). Evidence suggests that host–microbe interactions may extend beyond the local environment to peripheral tissues (Marsland et al., 2015). Preclinical and human studies have demonstrated that maternal antibiotic administration during prenatal and intrapartum periods alters the bacterial composition and diversity of the offspring's intestinal microbiota (Gonzalez-Perez et al., 2016; Yoshimoto et al., 2018; Dierikx et al., 2020; Zimmermann and Curtis, 2020). Microbiota profiles play a crucial role in intestinal barrier function and intestinal maturation in germ-free mice and human infants (Reinhardt et al., 2012; Sommer and Bäckhed, 2013; Kelly et al., 2015; Selma-Royo et al., 2020). However, the effects of maternal antibiotic treatment (MAT) during pregnancy on intestinal development and the relationship among MAT, the intestinal microbiota, and intestinal injury in neonates remain unknown. This study investigates the effects of MAT during pregnancy on intestinal microbiota and intestinal development in neonatal mice.

MATERIALS AND METHODS

Animals and Experimental Protocol

Our study was approved by the Institutional Animal Care and Use Committee of Taipei Medical University (license number LAC-2019-0290) and according to an Association for Assessment and Accreditation of Laboratory Animal Care approved protocol. Six time-dated pregnant C57BL/6N mice were housed in individual metal cages with hardwood chip bedding on a 12-h light–dark cycle and free access to laboratory food of a standard chow diet (Rodent Laboratory Chow no. 5001, Ralston Purina Company, St. Louis, MO, United States) and water. The facility temperature was maintained at 20–23°C, and the relative humidity was between 36 and 57%; at the same time, minimal environmental stress and basic environmental enrichment were carried out in strict accordance with the recommendations with our institutional guidelines. The mice were allowed to deliver vaginally at term. At timed intervals, two mice in the MAT group were fed sterile drinking water containing antibiotics (ampicillin, gentamicin, and vancomycin; 1 mg/ml) often prescribed to pregnant women and human newborns, starting from gestational day 15 to delivery (Gray et al., 2017). Two control and two antibiotic-treated dams gave birth to 9 and 14 pups. The diet of the mothers was continued throughout the nursing time until the analysis of the offspring. Each mother was housed with her offspring in a single cage, and all neonates (both male and female) were breastfed throughout the study. The control dams were fed sterile drinking water. Antibiotic administration was halted immediately after birth. The current study was designed and reported in adherence to the ARRIVE Essential 10: Compliance Questionnaire.

Mouse Tissue Collection

The animals were euthanized with an overdose of isoflurane on postnatal day 7. The abdomen was opened through a midline incision, 2 cm of the lower intestine from the anus to the colon was harvested, and the microbiota was sampled using a culture-independent approach (community sequencing of the 16S rRNA gene using the Illumina MiSeq). The instruments were rinsed with ethanol and flamed before each harvest, and the tissues were excised, placed in tubes containing 1 ml of sterile water, and homogenized mechanically using the Tissue-Tearor (BioSpec Products, Bartlesville, OK, United States). The tissue homogenizer was cleaned and rinsed with ethanol and water after each sample was obtained. Water control samples from homogenization that had been exposed to clean instruments were sequenced as procedural controls. The last 2 cm of the terminal ileum was excised, fixed with formalin, and embedded in paraffin for histological evaluation. A part of the ileum was flushed with saline to remove residual fecal matter and immediately fresh-frozen in liquid nitrogen for protein isolation.

16S rDNA Gene Sequencing and Next-Generation Sequencing Analysis

The protocol followed in this study for 16S rDNA analysis is described by Yang et al. (2020). In brief, 16S rDNA was purified from fecal samples with a QIAamp Fast DNA Stool Mini Kit (QIAGEN, Germany) and from lung tissues with a QIAamp DNA Microbiome Kit (QIAGEN, Germany). 16S rRNA gene amplification and library construction were performed according to the protocols provided by Illumina.[1] V3-V4 region of bacterial 16S rRNA genes was amplified with the universal bacterial primers 341F (5'-CCTACGGGNGGCWGCAG-3') and 805R (5'-GACTACHVGGGTATCTAATCC-3') containing Illumina overhang adapter sequences in the forward (5'-TCGTCGGCAGCGTCAGATGTGTATAAGAGACAG-3') and reverse (5'-GTCTCGTGGGCTCGGAGATGTGTATAAGAGACAG-3') primers using a limited cycle PCR. Illumina sequencing adapters and dual-index barcodes were added to the amplicon target using a Nextera XT Index kit. Quantification and quality of the libraries were checked using a QSep100 Analyzer (BiOptic Inc., Taiwan). Finally, the libraries were normalized and pooled in an equimolar ratio and sequenced with an Illumina MiSeq sequencer. The code of the 16S analysis was supported by Dr. IH Lin, and the information could be found at the Web site https://github.com/ycl6/16S-rDNA-V3-V4. The gene-specific sequences used in this protocol target the 16S V3 and V4 regions and were removed from the demultiplexed, paired reads using Cutadapt (v 1.12). The filtered reads were processed in the R environment (v 3.6.1) using R package DADA2 (v 1.14.1) following the procedure described by Callahan et al. (2016). Briefly, the forward and reversed reads were filtered and trimmed based on the read quality score and read length. Dereplication was then performed to merge identical reads; then, reads were subjected to the denoise DADA2 algorithm which alternate between error-rate estimation and sample composition inference until they

[1]https://support.illumina.com/downloads/16S_metagenomic_sequencing_library_preparation.html

converge on a jointly consistent solution. Finally, the paired reads were merged that required a minimal of 20 bp overlap and chimeras were subsequently removed. Taxonomy assignment was performed using the SILVA database (v 138) as a reference, with minimum bootstrap confidence of 80. Multiple sequence alignment of the SVs was performed using DECIPHER (v 2.14.0), and a phylogenetic tree was constructed from the alignment using phangorn, v 2.5.5 (Schliep, 2011; Quast et al., 2013). The count table, taxonomy assignment results, and phylogenetic tree were consolidated into a phyloseq object, community analysis, and Bray–Curtis distances were performed using phyloseq (v 1.30.0; McMurdie and Holmes, 2013). The alpha diversity indices were calculated using the estimate_richness function of the phyloseq package. The adonis and betadisper functions from the vegan package (v 2.5.6) were used for statistical analysis of the dissimilarity of composition between groups and homogeneity of dispersion, respectively. The enrichment analysis between groups was analysed using the linear discriminant analysis (LDA) effect size (LEfSe) method with Wilcoxon-Mann-Whitney test (at $\alpha = 0.05$) and logarithmic LDA score more than 2 (Segata et al., 2011). Sequence reads were input into the European Nucleotide Archive under the accession number PRJEB43913.

Histology

The ileum was separated into 5-μm sections, stained with hematoxylin and eosin, and examined through light microscopy for evaluation of intestinal morphology. The intestinal mucosal injury was scored on a scale of 0–5, where 0 = normal mucosal villi, 1 = subepithelial space at the villus tips and frequent capillary congestion, 2 = extension of the subepithelial space with the moderate lifting of the epithelial layer from the lamina propria, 3 = massive epithelial lifting down the sides of the villi with occasionally denuded villi tips, 4 = denuded villi with dilation of the lamina propria and capillaries, and 5 = disintegration of the lamina propria, hemorrhage, and ulceration (Chiu et al., 1970). The sections for goblet cell quantification were stained with Alcian blue staining, and the number of goblet cells per 100 epithelial cells was counted (Elgin et al., 2019).

Immunohistochemistry

After routine deparaffinization, the slides were immersed in a 0.01 mol/L sodium citrate buffer (pH 6.0) for heat-induced epitope retrieval. To block endogenous peroxidase activity and nonspecific antibody binding, the sections were preincubated for 1 h at room temperature in 0.1 mol/L phosphate-buffered saline containing 10% normal goat serum and 0.3% H_2O_2. All sections were incubated with the following primary antibodies for 20 h at 4°C: mouse monoclonal antioccludin, rat monoclonal anti-ZO-1 (both antioccludin and anti-ZO-1 were 1:20 diluted; Santa Cruz Biotechnology Inc., CA, United States), rabbit monoclonal anti-proliferating cell nuclear antigen (anti-PCNA; 1:100; Abcam, Cambridge, MA, United States), mouse monoclonal anti-vascular endothelial growth factor (anti-VEGF) and anti-CD68, and rat monoclonal anti-CD45R (all three antibodies were diluted at a 1:50 ratio; Santa Cruz Biotechnology). The sections were then treated for 1 h at 37°C with biotinylated goat anti-mouse IgG, goat anti-rat IgG, or goat anti-rabbit IgG (1:200; Jackson ImmunoResearch Laboratories Inc., PA, United States) before undergoing a reaction with reagents from an avidin–biotin complex kit (Vector, CA, United States). A diaminobenzidine substrate kit (Vector, CA, United States) was used to visualize the brown reaction products in accordance with the manufacturer's instructions. All immunostained sections were viewed and photographed using an Olympus BX43 microscope. The quantification method for PCNA-positive cells and CD45- and CD68-positive stained cells was modified from Şensoy and Öznurlu (2019), the cells were counted in a total of 100 crypt cells, and the results were recorded as the percentage (%) of positive cells.

Intestinal Cytokine Levels

Intestinal tissues were homogenized in 1 ml of ice-cold lysis buffer containing 1% Nonidet P-40, 0.1% sodium dodecyl sulfate, 0.01 m deoxycholic acid, and a complete protease cocktail inhibitor. Cell extracts were centrifuged, and the levels of interleukin (IL)-1β and IL-6 in supernatants were measured with an enzyme-linked immunosorbent assay kit (Cloud-Clone Corp., Houston, TX, United States).

Statistical Analysis

All data are presented as the mean ± SD. A test for normality of variances was conducted using the Shapiro–Wilk test. Normally distributed data were analyzed using Student's *t*-test. Non-normally distributed data were analyzed using the Mann–Whitney *U* test. The Kaplan–Meier method was used to determine the survival rate, and a log-rank test was used to compare groups. Differences were considered statistically significant at $p < 0.05$.

RESULTS

Total Intestinal Commensal Bacteria at Birth, and Survival Rate and Body Weight on Postnatal Day 7

Maternal antibiotic treatment significantly reduced the number of commensal bacteria in newborn mice compared with control newborns ($p < 0.05$; **Figure 1A**). Three control and three antibiotic-treated dams gave birth to 16 and 19 pups, respectively. At birth, seven mice from the control group and five mice from the MAT group were killed and their lower intestinal tract was used to determine the total bacterial load, which was quantified using qPCR with universal bacterial primers (forward: 5'-AAACTCAAAKGAATTGACGG-3'; reverse: 5'-CTCACRRCACGAGCTGA-3'). The rest nine mice born to the control dams survived (**Figure 1B**). Three mice and one mouse born to the antibiotic-treated dams died, on postnatal days 5 and 6, respectively. The mice born to control and antibiotic-treated dams had comparable survival rates. The mice born to the antibiotic-treated dams had significantly lower body weights at birth and on postnatal day 7 than did the mice born to the control dams ($p < 0.001$; **Figures 1C,D**).

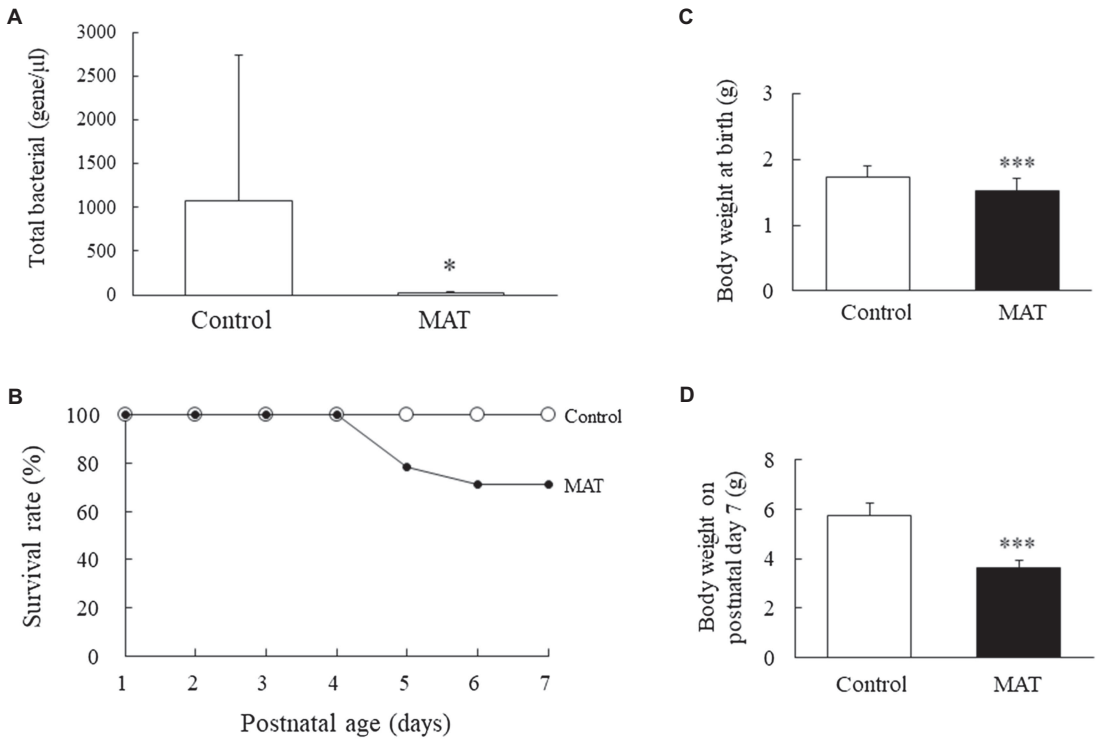

FIGURE 1 | Effects of MAT on **(A)** total intestinal commensal bacteria at birth, **(B)** survival rate, **(C)** body weight at birth, and **(D)** body weight on postnatal day 7. MAT significantly reduced the number of commensal bacteria in newborn mice compared with that in the control newborns. The survival rates were comparable between the mice born to control and antibiotic-treated dams. The mice born to the antibiotic-treated dams exhibited significantly lower body weights at birth and on postnatal day 7 than that of the mice born to the control dams. $^{*}p < 0.05$; $^{***}p < 0.001$. MAT, maternal antibiotic treatment.

MAT Altered the Intestinal Microbiota Composition

We analyzed the taxonomic community structure of the intestinal microbiome on postnatal day 7 to determine its response to MAT (**Figure 2A**). At the phylum level, the intestinal microbiome in the control and MAT groups contained four major bacterial phyla (%): *Actinobacteria* (2.5 ± 3.1 and 1.3 ± 1.3, respectively), *Bacteroidetes* (37.3 ± 8.2 and 29.2 ± 8.3, respectively), *Firmicutes* (45.9 ± 4.7 and 39.2 ± 3.0, respectively), and *Proteobacteria* (11.8 ± 7.5 and 27.8 ± 10.8, respectively). The first three phyla accounted for >95% of the sequences in the two groups. MAT significantly reduced the relative abundance of *Bacteroidetes* ($p < 0.05$) and *Firmicutes* ($p < 0.01$) and significantly increased the relative abundance of *Proteobacteria* ($p < 0.01$) in the intestine compared with the control group. Although the intestine microbiota composition was distinct between the control and MAT groups, MAT group exhibited lower Shannon diversity and Simpson diversity and the differences were not statistically significant ($p = 0.079$ and $p = 0.11$, respectively; **Figure 2B**). Nonmetric multidimensional scaling revealed that the intestinal microbiome in the control group was significantly different from that in the MAT group ($p < 0.000999$; **Figure 2C**). To identify microbial taxa affected by MAT, linear discriminant analysis effect size (LEfSe) analysis was performed, which revealed significant differences in relative bacterial abundance at the family level (**Figure 2D**).

MAT Induced the Intestinal Injury and Reduced Tight Junction Protein Expression

Representative immunohistochemistry and Western blotting results for occludin and ZO-1 are presented in **Figure 3**. The mice born to the control dams exhibited a normal intestinal wall configuration, a well-defined striated border at the luminal surface, and prominent goblet cells in the epithelium (**Figure 3A**). Those born to antibiotic-treated dams exhibited fewer goblet cells in the epithelium, dilated capillaries and lacteal ducts in the lamina propria of the villi, separated lamina propria in the basal portion of the mucosa from the submucosa, and a significantly (5.5-fold) higher intestinal injury score compared with the mice born to the control dams ($p < 0.05$; **Figure 3B**). The immunoreactivity of ZO-1 and occludin was observed on the cell membrane between adjacent intestinal epithelial cells (**Figure 3A**). We observed an intact construct of ZO-1 and occludin staining in the mice born to the control dams. The mice born to the antibiotic-treated dams exhibited disrupted ZO-1 and occludin immunohistochemistry between adjacent enterocytes and significantly (0.4-fold) lower ZO-1 and occludin protein

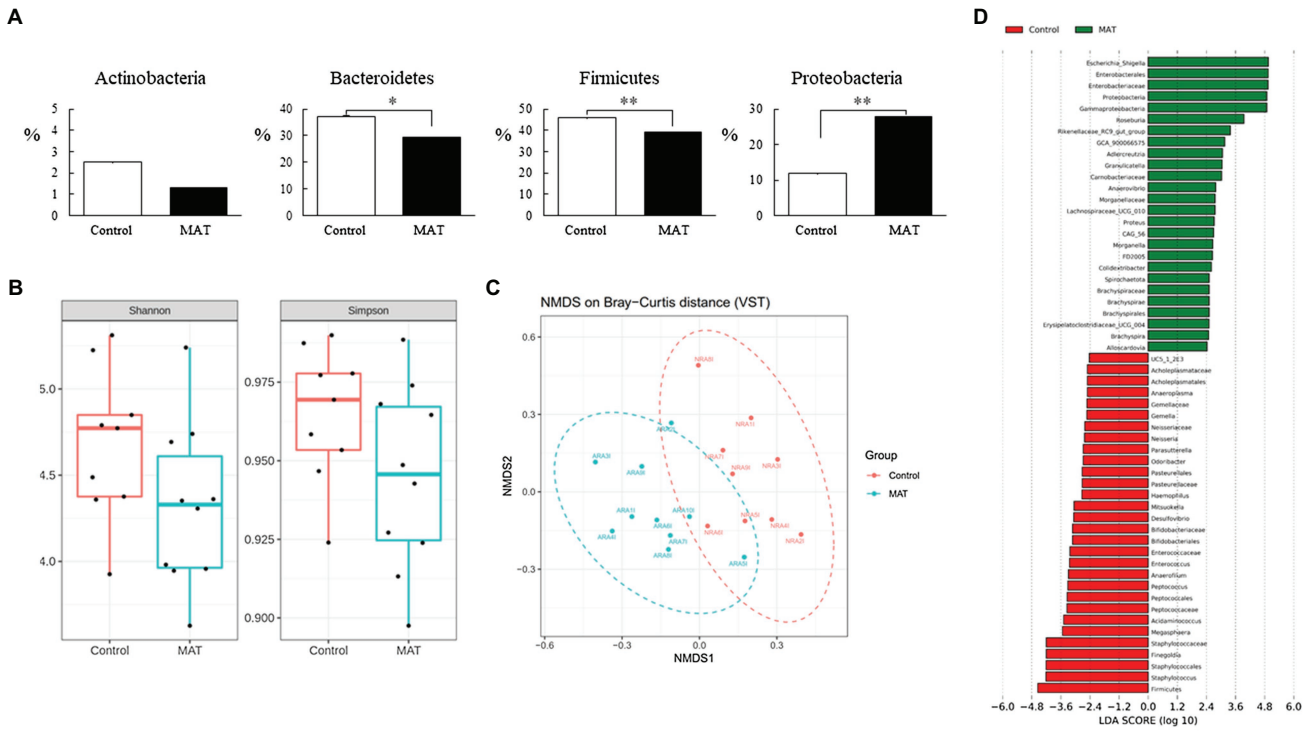

FIGURE 2 | Effects of MAT on **(A)** bacterial composition at the phylum level, **(B)** α diversity, **(C)** NMDS, and **(D)** histogram of the linear discriminant analysis scores of bacterial at the family level of the intestinal microbiota in 7-day-old mice. MAT altered the bacterial composition and diversity of the intestinal microbiota in 7-day-old offspring. MAT significantly reduced the relative abundances of *Bacteroidetes* and *Firmicutes* and significantly increased the relative abundance of *Proteobacteria* in the intestine compared with the abundances in the control group. No significant differences in Shannon diversity or Simpson diversity were observed between the control and MAT groups. NMDS revealed that the intestinal microbiome in the control group was significantly different from that in the MAT group. Bacterial taxa significantly differed across the control and MAT groups identified by LEfSe using the default parameters. $^{*}p < 0.05$; $^{**}p < 0.01$. NMDS, nonmetric multidimensional scaling; and MAT, maternal antibiotic treatment.

expression levels compared with the mice born to the control dams ($p < 0.05$, **Figure 3B**).

MAT Reduced the Numbers of Intestinal Goblet Cells and PCNA-Positive Cells and VEGF Protein Expression

We quantified the goblet cells and PCNA-positive cells to assess the components of innate immunity and proliferation in the intestine, respectively (**Figure 4A**). The immunoreactivity for PCNA was localized to the nucleus and was observed along the epithelium of the intestinal mucosa and in the basal area of the intestinal crypts. Dark brown VEGF-positive staining was localized at the apical cytoplasm of the epithelial cells in both groups; only mice born to the control dams displayed positive results for the immunostaining of VEGF on the endothelial cells of blood vessels in the lamina propria. The mice born to the control dams exhibited more prominent immunoreactivity for PCNA and VEGF staining. Those born to the antibiotic-treated dams had significantly (0.7-fold, $p < 0.001$) fewer mucus-positive goblet cells and PCNA-positive cells and significantly (0.66-fold, $p < 0.01$) lower VEGF protein expression than did the mice born to the control dams (**Figure 4B**).

MAT Increased the Numbers of Intestinal CD45- and CD68-Positive Cells and Cytokines

CD45 and CD68 immunoreactivity was observed on the cytoplasm and the cell membrane of the small lymphocytes (**Figure 5A**). The CD45- and CD68-positive cells were scattered over the lamina propria of the villi and between the epithelial cells of the intestinal mucosa. The mice born to the antibiotic-treated dams exhibited a significantly (1.35-fold, $p < 0.05$) higher percentage of CD45- and CD68-positive cells and (1.32-fold and 1.57-fold, respectively, $p < 0.001$) higher IL-1β and IL-6 expression levels than those born to the control dams (**Figures 5B,C**).

DISCUSSION

Our *in vivo* model demonstrated that MAT during pregnancy suppressed the intestinal microbiota and reduced the body weight of offspring at birth. Maternal antibiotic exposure altered the bacterial composition of intestinal microbiota, induced intestinal injury and inflammation, inhibited vascularization and cellular proliferation, and disrupted the intestinal barrier in neonatal mice. These findings suggest

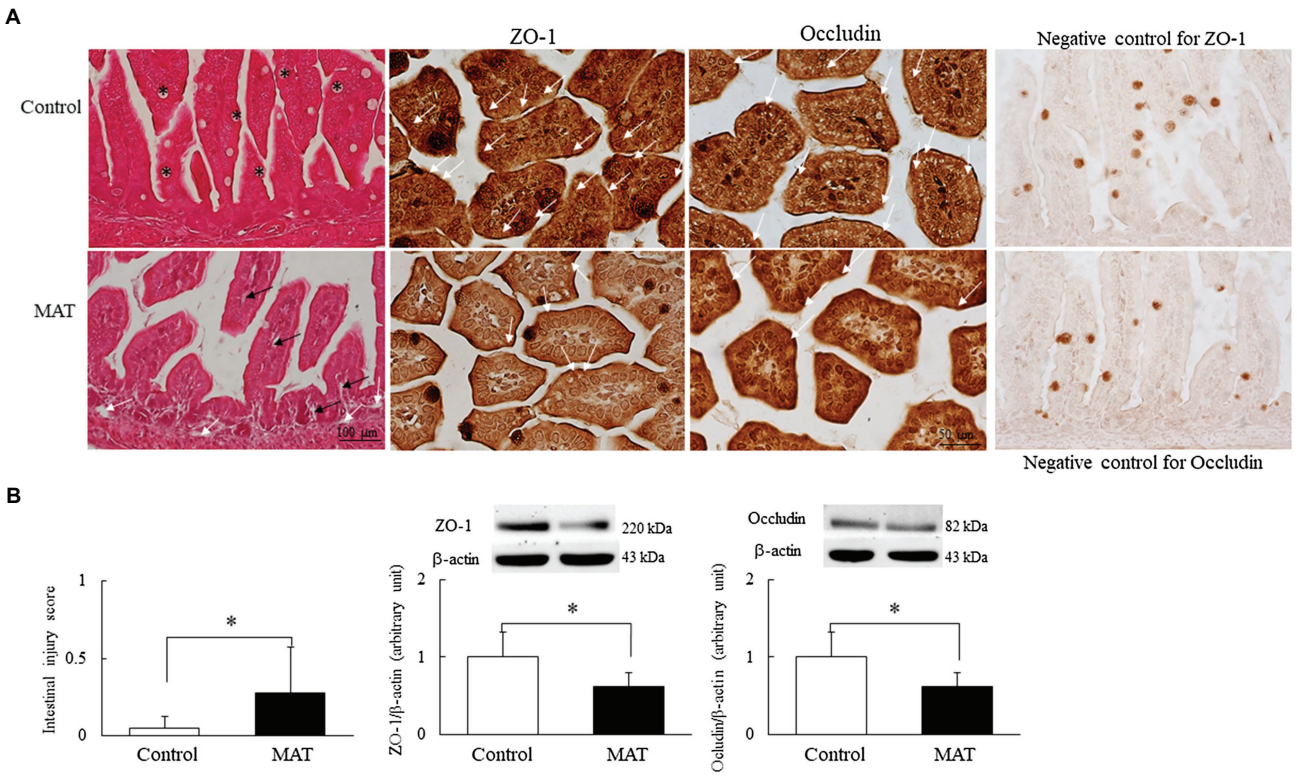

FIGURE 3 | Effects of MAT on **(A)** immunohistochemistry of the ileum and **(B)** intestinal injury score and Western blotting of tight junction proteins in 7-day-old mice. Compared with the mice born to the control dams, the mice born to the antibiotic-treated dams exhibited fewer goblet cells (asterisk) in the epithelium and a significantly higher intestinal injury score; they also exhibited dilated capillaries and lacteal ducts in the lamina propria of the villi (black arrow) and separated lamina propria in the basal portion of the mucosa from the submucosa (white arrow). Mice born to the control dams exhibited intact construct of ZO-1 and occludin staining (white arrow). Those born to the antibiotic-treated dams exhibited disrupted ZO-1 and occludin immunohistochemistry between adjacent enterocytes and significantly lower ZO-1 and occludin protein expression levels than the mice born to the control dams ($n = 9$). $^*p < 0.05$. MAT, maternal antibiotic treatment.

that the administration of antibiotics to women during pregnancy and the subsequent alterations to intestinal microbiota and intestinal development can cause short-term adverse effects.

Rat pups born to dams treated with perinatal antibiotics (amoxicillin or vancomycin) from day 8 prior to delivery to postnatal week 4 gained less weight than did pups born to control dams (Tulstrup et al., 2018). However, the effects of maternal antibiotic exposure during pregnancy on postnatal body weights are unknown. In this study, mice exposed to prenatal maternal antibiotics (ampicillin, gentamicin, and vancomycin) from gestational day 15 to delivery exhibited significantly lower body weights on postnatal day 7 than did mice exposed to sterile drinking water. This effect was not dependent on litter size but was associated with a reduced number of commensal bacteria in newborn mice born to antibiotic-treated dams. These results suggest that maternal antibiotic exposure during pregnancy alters body growth in the postnatal period, indicating that in utero antibiotic exposure alters organogenesis (Vidal et al., 2013). We demonstrated that MAT exposure increases mice mortality, although the survival rates were comparable between the mice born to the control dams and those born to the antibiotic-treated dams.

In this study, we found that MAT during pregnancy suppressed the development of the intestinal microbiota and disrupted intestinal development, as demonstrated by decreased numbers of goblet cells and PCNA-positive cells and decreased VEGF and tight junction protein expression. These results support the previous findings that the intestinal microbiota is crucial for intestinal development through the promotion of mucus production, cellular proliferation, vascularization, and preservation of epithelial junctions in germ-free mice and human infants (Reinhardt et al., 2012; Sommer and Bäckhed, 2013; Kelly et al., 2015; Selma-Royo et al., 2020). These findings suggest that antibiotics administration during pregnancy should be cautious and the manipulation of the intestinal microbiota might potentially prevent intestinal injury and promote intestinal development in antibiotic-exposed infants.

We demonstrated that MAT during pregnancy increases intestinal cytokine (IL-1β and IL-6) levels in neonatal mice. We also quantified intestinal lymphocyte populations of CD45- and CD68-positive stained cells and demonstrated that MAT

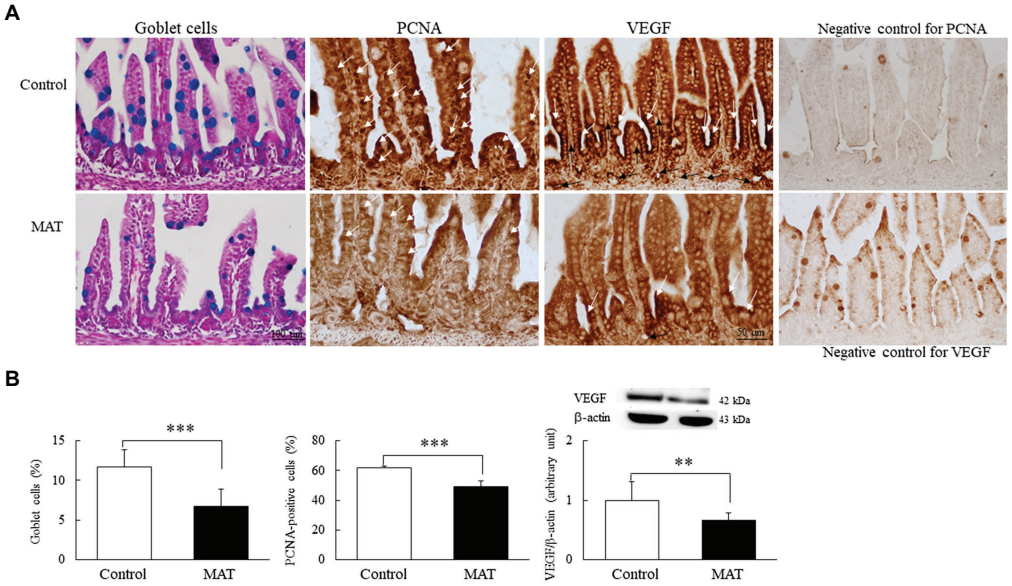

FIGURE 4 | Effects of MAT on **(A)** immunohistochemistry results and **(B)** results of quantitative analysis of goblet cells and PCNA-positive cells and Western blotting of VEGF in 7-day-old mice. The immunoreactivity for PCNA (white arrow) was localized to the nucleus and appeared along the epithelium of the intestinal mucosa and in the basal area of the intestinal crypts. Dark brown VEGF-positive staining (white arrow) was localized at the apical cytoplasm of the epithelial cells in both groups, and the VEGF-positive endothelial cells (black arrow) of blood vessels were observed in the lamina propria of the control group. The mice born to the control dams demonstrated more prominent immunoreactivity for PCNA and VEGF staining. The mice born to the antibiotic-treated dams exhibited significantly fewer mucus-positive goblet cells (blue stained) and PCNA-positive cells and significantly lower VEGF protein expression than did the mice born to the control dams ($n = 9$). $^{**}p < 0.01$; $^{***}p < 0.001$. MAT, maternal antibiotic treatment; PCNA, proliferating cell nuclear antigen; and VEGF, vascular endothelial growth factor.

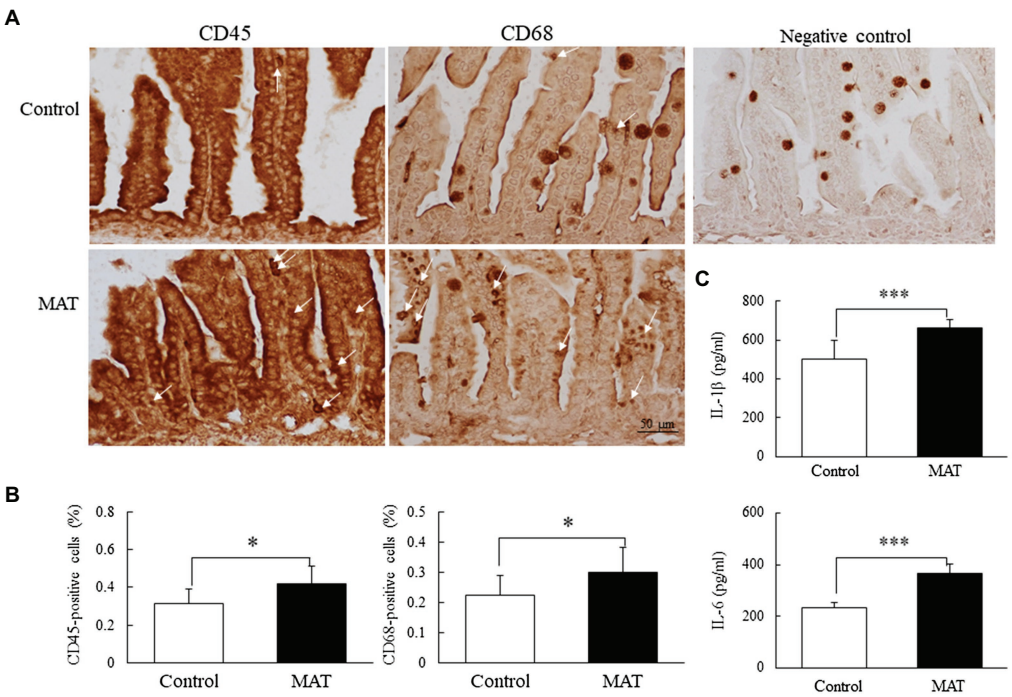

FIGURE 5 | Effects of MAT on **(A)** immunohistochemistry results, **(B)** results of quantitative analysis of CD45 and CD68 cells, and **(C)** cytokines in 7-day-old mice. CD45 and CD68 immunoreactivity was observed on the cytoplasm and cell membrane of the small lymphocytes. The CD45- and CD68-positive cells (white arrow) were scattered over the lamina propria and between the epithelial cells of the intestinal mucosa. The mice born to antibiotic-treated dams exhibited significantly higher percentages of CD45- and CD68-positive cells and higher IL-1β and IL-6 expression levels than did those born to control dams. $^{*}p < 0.05$; $^{***}p < 0.001$. MAT, maternal antibiotic treatment.

during pregnancy increases the numbers of these cells. The results suggest that CD45 and CD68 cells produce cytokines, which is compatible with the finding that type 3 innate lymphoid cells in the neonatal intestine produce the cytokines IL-17 and IL-22 (Niu et al., 2020).

In this study, we used a combination of ampicillin, gentamicin, and vancomycin because they are the most commonly prescribed antibiotics during pregnancy (Mylonas, 2011). We demonstrated that MAT during pregnancy altered the intestinal bacterial composition, induced intestinal injury and inflammation, and disrupted the intestinal development in neonatal mice. These findings suggest that antibiotics should only be applied to pregnant women if antibiotics are really needed. Further studies are needed to evaluate the effect of each antibiotic on intestinal microbiota and development in the offspring.

Our study has several limitations. First, we did not evaluate the maternal intestinal microbiota at the end of antibiotic treatment. Studies have demonstrated that maternal antibiotic exposure during pregnancy disturbs the maternal and fetal intestinal microbiota and affects the health of the offspring (Calatayud et al., 2019; Younge et al., 2019). However, the effects of antibiotics on intestine development in pregnant mice were largely unknown. Second, we did not evaluate the effects of MAT during pregnancy on intestinal permeability in the offspring, though studies have demonstrated that MAT increases colonic permeability on postnatal day 14 in swine offspring and that a disrupted intestinal barrier is associated with impaired intestinal function in hyperoxia-exposed newborn rats (Arnal et al., 2015; Chou and Chen, 2017). Third, maternal antibiotic administration was halted immediately after birth and we measured the intestinal microbiota and intestinal development on postnatal day 7. We did not investigate the effects of MAT during pregnancy through immediate postnatal period in the offspring mice. These might explain the differences in bacterial composition, and tight junction protein expression between the control and MAT groups was not large. Fourth, we did not measure immunological parameters to elucidate the mechanisms underlying impaired intestinal development.

CONCLUSION

In conclusion, this study demonstrated that MAT during pregnancy alters the intestinal microbiota, increases intestinal injury and inflammation, inhibits intestinal cellular proliferation and vascularization, and disrupts the intestinal barrier in neonatal mice. Research on intestinal development after prenatal antibiotic exposure in neonatal mice will increase our understanding of intestinal barrier function and provide strategies for the prevention of long-term adverse effects of MAT during pregnancy. Avoiding antibiotics during pregnancy and the manipulation of intestinal microbiota has the potential to prevent and treat the intestinal injury in infants exposed to prenatal antibiotics. Further studies are required to explore the mechanisms that connect MAT during pregnancy with impaired intestinal development in neonates.

DATA AVAILABILITY STATEMENT

The datasets presented in this study can be found in online repositories. The names of the repository and accession number(s) can be found at European Nucleotide Archive under the accession number PRJEB43913.

ETHICS STATEMENT

This animal study was approved by the Institutional Animal Care and Use Committee of Taipei Medical University (LAC-2019-0290).

AUTHOR CONTRIBUTIONS

C-MC: study design, acquisition and analysis of the data, and drafting and final approval of the manuscript. H-CC and Y-CY: acquisition and analysis of the data, and drafting and final approval of the manuscript. All authors contributed to the article and approved the submitted version.

FUNDING

This study was supported by a grant from the Ministry of Science and Technology in Taiwan (MOST 109-2314-B038-073).

ACKNOWLEDGMENTS

We would like to acknowledge the analytical and technological support provided by Taipei Medical University's Core Laboratory of Human Microbiome.

REFERENCES

Alhasan, M. M., Cait, A. M., Heimesaat, M. M., Blaut, M., Klopfleisch, R., Wedel, A., et al. (2020). Antibiotic use during pregnancy increases offspring asthma severity in a dose-dependent manner. *Allergy* 75, 1979–1990. doi: 10.1111/all.14234

Arnal, M. E., Zhang, J., Erridge, C., Smidt, H., and Lallès, J. P. (2015). Maternal antibiotic-induced early changes in microbial colonization selectively modulate colonic permeability and inducible heat shock proteins, and digesta concentrations of alkaline phosphatase and TLR-stimulants in swine offspring. *PLoS One* 10:e0118092. doi: 10.1371/journal.pone.0118092

Belkaid, Y., and Hand, T. W. (2014). Role of the microbiota in immunity and inflammation. *Cell* 157, 121–141. doi: 10.1016/j.cell.2014.03.011

Blaser, M. J., and Bello, M. G. (2014). Maternal antibiotic use and risk of asthma in offspring. *Lancet Respir. Med.* 2:e16. doi: 10.1016/S2213-2600(14)70219-X

Bookstaver, P. B., Bland, C. M., Griffin, B., Stover, K. R., Eiland, L. S., McLaughlin, M., et al. (2015). A review of antibiotic use in pregnancy. *Pharmacotherapy* 35, 1052–1062. doi: 10.1002/phar.1649

Broe, A., Pottegård, A., Lamont, R. F., Jørgensen, J. S., and Damkier, P. (2014). Increasing use of antibiotics in pregnancy during the period 2000–2010: prevalence, timing, category, and demographics. *BJOG* 121, 988–996. doi: 10.1111/1471-0528.12806

Calatayud, M., Koren, O., and Collado, M. C. (2019). Maternal microbiome and metabolic health program microbiome development and health of the offspring. *Trends Endocrinol. Metab.* 30, 735–744. doi: 10.1016/j.tem.2019.07.021

Callahan, B. J., Sankaran, K., Fukuyama, J. A., McMurdie, P. J., and Holmes, S. P. (2016). Bioconductor workflow for microbiome data analysis: from raw reads to community analyses. *F1000Res.* 5:1492. doi: 10.12688/f1000research.8986.1

Chiu, C. J., Scott, H. J., and Gurd, F. N. (1970). Intestinal mucosal lesion in low-flow states. II. The protective effect of intraluminal glucose as energy substrate. *Arch. Surg.* 101, 484–488. doi: 10.1001/archsurg.1970.01340280036010

Chou, H. C., and Chen, C. M. (2017). Neonatal hyperoxia disrupts the intestinal barrier and impairs intestinal function in rats. *Exp. Mol. Pathol.* 102, 415–421. doi: 10.1016/j.yexmp.2017.05.006

Dierikx, T. H., Visser, D. H., Benninga, M. A., van Kaam, A. H. L. C., de Boer, N. K. H., de Vries, R., et al. (2020). The influence of prenatal and intrapartum antibiotics on intestinal microbiota colonisation in infants: a systematic review. *J. Infect.* 81, 190–204. doi: 10.1016/j.jinf.2020.05.002

Elgin, T. G., Fricke, E. M., Gong, H., Reese, J., Mills, D. A., Kalantera, K. M., et al. (2019). Fetal exposure to maternal inflammation interrupts murine intestinal development and increases susceptibility to neonatal intestinal injury. *Dis. Model. Mech.* 12:dmm040808. doi: 10.1242/dmm.040808

Gonzalez-Perez, G., Hicks, A. L., Tekieli, T. M., Radens, C. M., Williams, B. L., Lamousé-Smith, E. S., et al. (2016). Maternal antibiotic treatment impacts development of the neonatal intestinal microbiome and antiviral immunity. *J. Immunol.* 196, 3768–3779. doi: 10.4049/jimmunol.1502322

Gray, J., Oehrle, K., Worthen, G., Alenghat, T., Whitsett, J., Deshmukh, H., et al. (2017). Intestinal commensal bacteria mediate lung mucosal immunity and promote resistance of newborn mice to infection. *Sci. Transl. Med.* 9:eaaf9412. doi: 10.1126/scitranslmed.aaf9412

Kelly, C. J., Zheng, L., Campbell, E. L., Saeedi, B., Scholz, C. C., Bayless, A. J., et al. (2015). Crosstalk between microbiota-derived short-chain fatty acids and intestinal epithelial HIF augments tissue barrier function. *Cell Host Microbe* 17, 662–671. doi: 10.1016/j.chom.2015.03.005

Loewen, K., Monchka, B., Mahmud, S. M., and Azad, M. B. (2018). Prenatal antibiotic exposure and childhood asthma: a population-based study. *Eur. Respir. J.* 52:1702070. doi: 10.1183/13993003.02070-2017

Marsland, B. J., Trompette, A., and Gollwitzer, E. S. (2015). The gut-lung axis in respiratory disease. *Ann. Am. Thorac. Soc.* 12(Suppl. 2), S150–S156. doi: 10.1513/AnnalsATS.201503-133AW

McMurdie, P. J., and Holmes, S. (2013). Phyloseq: an R package for reproducible interactive analysis and graphics of microbiome census data. *PLoS One* 8:e61217. doi: 10.1371/journal.pone.0061217

Miller, J. E., Wu, C., Pedersen, L. H., de Klerk, N., Olsen, J., Burgner, D. P., et al. (2018). Maternal antibiotic exposure during pregnancy and hospitalization with infection in offspring: a population-based cohort study. *Int. J. Epidemiol.* 47, 561–571. doi: 10.1093/ije/dyx272

Mylonas, I. (2011). Antibiotic chemotherapy during pregnancy and lactation period: aspects for consideration. *Arch. Gynecol. Obstet.* 283, 7–18. doi: 10.1007/s00404-010-1646-3

Niu, X., Daniel, S., Kumar, D., Ding, E. Y., Savani, R. C., Koh, A. Y., et al. (2020). Transient neonatal antibiotic exposure increases susceptibility to late-onset sepsis driven by microbiota-dependent suppression of type 3 innate lymphoid cells. *Sci. Rep.* 10:12974. doi: 10.1038/s41598-020-69797-z

Palm, N. W., de Zoete, M. R., and Flavell, R. A. (2015). Immune-microbiota interactions in health and disease. *Clin. Immunol.* 159, 122–127. doi: 10.1016/j.clim.2015.05.014

Quast, C., Pruesse, E., Yilmaz, P., Gerken, J., Schweer, T., Yarza, P., et al. (2013). The SILVA ribosomal RNA gene database project: improved data processing and web-based tools. *Nucleic Acids Res.* 41, D590–D596. doi: 10.1093/nar/gks1219

Reed, B. D., Schibler, K. R., Deshmukh, H., Ambalavanan, N., and Morrow, A. L. (2018). The impact of maternal antibiotics on neonatal disease. *J. Pediatr.* 197, 97–103. doi: 10.1016/j.jpeds.2018.01.056

Reinhardt, C., Bergentall, M., Greiner, T. U., Schaffner, F., Ostergren-Lundén, G., Petersen, L. C., et al. (2012). Tissue factor and PAR1 promote microbiota-induced intestinal vascular remodelling. *Nature* 483, 627–631. doi: 10.1038/nature10893

Schliep, K. P. (2011). Phangorn: phylogenetic analysis in R. *Bioinformatics* 27, 592–593. doi: 10.1093/bioinformatics/btq706

Segata, N., Izard, J., Waldron, L., Gevers, D., Miropolsky, L., Garrett, W. S., et al. (2011). Metagenomic biomarker discovery and explanation. *Genome Biol.* 12:R60. doi: 10.1186/gb-2011-12-6-r60

Selma-Royo, M., Calatayud Arroyo, M., García-Mantrana, I., Parra-Llorca, A., Escuriet, R., Martínez-Costa, C., et al. (2020). Perinatal environment shapes microbiota colonization and infant growth: impact on host response and intestinal function. *Microbiome* 8:167. doi: 10.1186/s40168-020-00940-8

Şensoy, E., and Öznurlu, Y. (2019). Determination of the changes on the small intestine of pregnant mice by histological, enzyme histochemical, and immunohistochemical methods. *Turk. J. Gastroenterol.* 30, 917–924. doi: 10.5152/tjg.2019.18681

Sommer, F., and Bäckhed, F. (2013). The gut microbiota-masters of host development and physiology. *Nat. Rev. Microbiol.* 11, 227–238. doi: 10.1038/nrmicro2974

Tulstrup, M. V., Roager, H. M., Thaarup, I. C., Frandsen, H. L., Frøkiær, H., Licht, T. R., et al. (2018). Antibiotic treatment of rat dams affects bacterial colonization and causes decreased weight gain in pups. *Commun. Biol.* 1:145. doi: 10.1038/s42003-018-0140-5

Vidal, A. C., Murphy, S. K., Murtha, A. P., Schildkraut, J. M., Soubry, A., Huang, Z., et al. (2013). Associations between antibiotic exposure during pregnancy, birth weight and aberrant methylation at imprinted genes among offspring. *Int. J. Obes.* 37, 907–913. doi: 10.1038/ijo.2013.47

Yang, Y. S. H., Chang, H. W., Lin, I. H., Chien, L. N., Wu, M. J., Liu, Y. R., et al. (2020). Long-term proton pump inhibitor administration caused physiological and microbiota changes in rats. *Sci. Rep.* 10:866. doi: 10.1038/s41598-020-57612-8

Yoshimoto, A., Uebanso, T., Nakahashi, M., Shimohata, T., Mawatari, K., Takahashi, A., et al. (2018). Effect of prenatal administration of low dose antibiotics on gut microbiota and body fat composition of newborn mice. *J. Clin. Biochem. Nutr.* 62, 155–160. doi: 10.3164/jcbn.17-53

Younge, N., McCann, J. R., Ballard, J., Plunkett, C., Akhtar, S., Araújo-Pérez, F., et al. (2019). Fetal exposure to the maternal microbiota in humans and mice. *JCI Insight* 4:e127806. doi: 10.1172/jci.insight.127806

Zimmermann, P., and Curtis, N. (2020). Effect of intrapartum antibiotics on the intestinal microbiota of infants: a systematic review. *Arch. Dis. Child. Fetal Neonatal Ed.* 105, 201–208. doi: 10.1136/archdischild-2018-316659

Conflict of Interest: The authors declare that the research was conducted in the absence of any commercial or financial relationships that could be construed as a potential conflict of interest.

frontiers in Microbiology

ORIGINAL RESEARCH
published: 21 June 2021
doi: 10.3389/fmicb.2021.615416

Correlations Between Intestinal Microbial Community and Hematological Profile in Native Tibetans and Han Immigrants

Yan Ma[1,2,3], *Qin Ga*[1,2,3], *Ri-Li Ge*[1,2,3] *and Shuang Ma*[1,2,3]*

[1]Research Center for High Altitude Medicine, Qinghai University Medical College, Xining, China, [2]Key Laboratory for Application of High Altitude Medicine in Qinghai Province, Qinghai University, Xining, China, [3]Qinghai-Utah Joint Research Key Lab for High Altitude Medicine, Qinghai University Medical College, Xining, China

OPEN ACCESS

Edited by:
Joao Inacio,
University of Brighton,
United Kingdom

Reviewed by:
Monica Di Paola,
University of Florence, Italy
Huan Li,
Lanzhou University, China

***Correspondence:**
Shuang Ma
shuang-cool@126.com

Specialty section:
This article was submitted to Microbial Symbioses, a section of the journal Frontiers in Microbiology

Received: 13 October 2020
Accepted: 21 May 2021
Published: 21 June 2021

Citation:
Ma Y, Ga Q, Ge R-L and Ma S (2021) Correlations Between Intestinal Microbial Community and Hematological Profile in Native Tibetans and Han Immigrants. Front. Microbiol. 12:615416. doi: 10.3389/fmicb.2021.615416

Hematological features are one of the best-known aspects of high-altitude adaptation in Tibetans. However, it is still unclear whether the intestinal microbiota is associated with the hematology profile. In this study, routine blood tests and 16S rRNA gene sequencing were used to investigate the differences in the intestinal microbiota and hematological parameters of native Tibetan herders and Han immigrants sampled at 3,900 m. The blood test results suggested that the platelet counts (PLTs) were significantly higher in native Tibetans than the Han immigrants. The feces of the native Tibetans had significantly greater microbial diversity (more different species: Simpson's and Shannon's indices) than that of the Han immigrants. The native Tibetans also had a different fecal microbial community structure than the Han immigrants. A Bray–Curtis distance-based redundancy analysis and envfit function test showed that body mass index (BMI) and PLT were significant explanatory variables that correlated with the fecal microbial community structure in native Tibetans. Spearman's correlation analysis showed that *Megamonas* correlated positively with BMI, whereas *Bifidobacterium* correlated negatively with BMI. *Alistipes* and *Parabacteroides* correlated positively with the PLT. *Succinivibrio* correlated positively with SpO_2. *Intestinibacter* correlated negatively with the red blood cell count, hemoglobin, and hematocrit (HCT). *Romboutsia* correlated negatively with HCT, whereas *Phascolarctobacterium* correlated positively with HCT. A functional analysis showed that the functional capacity of the gut microbial community in the native Tibetans was significantly related to carbohydrate metabolism. These findings suggest that the hematological profile is associated with the fecal microbial community, which may influence the high-altitude adaptation/acclimatization of Tibetans.

Keywords: fecal microbiota, high-altitude adaptation, Tibetan, Han immigrant, hematological profile

INTRODUCTION

The Tibetan Plateau is both the largest and highest plateau in the world, with a mean elevation of 4,500 m (Zhao et al., 2019), and is therefore considered as the "roof of the world." It has special environmental conditions, such as low atmospheric pressure, low temperature, low relative humidity, and high solar radiation (Zhao et al., 2018). On the Tibetan Plateau, the main indigenous population is the Tibetans, whereas the Han population constitutes the majority of the immigrant population. Han individuals and other unacclimatized or susceptible people who ascend to altitudes >2,500 m can experience physiological responses during rapid ascent that may be life-threatening (Roach et al., 2018). Increased red blood cell (RBC) counts, packed cell volumes, or high hemoglobin concentrations are frequently observed in physiological responses to high altitude. Patients with chronic mountain sickness are characterized by excessive erythrocytosis (Moore et al., 2010). Hypoxia also alters the proteome of platelets, favoring a prothrombotic phenotype, increasing platelet reactivity, which increases the risk of thrombotic diseases in chronically hypoxic individuals (Rocke et al., 2018). However, Tibetans have been living at high altitudes for thousands of years (Meyer et al., 2017), have established perfectly adapted mechanisms for high-altitude living, and display a suite of adaptive physiological traits: increased resting ventilation, reduced arterial oxygen content, blunted hypoxic ventilation response and pulmonary vasoconstriction response, and a reduced incidence of low birth weight (Jianguo et al., 2002; Beall, 2006, 2007; Tianyi and Kayser, 2006). Lowland individuals (Han) can acclimatize to altitude to mitigate the effects of high-altitude exposure, and during this acclimatization, most changes occur over a period of days up to a few weeks (Muza et al., 2010; West et al., 2012; Qian-Qian et al., 2013). This process does not restore the individual's performance to that at sea level, nor to one that is completely the same as that of the native population (Yang et al., 2018). Although many genome-wide association studies have identified differences in several genes, such as endothelial PAS domain containing protein 1 (*EPAS1*) and egl-9 family hypoxia inducible factor (*EGLN1*), which are responsible for the genetic adaptation of native highlanders (Simonson et al., 2010; Lorenzo et al., 2014; Arciero et al., 2018; Storz, 2021), limited information is available on the association between the intestinal microbiome, or "second genome" (Grice and Segre, 2012), and the hematology of these natives. Trillions of microorganisms inhabit the human body, strongly colonizing the gastrointestinal tract and outnumbering our own cells (Sohail et al., 2019). Most microbes reside in the gastrointestinal tract, have coevolved with their hosts, and have profound effects on human physiology and nutrition (Turnbaugh et al., 2006; Tremaroli and Bäckhed, 2012).

Short or chronic exposure of humans or animals to hypoxia (the most typical characteristic of high altitude) can affect the composition of the intestinal microbiota (Brigitta et al., 2005; Atanu et al., 2013; Lucking et al., 2018; Zhang et al., 2019). It appears that some indigenous high-altitude humans and animals tend to carry several common genes and some common intestinal microbes that may be related to their adaptation to altitude (Ge et al., 2013; Kang et al., 2016; Li et al., 2016, 2018; Zhang et al., 2016a,b; Lan et al., 2017; Arciero et al., 2018; Bai et al., 2018). These findings suggest that the host genome and the intestinal microbiome have coevolved under the selection pressure exerted by high altitude.

Among the majority populations on the Tibetan Plateau, the native Tibetan and Han immigrants living at same high altitude display significant differences in compositions of their intestinal microbiota (Kang et al., 2016). This is also true of members of the same ethnic group living at different altitudes (Lan et al., 2017). Diet, body mass index (BMI), lifestyle, and age also influence the community composition and structure of the intestinal microbial in native Tibetans and Han immigrants (Li and Zhao, 2015; Lan et al., 2017; Li et al., 2018).

Recent studies have indicated that the intestinal microbiota not only regulates mucosal immunity but also contributes to hematopoiesis. The gut microbiota sustains hematopoiesis. Hematopoietic changes are associated with a significant contraction of the fecal microbiome and are partially rescued by the transfer of fecal microbiota. Platelet counts (PLTs) are consistently and significantly increased in antibiotic-treated mice compared with those in control mice (Josefsdottir et al., 2017; Staffas et al., 2018; Han et al., 2021). Metabolites from the intestinal microbiota, such as short-chain fatty acids (SCFAs), contribute to the production of hematopoietic precursors in specific-pathogen-free (SPF) mice (Trompette et al., 2014). Some of the best-known aspects of high-altitude acclimatization and adaptation involve the hematological system, such as the changes in RBC numbers per unit volume, the hemoglobin (Hb) concentration, and the PLT or activation (West et al., 2012; Shang et al., 2019). However, the association between the intestinal microbiota and the hematological parameters of natives and immigrants living at high altitudes is still unclear. This prompted us to investigate the composition and diversity of the intestinal microbiota in native Tibetans and Han immigrants, and the potential relationship between their intestinal microbial profiles and host hematological parameters during exposure to high altitude.

MATERIALS AND METHODS

Ethics Statement

All the experiments were approved by and performed in accordance with the guidelines and regulations of the Ethics Committee of Qinghai University, Xining, China. Written informed consent was obtained from all the participants and submitted to the Ethics Committee.

Subjects

The native Tibetan herders (n = 26) were living at an altitude of 3,900 m in Da Ri county (33°45'3.83 N, 99°39' E), Guoluo Tibetan Autonomous Prefecture, Qinghai–Tibet Plateau.

The Chinese Han immigrants (n = 5) had migrated to Da Ri earlier than a year ago. All the enrolled subjects were healthy, with no history of gastrointestinal disease, liver disease, hypertension, or diabetes, as demonstrated by their medical histories and physical examinations.

Blood Sample Collection and Analysis

Venous blood samples (2 ml) were collected with venipuncture into an EDTA-K2 anticoagulant Vacutainer tubes and then analyzed with BM-2300 fully automated blood cell analyzer (Mindray, Shenzhen, China) within 30 min of the blood drawing.

Fecal Sample Collection

Approximately 5 g of fresh feces was collected from each participant and placed in two sterile 5-ml tubes, which were immediately transferred to liquid nitrogen and then stored at −80°C.

Fecal Microbiome Analysis

DNA Extraction

The total genomic DNA from each fecal sample was extracted with the PowerFecal™ DNA Isolation Kit (Mo Bio Laboratories, Carlsbad, CA, United States), according to the manufacturer's instructions. The DNA purity was assessed on 1% agarose gels. The DNA purity and concentration were also calculated with an optical density (OD) analysis at wavelengths of 260 and 280 nm, as the OD_{260}/OD_{280} ratio, with a NanoPhotometer® spectrophotometer (Implen, Munich, Germany). The DNA concentrations were measured with the Qubit® dsDNA Assay Kit in a Qubit® 2.0 Fluorometer (Life Technologies, Camarillo, CA, United States).

16S rRNA Gene Sequencing and Data Analysis

16S rRNA gene sequencing was performed by Novogene Bioinformatics Technology Co., Ltd., China. Briefly, the DNA samples were diluted to 1 ng/μl in sterile water and then PCR amplified with the 515F/806R primer set (515F: 5'-GTGCCAGCMGCCGCGGTAA-3', 806R: 5'-XXXXXXGG ACTACHVGGGTATCTAAT-3'), which targets the V4 region of the bacterial 16S rRNA. The reverse primer contained a 6-bp error-correcting barcode unique to each sample. All PCRs were performed with Phusion® High-Fidelity PCR Master Mix (New England Biolabs [Beijing] Ltd., Beijing, China). The PCR products were mixed with the same volume of 1 × loading buffer (containing SYB Green dye) and separated electrophoretically on 2% agarose gels for confirmation. Samples with bright major bands of 400–450 bp were isolated for further analysis. All the PCR products were purified with the GeneJET Gel Extraction Kit (Thermo Scientific, Waltham MA, United States). Sequencing libraries were generated with the TruSeq® DNA PCR-Free Sample Preparation Kit (Illumina, San Diego, CA, United States), according to the protocol described by the manufacturer, and index codes were added. After the quality of the libraries was assessed, they were sequenced on the Illumina HiSeq 2500 platform (Illumina), and 250-bp paired-end reads were generated.

Data Analysis

Student's t-test was used to test the significance of differences in age, gender, height, weight, BMI, oxyhemoglobin saturation measured with a pulse oximeter (SpO_2), RBCs, Hb, hematocrit (HCT), and PLT between the native Tibetans and Han immigrants.

After 16S rRNA gene sequencing, the paired-end reads were merged with FLASH (Magoč and Salzberg, 2011). The raw tags were quality filtered under specific filtering conditions to obtain high-quality clean tags (Bokulich et al., 2013), according to the QIIME quality-controlled process (Caporaso et al., 2010). The tags were then compared with the reference database (Genomes OnLine Database, GOLD)[1] using the UCHIME algorithm (Edgar et al., 2011), to detect chimeric sequences, which were then removed (Haas et al., 2011). Uparse (Edgar, 2013) was used to identify the operational taxonomic units (OTUs) by constructing an OTU table. Sequences with ≥97% similarity were assigned to the same OTU. Representative sequences for each OTU were screened for further annotation. The Green Gene Database (Desantis et al., 2006) was used with the RDP Classifier algorithm (Wang et al., 2007) to annotate each representative sequence with taxonomic information. Multiple sequence alignments were constructed with MUSCLE (Edgar, 2004). The numbers of common and unique OTUs were presented in Venn diagrams using BioVenn.[2] Student's t-test was used to test the significance of differences in the relative abundances of Firmicutes and Bacteroidetes. The Mann–Whitney U test was used to test the significance of differences in unclassified *Prevotellaceae*, *Bacteroides*, *Faecalibacterium*, and the Firmicutes/Bacteroidetes (F/B) ratio between the groups. The Mann–Whitney U test was used to test the significance of differences in Ace, Chao 1, Simpson's index, and Shannon's index between groups. The differences in the overall community compositions and structures of both groups were visualized with the nonmetric multidimensional scaling (NMDS) ordination plots of Jaccard and with Bray–Curtis distance matrices. A MetaStats analysis was used to identify bacterial taxa differentially represented in the groups at the genus or higher taxonomic levels, and values of p were corrected with the Benjamini–Hochberg false discovery rate method to determine the values of q (White et al., 2009). The linear discriminant analysis (LDA) effect size (LEfSe), which takes into account both statistical significance and biological relevance, was used to search for taxa whose relative abundances differed significantly between the groups, with a default LDA of four (Segata et al., 2011). A Bray–Curtis distance-based redundancy analysis (dbRDA; Clarke and Ainsworth, 1993) and the variance inflation factor (Sheik et al., 2012) function in the "vegan" package of R were used to evaluate the linkages between the fecal microbiota and environmental attributes. The influences of environmental factors on the distributions of genera were calculated with the "envfit" function, which uses multivariate

[1]http://drive5.com/uchime/uchime_download.html
[2]http://www.biovenn.nl/index.php

ANOVA for categorical variables and linear correlations for continuous variables. Correlations between age, BMI, SpO_2, RBC, Hb, HCT, PLT, and the bacterial communities were assessed with Spearman's correlation analysis (Segata et al., 2011) using the "pheatmap" package in R.

The functional profiles of the microbial communities were predicted with Tax4Fun (AβHauer et al., 2015) with the nearest-neighbor method, based on the minimum 16S rRNA sequence similarity. The Kyoto Encyclopedia of Genes and Genomes (KEGG) database prokaryotic whole-genome 16S rRNA gene sequence was extracted and aligned with the SILVA SSU Ref NR database using the BLASTN algorithm to establish a correlation matrix. The prokaryotic whole-genome functional information from the KEGG database, annotated by UProC and PAUDA, was mapped to do the SILVA database function annotation. The sequenced samples were clustered out of the OTU using the SILVA database sequence as the reference sequence to obtain functional annotation information.

RESULTS

Sample Characteristics

In this study, we compared the age, sex, height, weight, BMI, and hematological parameters of native Tibetans and the Han immigrants. The native Tibetans had significantly higher PLT than the Han immigrants ($p < 0.05$; **Table 1**), whereas age, sex, height, weight, BMI, SpO_2, RBC, Hb, and HCT did not differ significantly between the two groups ($p > 0.05$; **Table 1**). The main food of the native Tibetans was roasted barley flour, buttered tea, cheese, and meat, whereas the daily staples of the Han immigrants were noodles, rice, and vegetables.

HiSeq Sequencing

The fecal microbiotal compositions were determined by sequencing the 16S rRNA gene in 31 samples from the two groups with the HiSeq platform. A total of 2,674,262 raw reads were obtained. After the low-quality sequences, chimeric sequences, and those that were not classified as bacteria were removed, 2,392,645 sequences remained, with an average number of 77,182 sequences per sample (range 46,224–2,392,645) and an average read length of 253 bp. A clustering analysis assigned the microbial sequences from the samples that shared 97% similarity to the same OTUs. In total, 2,205 OTUs were identified. Rarefaction curves showed that a plateau level was reached in all samples (**Supplementary Figure S1**), indicating that our sequencing depth was sufficient, and that those additional sequences may identify some rare bacterial species.

TABLE 1 | Characteristic of the native Tibetans and Han immigrants in Da Ri.

	Native Tibetan	Immigrant Han	Value of *p*
N	26	5	
Age (years)	42.73 ± 18.09	48.2 ± 1.30	0.511
Sex (male/female)	19/7	4/1	1.000
Height (cm)	162.96 ± 8.67	165.40 ± 7.23	0.561
Weight (kg)	62.57 ± 11.85	58.80 ± 9.60	0.509
BMI	19.12 ± 2.95	17.78 ± 2.89	0.359
SpO_2 (%)	83.54 ± 6.56	86.00 ± 1.87	0.418
RBC (10*12/L)	5.65 ± 0.86	5.17 ± 0.81	0.263
Hb (g/L)	162.46 ± 26.61	156.40 ± 22.76	0.638
HCT (%)	58.60 ± 12.45	56.86 ± 8.29	0.768
PLT (10*9/L)	257.34 ± 61.02	189.40 ± 57.22	0.029

Values are means ± SD. Data were analyzed with the Student's t-test to compare the variables between the groups. BMI, body mass index; SpO_2, oxyhemoglobin saturation measured with a pulse oximeter; RBC, red blood cells; Hb, hemoglobin; HCT, hematocrit; and PLT, platelet count.

Taxonomic Analysis

Of the total OTUs, 970 (43.9%) were common to the native Tibetans and Han immigrants, whereas 961 OTUs (43.5%) were unique to the native Tibetans, and 274 OTUs (12.4%) were unique to the Han immigrants. The fecal microbiota compositions of each group at phylum and genus levels are shown in **Figure 1**. The fecal microbiotas of the native Tibetans and Han immigrants were dominated by the following phyla: Firmicutes (49.5 and 60.2%, respectively), Bacteroidetes (32.8 and 29.3%, respectively), Proteobacteria (11.3 and 4.3%, respectively), and Actinobacteria (5.7 and 4.9%, respectively). Other rare phyla (mean relative abundance <1%) included Verrucomicrobia, Tenericutes, Melainabacteria, Euryarchaeota, and Planctomycetes. We found no significant differences in the relative abundances of Firmicutes and Bacteroidetes, or in the F/B ratios (Ruth et al., 2005) of the native Tibetans and Han immigrants ($p > 0.05$; **Supplementary Table S1**). At the genus level, 449 genera were detected. The four core taxa of the fecal bacteria in the native Tibetans were *unclassified Prevotellaceae* (13.69%), *Bacteroides* (8.30%), *Faecalibacterium* (6.62%), and *Blautia* (5.31%). The four core taxa of fecal bacteria in the Han immigrants were *Bacteroides* (21.79%), *Faecalibacterium* (9.96%), *unclassified Prevotellaceae* (8.85%), and *Veillonella* (6.91%). The relative abundance of *unclassified Prevotellaceae* was higher in the native Tibetans than in the Han immigrants, whereas the abundance of *Bacteroides* was higher in the Han immigrants than in the native Tibetans, but the differences were not statistically significant ($p > 0.05$; **Supplementary Table S2**).

α-Diversity Analysis

Four α-diversity measures were calculated: Simpson's index, Shannon's index, the abundance-based coverage estimator (Ace) index, and Chao 1. We found no significant differences in community richness (Ace and Chao 1) between the native Tibetans and the Han immigrants ($p > 0.05$; **Table 1**), but the native Tibetan feces had significantly greater microbial diversity (more different species, Simpson's and Shannon's indices) than that of the Han immigrants ($p < 0.05$; **Table 2**).

β-Diversity Analysis

The relationship between the community structures of the microbiota of the native Tibetans and Han immigrants was examined with NMDS ordination plots, which revealed clear differences in the community compositions and structures of the two groups (**Figure 2**).

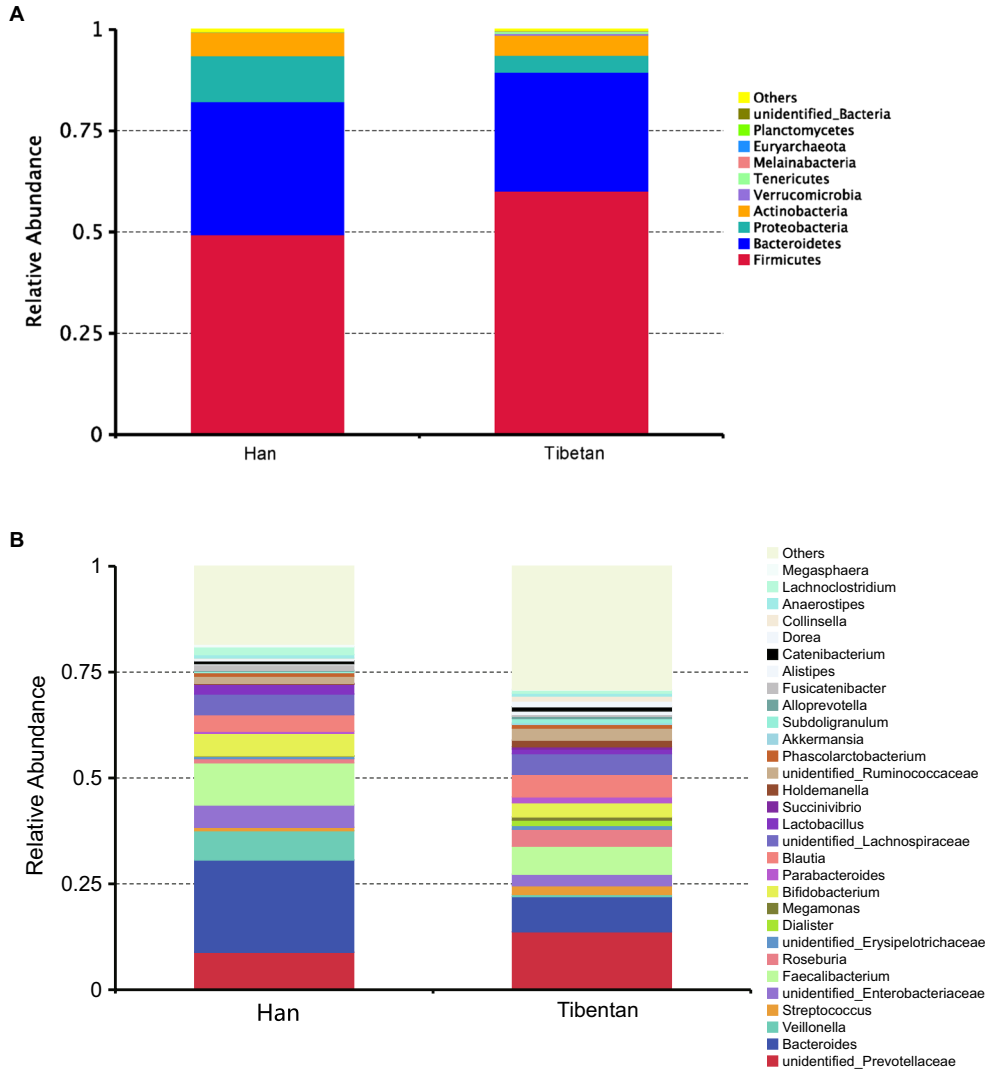

FIGURE 1 | Community composition of fecal microbiota in native Tibetans and Han immigrants. In the stacked bar chart, each bar represents the average relative abundance of each bacterial taxon. The taxa with high relative abundances at the phylum (top 10, **A**) and genus levels (top 30, **B**) are shown.

TABLE 2 | Fecal microbial diversity and richness in the native Tibetans and Han immigrants.

Group	Shannon's index	Simpson's index	Ace	Chao 1
Native Tibetan	5.53 ± 0.43	0.94 ± 0.01	644.52 ± 151.59	641.37 ± 150.44
Immigrant Han	4.60 ± 0.62	0.88 ± 0.40	645.59 ± 194.35	639.40 ± 190.97
Value of *p*	0.001	0.001	0.856	0.658

Values are means ± SD. Differences between the groups were analyzed with the Mann–Whitney U test.

Differences in Fecal Microbiota of Native Tibetans and Han Immigrants

Of the total OTUs, 961 OTUs (43.5%) were unique to the native Tibetans, and 274 OTUs (12.4%) were unique to the Han immigrants.

A MetaStats analysis of the most-abundant taxa was used to identify the bacterial taxa that differed significantly between the two groups. **Figure 3A** shows that six bacterial taxa were significantly more abundant ($p < 0.05$) in the fecal microbial of the native Tibetans (*Holdemanella*, *Subdoligranulum*, *Alistipes*, *Dorea*, *Collinsella*, and *Roseburia*) than in that of the Han immigrants. An LEfSe analysis was also conducted to detect the bacterial taxa that differed significantly between the groups. *Roseburia* was significantly more abundant in the fecal microbiota of the native Tibetans than in that of the Han immigrants (**Figure 3B**).

Correlations Between Fecal Microbiota and Age, BMI, SpO_2, RBC, Hb, HCT, and PLT

A Spearman's correlation matrix was generated to examine the correlations between age, BMI, SpO_2, RBC, Hb, HCT, PLT, and the bacterial genera. As shown in **Figure 4**,

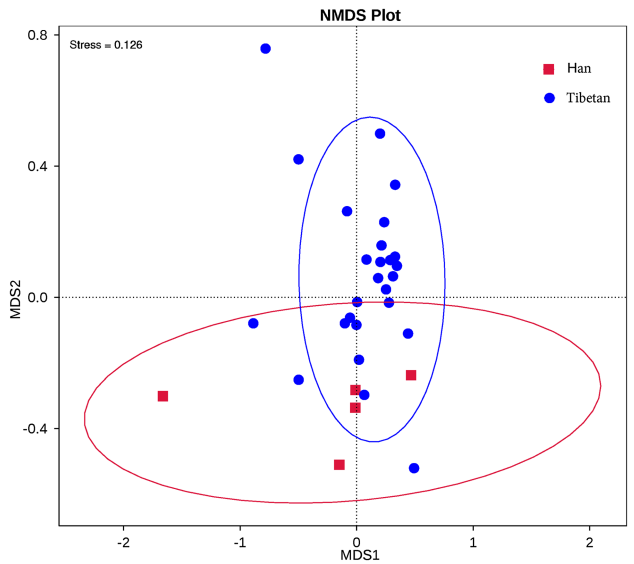

FIGURE 2 | Nonmetric multidimensional scaling (NMDS) showed distinct fecal bacterial communities in the native Tibetans and Han immigrants. Each symbol represents the fecal microbiota of one sample. NMDS plots were derived from the Bray–Curtis distances between the groups.

significant associations were identified between the fecal microbiota and age, BMI, SpO_2, RBC, Hb, HCT, and PLT. A correlation analysis revealed that genus *unclassified Prevotellaceae* correlated positively with BMI ($r = 0.42$, $p < 0.05$); *Megamonas* correlated positively with BMI ($r = 0.42$, $p < 0.05$); *Bifidobacterium* correlated negatively with BMI ($r = -0.41$, $p < 0.05$); *Alistipes* correlated positively with PLT ($r = 0.52$, $p < 0.01$); *Parabacteroides* correlated positively with PLT ($r = 0.36$, $p < 0.05$); *Bacteroides* correlated positively with age ($r = 0.36$, $p < 0.05$); *Lactobacillus* correlated positively with age ($r = 0.42$, $p < 0.05$); *unclassified Ruminococcaceae* correlated negatively with age ($r = -0.41$, $p < 0.05$) and positively with SpO_2 ($r = 0.44$, $p < 0.05$); *Succinivibrio* correlated positively with SpO_2 ($r = 0.43$, $p < 0.05$); *unidentified Clostridiales* correlated negatively with RBC ($r = -0.42$, $p < 0.05$); *Intestinibacter* correlated negatively with RBC ($r = -0.56$, $p < 0.01$), Hb ($r = -0.48$, $p < 0.01$), and HCT ($r = -0.31$, $p < 0.05$); *Romboutsia* correlated negatively with HCT ($r = -0.36$, $p < 0.05$); *Phascolarctobacterium* correlated positively with HCT ($r = 0.40$, $p < 0.05$); and *Roseburia* correlated positively with BMI ($r = 0.33$, $p = 0.06$), RBC ($r = 0.33$, $p = 0.06$), Hb ($r = 0.31$, $p = 0.08$), HCT ($r = 0.31$, $p = 0.08$), and PLT ($r = 0.34$, $p = 0.05$).

To determine whether BMI or other variables had an additional effect on the fecal microbial community structure, we performed a Bray–Curtis dbRDA. Age, BMI, SpO_2, RBC, Hb, HCT, and PLT were associated with the microbial community structure (**Figure 5**). Furthermore, an envfit function test showed that BMI and PLT were significant explanatory variables (**Table 3**).

Functional Profiles of Fecal Microbiota in Native Tibetans and Han Immigrants

To further investigate the functional capacities of the fecal microbial communities in the native Tibetans and Han immigrants, Tax4Fun was used to examine the functional profiles of the fecal microbiota in the two groups. **Figure 6** shows the 35 most-abundant pathways at the third level of KEGG pathways. Of these 35 pathways, 27 were more abundant in the fecal microbial community of the native Tibetans than in that of the Han immigrants. The functional capacities of the intestinal microbial communities in the native Tibetans were enriched in metabolism (pyruvate metabolism; butanoate metabolism; alanine, aspartate, and glutamate metabolism; glycolysis and gluconeogenesis; starch and sucrose metabolism; amino sugar and nucleotide sugar metabolism; glycine, serine, and threonine metabolism; purine and pyrimidine metabolism; and carbon fixation pathways in prokaryotes) and genetic information processing (ribosome biogenesis; DNA repair and recombination proteins; homologous recombination; mismatch repair; chaperones and folding catalysts; chromosome and associated proteins; and DNA replication proteins). Eight pathways (transporters; cysteine and methionine metabolism; ABC transporters; transfer RNA biogenesis; quorum sensing; amino acid related enzymes; secretion system; and aminoacyl tRNA biosynthesis) were enriched in the fecal microbial community of the Han immigrants.

DISCUSSION

In this study, we focused on the composition, structure, and diversity of the gut microbiota in two ethnic groups (Tibetan and Chinese Han), living at high altitude (Qinghai), and their correlations with some explanatory factors, especially hematological parameters.

Previous studies have shown that altitude and ethnicity affect the intestinal bacterial profiles of Tibetans (Kang et al., 2016; Lan et al., 2017). Diet, BMI, lifestyle, and age also influence the composition and structure of the Tibetans' intestinal microbial communities (Li and Zhao, 2015; Lan et al., 2017; Li et al., 2018). However, few studies have examined the association between intestinal microbial profiles and hematological parameters. Our results show that age, BMI, SpO_2, RBC, Hb, HCT, and PLT correlated with the intestinal microbial community structure, and that BMI and PLT were significant explanatory variables. The genus *Megamonas* correlated positively with BMI, whereas *Bifidobacterium* was negatively associated with BMI. The microbiota of obese subjects contain increased numbers of *Megamonas* (Chiu et al., 2014) and reduced numbers of *Bifidobacterium* (Million et al., 2012). In this study, *Alistipes* and *Parabacteroides* correlated positively with PLT. *Parabacteroides species* modulate the host metabolism by the produce of succinate and secondary bile acids (Wang et al., 2019). Bile acid receptors and platelet-activating factor receptors are numbers of the G-protein-coupled receptors family, which

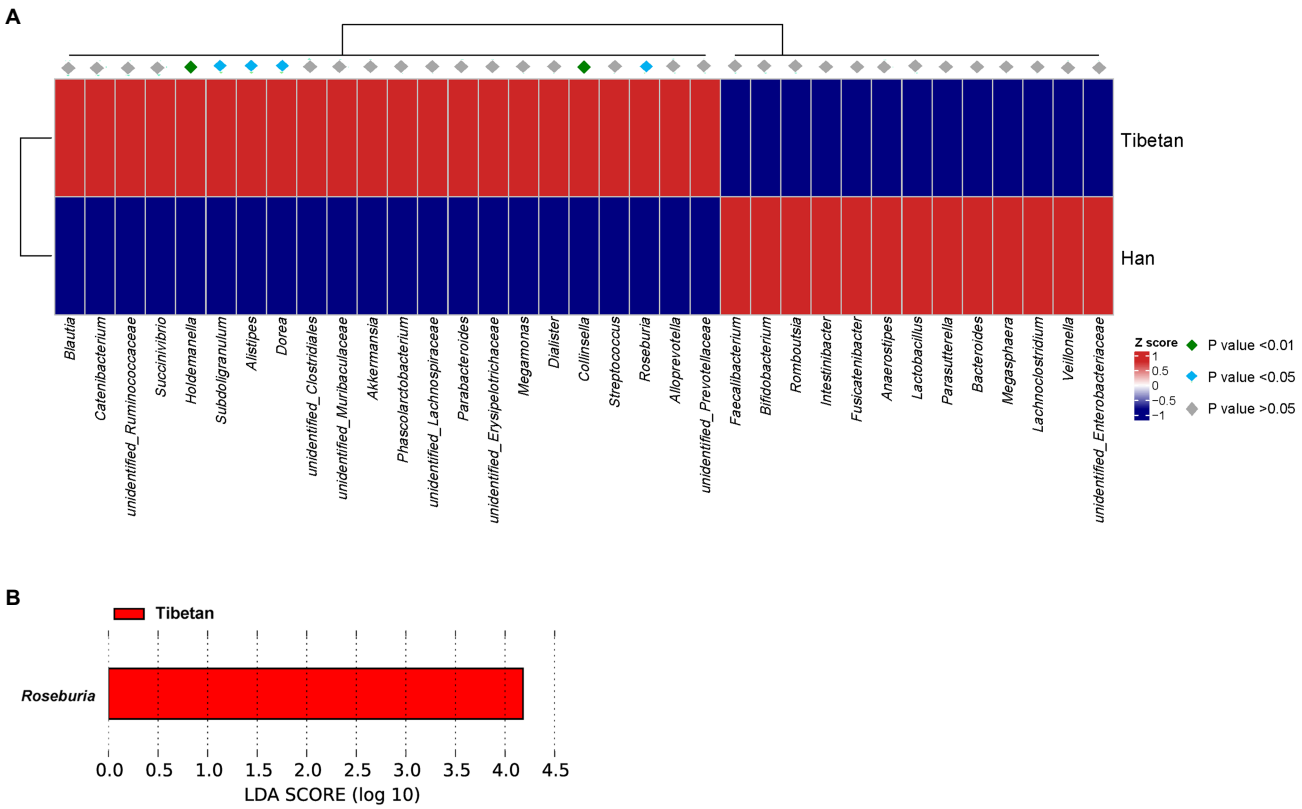

FIGURE 3 | Bacterial taxa that differed significantly between native Tibetans and Han immigrants were identified with: **(A)** a MetaStats analysis, in which the abundances of the 35 most significantly different taxa in the two groups are shown in a heatmap, $p < 0.05$, $q < 0.05$; **(B)** a linear discriminant analysis (LDA) effect size (LEfSe), using the default parameters. A histogram of the LDA scores computed for the bacterial taxa that differed in abundances in the two groups is shown.

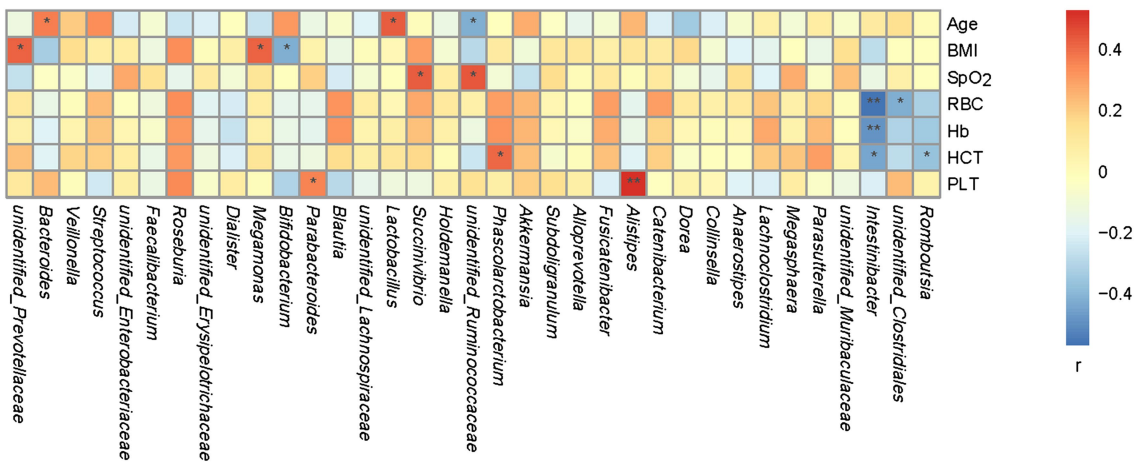

FIGURE 4 | Spearman's association analysis of bacterial genera and age, BMI, SpO_2, RBC, Hb, HCT, and PLT. *r* indicates Spearman's correlation coefficient. Cells are colored based on the value of *r* between significantly altered genera and age, body mass index (BMI), oxyhemoglobin saturation measured with a pulse oximeter (SpO_2), red blood cells (RBC), hemoglobin (Hb), hematokrit (HCT), and platelet count (PLT). Red represents a significantly positive correlation, blue represents a significant negative correlation, and white represents no significant correlation. $^*p < 0.05$; $^{**}p < 0.01$.

are activated by lipid-derived endogenous ligands (Cooper et al., 2017). Cholesterol, cholic acid, ursodeoxycholic acid, deoxycholic acid, and tauroursodeoxycholic acid affect platelet activation through adenosine diphosphate (ADP; Baele et al., 1980; McGregor et al., 1980; Tan et al., 2012). The platelets of highlanders are hyperactive, and the platelet transcriptome

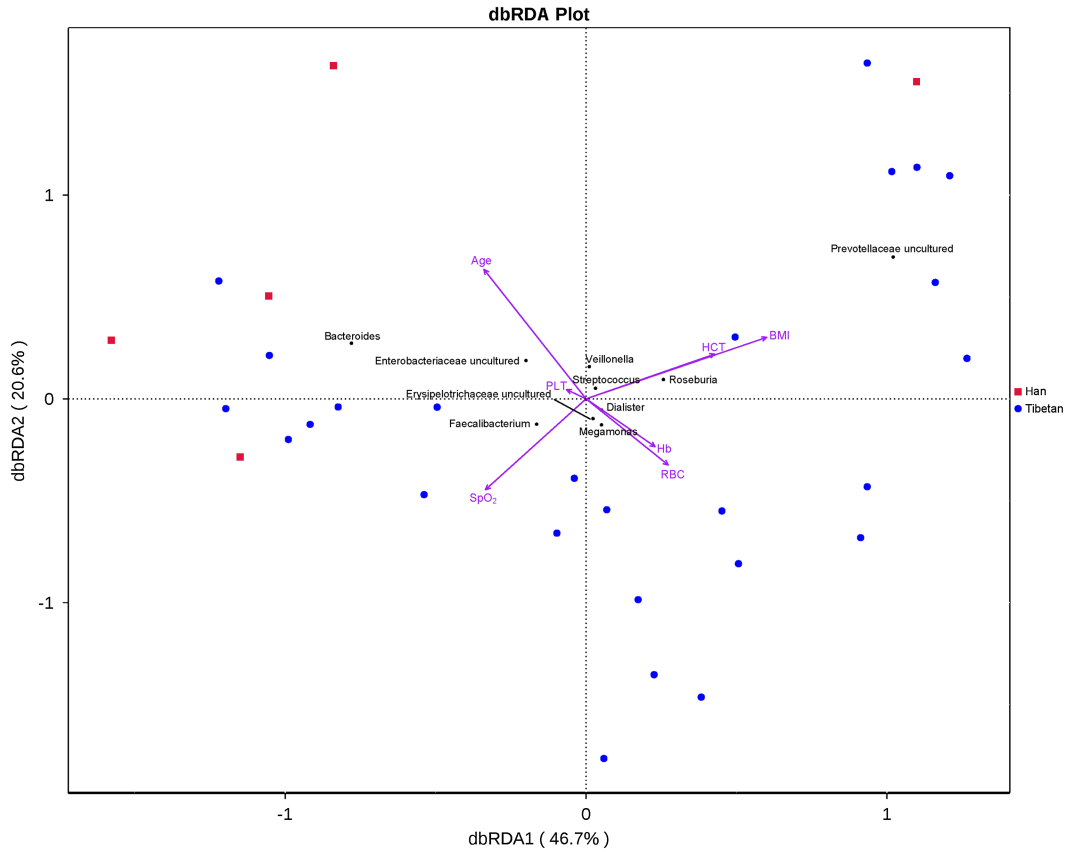

FIGURE 5 | Bray–Curtis distance-based redundancy analysis (dbRDA) of the fecal microbiota and explanatory variables in native Tibetans and Han immigrants.

TABLE 3 | dbRDA envfit analysis of the correlation between fecal microbiota and explanatory variables in native Tibetans and Han immigrants.

	RDA1	RDA2	r^2	*p*
BMI	0.973172	0.230079	0.308357	0.0059
PLT	−0.04598	0.998943	0.434019	0.0005

RDA1 and RDA2 are the cosines of the angles between the arrows of the explanatory variables and the sorting axes. r^2, the goodness of fit statistic, is the squared correlation coefficient.

and proteome are markedly altered under chronic exposure to high altitudes, together with increased circulating ADP (Shang et al., 2019). *Succinivibrio*, which correlated positively with SpO_2, ferments carbohydrates and generates succinate, acetate, formate, and lactate (Bryant, 2015). *Intestinibacter* was negatively associated with RBC, Hb, and HCT and is reportedly associated with resistance to oxidative stress (Forslund et al., 2015). *Romboutsia* was negatively associated with HCT, whereas *Phascolarctobacterium* correlated positively with HCT. *Romboutsia* currently includes three species, and *R. timonensis* has only been isolated from the right colon of a human with a severe anemia. *Phascolarctobacterium* is a producer of SCFAs, including acetate and propionate. The gut microbiota sustains hematopoiesis (Chen et al., 2020). The harvesting of nutrients from the diet is a well-recognized feature of the symbiotic relationship between the microbiota and its host throughout evolution (Baeckhed et al., 2005). A previous study reported that energy harvested from the diet is a critical mechanism by which the gut microbiota contributes to hematopoiesis after bone-marrow transplantation (Staffas et al., 2018) and hematopoietic stem cell transplantation (Staffas and Brink, 2019).

Altitude may exert an important effect on the human energy balance, and the energy demands of highlanders are high (Kayser and Verges, 2013). High F/B ratios and a high proportion of Firmicutes have been shown to be associated with the highly efficient extraction of energy from food (Turnbaugh et al., 2008). Our results show that there were no differences in the high relative abundances of Firmicutes and Bacteroidetes or in the F/B ratios of the Tibetans and Chinese Han living in the same high-altitude area. Similar results were reported by Li and Zhao (2015), who found that the F/B ratio was higher, Firmicutes was significantly more abundant, and Bacteroidetes was significantly less abundant in the intestinal microbiota of Tibetans and Han immigrants living at high altitudes than in Han subjects living at low altitudes. Interestingly, obese people show similar changes in Firmicutes and Bacteroidetes to those

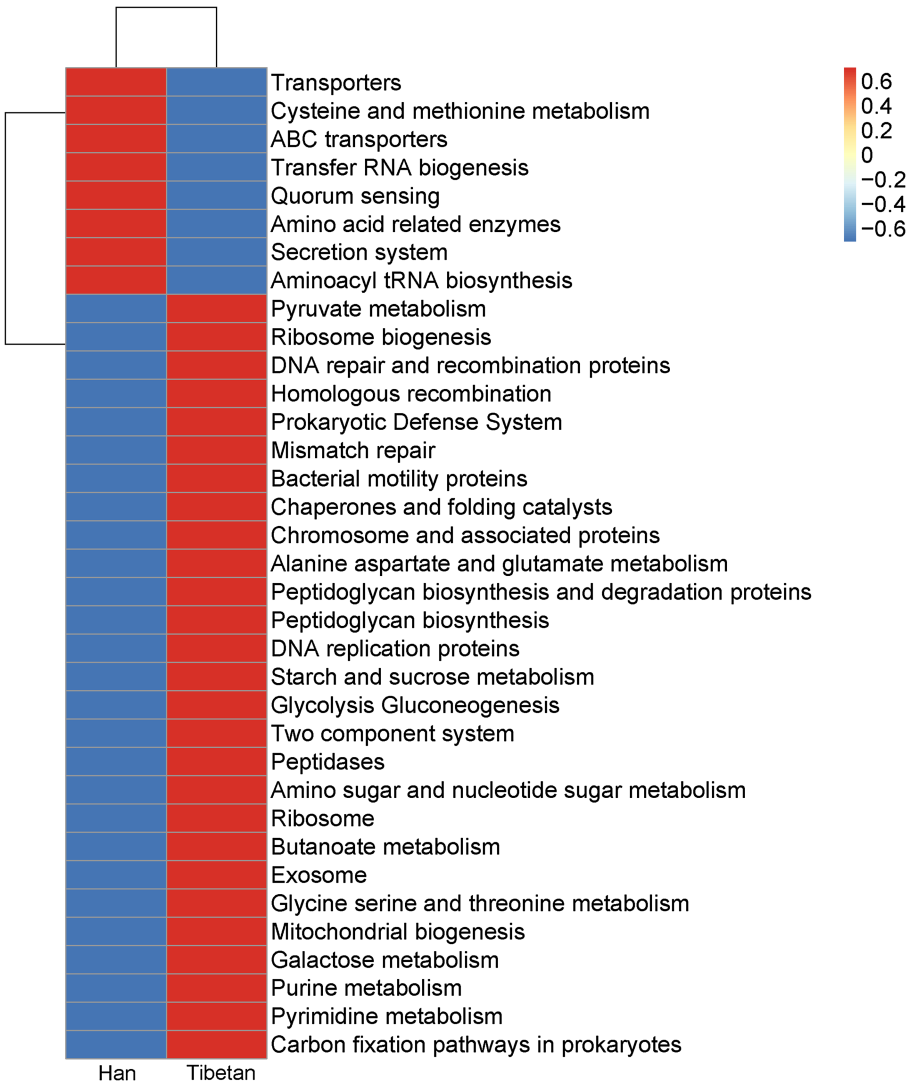

FIGURE 6 | Functional profiles of the fecal microbial communities in native Tibetans and Han immigrants. The 35 most-abundant pathways at the third level of KEGG pathways are shown in a heatmap.

of highlanders with a "normal" BMI according to accepted standards (Tan, 2004; Ley et al., 2006).

In this study, we observed that the genera *Subdoligranulum*, *Roseburia*, *Alistipes*, *Holdemanella*, *Collinsella*, and *Dorea* were significantly more abundant in the fecal bacteria of the native Tibetans than in those of the Han immigrants. *Subdoligranulum* and *Roseburia* produce butyrate from complex carbohydrates and plant polysaccharides (Duncan et al., 2002; Holmstrøm et al., 2004), and butyrate is a major SCFA product from an intestinal source, providing at least 60–70% of the energy requirements of colonocytes (Hamer et al., 2008). SCFAs act not only as energy sources for the colonic epithelium but also as systemic nutrients. SCFA levels can directly affect the substrate and energy metabolism in the peripheral tissues, such as adipose tissues, skeletal muscle, and liver (Canfora et al., 2015). SCFA producers are also responsible for regulating the protection of cells from oxidative stress (Ticinesi et al., 2018). Notably, SCFAs have been shown to contribute to the production of hematopoietic precursors in SPF mice (Trompette et al., 2014). A high-fat diet was associated with an increased abundance of *Alistipes* relative to that associated with a lower-fat diet in healthy young adults in a 6-month randomized, controlled feeding trial (Wan et al., 2019). *Alistipes* is also more abundant in patients with type 2 diabetes (Qin et al., 2012). Tibetans frequently consume high-fat foods, such as buttered tea, cheese, and meat. However, in our study, the Tibetans had normal BMIs and no diabetes. *Holdemanella biformis* is associated with cholesterol, low-density lipoprotein–cholesterol (LDL-C), and free fatty acids (Brahe et al., 2015). The elevated lipid concentration in Tibetans might be attributable to increased lipid synthesis (Ge et al., 2012). *Collinsella* can alter the intestinal absorption of cholesterol, reducing glycogenesis in the liver and increasing triglyceride

synthesis, and the abundance of *Collinsella* correlates positively with circulating insulin (Gomez-Arango et al., 2018). Therefore, it is possible that having more *Subdoligranulum*, *Roseburia*, *Alistipes*, *Holdemanella*, and *Collinsella* in the intestine is beneficial for energy capture. The functional capacity of the intestinal microbial communities in the native Tibetans showed that metabolism, especially carbohydrate metabolism (pyruvate metabolism; butanoate metabolism; alanine, aspartate, and glutamate metabolism; glycolysis and gluconeogenesis; starch and sucrose metabolism; and amino sugar and nucleotide sugar metabolism), is one of the most frequent functional classes annotated at the third level of the KEGG pathways. The metabolisms of pyruvate, butanoate, starch, and sucrose are important in the fermenting of nonabsorbed carbohydrates to SCFAs. Carbohydrate metabolism, rather than lipid metabolism, is increased in the Tibetans (Ge et al., 2012). Like Tibetans, Sherpas are also from the Himalayan region and use the oxidation of carbohydrates over the oxidation of intramyocellular lipids and lipid substrates for their energy needs (Holden et al., 1995; Murray, 2009; Gilbertkawai et al., 2014). Interestingly, Sherpa and Aymara, who are also from high altitudes, have different gut microbiota compositions and potential functions. For example, *Treponema*, *Butyrivibrio*, and *RFN20* characterize the gut microbiota of Sherpa and Aymara, and metabolic functions, such as the synthesis and degradation of ketone bodies, vitamin B6 metabolism, the degradation of caprolactam, and the biosynthesis of the terpenoid backbone and unsaturated fatty acids, are elevated in those two populations (Quagliariello et al., 2019). Genetic, geographic, dietary structural, and cultural differences in the hosts may contribute to the diverse gut microbiota of the different high-altitude populations, supplying suitable strategies for each population to cope with its extreme environment.

We also found that the feces of native Tibetans contain significantly greater bacterial diversity than those of the Han immigrants, whereas there was no significant difference in the microbial community richness in the two groups. Increased diversity and redundancy within a microbial community enhance the stability of the ecosystem, including its resistance to acute toxic effects and its general resilience (Konopka, 2009). As the altitude increases, Tibetans display greater intestinal microbial diversity and richness than Tibetans living at lower altitudes (Lan et al., 2017). However, Han individuals living at high altitudes show a reduction in their total intestinal bacteria compared with those of Han individuals living at lower altitudes (Lan et al., 2017). These findings suggest that the more primitive lifestyle of the Tibetans may be associated with the high microbial diversity and richness observed at higher altitudes than is observed at lower altitudes. Urbanization is also related to a loss of intestinal microbial diversity in humans (Winglee et al., 2017), and the urbanization of Tibetan herdsmen has affected the β-diversity of their microbiota community (Li et al., 2018). The functional redundancy of the microbial community could decrease in Han people who migrate to higher altitudes, thus weakening the stability of the ecosystem.

The study subjects were carefully selected, so that the indigenous Tibetans had been living in Da Ri for generations, and the Han individuals had been living in the same region for more than 1 year. And the Han individuals who enrolled were without travel between Da Ri and low altitudes during their residence. It is the major reason that this study had a limited number of samples in the Han immigrants group. Although this preliminary study was performed on a limited sample size, it extends the series of recent studies of the association between the gut microbiota and high-altitude adaptation/acclimatization, and provides valuable information on the fecal microbial communities and hematological profiles in highlanders. Importantly, future studies must be based on larger sample sizes and confirm the interaction between the gut microbiota and hematopoiesis in high-altitude populations.

CONCLUSION

Our findings on the compositions and diversity of the fecal microbiota in native Tibetans and Han immigrants living at high altitude indicate that the taxa associated with energy metabolism (such as SCFAs production) were more enriched in the fecal microbiota of the natives Tibetan than that of the Han immigrants. Correspondingly, functional annotations related to carbohydrate metabolism (such as SCFAs-related pathways) were also enriched in the fecal microbiota of the native Tibetans relative to those in the Han immigrants. These bacteria probably allow Tibetans to obtain more energy from food to meet their energy demands at high altitude. BMI, age, SpO_2, RBC, Hb, HCT, and PLT correlated with the intestinal microbial community structure in the highlanders. Some taxa (such as *Alistipes* or *Parabacteroides*) showed positive or negative associations with BMI and the hematological parameters. Our study provides valuable insights into the possible relationships between the fecal microbial communities and hematological profiles in Tibetans. The mechanisms underlying the effects of the intestinal microbiota on the hematological parameters in highlanders require further large-scale studies. The range of microbial products that signal to the host to influence normal hematopoiesis and the microbial species from which they derive is yet to be clarified.

DATA AVAILABILITY STATEMENT

The datasets presented in this study can be found in online repositories. The names of the repository/repositories and accession number(s) can be found at FigShare, https://figshare.com/s/f477aa8a35c4ecb9f06a; doi: 10.6084/m9.figshare.14503209.

ETHICS STATEMENT

The studies involving human participants were reviewed and approved by the Ethics Committee of Qinghai University, Xining, China. The patients/participants provided their written informed consent to participate in this study.

AUTHOR CONTRIBUTIONS

YM and SM designed the experiments. YM, QG, and SM performed the experiments. YM analyzed the data and wrote the manuscript. R-LG provided financial support. All authors contributed to the article and approved the submitted version.

FUNDING

This research was supported by the National Natural Science Foundation of China (Nos. 31571231 and 81660707).

ACKNOWLEDGMENTS

We thank Janine Miller, PhD, from Liwen Bianji, Edanz Editing China, for editing the English text of a draft of this manuscript.

SUPPLEMENTARY MATERIAL

The Supplementary Material for this article can be found online at https://www.frontiersin.org/articles/10.3389/fmicb.2021.615416/full#supplementary-material

REFERENCES

Arciero, E., Kraaijenbrink, T., Haber, M., Mezzavilla, M., Ayub, Q., Wang, W., et al. (2018). Demographic history and genetic adaptation in the Himalayan region inferred from genome-wide SNP genotypes of 49 populations. *Mol. Biol. Evol.* 35, 1916–1933. doi: 10.1093/molbev/msy094

Atanu, A., Chiranjit, M., Kuntal, G., Bikas Ranjan, P., and Keshab Chandra, M. (2013). Dynamics of predominant microbiota in the human gastrointestinal tract and change in luminal enzymes and immunoglobulin profile during high-altitude adaptation. *Folia Microbiol.* 58, 523–528. doi: 10.1007/s12223-013-0241-y

AβHauer, K. P., Bernd, W., Rolf, D., and Peter, M. (2015). Tax4Fun: predicting functional profiles from metagenomic 16S rRNA data. *Bioinformatics* 31, 2882–2884. doi: 10.1093/bioinformatics/btv287

Baeckhed, F., Ley, R. E., Sonnenburg, J. L., Peterson, D. A., and Gordon, J. I. (2005). Host-bacterial mutualism in the human intestine. *Science* 307, 1915–1920. doi: 10.1126/science.1104816

Baele, G., Beke, R., and Barbier, F. (1980). In vitro inhibition of platelet aggregation by bile salts. *Thromb. Haemost.* 43, 62–64.

Bai, X., Lu, S., Yang, J., Jin, D., Pu, J., Díaz, M. S., et al. (2018). Precise fecal microbiome of the herbivorous Tibetan antelope inhabiting high-altitude alpine plateau. *Front. Microbiol.* 9:2321. doi: 10.3389/fmicb.2018.02321

Beall, C. M. (2006). Andean, Tibetan, and Ethiopian patterns of adaptation to high-altitude hypoxia. *Integr. Comp. Biol.* 46, 18–24. doi: 10.1093/icb/icj004

Beall, C. M. (2007). Two routes to functional adaptation: Tibetan and Andean high-altitude natives. *Proc. Natl. Acad. Sci. U. S. A.* 104, 8655–8660. doi: 10.1073/pnas.0701985104

Bokulich, N. A., Subramanian, S., Faith, J. J., Gevers, D., Gordon, J. I., Knight, R., et al. (2013). Quality-filtering vastly improves diversity estimates from Illumina amplicon sequencing. *Nat. Methods* 10, 57–59. doi: 10.1038/nmeth.2276

Brahe, L. K., Chatelier, E. L., Prifti, E., Pons, N., Kennedy, S., Hansen, T., et al. (2015). Specific gut microbiota features and metabolic markers in postmenopausal women with obesity. *Nutr. Diabetes* 5:e159. doi: 10.1038/nutd.2015.9

Brigitta, K., Wieland, S., Marcus, S., Andreas, R., Olaf, R., and Monika, K. (2005). Microbial and immunological responses relative to high-altitude exposure in mountaineers. *Med. Sci. Sports Exerc.* 37, 1313–1318. doi: 10.1249/01.mss.0000174888.22930.e0

Bryant, M. P. (2015). "Succinivibrio," in *Bergey's Manual of Systematics of Archaea and Bacteria*. ed. M. P. Bryant (New Jersy, USA: John Wiley & Sons, Inc.), 1–3.

Canfora, E. E., Jocken, J. W., and Blaak, E. E. (2015). Short-chain fatty acids in control of body weight and insulin sensitivity. *Nat. Rev. Endocrinol.* 11, 577–591. doi: 10.1038/nrendo.2015.128

Caporaso, J. G., Kuczynski, J., Stombaugh, J., Bittinger, K., Bushman, F. D., Costello, E. K., et al. (2010). QIIME allows analysis of high-throughput community sequencing data. *Nat. Methods* 7, 335–336. doi: 10.1038/nmeth.f.303

Chen, J., Zhang, S., Feng, X., Wu, Z., and Mock, B. A. (2020). Conventional co-housing modulates murine gut microbiota and hematopoietic gene expression. *Int. J. Mol. Sci.* 21:6143. doi: 10.3390/ijms21239314

Chiu, C.-M., Huang, W.-C., Weng, S.-L., Tseng, H.-C., Liang, C., Wang, W.-C., et al. (2014). Systematic analysis of the association between gut flora and obesity through high-throughput sequencing and bioinformatics approaches. *Biomed. Res. Int.* 2014:906168. doi: 10.1155/2014/906168

Clarke, K. R., and Ainsworth, M. (1993). A method of linking multivariate community structure to environmental variables. *Mar. Ecol. Prog.* 92, 205–219. doi: 10.3354/meps092205

Cooper, A., Singh, S., Hook, S., Tyndall, J. D., and Vernall, A. J. (2017). Chemical tools for studying lipid-binding class AG protein–coupled receptors. *Pharmacol. Rev.* 69, 316–353. doi: 10.1124/pr.116.013243

Desantis, T. Z., Hugenholtz, P., Larsen, N., Rojas, M., Brodie, E. L., Keller, K., et al. (2006). Greengenes, a chimera-checked 16S rRNA gene database and workbench compatible with ARB. *Appl. Environ. Microbiol.* 72, 5069–5072. doi: 10.1128/AEM.03006-05

Duncan, S. H., Hold, G. L., Barcenilla, A., Stewart, C. S., and Flint, H. J. (2002). *Roseburia intestinalis* sp. nov., a novel saccharolytic, butyrate-producing bacterium from human faeces. *Int. J. Syst. Evol. Microbiol.* 52, 1615–1620. doi: 10.1099/00207713-52-5-1615

Edgar, R. C. (2004). MUSCLE: multiple sequence alignment with high accuracy and high throughput. *Nucleic Acids Res.* 32, 1792–1797. doi: 10.1093/nar/gkh340

Edgar, R. C. (2013). UPARSE: highly accurate OTU sequences from microbial amplicon reads. *Nat. Methods* 10, 996–998. doi: 10.1038/nmeth.2604

Edgar, R. C., Haas, B. J., Clemente, J. C., Christopher, Q., and Rob, K. (2011). UCHIME improves sensitivity and speed of chimera detection. *Bioinformatics* 27, 2194–2220. doi: 10.1093/bioinformatics/btr381

Forslund, K., Hildebrand, F., Nielsen, T., Falony, G., Le Chatelier, E., Sunagawa, S., et al. (2015). Disentangling type 2 diabetes and metformin treatment signatures in the human gut microbiota. *Nature* 528, 262–266. doi: 10.1038/nature15766

Ge, R. L., Cai, Q., Shen, Y. Y., San, A., Ma, L., Zhang, Y., et al. (2013). Draft genome sequence of the Tibetan antelope. *Nat. Commun.* 4:1858. doi: 10.1038/ncomms2860

Ge, R. L., Simonson, T. S., Cooksey, R. C., Tanna, U., Qin, G., Huff, C. D., et al. (2012). Metabolic insight into mechanisms of high-altitude adaptation in Tibetans. *Mol. Genet. Metab.* 106, 244–247. doi: 10.1016/j.ymgme.2012.03.003

Gilbertkawai, E. T., Milledge, J. S., Grocott, M. P., and Martin, D. S. (2014). King of the mountains: Tibetan and Sherpa physiological adaptations for life at high altitude. *Physiology* 29, 388–402. doi: 10.1152/physiol.00018.2014

Gomez-Arango, L. F., Barrett, H. L., Wilkinson, S. A., Callaway, L. K., McIntyre, H. D., Morrison, M., et al. (2018). Low dietary fiber intake increases *Collinsella* abundance in the gut microbiota of overweight and obese pregnant women. *Gut Microbes* 9, 189–201. doi: 10.1080/19490976.2017.1406584

Grice, E. A., and Segre, J. A. (2012). The human microbiome: our second genome*. *Annu. Rev. Genomics Hum. Genet.* 13, 151–170. doi: 10.1146/annurev-genom-090711-163814

Haas, B. J., Gevers, D., Earl, A. M., Feldgarden, M., Ward, D. V., Giannoukos, G., et al. (2011). Chimeric 16S rRNA sequence formation and detection in Sanger and 454-pyrosequenced PCR amplicons. *Genome Res.* 21, 494–504. doi: 10.1101/gr.112730.110

Hamer, H. M., Jonkers, D., Venema, K., Vanhoutvin, S., Troost, F. J., and Brummer, R. J. (2008). Review article: the role of butyrate on colonic function. *Aliment. Pharmacol. Ther.* 27, 104–119. doi: 10.1111/j.1365-2036.2007.03562.x

Han, H., Yan, H., and King, K. Y. (2021). Broad-spectrum antibiotics deplete bone marrow regulatory T cells. *Cell* 10:277. doi: 10.3390/cells10020277

Holden, J. E., Stone, C. K., Clark, C. M., Brown, W. D., Nickles, R. J., Stanley, C., et al. (1995). Enhanced cardiac metabolism of plasma glucose in high-altitude natives: adaptation against chronic hypoxia. *J. Appl. Physiol.* 79, 222–228. doi: 10.1152/jappl.1995.79.1.222

Holmstrøm, K., Collins, M. D., Møller, T., Falsen, E., and Lawson, P. A. (2004). *Subdoligranulum variabile* gen. nov., sp. nov. from human feces. *Anaerobe* 10, 197–203. doi: 10.1016/j.anaerobe.2004.01.004

Jianguo, Z., Haifeng, Z., and Zhaonian, Z. (2002). Reserved higher vagal tone under acute hypoxia in Tibetan adolescents with long-term migration to sea level. *Jpn. J. Physiol.* 52, 51–56. doi: 10.2170/jjphysiol.52.51

Josefsdottir, K. S., Baldridge, M. T., Kadmon, C. S., and King, K. Y. (2017). Antibiotics impair murine hematopoiesis by depleting the intestinal microbiota. *Blood* 129, 729–739. doi: 10.1182/blood-2016-03-708594

Kang, L., Zeng, D., Gesang, L., Hong, W., Zhou, Y., Du, Y., et al. (2016). Comparative analysis of gut microbiota of native Tibetan and Han populations living at different altitudes. *PLoS One* 11:e0155863. doi: 10.1371/journal.pone.0155863

Kayser, B., and Verges, S. (2013). Hypoxia, energy balance and obesity: from pathophysiological mechanisms to new treatment strategies. *Obesity Rev.* 14, 579–592. doi: 10.1111/obr.12034

Konopka, A. (2009). What is microbial community ecology? *ISME J.* 3, 1223–1230. doi: 10.1038/ismej.2009.88

Lan, D., Ji, W., Lin, B., Chen, Y., Huang, C., Xiong, X., et al. (2017). Correlations between gut microbiota community structures of Tibetans and geography. *Sci. Rep.* 7:16982. doi: 10.1038/s41598-017-17194-4

Ley, R. E., Turnbaugh, P. J., Samuel, K., and Gordon, J. I. (2006). Microbial ecology: human gut microbes associated with obesity. *Nature* 444, 1022–1023. doi: 10.1038/4441022a

Li, H., Li, T., Beasley, D. A. E., Heděnec, P., Xiao, Z., Zhang, S., et al. (2016). Diet diversity is associated with beta but not alpha diversity of pika gut microbiota. *Front. Microbiol.* 7:1169. doi: 10.3389/fmicb.2016.01169

Li, H., Li, T., Li, X., Wang, G. H., Lin, Q., and Qu, J. (2018). Gut microbiota in Tibetan herdsmen reflects the degree of urbanization. *Front. Microbiol.* 9:1745. doi: 10.3389/fmicb.2018.01745

Li, L., and Zhao, X. (2015). Comparative analyses of fecal microbiota in Tibetan and Chinese Han living at low or high altitude by barcoded 454 pyrosequencing. *Sci. Rep.* 5:14682. doi: 10.1038/srep18610

Lorenzo, F. R., Huff, C., Myllymäki, M., Olenchock, B., Swierczek, S., Tashi, T., et al. (2014). A genetic mechanism for Tibetan high-altitude adaptation. *Nat. Genet.* 46, 951–956. doi: 10.1038/ng.3067

Lucking, E. F., O'Connor, K. M., Strain, C. R., Fouhy, F., Bastiaanssen, T. F. S., Burns, D. P., et al. (2018). Chronic intermittent hypoxia disrupts cardiorespiratory homeostasis and gut microbiota composition in adult male guinea-pigs. *EBioMedicine* 38, 191–205. doi: 10.1016/j.ebiom.2018.11.010

Magoč, T., and Salzberg, S. L. (2011). FLASH: fast length adjustment of short reads to improve genome assemblies. *Bioinformatics* 27, 2957–2963. doi: 10.1093/bioinformatics/btr507

McGregor, L., Morazain, R., and Renaud, S. (1980). A comparison of the effects of dietary short and long chain saturated fatty acids on platelet functions, platelet phospholipids, and blood coagulation in rats. *Lab. Investig.* 43, 438–442.

Meyer, M., Aldenderfer, M., Wang, Z., Hoffmann, D., Dahl, J., Degering, D., et al. (2017). Permanent human occupation of the central Tibetan Plateau in the early Holocene. *Science* 355, 64–67. doi: 10.1126/science.aag0357

Million, M., Maraninchi, M., Henry, M., Armougom, F., Richet, H., Carrieri, P., et al. (2012). Obesity-associated gut microbiota is enriched in *Lactobacillus reuteri* and depleted in *Bifidobacterium animalis* and *Methanobrevibacter smithii*. *Int. J. Obes.* 36, 817–825. doi: 10.1038/ijo.2011.153

Moore, L. G., Niermeyer, S., and Zamudio, S. (2010). Human adaptation to high altitude: regional and life-cycle perspectives. *Am. J. Phys. Anthropol.* 107, 25–64. doi: 10.1002/(sici)1096-8644(1998)107:27+<25::aid-ajpa3>3.0.co;2-l

Murray, A. J. (2009). Metabolic adaptation of skeletal muscle to high altitude hypoxia: how new technologies could resolve the controversies. *Genome Med.* 1:117. doi: 10.1186/gm117

Muza, S. R., Beidleman, B. A., and Fulco, C. S. (2010). Altitude preexposure recommendations for inducing acclimatization. *High Alt. Med. Biol.* 11, 87–92. doi: 10.1089/ham.2010.1006

Qian-Qian, P., Zhuoma, B., Chao-Ying, C., Lei, L., Ji, Q., Quzhen, G., et al. (2013). Physiological responses and evaluation of effects of BMI, smoking and drinking in high altitude acclimatization: a cohort study in Chinese Han young males. *PLoS One* 8:e79346. doi: 10.1371/journal.pone.0079346

Qin, J., Li, Y., Cai, Z., Li, S., Zhu, J., Zhang, F., et al. (2012). A metagenome-wide association study of gut microbiota in type 2 diabetes. *Nature* 490, 55–60. doi: 10.1038/nature11450

Quagliariello, A., Paola, M., Fanti, S. D., Gnecchi-Ruscone, G. A., and Filippo, C. D. (2019). Gut microbiota composition in Himalayan and Andean populations and its relationship with diet, lifestyle and adaptation to the high-altitude environment. *J. Anthropol. Sci.* 96, 189–208. doi: 10.4436/JASS.97007

Roach, R. C., Hackett, P. H., Oelz, O., Bärtsch, P., Luks, A. M., Macinnis, M. J., et al. (2018). The 2018 Lake Louise acute mountain sickness score. *High Alt. Med. Biol.* 19, 4–6. doi: 10.1089/ham.2017.0164

Rocke, A., Paterson, G., Barber, M., Jackson, A., Main, S., Stannett, C., et al. (2018). Thromboelastometry and platelet function during acclimatization to high altitude. *Thromb. Haemost.* 118, 63–71. doi: 10.1160/TH17-02-0138

Ruth, E. L., Fredrik, B. C., Peter, T., Catherine, A. L., Robin, D. K., and Jeffrey, I. G. (2005). Obesity alters gut microbial ecology. *Proc. Natl. Acad. Sci. U. S. A.* 102, 11070–11075. doi: 10.1073/pnas.0504978102

Segata, N., Izard, J., Waldron, L., Gevers, D., Miropolsky, L., Garrett, W. S., et al. (2011). Metagenomic biomarker discovery and explanation. *Genome Biol.* 12:R60. doi: 10.1186/gb-2011-12-6-r60

Shang, C., Wuren, T., Ga, Q., Bai, Z., Guo, L., Eustes, A. S., et al. (2019). The human platelet transcriptome and proteome is altered and pro-thrombotic functional responses are increased during prolonged hypoxia exposure at high altitude. *Platelets* 31, 33–42. doi: 10.1080/09537104.2019.1572876

Sheik, C. S., Mitchell, T. W., Rizvi, F. Z., Rehman, Y., Faisal, M., Hasnain, S., et al. (2012). Exposure of soil microbial communities to chromium and arsenic alters their diversity and structure. *PLoS One* 7:e40059. doi: 10.1371/journal.pone.0040059

Simonson, T., Yang, Y., Huff, C., Yun, H., Qin, G., Witherspoon, D., et al. (2010). Genetic evidence for high-altitude adaptation in Tibet. *Science* 329, 72–75. doi: 10.1126/science.1189406

Sohail, M. U., Yassine, H. M., Sohail, A., and Thani, A. (2019). Impact of physical exercise on gut microbiome, inflammation, and the pathobiology of metabolic disorders. *Rev. Diabet. Stud.* 15, 35–48. doi: 10.1900/RDS.2019.15.35

Staffas, A., and Brink, M. (2019). The intestinal flora is required for post-transplant hematopoiesis in recipients of a hematopoietic stem cell transplantation. *Bone Marrow Transplant.* 54, 756–758. doi: 10.1038/s41409-019-0612-3

Staffas, A., da Silva, M. B., Slingerland, A. E., Lazrak, A., Bare, C. J., Holman, C. D., et al. (2018). Nutritional support from the intestinal microbiota improves hematopoietic reconstitution after bone marrow transplantation in mice. *Cell Host Microbe* 23, 447–457. doi: 10.1016/j.chom.2018.03.002

Storz, J. F. (2021). High-altitude adaptation: mechanistic insights from integrated genomics and physiology. *Mol. Biol. Evol.* 1–15. doi: 10.1093/molbev/msab064 [Epub ahead of print].

Tan, J., Reddy, E., Murphy, D., Keely, S., and O'Neill, S. (2012). "Bile acids differentially impact on platelet activation." in *BMC Proceedings. Vol. 6*. November 4–5, 2011; Dublin, Ireland (Springer).

Tan, K. (2004). Appropriate body-mass index for Asian populations and its implications for policy and intervention strategies." *Lancet* 363, 157–163. doi: 10.1016/S0140-6736(03)15268-3

Tianyi, W. U., and Kayser, B. (2006). High altitude adaptation in Tibetans. *High Alt. Med. Biol.* 7, 193–208. doi: 10.1089/ham.2006.7.193

Ticinesi, A., Milani, C., Guerra, A., Allegri, F., Lauretani, F., Nouvenne, A., et al. (2018). Understanding the gut–kidney axis in nephrolithiasis: an analysis of the gut microbiota composition and functionality of stone formers. *Gut* 67, 2097–2106. doi: 10.1136/gutjnl-2017-315734

Tremaroli, V., and Bäckhed, F. (2012). Functional interactions between the gut microbiota and host metabolism. *Nature* 489, 242–249. doi: 10.1038/nature11552

Trompette, A., Gollwitzer, E. S., Yadava, K., Sichelstiel, A. K., Sprenger, N., Ngom-Bru, C., et al. (2014). Gut microbiota metabolism of dietary fiber influences allergic airway disease and hematopoiesis. *Nat. Med.* 20, 159–166. doi: 10.1038/nm.3444

Turnbaugh, P. J., Backhed, F., Fulton, L., and Gordon, J. I. (2008). Diet-induced obesity is linked to marked but reversible alterations in the mouse distal gut microbiome. *Cell Host Microbe* 3, 213–223. doi: 10.1016/j.chom.2008.02.015

Turnbaugh, P. J., Ley, R. E., Mahowald, M. A., Magrini, V., Mardis, E. R., and Gordon, J. I. (2006). An obesity-associated gut microbiome with increased capacity for energy harvest. *Nature* 444, 1027–1031. doi: 10.1038/nature05414

Wan, Y., Wang, F., Yuan, J., Li, J., Jiang, D., Zhang, J., et al. (2019). Effects of dietary fat on gut microbiota and faecal metabolites, and their relationship with cardiometabolic risk factors: a 6-month randomised controlled-feeding trial. *Gut* 68, 1417–1429. doi: 10.1136/gutjnl-2018-317609

Wang, K., Liao, M., Zhou, N., Bao, L., Ma, K., Zheng, Z., et al. (2019). *Parabacteroides distasonis* alleviates obesity and metabolic dysfunctions via production of succinate and secondary bile acids. *Cell Rep.* 26, 222.e5–235.e5. doi: 10.1016/j.celrep.2018.12.028

Wang, Q., Garrity, G. M., Tiedje, J. M., and Cole, J. R. (2007). Naive Bayesian classifier for rapid assignment of rRNA sequences into the new bacterial taxonomy. *Appl. Environ. Microbiol.* 73, 5261–5267. doi: 10.1128/AEM.00062-07

West, J. B., Schoene, R. B., Luks, A. M., and Milledge, J. S. (2012). *High Altitude Medicine and Physiology*. Boca Raton: CRC Press.

White, J. R., Nagarajan, N., and Pop, M. (2009). Statistical methods for detecting differentially abundant features in clinical metagenomic samples. *PLoS Comput. Biol.* 5:e1000352. doi: 10.1371/journal.pcbi.1000352

Winglee, K., Howard, A. G., Sha, W., Gharaibeh, R. Z., Liu, J., Jin, D., et al. (2017). Recent urbanization in China is correlated with a Westernized microbiome encoding increased virulence and antibiotic resistance genes. *Microbiome* 5:121. doi: 10.1186/s40168-017-0338-7

Yang, Y., Zha-Xi, D. J., Mao, W., Zhi, G., Feng, B., and Chen, Y. D. (2018). Comparison of echocardiographic parameters between healthy highlanders in Tibet and lowlanders in Beijing. *High Alt. Med. Biol.* 19, 259–264. doi: 10.1089/ham.2017.0094

Zhang, Q., Gou, W., Wang, X., Zhang, Y., Ma, J., Zhang, H., et al. (2016a). Genome resequencing identifies unique adaptations of Tibetan chickens to hypoxia and high-dose ultraviolet radiation in high-altitude environments. *Genome Biol. Evol.* 8, 765–776. doi: 10.1093/gbe/evw032

Zhang, W., Jiao, L., Liu, R., Zhang, Y., Ji, Q., Zhang, H., et al. (2019). The effect of exposure to high altitude and low oxygen on intestinal microbial communities in mice. *PLoS One* 13:e0203701. doi: 10.1371/journal.pone.0203701

Zhang, Z., Xu, D., Li, W., Hao, J., Wang, J., Xin, Z., et al. (2016b). Convergent evolution of rumen microbiomes in high-altitude mammals. *Curr. Biol.* 26, 1873–1879. doi: 10.1016/j.cub.2016.05.012

Zhao, P., Xu, X., Chen, F., Guo, X., Zheng, X., Liu, L., et al. (2018). The third atmospheric scientific experiment for understanding the earth–atmosphere coupled system over the Tibetan Plateau and its effects. *Bull. Am. Meteorol. Soc.* 99, 757–776. doi: 10.1175/BAMS-D-16-0050.1

Zhao, Q., Ding, Y., Wang, J., Gao, H., Zhang, S., Zhao, C., et al. (2019). Projecting climate change impacts on hydrological processes on the Tibetan Plateau with model calibration against the glacier inventory data and observed streamflow. *J. Hydrol.* 573, 60–81. doi: 10.1016/j.jhydrol.2019.03.043

Conflict of Interest: The authors declare that the research was conducted in the absence of any commercial or financial relationships that could be construed as a potential conflict of interest.

frontiers in Microbiology

PERSPECTIVE
published: 10 February 2022
doi: 10.3389/fmicb.2021.709421

Altered Ecology of the Respiratory Tract Microbiome and Nosocomial Pneumonia

Ana Elena Pérez-Cobas[1]*, *Fernando Baquero*[1,2], *Raúl de Pablo*[3], *María Cruz Soriano*[3] and *Teresa M. Coque*[1,4]

[1] Department of Microbiology, Ramón y Cajal Institute for Health Research (IRYCIS), Ramón y Cajal University Hospital, Madrid, Spain, [2] CIBER in Epidemiology and Public Health (CIBERESP), Madrid, Spain, [3] Intensive Care Department, Ramón y Cajal University Hospital, Madrid, Spain, [4] CIBER in Infectious Diseases (CIBERINFEC), Madrid, Spain

Nosocomial pneumonia is one of the most frequent infections in critical patients. It is primarily associated with mechanical ventilation leading to severe illness, high mortality, and prolonged hospitalization. The risk of mortality has increased over time due to the rise in multidrug-resistant (MDR) bacterial infections, which represent a global public health threat. Respiratory tract microbiome (RTM) research is growing, and recent studies suggest that a healthy RTM positively stimulates the immune system and, like the gut microbiome, can protect against pathogen infection through colonization resistance (CR). Physiological conditions of critical patients and interventions as antibiotics administration and mechanical ventilation dramatically alter the RTM, leading to dysbiosis. The dysbiosis of the RTM of ICU patients favors the colonization by opportunistic and resistant pathogens that can be part of the microbiota or acquired from the hospital environments (biotic or built ones). Despite recent evidence demonstrating the significance of RTM in nosocomial infections, most of the host-RTM interactions remain unknown. In this context, we present our perspective regarding research in RTM altered ecology in the clinical environment, particularly as a risk for acquisition of nosocomial pneumonia. We also reflect on the gaps in the field and suggest future research directions. Moreover, expected microbiome-based interventions together with the tools to study the RTM highlighting the "omics" approaches are discussed.

Keywords: respiratory tract microbiome (RTM), ecology, nosocomial pneumonia, intensive care unit (ICU), dysbiosis, antibiotic resistance genes (ARGs)

OPEN ACCESS

Edited by:
Lucas David Bowler, University of Brighton, United Kingdom

Reviewed by:
Felipe Hernandes Coutinho, Spanish National Research Council (CSIC), Spain
Teresa Nogueira, Instituto Nacional Investigaciao Agraria e Veterinaria (INIAV), Portugal

***Correspondence:**
Ana Elena Pérez-Cobas
anaelena.perez@salud.madrid.org

Specialty section:
This article was submitted to Microbial Symbioses, a section of the journal Frontiers in Microbiology

Received: *13 May 2021*
Accepted: *21 December 2021*
Published: *10 February 2022*

Citation:
Pérez-Cobas AE, Baquero F, de Pablo R, Soriano MC and Coque TM (2022) Altered Ecology of the Respiratory Tract Microbiome and Nosocomial Pneumonia. Front. Microbiol. 12:709421. doi: 10.3389/fmicb.2021.709421

INTRODUCTION

The respiratory tract is an organ system that goes from the nostrils to the lung alveoli. It is divided into the suprathoracic (upper) respiratory tract (URT) and the intrathoracic (lower) respiratory tract (LRT) with a surface of roughly 100 square meters (Ross and Pawlina, 2016). Through the years, several studies have revealed the existence of a resident microbial ecosystem inhabiting airway surfaces: the respiratory tract microbiome (RTM) (Man et al., 2017), is particularly dense in the URT. As the gastrointestinal microbiome (GIM), the RTM constitutes a continuous ecosystem with a longitudinal and transversal gradient of microbial diversity from the nasal and oral cavities to the alveoli (Bassis et al., 2015). However, RTM and GIM differ in biomass, diversity and taxonomic composition. In healthy individuals, the complexity and biomass of the GIM increase from the

stomach to the colon, reaching up to 10^{10}-10^{12} CFUs/mL (Martinez-Guryn et al., 2019). In the RTM, the oropharynx has a high bacterial density (10^7-10^8 CFU/ml), but when moving from the mouth to the lungs, there is a progressive decrease, reaching 10^4-10^5 bacterial cells per mL of alveolar intraluminal fluid (Schneeberger et al., 2019). The RTM composition is influenced by the local microbiological growth conditions determined by the nutrient availability, the micro-geography, and the physicochemical conditions such as the mucociliary escalator, oxygen tension, blood flow, pH, temperature, human immune system interactions, and environmental factors (Dickson et al., 2014). The primary source of microorganisms of the RTM is the oropharynx, eventually migrating to the LRT by microaspiration and mucosal dispersion (Bassis et al., 2015; Venkataraman et al., 2015; Dickson et al., 2017). A current model of the ecology of the RTM is known as the "adapted island model of the lung" (Dickson et al., 2014), and it resembles a biogeographical process, which is derived from the equilibrium model proposed by MacArthur and Wilson (1963) of island biogeography (MacArthur and Wilson, 1963). The "adapted model" indicates that the microbial richness in the RTM is based on the balance of immigration (mucosal extension, micro-aspiration) and elimination (ciliary clearance, cough, antimicrobial immunity mechanisms) of species to the lung from the URT. Basically, the RTM structure depends on the rates of stochastic migration, growth, extinction, and epidemic propagation of members of the microbial community, processes that are influenced by anatomical, physiological and clinical factors (Dickson et al., 2014, 2015). This model would help to explain the gradient of microbial diversity, biomass, and complexity decreasing from the oral cavity to the lung. Dickson and colleagues stated that, in health, the lung microbiome is more influenced by microbial immigration and elimination than by local growing conditions. However, local growth conditions are more critical during advanced clinical diseases. This microbiome-based ecological model provides a theoretical framework for pathogen infection, more accurate than the traditional view of pneumonia based on the rapid growth of an invader to a sterile lung.

The bacterial composition of the healthy RTM mainly comprises Firmicutes, Bacteroidetes, and Proteobacteria, which are three of the four predominant phyla in all human site-specific microbiomes. The most abundant genera are *Streptococcus*, *Prevotella*, or *Veillonella*, which also predominate in the oral microbiome (Araghi, 2020). Only a few studies have characterized other RTM members as fungi, archaea, or viruses (Marsland and Gollwitzer, 2014; Man et al., 2017). With the possible exception of Saccharomycetes (as the genus *Candida*) in the oropharynx, it is difficult to ascertain if at lower (sub-tracheal) levels there is a normal established "respiratory mycobiome," if the fungi found in the RTM correspond to inhaled environmental fungi, or if a subset of them is less prone to physiological clearance. The healthy respiratory mycobiome is enriched in environmental fungi from the phyla Ascomycota and Basidiomycota, the most common also in the GIT (Tipton et al., 2017). Many fungi correspond to Eremothecium, Systenostrema, Cladosporium genera, and Davidiellaceae family that, together with Saccharomycetes, are also the most common taxa in the GIT. The LRT's virome remains largely unexplored, especially in healthy people. Nonetheless, similar to the gut virome, eukaryotic viruses and many bacteriophages have been described in different studies (Marsland and Gollwitzer, 2014; Mitchell et al., 2016). Some studies point to a function of the respiratory virome in priming and modulating host immune response, as well as the control of other microbial species within the lungs (Mitchell et al., 2016). The factors shaping the virome diversity remain unknown, although the its composition in the respiratory tract appears to be determined by the host health and the presence of specific resident bacterial populations in the bronchi, as it has been suggested in cystic fibrosis (Willner et al., 2009, 2012). A metagenomic study of the virome after lung transplantation based on allograft bronchoalveolar lavage (BAL) samples showed that the respiratory tracts of lung transplant recipients were enriched in complex populations of anelloviruses (Young et al., 2015). Viral loads have also been correlated with bacterial dysbiosis which influences transplant outcomes and suggests that viral-bacterial interactions are critical for microbiome-immune system equilibrium and, thus, to its physiology. Moreover, the high abundance of bacteriophages in the RTM deserves in-depth research to determine if they play similar roles as those observed in the GIM, namely, controlling microbial homeostasis (blooms, microbial composition, diversity, metabolism, and facilitating horizontal gene transfer (HGT) (Maurice, 2019; Sutton and Hill, 2019). Methanogenic archaea have been detected in the nasal, GIT, skin, and lung microbiomes, and the phylum Woesearchaeota is apparently associated with the lungs (Koskinen et al., 2017). However, besides a few descriptive studies, the function of the non-bacterial fraction of the RTM deserves to be further analyzed.

The RTM ecology is an emerging research area gaining attention since several studies showed the beneficial role of microbial inhabitants in the stimulation of the immune system and the protection against pathogen (colonization resistance, CR), as it has been extensively documented for the intestinal microbiome (examples reported by Thibeault et al., 2021). The microbiome homeostasis can be transiently disturbed, for instance, by antibiotic usage, application of medical equipment (intubation, ventilators), transient abnormal events (aspiration), or particular diseases (viral diseases might reduce the effectiveness of the bronchial clearance escalator) allowing some pathogens to overgrow and boosting the colonization and, ultimately to cause infection at LRT. Most of the studies related to the RTM have been focused on particular chronic respiratory diseases, such as microbial populations colonizing the lung in cystic fibrosis (reviewed in O'Toole, 2018; Françoise and Héry-Arnaud, 2020). In this disease, the respiratory tract hyper viscosity promotes polymicrobial proliferation and dysbiosis along the respiratory tract (Françoise and Héry-Arnaud, 2020). The most frequent bacteria associated with cystic fibrosis chronic colonization are *Pseudomonas aeruginosa*, *Staphylococcus aureus*, *Stenothrophomonas maltophilia*, *Burkholderia*, and *Pandoraea*, which frequent co-colonize. However, oral-cavity-related microorganisms are also present as *Actinomyces*, *Fusobacterium*, *Gemella*, *Granulicatella*, *Neisseria*, *Porphyromonas*, *Prevotella*, *Rothia*, *Streptococcus*, *Haemophilus*,

or *Veillonella*. Interestingly, predator bacteria in the RTM-LRT as *Bdellovibrio* and *Vampirovibrio*, and bacterial parasites of the phylum Parcubacteria can be found in cystic fibrosis patients (Caballero et al., 2017), This last work suggests a possible role of predator bacteria from the RTM in controlling chronic colonization by pathogens in early colonization stages of cystic fibrosis, highlighting the involvement of the RTM bacterial fraction in fighting pathogenic bacterial populations.

Here, we present our perspective regarding research in altered RTM ecology in the clinical environment, increasing the probability for acquiring nosocomial pneumonia in high-risk hospital areas as ICUs, and discuss recent advances on the topic. We also discuss the gaps in the field, the future of microbiome-based interventions to prevent and treat nosocomial pneumonia, and the contribution of "omics" approaches to understanding the role of the RTM dynamics in the onset of respiratory infections.

THE RESPIRATORY MICROBIOME ECOLOGY IN NOSOCOMIAL PNEUMONIA

Acute LRT infections, pneumonia or exacerbations of chronic bronchitis, are the leading cause of mortality and morbidity worldwide (Troeger et al., 2018). In the elderly, the progression of pneumonia happens fast, with poor prognosis, primarily associated with hospitalization, and high mortality rate frequently in ICUs (Henig and Kaye, 2017). Nosocomial pneumonia, a lung alveoli infection that mostly bacteria, but also viruses, or fungi can cause comprises hospital-acquired and ventilator-associated pneumonia and is of significant public health concern since it is frequently caused by multidrug-resistant (MDR) pathogens acquired within the hospital environment (Denys and Relich, 2014). Ventilator-associated pneumonia is the first cause of nosocomial infection in mechanically ventilated patients and the second most common one at intensive care units (ICU), with long-term infections often caused by MDR bacteria (Kalanuria et al., 2014). This scenario has worsened during the COVID-19 pandemic due to the dramatic increase in SARS-CoV-2 secondary infections and the over-use of antibiotics, leading to a remarkable increase of MDR infections and antibiotic resistance gene (ARGs) transmission (Feldman and Anderson, 2021; Langford et al., 2021; Soriano et al., 2021). The microbiome's contribution to innate and adaptive immune responses suggests that a healthy microbiome may be a factor contributing to a lower case fatality ratio from COVID-19 (Khatiwada and Subedi, 2020; Janda et al., 2021). On the other hand, microbiome dysbiosis could be associated with poor immune response and worse disease outcomes (Stavropoulou et al., 2021). The field is new and available studies regarding the COVID-19 microbiome have reported contradictory results (Yamamoto et al., 2021). One of the factors leading to contradictions seems to be confounders such as mechanical ventilation in ICU patients, altering the RTM community structure, including the abundance of oral taxa previously associated with COVID-19 (Lloréns-Rico et al., 2021). Studies sampling the infected lungs directly through bronchoscopy have proven to be the most accurate so far for identifying microbiological and immunologic alveolar signatures associated with SARS-CoV-2 infection (Dickson, 2021). A work based on 142 patients who underwent bronchoscopy showed that clinical outcomes could be partly explained by alveolar viral abundance, and colonization by URT microbiome-derived bacteria (*Mycoplasma salivarium*), and poor adaptive immune response (Sulaiman et al., 2021).

An ecological model of pneumonia proposes that the RTM equilibrium is displaced toward a state of dysbiosis characterized by low microbial diversity, high microbial burden, and host inflammatory response (Dickson et al., 2014). Whether dysbiosis is the cause or the effect of the pneumonic disease remains obscure. In fact, the role and dynamics of the RTM microbiome in critical patients have been scarcely investigated, and therefore microbiome-directed interventions have not been included in clinical guidelines. Certainly, RTM disruption can be influenced by physiological circumstances altering the local ecology (Dickson et al., 2016), including: (1) inflammation, alteration of metabolites profile, and weakened local defense mechanisms by infections (i.e., virus), favoring bacterial stochastic migration and growth (Madhi and Klugman, 2004; Gu et al., 2019); (2) abnormal chemical composition of the bronchi, as in cystic fibrosis (Goldman et al., 1997); (3) anatomical abnormalities and other conditions leading to obstruction, as in bronchiectasis, cystic fibrosis, chronic obstructive lung disease, pulmonary edema (which can be secondary to sepsis), or lung cancer (Hogg et al., 1970; Peteranderl et al., 2017; Vengoechea et al., 2019); (4) external harmful conditions, as long-term exposure to cold, leading to mucosal vasoconstriction in the respiratory tract mucosa and suppression of immune responses, or allergenic drivers for asthma (Depner et al., 2017); (5) increased bacterial migration (i.e., thorough aspiration of gastric fluids, altered oral microbiome, intubation, unconsciousness, supine position), and decreased elimination process (unconsciousness, intubation, sedatives, head raised, impaired mucociliary clearance) (Dickson, 2016); (6) underlying diseases and medical interventions (i.e., therapeutical immunosuppression, intubation, mechanical ventilation, or long-term antibiotic therapy) favoring colonization of opportunistic pathogens.

Nosocomial pneumonia can be endogenous, caused by opportunistic pathogens as *Streptococcus pneumoniae* or *Haemophilus influenzae*, which are part of the healthy human RTM. This pneumonia generally appears soon after admission. However, late-onsent cases of pneumonia development frequently involve hospital-acquired MDR pathogens, including *P. aeruginosa*, Enterobacteriaceae producing extended-spectrum-beta-lactamases (ESBL), and/or carbapenemases, and methicillin-resistant *Staphylococcus aureus* (MRSA), which are often selected and spread in the ICU environment (Denys and Relich, 2014). The pathogen-centric view of infectious diseases has recently moved toward an ecological perspective based on host-pathogen-microbiome-environment interactions (Wu and Segal, 2018). In this context, nosocomial pneumonia represents a complex scenario where several factors may play a role in the onset and the outcome of the infection (**Figure 1**).

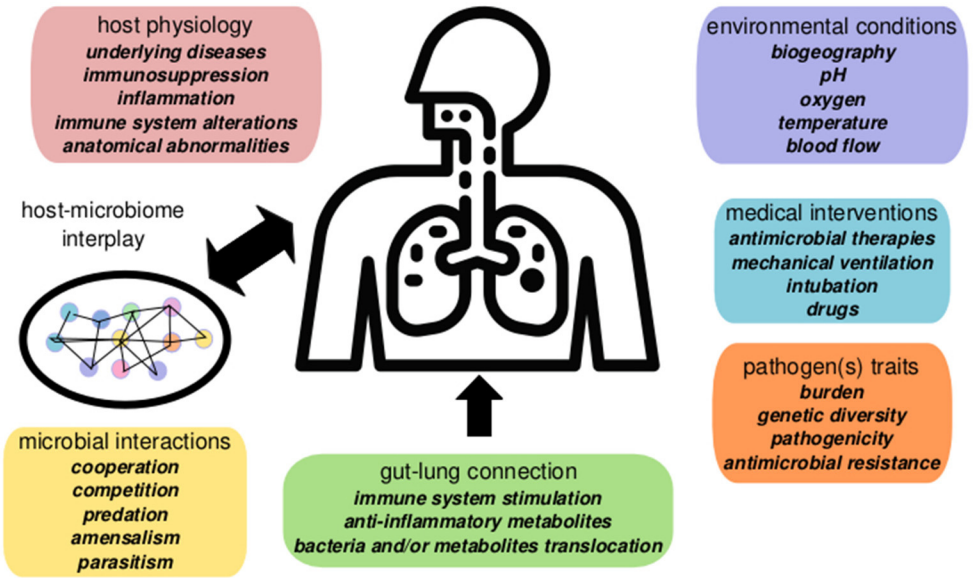

FIGURE 1 | Summary of factors involved in nosocomial pneumonia dynamics in critical patients. Pneumonia evolution and outcome are influenced by host interplay with the respiratory microbiome determined by the microenvironment, microbial interactions, and host physiology. The gut microbiome contributes to pneumonia responses via the gut-lung axis (gut microbiome changes alter systemic and lung physiology). Environmental conditions and clinical factors, as mechanical ventilation, or antibiotics, also play a significant role in disease, altering the microbiome ecology and the pathogen(s) population dynamics.

EFFECT OF ANTIBIOTICS AND OTHER MEDICAL INTERVENTIONS IN THE RTM OF CRITICAL PATIENTS

The intense use of broad-spectrum antibiotics in the ICU favors the selection of resistant bacteria (i.e., *P. aeruginosa*, MRSA, multi-resistant Enterobacterales) or paranasal viruses established in the oral-nasopharyngeal cavity, which can colonize and eventually cause respiratory infections (Bert and Lambert-Zechovsky, 1996; Volakli et al., 2010). In this respect, RTM contribution to pneumonia development and severity, or the eventual implication in the transmission of antimicrobial resistance (AMR) remains poorly analyzed. As well as systemic alteration through depletion of the GIT microbiome, antibiotic usage locally affects the RTM during respiratory infections, especially in ventilated-associated pneumonia (Fernández-Barat et al., 2020). The administration of antimicrobial drugs transiently disrupts the RTM homeostasis and thus, impair CR capacity (Fernández-Barat et al., 2020; Pettigrew et al., 2020). It results in local selection and overgrowth of resistant pathogenic and opportunistic species, increasing the chances of co-infections. However, the effects of doses, the length of therapy, the route of administration, and the spectrum of the antibiotics in the ecology of RTM have not been fully characterized, especially considering that classic antibiotic therapy of respiratory tract infections is directed to pathogen eradication (Dagan et al., 2001; Ball et al., 2002). Further research on the influence of common antibiotics used in ICU medicine on RTM composition and resistome is necessary to implement more efficient interventions.

Moreover, the ARG reservoirs and transmission mechanisms in the human respiratory microbiome remain poorly characterized, particularly in ICU patients (Kim and Cha, 2021). An interesting study based on metatranscriptomics and 16S rRNA-gene sequencing revealed that response to influenza infection could indirectly affect the expression of ARGs in the respiratory tract by impacting the microbiome diversity and overall the microbial gene transcription (Zhang et al., 2020). In this connection, *S. pneumoniae*, a common respiratory pathogen, can kill closely related bacteria (a phenomenon known as fratricide) by competence-activated killing factors (bacteriocins). The killing leads to HGT by acquiring exogenous DNA from the dead cells, including ARGs (Veening and Blokesch, 2017). Another exciting example related to ARGs acquisition is the case of *Acinetobacter* species which are MDR pathogens causing respiratory infections. Cooper and colleagues showed a predator-prey dynamics where *Acinetobacter baylyi* using its type VI Secretion System (T6SS), lyses and acquires genes through HGT from neighboring *Escherichia coli* cells, including ARGs (Cooper et al., 2017). Similar to species as *A. baylyi* or *Vibrio cholerae* a T6SS-dependent killing of neighboring bacterial cells promoting the uptake of foreign DNA could lead to antibiotic resistance or virulence in other bacteria associated with respiratory infections as *Pseudomonas* or *Ralstonia* (Ringel et al., 2017). These strategies contribute to the fitness of the stronger competitor or the predator bacteria by acquiring beneficial adaptive traits, including the uptake of plasmids and ARGs.

Among medical ICU interventions, ventilation is one of the main factors shaping the composition of the respiratory microbiome. The significant variability between the few available

mechanically-ventilated patient-based studies is a challenge for establishing conclusions (Fromentin et al., 2021). As expected, the microbiome in ICU ventilated patients is more disturbed than in non-ventilated individuals as it reflects the decrease of the alpha-diversity with the duration of mechanic ventilation and the frequent overgrowth of one or a few species (Kelly et al., 2016; Zakharkina et al., 2017). Besides differences in the alpha diversity, the RTM in mechanically ventilated patients shows differences in the composition and the abundance of microbial entities when compared to controls (Emonet et al., 2019). Emonet and colleagues identified early markers associated with the development of ventilator-associated pneumonia (Emonet et al., 2019). Dickson et al. performed a prospective, observational cohort study in critically ill patients with mechanical ventilation. The authors found that bacterial burden and composition of the RTM predict the ICU-patient outcome (Dickson et al., 2020). More studies of this nature would significantly improve the prevention and diagnosis of ventilator-associated pneumonia by identifying the risk, severity, and evolution of RTM markers. The diagnosis, prognosis, and therapies should consider all these factors to adopt a precise medical approach to manage respiratory infections.

GUT-LUNG AXIS IN RESPIRATORY INFECTIONS

The microbial gut-lung axis (cross-talk between the intestinal and the respiratory microbiotas) seems to work through systemic dissemination of beneficial anti-inflammatory and antimicrobial metabolites, such as short-chain fatty acids (SCFAs) or by the stochastic propagation of bacteria (Dumas et al., 2018). Mice studies have proved that the GIM is protective against respiratory infection through pulmonary immune system stimulation (Budden et al., 2017). Gut microbiome perturbations are linked with altered immune responses and homeostasis in the airways (Dang and Marsland, 2019). Note that gut microbiota dysbiosis generally results in the overgrowth of subpopulations of Proteobacteria (e.g., some genus/families of Gammaproteobacteria) present as minority populations in the gut, which frequently colonize the upper intestine, thus increasing the chances of reaching the respiratory tract. This often occurs under antibiotic therapy and underlying patient conditions such as obesity and under-nutrition. In cystic fibrosis, changes in the dominance of certain species in the GIM are followed by an increase of the same species in the respiratory tract (Madan et al., 2012).

The gut-lung axis might become harmful in circumstances of famine and during critical illness. In the ICU, the customary use of anti-acid therapy (facilitating stomach-esophageal-mouth-tracheal colonization) might contribute to gut-respiratory transmission. The abdominal cavity (peritoneum) and the thoracic cavity (pleura) are neighbor spaces separated by a dynamic and not totally hermetic membrane (diaphragm), and then pneumonia is frequently associated with peritonitis (Muniz et al., 2015). Recently, patients with COVID-19, besides the evident pulmonary infection, have been reported to present gastrointestinal symptoms, pointing to the gut-lung axis as a strategy to prevent and treat the disease (He et al., 2020). The basis and mechanisms of the gut-lung axis in respiratory infections needs to be addressed by combining animal model and clinical analyses. Longitudinal sampling of the gut and the RTM from ICU patients would provide much knowledge on directionality and connection among both systems. Also, whole-genome comparisons of species present in the GIM and RTM could cast some light on connectivity of both ecological spaces.

"THE BLACK HOLE" OF THE RTM IN HEALTH AND DISEASE

The RTM field is in its infancy, and the role of the RTM for host physiology in health and disease is far from being understood. More than knowledge gaps or pieces of information, there is a "black hole" regarding the ecology of the RTM and the consequences derived from its disturbances. One of the main gaps in the field is the poor knowledge of the healthy RTM baseline data, especially regarding the LRT. The area involved in the nutrients acquisition, which is the primary function of the gastrointestinal tract, has evolved (acidity, bile, peristalsis) to contain a minimum microbial load. Similarly, the area involved in oxygen acquisition by the respiratory tract has evolved to be very poorly colonized (mucociliary escalator, cough reflex). Whether a normal indigenous RTM in the LRT persists over time or is constant community immigration from the URT is a matter of debate and challenge. Until the development of high-throughput sequencing approaches, the LRT colonizers in the absence of infection have been disregarded. This fact was primarily due to the failure to grow lung microbes in routine microbiological cultures (Bos and Kalil, 2019). Moreover, collecting clinical samples suitable for describing the LRT microbiome, such as tracheal aspirates or BALs, is an invasive procedure that makes it quite challenging for performance on non-hospitalized healthy individuals and does not prevent oropharyngeal contamination.

Like any microbial ecosystem, the RTM functions through microbial interactions taking place in the tract niches with a strong influence on the host through the immune system, and the environment, especially in a body part in constant air exchange. Most of the ecological processes that may occur in this microbiome, including diversity dynamics, stability, resistance, resilience, or microbial interactions (i.e., cooperation, competition, amensalism) are poorly understood. Furthermore, the identification of "keystone" microorganisms (those with a substantial impact on the performance of ecosystems that, when affected, have a significant effect on the whole arrangement as key-nodes in a network) and their microbial interactions (network's edges), generally involving mechanisms such as metabolite exchange, metabolite conversion, signaling, or genetic exchange, remain largely unknown. Identifying the RTM composition, the microbial interactions, and the mechanisms involved in CR are becoming relevant to define a "healthy microbiome" along the respiratory tract and to understand the impact of clinical and environmental factors that

lead to dysbiosis. The development of accurate, personalized microbiome-based treatments would significantly remodel the management of patients with respiratory diseases.

The detection of microbial eukaryotes (fungi and protozoa), archaea, and viruses have been neglected in RTM research. However, through the application of "omics," the RTM composition of non-bacterial microorganisms is starting to be described (Koskinen et al., 2017; Xu et al., 2017; Pérez-Cobas et al., 2020a). The mycobiome and virome should be considered a high priority due to the contribution of viruses and fungi in the development of respiratory infections (Wu and Segal, 2018). In pneumonia and other infectious diseases, intra- (bacteria-bacteria, fungi-fungi) and inter-kingdom interactions (bacteria-fungi, bacteria-viruses) seem to influence the severity of the infections and might have a role in host-microbiome equilibrium restoration after disease remission (Molyneaux et al., 2013; Pérez-Cobas et al., 2020a). Since the microbial ecosystem works as a network of connections, it is wise to consider bacteria and their interactions with other kingdoms to treat infections. On the one hand, that would indirectly allow targeting infections through their co-dependent partners disrupting the whole dysbiotic consortium. On the other hand, knowing the network of beneficial partners would also make it possible to stimulate a set of microorganisms that might contribute to accelerating health recovery through microbiome restoration.

MICROBIOME-BASED INTERVENTIONS TO TREAT NOSOCOMIAL RESPIRATORY INFECTIONS

As previously stated, hospitalized patients are generally under antibiotic therapy, especially critical ones in the ICUs with mechanical ventilation, long-term stays, and immunosuppression. Thibeault et al. recommend a personalized and rational use of antibiotics, the monitorization of the treatment, and frequent and continuous reevaluation of the therapeutic regimen as a strategy to overcome the effect of antimicrobials on the microbiota (Thibeault et al., 2021). A good choice of pathogen-focused antibiotics should effectively kill the pathogen while causing minimized damage to the microbiota. Research on the effect of the clinical most used antibiotic combinations in the RTM would improve the antibiotics therapy choices in ICU patients.

Probiotics (administered living bacteria beneficial for health) have been applied to restore the gut microbiome in several conditions associated with antibiotics treatments, although studies of its efficacy have yielded heterogeneous but moderately positive effects (Hempel et al., 2012; Goldenberg et al., 2018). They can be administered combined with prebiotics (diet components that positively stimulate the microbiome leading to benefit for host physiology), the combination being called synbiotics. Preliminary studies suggest a positive effect of probiotics and synbiotics and high safety in nosocomial and ventilator-associated pneumonia patients. These studies correspond to different and heterogeneous clinical trials and, thus, are not conclusive (Liu et al., 2012; van Ruissen et al., 2019; Batra et al., 2020) which makes it necessary to increase the efforts in this area. Targeting the respiratory microbiome directly through the airways (i.e., inhalation) would be helpful to progress in the prevention and therapy of nosocomial pneumonia.

Fecal microbiota transplantation (FMT) is a promising approach that has been successfully applied to restore the microbiome of patients under recurrent *Clostridium difficile* (Juul et al., 2018). Some clinical studies on *C. difficile* showed that FMT, along side the microbiome equilibrium recovery, reduces intestinal colonization by MDR bacteria (Millan et al., 2016; Saha et al., 2019; Ghani et al., 2020). Also, mouse model studies showed that intestinal and URT microbiome restoration could re-establish the pulmonary immune defenses against bacterial and viral infections through mechanisms as enhancing primary alveolar macrophage function (Schuijt et al., 2016; Brown et al., 2017; Sencio et al., 2021). The set-up and application of this methodology to target the respiratory microbiome could significantly improve patient response to treatments and impede AMR transmission. FMT could restore the protection capacity against nosocomial infections by MDR bacteria, a current major problem in the ICU environment. Besides probiotics and FMT the possibility of a cocktail of known species involved in CR against pathogens, immune system homeostasis, and respiratory microbiome ecology restoration (keystone species) would represent a milestone in targeted microbiome interventions.

As the FMT stimulation of the intestine activates the immune lung responses, another way to cure respiratory infections via the gut-lung axis is by stimulation of the production of gut microbe-derived metabolites, such as the SCFAs or polyamines that have positive systemic effects (Rooks and Garrett, 2016). Various studies have shown that SCFAs are known to stimulate the immune system protecting against viral and secondary bacterial respiratory infections (reviewed in Sencio et al., 2021). Animal and clinical studies using supplementation with these metabolites or stimulation of the growth of producers could contribute to preventing and better fighting against respiratory infections.

Although still in a very early stage, the bacteriophage-based therapies seem very promising to fight pneumonia caused by MDR bacteria (Wunderink, 2019). A recent report showed high levels of bacterial clearance after the administration of an intravenous and aerosol four-phage cocktail to a patient with in a multilobe cavitary resistant *Pseudomonas* infection (Maddocks et al., 2019). Another study shows how an intravenous cocktail of four bacteriophages was as effective as teicoplanin in improving survival and decreasing bacterial load in a mouse model of pneumonia by MRSA (Prazak et al., 2019). Another approach is a vaccination to reduce the antimicrobial resistance burden by targeting bacterial pathogens that can be resistant. When focused on lung pathogens, vaccination against S. pneumoniae and H. influenzae to reduce high mortality bacterial complications like pneumonia or sepsis lead to a reduction in antibiotic-resistant lineages (Ginsburg and Klugman, 2017). Bacteriophage-based pathogen elimination and vaccination act against specific agents and are partially effective when co-infections are in a dysbiotic microbiome environment. A disturbed microbiome is ineffective

in stimulating specific immune system pathways involved in protections against infections.

The restoration of the immune system capacity through local stimuli is a novel prophylactic strategy that has been successfully tested in mice. Specifically, direct applications of IgA, IL-22, or antibodies that block IL-10 help protect microbiota-depleted mice from bacterial pneumonia (reviewed in Thibeault et al., 2021). Robak and colleagues showed that depletion of microbiota by antibiotics inhibited TLR-dependent production of a proliferation-inducing ligand (APRIL), leading to a deficiency in a secondary IgA in mice and human ICU patient's lungs (Robak et al., 2018). Furthermore, since the IgA contributes to defense against *P. aeruginosa*, the authors also demonstrated that after transnasal direct application in antibiotic-treated mice, *P. aeruginosa*-binding IgA provided resistance to infection. Further research combining targeted approaches as bacteriophage therapy or vaccination with restore-based ones as probiotics or prebiotics is promising.

FUTURE DIRECTIONS: NEXT STEPS IN THE RTM RESEARCH

The "omics" have transformed research in clinical microbiology and infectious diseases, contributing to understand microbiome ecology in health and disease (Relman, 2011). The RTM is generally approached from samples such as sputum, tracheal aspirates, or BALs that generally present low biomass, high host contamination, frequent manipulation-derived contaminations, making marker genes sequencing a suitable option (Perez-Cobas and Buchrieser, 2019). So far, the most applied culture-independent methodology to analyze microbial communities' diversity and composition is marker gene sequencing such as 16S rRNA for archaea and bacteria and internal transcribed spacer (ITS) for fungi (Fromentin et al., 2021). Marker genes derived data provided a vision on the relative abundance of the taxa; however, the absolute abundance values are often not estimated. Therefore, the marker genes approach combined with quantification methods of the selected fractions such as qPCR, spikes, or droplet-digital PCR will be relevant to have a more accurate picture of the microbiome evolution during disease, considering not only the relative abundance but the biomass dynamics (Dickson et al., 2020; Pérez-Cobas et al., 2020a).

On the other hand, the omics field is evolving toward the shotgun metagenomic sequencing, which allows characterizing whole metagenomes, reaching a strain level of resolution, and exploring the diversity of non-bacterial diversity such as eukaryotes and viruses (Pérez-Cobas et al., 2020b). However, the low microbial biomass and the enrichment in human cells of respiratory samples complicate the application of metagenomics approaches. Recent-developed protocols deplete human and extracellular DNA from low-biomass abundance samples, yield optimized microbiome profiles, and allow quantifying live microbial load (Marotz et al., 2018, 2021; Nelson et al., 2019). Respiratory clinical samples enriched in microbial cells will enable the application of other omics more focused on understanding the RTM's metabolic, enzymatic, and functional capacities, including meta-metabolomics, metaproteomics, or metatranscriptomics. As previously stated, AMR is a major problem to treat critical patients with pneumonia, and the contribution of the RTM to the acquisition, development, or maintenance of AMR is practically unknown. Besides shotgun metagenomics, future studies should include specific characterization of the resistome and mobilome based on novel targeted-metagenomics (Lanza et al., 2018). More investigation focusing on bacteriophages that are frequent carriers of resistances is needed to fully understand ARGs dynamics and transmission. For instance, a method set-up for skin and wound swabs allows several hundred-fold enrichment of viral DNA, improving viromics performance (Verbanic et al., 2019).

Culture-independent approaches will contribute to obtain the RTM whole picture of diversity, composition, metabolism, expression, ARGs, shedding light on its ecology and physiological role. Together with clinical and environmental variables, this biological information would allow identifying biomarkers of illness prognosis and severity, leading to significant improvement of diagnostic tools, and personalized therapeutic regimens. To complement and test omic-derived data, culturomics, *in vitro* studies, animal models, and longitudinal human clinical studies are necessary to understand the lung microbiome's ecology in infectious diseases and further develop microbiome-based therapies.

DATA AVAILABILITY STATEMENT

The original contributions presented in the study are included in the article/supplementary material, further inquiries can be directed to the corresponding authors.

AUTHOR CONTRIBUTIONS

The manuscript was written by AEP-C, FB, TC, RP, and MCS. All authors listed have made a substantial, direct, and intellectual contribution to the work and approved it for publication.

FUNDING

Lab research in this topic was supported by grants funded by Fundación Ramón Areces (BIOMETASEP), and the Instituto de Salud Carlos III (PI18/1942) co-funded by the European Regional Development Fund (ERDF, A way to achieve Europe). Also supported by InGEMICS-CM (B2017/BMD-3691), funded by Comunidad de Madrid (Spain) and CIBER (CIBER in Infectious Diseases, CIBERINFEC CB21/13/00084) and (CIBER in Epidemiology and Public Health, CIBERESP; CB06/02/0053), integrated in the Spanish 2013-2016 I+D+i State Plan and funded by Instituto de Salud Carlos III. AEP-C is recipient of a Grant for the Attraction of Talent within the Comunidad de Madrid (Grant No. 2019-T2/BMD-12874).

ACKNOWLEDGMENTS

The authors sincerely acknowledge the continuous support and collaboration of nursing and medical staff at the Intensive Medicine Department of the Hospital Universitario Ramón y Cajal.

REFERENCES

Araghi, A. (2020). The lung microbiome and pneumonia: where precision medicine meets pulmonology. *Pulmonology* 26, 333–334. doi: 10.1016/j.pulmoe.2020.04.005

Ball, P., Baquero, F., Cars, O., File, T., Garau, J., Klugman, K., et al. (2002). Antibiotic therapy of community respiratory tract infections: strategies for optimal outcomes and minimized resistance emergence. *J. Antimicrob. Chemother*. 49, 31–40. doi: 10.1093/jac/49.1.31

Bassis, C. M., Erb-Downward, J. R., Dickson, R. P., Freeman, C. M., Schmidt, T. M., Young, V. B., et al. (2015). Analysis of the upper respiratory tract microbiotas as the source of the lung and gastric microbiotas in healthy individuals. *MBio* 6, 1–10. doi: 10.1128/mBio.00037-15

Batra, P., Soni, K. D., and Mathur, P. (2020). Efficacy of probiotics in the prevention of VAP in critically ill ICU patients: an updated systematic review and meta-analysis of randomized control trials. *J. Intensive Care* 8, 1–14. doi: 10.1186/s40560-020-00487-8

Bert, F., and Lambert-Zechovsky, N. (1996). Sinusitis in mechanically ventilated patients and its role in the pathogenesis of nosocomial pneumonia. *Eur. J. Clin. Microbiol. Infect. Dis. Off. Publ. Eur. Soc. Clin. Microbiol*. 15, 533–544. doi: 10.1007/BF01709360

Bos, L. D. J., and Kalil, A. C. (2019). Changes in lung microbiome do not explain the development of ventilator-associated pneumonia. *Intensive Care Med*. 45, 1133–1135. doi: 10.1007/s00134-019-05691-1

Brown, R. L., Sequeira, R. P., and Clarke, T. B. (2017). The microbiota protects against respiratory infection via GM-CSF signaling. *Nat. Commun.* 8:1512. doi: 10.1038/s41467-017-01803-x

Budden, K. F., Gellatly, S. L., Wood, D. L. A., Cooper, M. A., Morrison, M., Hugenholtz, P., et al. (2017). Emerging pathogenic links between microbiota and the gut-lung axis. *Nat. Rev. Microbiol*. 15, 55–63. doi: 10.1038/nrmicro.2016.142

Caballero, J., Vida, R., Cobo, M., Maiz, L., Suarez, L., Galeano, J., et al. (2017). Individual patterns of complexity in including predator bacteria, over a 1-year period. *MBio* 8:e00959–17. doi: 10.1128/mBio.00959-17

Cooper, R. M., Tsimring, L., and Hasty, J. (2017). Inter-species population dynamics enhance microbial horizontal gene transfer and spread of antibiotic resistance. *Elife* 6:e67995. doi: 10.7554/eLife.25950

Dagan, R., Klugman, K. P., Craig, W. A., and Baquero, F. (2001). Evidence to support the rationale that bacterial eradication in respiratory tract infection is an important aim of antimicrobial therapy. *J. Antimicrob. Chemother*. 47, 129–140. doi: 10.1093/jac/47.2.129

Dang, A. T., and Marsland, B. J. (2019). Microbes, metabolites, and the gut-lung axis. *Mucosal Immunol*. 12, 843–850. doi: 10.1038/s41385-019-0160-6

Denys, G. A., and Relich, R. F. (2014). Antibiotic resistance in nosocomial respiratory infections. *Clin. Lab. Med*. 34, 257–270. doi: 10.1016/j.cll.2014.02.004

Depner, M., Ege, M. J., Cox, M. J., Dwyer, S., Walker, A. W., Birzele, L. T., et al. (2017). Bacterial microbiota of the upper respiratory tract and childhood asthma. *J. Allergy Clin. Immunol.* 139, 826–834.e13. doi: 10.1016/j.jaci.2016.05.050

Dickson, R. P. (2016). The microbiome and critical illness. *Lancet. Respir. Med*. 4, 59–72. doi: 10.1016/S2213-2600(15)00427-0

Dickson, R. P. (2021). Lung microbiota and COVID-19 severity. *Nat. Microbiol*. (2021) 610, 1217–1218. doi: 10.1038/s41564-021-00969-x

Dickson, R. P., Erb-Downward, J. R., Freeman, C. M., McCloskey, L., Beck, J. M., Huffnagle, G. B., et al. (2015). Spatial variation in the healthy human lung microbiome and the adapted island model of lung biogeography. *Ann. Am. Thorac. Soc*. 12, 821–830. doi: 10.1513/AnnalsATS.201501-029OC

Dickson, R. P., Erb-Downward, J. R., Freeman, C. M., McCloskey, L., Falkowski, N. R., Huffnagle, G. B., et al. (2017). Bacterial topography of the healthy human lower respiratory tract. *MBio*. doi: 10.1128/mBio.02287-16

Dickson, R. P., Erb-Downward, J. R., and Huffnagle, G. B. (2014). Towards an ecology of the lung: new conceptual models of pulmonary microbiology and pneumonia pathogenesis. *Lancet Respir. Med*. 2, 238–246. doi: 10.1016/S2213-2600(14)70028-1

Dickson, R. P., Erb-Downward, J. R., Martinez, F. J., and Huffnagle, G. B. (2016). The microbiome and the respiratory tract. *Annu. Rev. Physiol*. 78, 481–504. doi: 10.1146/annurev-physiol-021115-105238

Dickson, R. P., Schultz, M. J., Van Der Poll, T., Schouten, L. R., Falkowski, N. R., Luth, J. E., et al. (2020). Lung microbiota predict clinical outcomes in critically ill patients. *Am. J. Respir. Crit. Care Med*. 201, 555–563. doi: 10.1164/rccm.201907-1487OC

Dumas, A., Bernard, L., Poquet, Y., Lugo-Villarino, G., and Neyrolles, O. (2018). The role of the lung microbiota and the gut-lung axis in respiratory infectious diseases. *Cell Microbiol*. 20:e12966. doi: 10.1111/cmi.12966

Emonet, S., Lazarevic, V., Leemann Refondini, C., Gaïa, N., Leo, S., Girard, M., et al. (2019). Identification of respiratory microbiota markers in ventilator-associated pneumonia. *Intensive Care Med*. 45, 1082–1092. doi: 10.1007/s00134-019-05660-8

Feldman, C., and Anderson, R. (2021). The role of co-infections and secondary infections in patients with COVID-19. *Pneumonia* 13:5. doi: 10.1186/s41479-021-00083-w

Fernández-Barat, L., López-Aladid, R., and Torres, A. (2020). Reconsidering ventilator-associated pneumonia from a new dimension of the lung microbiome. *EBioMedicine* 60:102590. doi: 10.1016/j.ebiom.2020.102995

Françoise, A., and Héry-Arnaud, G. (2020). The microbiome in cystic fibrosis pulmonary disease. *Genes* 11:536. doi: 10.3390/genes11050536

Fromentin, M., Ricard, J. D., and Roux, D. (2021). Respiratory microbiome in mechanically ventilated patients: a narrative review. *Intensive Care Med*. 47, 292–306. doi: 10.1007/s00134-020-06338-2

Ghani, R., Mullish, B. H., McDonald, J. A. K., Ghazy, A., Williams, H. R. T., Brannigan, E. T., et al. (2020). Disease prevention not decolonization: a model for fecal microbiota transplantation in patients colonized with multidrug-resistant organisms. *Clin. Infect. Dis*. 72:3. doi: 10.1093/cid/ciaa948

Ginsburg, A. S., and Klugman, K. P. (2017). Vaccination to reduce antimicrobial resistance. *Lancet Glob. Heal.* 5:e1176–e1177. doi: 10.1016/S2214-109X(17)30364-9

Goldenberg, J. Z., Mertz, D., and Johnston, B. C. (2018). Probiotics to prevent clostridium difficile infection in patients receiving antibiotics. *JAMA* 320, 499–500. doi: 10.1001/jama.2018.9064

Goldman, M. J., Anderson, G. M., Stolzenberg, E. D., Kari, U. P., Zasloff, M., and Wilson, J. M. (1997). Human beta-defensin-1 is a salt-sensitive antibiotic in lung that is inactivated in cystic fibrosis. *Cell* 88, 553–560. doi: 10.1016/S0092-8674(00)81895-4

Gu, L., Deng, H., Ren, Z., Zhao, Y., Yu, S., Guo, Y., et al. (2019). Dynamic changes in the microbiome and mucosal immune microenvironment of the lower respiratory tract by influenza virus infection. *Front. Microbiol*. 10:2491. doi: 10.3389/fmicb.2019.02491

He, L.-H., Ren, L.-F., Li, J.-F., Wu, Y.-N., Li, X., and Zhang, L. (2020). Intestinal flora as a potential strategy to fight SARS-CoV-2 infection. *Front. Microbiol*. 11:1388. doi: 10.3389/fmicb.2020.01388

Hempel, S., Newberry, S. J., Maher, A. R., Wang, Z., Miles, J. N. V., Shanman, R., et al. (2012). Probiotics for the prevention and treatment of antibiotic-associated diarrhea: a systematic review and meta-analysis. *JAMA* 307, 1959–1969. doi: 10.1001/jama.2012.3507

Henig, O., and Kaye, K. S. (2017). Bacterial pneumonia in older adults. *Infect. Dis. Clin. North Am*. 31, 689–713. doi: 10.1016/j.idc.2017.07.015

Hogg, J. C., Williams, J., Richardson, J. B., Macklem, P. T., and Thurlbeck, W. M. (1970). Age as a factor in the distribution of lower-airway conductance and in the pathologic anatomy of obstructive lung disease. *N. Engl. J. Med*. 282, 1283–1287. doi: 10.1056/NEJM197006042822302

Janda, L., Mihalčin, M., and Štastná, M. (2021). Is a healthy microbiome responsible for lower mortality in COVID-19? *Biologia* 76:1. doi: 10.2478/s11756-020-00614-8

Juul, F. E., Garborg, K., Bretthauer, M., Skudal, H., Øines, M. N., Wiig, H., et al. (2018). Fecal microbiota transplantation for primary *Clostridium difficile* infection. *N. Engl. J. Med*. 378, 2535–2536. doi: 10.1056/NEJMc1803103

Kalanuria, A. A., Zai, W., and Mirski, M. (2014). Ventilator-associated pneumonia in the ICU. *Crit. Care* 18, 1–8. doi: 10.1186/cc13775

Kelly, B. J., Imai, I., Bittinger, K., Laughlin, A., Fuchs, B. D., Bushman, F. D., et al. (2016). Composition and dynamics of the respiratory tract microbiome in intubated patients. *Microbiome* 4, 1–13. doi: 10.1186/s40168-016-0151-8

Khatiwada, S., and Subedi, A. (2020). Lung microbiome and coronavirus disease 2019 (COVID-19): possible link and implications. *Hum. Microbiome J.* 17:100073. doi: 10.1016/j.humic.2020.100073

Kim, D. W., and Cha, C. J. (2021). Antibiotic resistome from the One-Health perspective: understanding and controlling antimicrobial resistance transmission. *Exp. Mol. Med*. 53, 301–309. doi: 10.1038/s12276-021-00569-z

Koskinen, K., Pausan, M. R., Perras, A. K., Beck, M., Bang, C., Mora, M., et al. (2017). First insights into the diverse human archaeome: specific detection of Archaea in the gastrointestinal tract, lung, and nose and on skin. *MBio* 8, 1–17. doi: 10.1128/mBio.00824-17

Langford, B. J., So, M., Raybardhan, S., Leung, V., Soucy, J.-P. R., Westwood, D., et al. (2021). Antibiotic prescribing in patients with COVID-19: rapid review and meta-analysis. *Clin. Microbiol. Infect. Off. Publ. Eur. Soc. Clin. Microbiol. Infect. Dis*. 27, 520–531. doi: 10.1016/j.cmi.2020.12.018

Lanza, V. F., Baquero, F., Martínez, J. L., Ramos-Ruíz, R., González-Zorn, B., Andremont, A., et al. (2018). In-depth resistome analysis by targeted metagenomics. *Microbiome* 6, 1–14. doi: 10.1186/s40168-017-0387-y

Liu, K., xiong, Zhu, Y., gang, Zhang, J., Tao, L., li, Lee, J. W., Wang, X., et al. (2012). Probiotics' effects on the incidence of nosocomial pneumonia in critically ill patients: A systematic review and meta-analysis. *Crit. Care* 16:R109. doi: 10.1186/cc11398

Lloréns-Rico, V., Gregory, A. C., Van Weyenbergh, J., Jansen, S., Van Buyten, T., Qian, J., et al. (2021). Clinical practices underlie COVID-19 patient respiratory microbiome composition and its interactions with the host. *Nat. Commun.* 121:6243. doi: 10.1038/s41467-021-26500-8

MacArthur, R. H., and Wilson, E. O. (1963). An equilibrium theory of insular zoogeography. *Evolution* 17:373. doi: 10.2307/2407089

Madan, J. C., Koestler, D. C., Stanton, B. A., Davidson, L., Moulton, L. A., Housman, M. L., et al. (2012). Serial analysis of the gut and respiratory microbiome in cystic fibrosis in infancy: interaction between intestinal and respiratory tracts and impact of nutritional exposures. *MBio* 3:e00251–12. doi: 10.1128/mBio.00251-12

Maddocks, S., Fabijan, A. P., Ho, J., Lin, R. C. Y., Ben Zakour, N. L., Dugan, C., et al. (2019). Bacteriophage therapy of ventilator-associated pneumonia and empyema caused by *Pseudomonas aeruginosa*. *Am. J. Respir. Crit. Care Med*. 200, 1179–1181. doi: 10.1164/rccm.201904-0839LE

Madhi, S. A., and Klugman, K. P. (2004). A role for *Streptococcus pneumoniae* in virus-associated pneumonia. *Nat. Med*. 10, 811–813. doi: 10.1038/nm1077

Man, W. H., De Steenhuijsen Piters, W. A. A., and Bogaert, D. (2017). The microbiota of the respiratory tract: gatekeeper to respiratory health. *Nat. Rev. Microbiol*. 15, 259–270. doi: 10.1038/nrmicro.2017.14

Marotz, C., Morton, J. T., Navarro, P., Coker, J., Belda-Ferre, P., Knight, R., et al. (2021). Quantifying live microbial load in human saliva samples over time reveals stable composition and dynamic load. *mSystems* 6, 1–16. doi: 10.1128/mSystems.01182-20

Marotz, C. A., Sanders, J. G., Zuniga, C., Zaramela, L. S., Knight, R., and Zengler, K. (2018). Improving saliva shotgun metagenomics by chemical host DNA depletion. *Microbiome* 6, 1–9. doi: 10.1186/s40168-018-0426-3

Marsland, B. J., and Gollwitzer, E. S. (2014). Host-microorganism interactions in lung diseases. *Nat. Rev. Immunol*. 14, 827–835. doi: 10.1038/nri3769

Martinez-Guryn, K., Leone, V., and Chang, E. B. (2019). Regional diversity of the gastrointestinal microbiome. *Cell Host Microbe* 26, 314–324. doi: 10.1016/j.chom.2019.08.011

Maurice, C. F. (2019). Considering the other half of the gut microbiome: bacteriophages. *mSystems* 4, 4–7. doi: 10.1128/mSystems.00102-19

Millan, B., Park, H., Hotte, N., Mathieu, O., Burguiere, P., Tompkins, T. A., et al. (2016). Fecal microbial transplants reduce antibiotic-resistant genes in patients with recurrent clostridium difficile infection. *Clin. Infect. Dis*. 62, 1479–1486. doi: 10.1093/cid/ciw185

Mitchell, A. B., Oliver, B. G. G., and Glanville, A. R. (2016). Concise clinical review translational aspects of the human respiratory virome. *Am. J. Respir. Crit. Care Med*. 194, 1458–1464. doi: 10.1164/rccm.201606-1278CI

Molyneaux, P. L., Mallia, P., Cox, M. J., Footitt, J., Willis-Owen, S. A. G., Homola, D., et al. (2013). Outgrowth of the bacterial airway microbiome after rhinovirus exacerbation of chronic obstructive pulmonary disease. *Am. J. Respir. Crit. Care Med*. 188, 1224–1231. doi: 10.1164/rccm.201302-0341OC

Muniz, B. F., Netto, G. M., Ferreira, M. J., Prata, L. O., Mayrink, C. C., Guimarães, Y. L., et al. (2015). Neutrophilic infiltration in lungs of mice with peritonitis in acid or basic medium. *Int. J. Clin. Exp. Med*. 8, 5812–5817.

Nelson, M. T., Pope, C. E., Marsh, R. L., Wolter, D. J., Weiss, E. J., Hager, K. R., et al. (2019). Human and extracellular DNA depletion for metagenomic analysis of complex clinical infection samples yields optimized viable microbiome profiles. *Cell Rep*. 26, 2227–2240.e5. doi: 10.1016/j.celrep.2019.01.091

O'Toole, G. A. (2018). Cystic fibrosis airway microbiome: overturning the old, opening the way for the new. *J. Bacteriol*. 200, 1–8. doi: 10.1128/JB.00561-17

Perez-Cobas, A. E., and Buchrieser, C. (2019). Analysis of the pulmonary microbiome composition of Legionella pneumophila-infected patients. *Methods Mol. Biol*. 1921, 429–443. doi: 10.1007/978-1-4939-9048-1_27

Pérez-Cobas, A. E., Ginevra, C., Rusniok, C., Jarraud, S., and Buchrieser, C. (2020a). Persistent legionnaires' disease and associated antibiotic treatment engender a highly disturbed pulmonary microbiome enriched in opportunistic microorganisms. *MBio* 11:e00889–20. doi: 10.1128/mBio.00889-20

Pérez-Cobas, A. E., Gomez-Valero, L., and Buchrieser, C. (2020b). Metagenomic approaches in microbial ecology: an update on whole-genome and marker gene sequencing analyses. *Microb. Genom.* 6:409. doi: 10.1099/mgen.0.000409

Peteranderl, C., Sznajder, J. I., Herold, S., and Lecuona, E. (2017). Inflammatory responses regulating alveolar ion transport during pulmonary infections. *Front. Immunol*. 8:446. doi: 10.3389/fimmu.2017.00446

Pettigrew, M. M., Tanner, W., and Harris, A. D. (2020). The lung microbiome and pneumonia. *J. Infect. Dis*. 223(12 Suppl 2):S241–5. doi: 10.1093/infdis/jiaa702

Prazak, J., Iten, M., Cameron, D. R., Save, J., Grandgirard, D., Resch, G., et al. (2019). Bacteriophages improve outcomes in experimental *Staphylococcus aureus* ventilator-associated pneumonia. *Am. J. Respir. Crit. Care Med*. 200, 1126–1133. doi: 10.1164/rccm.201812-2372OC

Relman, D. A. (2011). Microbial genomics and infectious diseases. *N. Engl. J. Med*. 365, 347–357. doi: 10.1056/NEJMra1003071

Ringel, P. D., Hu, D., and Basler, M. (2017). The role of type VI secretion system effectors in target cell lysis and subsequent horizontal gene transfeR. *Cell Rep*. 21, 3927–3940. doi: 10.1016/j.celrep.2017.12.020

Robak, O. H., Heimesaat, M. M., Kruglov, A. A., Prepens, S., Ninnemann, J., Gutbier, B., et al. (2018). Antibiotic treatment-induced secondary IgA deficiency enhances susceptibility to *Pseudomonas aeruginosa* pneumonia. *J. Clin. Invest*. 128:3535. doi: 10.1172/JCI97065

Rooks, M. G., and Garrett, W. S. (2016). Gut microbiota, metabolites and host immunity. *Nat. Rev. Immunol*. 16, 341–352. doi: 10.1038/nri.2016.42

Ross, M. H., and Pawlina, W. (2016). *Histology: A Text and Atlas : with Correlated Cell and Molecular Biology*. Wolters Kluwer Health. Available onine at: https://books.google.es/books?id=A7zooQEACAAJ

Saha, S., Tariq, R., Tosh, P. K., Pardi, D. S., and Khanna, S. (2019). Faecal microbiota transplantation for eradicating carriage of multidrug-resistant organisms: a systematic review. *Clin. Microbiol. Infect*. 25, 958–963. doi: 10.1016/j.cmi.2019.04.006

Schneeberger, P. H. H., Prescod, J., Levy, L., Hwang, D., Martinu, T., and Coburn, B. (2019). Microbiota analysis optimization for human bronchoalveolar lavage fluid. *Microbiome* 7, 1–16. doi: 10.1186/s40168-019-0755-x

Schuijt, T. J., Lankelma, J. M., Scicluna, B. P., De Sousa E Melo, F., Roelofs, J. J. T. H., De Boer, J. D., et al. (2016). The gut microbiota plays a protective role in the host defence against pneumococcal pneumonia. *Gut* 65, 575–583. doi: 10.1136/gutjnl-2015-309728

Sencio, V., Machado, M. G., and Trottein, F. (2021). The lung-gut axis during viral respiratory infections: the impact of gut dysbiosis on secondary disease outcomes. *Mucosal Immunol*. 14, 296–304. doi: 10.1038/s41385-020-00361-8

Soriano, M. C., Vaquero, C., Ortiz-Fernández, A., Caballero, A., Blandino-Ortiz, A., and de Pablo, R. (2021). Low incidence of co-infection, but high incidence of ICU-acquired infections in critically ill patients with COVID-19. *J. Infect*. 82:e20–e21. doi: 10.1016/j.jinf.2020.09.010

Stavropoulou, E., Kantartzi, K., Tsigalou, C., Konstantinidis, T., Voidarou, C., Konstantinidis, T., et al. (2021). Unraveling the interconnection patterns across lung microbiome, respiratory diseases, and COVID-19. *Front. Cell. Infect. Microbiol*. 10:892. doi: 10.3389/fcimb.2020.619075

Sulaiman, I., Chung, M., Angel, L., Tsay, J. C. J., Wu, B. G., Yeung, S. T., et al. (2021). Microbial signatures in the lower airways of mechanically ventilated COVID-19 patients associated with poor clinical outcome. *Nat. Microbiol*. 610, 1245–1258. doi: 10.1038/s41564-021-00961-5

Sutton, T. D. S., and Hill, C. (2019). Gut bacteriophage: current understanding and challenges. *Front. Endocrinol.* 10:784. doi: 10.3389/fendo.2019.00784

Thibeault, C., Suttorp, N., and Opitz, B. (2021). The microbiota in pneumonia: From protection to predisposition. *Sci. Transl. Med.* 13:eaba0501. doi: 10.1126/scitranslmed.aba0501

Tipton, L., Ghedin, E., and Morris, A. (2017). The lung mycobiome in the next-generation sequencing era. *Virulence* 8, 334–341. doi: 10.1080/21505594.2016.1235671

Troeger, C., Blacker, B., Khalil, I. A., Rao, P. C., Cao, J., Zimsen, S. R. M., et al. (2018). Estimates of the global, regional, and national morbidity, mortality, and aetiologies of lower respiratory infections in 195 countries, 1990-2016: a systematic analysis for the Global Burden of Disease Study 2016. *Lancet Infect. Dis.* 18, 1191–1210. doi: 10.1016/S1473-3099(18)30310-4

van Ruissen, M. C. E., Bos, L. D., Dickson, R. P., Dondorp, A. M., Schultsz, C., and Schultz, M. J. (2019). Manipulation of the microbiome in critical illness-probiotics as a preventive measure against ventilator-associated pneumonia. *Intensive Care Med. Exp.* 7, 1–12. doi: 10.1186/s40635-019-0238-1

Veening, J.-W., and Blokesch, M. (2017). Interbacterial predation as a strategy for DNA acquisition in naturally competent bacteria. *Nat. Rev. Microbiol.* 15, 621–629. doi: 10.1038/nrmicro.2017.66

Vengoechea, J. J., Ponce-Alonso, M., Figueredo, A. L., Micholé, E., Torralba, L., Errasti, J., et al. (2019). Changes in the pulmonary microbiome associated with lung cancer. *Eur. Respir. J.* 54, PA3663. doi: 10.1183/13993003.congress-2019.PA3663

Venkataraman, A., Bassis, C. M., Beck, J. M., Young, V. B., Curtis, J. L., Huffnagle, G. B., et al. (2015). Application of a neutral community model to assess structuring of the human lung microbiome. *MBio* 6, 1–9. doi: 10.1128/mBio.02284-14

Verbanic, S., Kim, C. Y., Deacon, J. M., and Chen, I. A. (2019). Improved single-swab sample preparation for recovering bacterial and phage DNA from human skin and wound microbiomes. *BMC Microbiol.* 19:214. doi: 10.1186/s12866-019-1586-4

Volakli, E., Spies, C., Michalopoulos, A., Groeneveld, A. J., Sakr, Y., and Vincent, J. L. (2010). Infections of respiratory or abdominal origin in ICU patients: what are the differences? *Crit. Care* 14:R32. doi: 10.1186/cc8909

Willner, D., Furlan, M., Haynes, M., Schmieder, R., Angly, F. E., Silva, J., et al. (2009). Metagenomic analysis of respiratory tract DNA viral communities in cystic fibrosis and non-cystic fibrosis individuals. *PLoS ONE* 4:7370. doi: 10.1371/journal.pone.0007370

Willner, D., Haynes, M. R., Furlan, M., Hanson, N., Kirby, B., Lim, Y. W., et al. (2012). Case studies of the spatial heterogeneity of DNA viruses in the cystic fibrosis lung. *Am. J. Respir. Cell Mol. Biol.* 46, 127–131. doi: 10.1165/rcmb.2011-0253OC

Wu, B. G., and Segal, L. N. (2018). The lung microbiome and its role in pneumonia. *Clin. Chest Med.* 39, 677–689. doi: 10.1016/j.ccm.2018.07.003

Wunderink, R. G. (2019). Turning the phage on treatment of antimicrobial-resistant pneumonia. *Am. J. Respir. Crit. Care Med.* 200, 1081–1082. doi: 10.1164/rccm.201908-1561ED

Xu, L., Zhu, Y., Ren, L., Xu, B., Liu, C., Xie, Z., et al. (2017). Characterization of the nasopharyngeal viral microbiome from children with community-acquired pneumonia but negative for Luminex xTAG respiratory viral panel assay detection. *J. Med. Virol.* 89, 2098–2107. doi: 10.1002/jmv.24895

Yamamoto, S., Saito, M., Tamura, A., Prawisuda, D., Mizutani, T., and Yotsuyanagi, H. (2021). The human microbiome and COVID-19: a systematic review. *PLoS ONE* 16:e0253293. doi: 10.1371/journal.pone.0253293

Young, J. C., Chehoud, C., Bittinger, K., Bailey, A., Diamond, J. M., Cantu, E., et al. (2015). Viral metagenomics reveal blooms of anelloviruses in the respiratory tract of lung transplant recipients. *Am. J. Transplant.* 15, 200–209. doi: 10.1111/ajt.13031

Zakharkina, T., Martin-Loeches, I., Matamoros, S., Povoa, P., Torres, A., Kastelijn, J. B., et al. (2017). The dynamics of the pulmonary microbiome during mechanical ventilation in the intensive care unit and the association with occurrence of pneumonia. *Thorax* 72, 803–810. doi: 10.1136/thoraxjnl-2016-209158

Zhang, L., Forst, C. V., Gordon, A., Gussin, G., Geber, A. B., Fernandez, P. J., et al. (2020). Characterization of antibiotic resistance and host-microbiome interactions in the human upper respiratory tract during influenza infection. *Microbiome* 8, 1–12. doi: 10.1186/s40168-020-00803-2

Conflict of Interest: The authors declare that the research was conducted in the absence of any commercial or financial relationships that could be construed as a potential conflict of interest.

Publisher's Note: All claims expressed in this article are solely those of the authors and do not necessarily represent those of their affiliated organizations, or those of the publisher, the editors and the reviewers. Any product that may be evaluated in this article, or claim that may be made by its manufacturer, is not guaranteed or endorsed by the publisher.

Advantages of publishing in Frontiers

OPEN ACCESS
Articles are free to read for greatest visibility and readership

FAST PUBLICATION
Around 90 days from submission to decision

HIGH QUALITY PEER-REVIEW
Rigorous, collaborative, and constructive peer-review

TRANSPARENT PEER-REVIEW
Editors and reviewers acknowledged by name on published articles

Frontiers
Avenue du Tribunal-Fédéral 34
1005 Lausanne | Switzerland

Visit us: www.frontiersin.org
Contact us: frontiersin.org/about/contact

REPRODUCIBILITY OF RESEARCH
Support open data and methods to enhance research reproducibility

DIGITAL PUBLISHING
Articles designed for optimal readership across devices

FOLLOW US
@frontiersin

IMPACT METRICS
Advanced article metrics track visibility across digital media

EXTENSIVE PROMOTION
Marketing and promotion of impactful research

LOOP RESEARCH NETWORK
Our network increases your article's readership